# Heating and Cooling in a Packed Bed

## A Major Qualifying Project

Submitted to the Faculty of the

WORCESTER POLYTECHNIC INSTITUTE

in partial fulfillment of the requirement for the

Degree of Bachelor of Science

in Chemical Engineering


Anthony DiNino _____

Emily Hartzell _____

Katherine Judge _____

Ashley Morgan _____


April 22, 2013


WPI

Approved:

_____

Anthony G. Dixon

## ABSTRACT

The purpose of this research was to examine heat transfer in wall-heated and wall-cooled packed beds. In previous research at Worcester Polytechnic Institute, cooling was found to trend higher than heating. Through changes in the computer model, calculated temperature profiles were closer to experimental profiles. When changing the experimental procedure to reduce re-packings, the trends in parameters were less scattered. Using these alterations, heating and cooling were found to be more similar than what was observed in the past.

## Executive Summary

This research examined heat transfer experiments in a packed bed. In industry, packed beds are used in applications such as separators, absorbers, strippers, and reactors. In order to design a safe process, it is necessary to know the heat transfer parameters of the bed. This ensures that the correct amount of heat is added or removed from the bed. It is important for exothermic reactions to ensure a run-away reaction does not occur. Conversely, if an insufficient amount heat is supplied to an endothermic reaction, the reaction may not yield the desired conversion. To properly model industrial reactors, they are first modeled on a small scale.

Pilot scale experiments have been performed at Worcester Polytechnic Institute for both steam-heated and water-cooled setups. In these past experiments, cooling has been found to produce higher heat transfer parameters than heating. Since heating and cooling have rarely been performed in the same research period using the same column and packing, this research conducted both experiments. The goal of the performing both experiments under the same conditions was to draw more definite conclusions about comparing heating and cooling.

For this research, heating and cooling experiments were performed using a two-inch brass column packed with ¼-inch ceramic spheres. Before the air entered the column, it was first passed through a calming section packed with ¼-inch metal spheres. This calming section helped to develop the velocity profile before the air entered the bed. For heating experiments, room temperature air was passed through the bed and steam condensed on the column walls. When cooling was performed, the air was pre-heated to about 95°C and then passed into the column with cooling water running through the jacket. The bed was packed to heights of 4, 6, 8, and 10 inches and a thermocouple cross and a Datalogger were used to collect the radial temperature profiles at each height.

A Generalized Inlet Profile Plug Flow (GIPPF) model was used to analyze the collected axial and radial temperatures in order to calculate heat transfer parameters. This model took the first bed height as the initial height and interpolated the experimental data to give a full inlet profile. This accounted for any heat losses that would occur in the calming section. When the dimensionless inlet profile interpolated by the model was compared to our experimental profile, it was found these graphs did not match. The produced model sometimes showed the dimensionless temperature at the center of the bed was approaching values greater than one. The problem with the model was that it was not including the center thermocouple and values at the center of the bed were actually being extrapolated. Since this was producing physically unreasonable results, the model was altered to include the center thermocouple.

Once the correct model was used, the heating experiments from this research were compared to past heating. It was found that the heating data from this research had more scatter than was previously observed and also was trending higher. The only difference, besides the

inclusion of the center thermocouple, was a change in experimental procedure. For this research, the bed was packed to all heights during one day with a constant airflow. For the previous heating research, the bed was packed to one height per day with changing airflow. Since the procedure used in this research comprised of more re-packing, which introduces scatter, the procedure from the previous research was used to collect heating and cooling data. The data was recollected and was once again compared to previous heating data. It was then found that the current heating data matched the previous heating data well and the scatter was significantly reduced.

Finally, once the corrected model and procedure were selected, heating and cooling were compared to each other. This research found heating and cooling to be very similar for lower Reynolds numbers and then heating began to trend slightly higher than cooling after Reynolds numbers of about 600. This contradicts what was observed in the past, where cooling was found to trend higher than heating for all Reynolds numbers studied.

After all of the results were compared, the current research came to the following conclusions and recommendations. Firstly, the corrected model which includes center thermocouple should be used to provide physically reasonable dimensionless temperature profiles. Secondly, to eliminate scatter produced from re-packing the bed, the bed should be packed to one height per day and the airflow should be varied. Lastly, for this research heating and cooling have been found to be more similar than what has been observed in the past. If there is a difference, it is smaller than what was previously found. Additionally heating seems to trend higher for Reynolds numbers above 600. However, since the data collected using the recommended procedure utilized only one packing structure and two weeks' worth of data, more research needs to be done. For future research, it is recommended that the same column and packing materials should be used for multiple packing structures using the recommended procedure. This will allow for more data to provide a clearer picture of the comparison of heating and cooling. After this is done, it is recommended that several different packing materials and columns sizes should be used to draw a more universal conclusion.

# TABLE OF CONTENTS

# List of Figures

# LIST OF TABLES

# List of Equations

## INTRODUCTION

Packed beds are columns packed with material providing more surface area for separations or catalysis. In industry, packed beds are used in applications such as separators, absorbers, strippers, and reactors. In designing these units, it is important to understand the heat transfer phenomena through the packing, as some reactors require heating or cooling systems to drive or control the reaction. This is, however, difficult to predict and model within packed beds since there are multiple modes at work. Heat transfer within packed bed reactors have been studied since the 1940's. Various studies have been done since the 1940's to try to understand the heat transfer phenomena in packed beds. Research in this field is directed towards designing models of the heat transfer with a bed, perfecting experimental equipment used to measure the heat transfer in packed beds, understanding how different packing materials and the relative sizes of the packing and column affect heat transfer, and creating correlations of heat transfer parameters to predict heat transfer rates at different flow conditions. Given the variety of different models and experimental methods in the literature, there is a large amount of disagreement in correlations of heat transfer parameters.

Heat transfer parameters have been determined experimentally for both experiments using wall-heated and wall-cooled packed beds. Traditionally these two methods have been considered equivalent; however, in 1946 Leva produced two different correlations for wall-heated and wall-cooled experiments. In his results he found that wall-cooled experiments showed more effective heat transfer than wall-heated experiments. The scientific community did not believe his findings and disregarded his work. Little work has been done since in directly comparing heat transfer in heating and cooling experiments.

Much of the work performed at Worcester Polytechnic Institute by both undergraduate and graduate students has been focused on applied mathematics and modeling heat transfer in packed beds. Originally this work was done solely using a wall heated column. In 2008, the experiments were shifted to cooling due to an unavailability of steam for one of the MQP projects. The results for these experiments, however, did not show the same heat transfer parameters obtained from the previous heating data from the same column and materials. As was observed by Leva in 1946, cooling was shown to trend higher than heating. This general

trend was later found by MQP groups performing cooling experiments. Since the cooling experiments have begun, no research has directly compared heating and cooling experiments performed by the same group within the same project. The objective of this research is to conduct both heating and cooling experiments to determine whether the trends observed by Leva and research groups at Worcester Polytechnic Institute are supported. If an observable difference is found between the two types of experiments, this research hopes to provide possible explanations for this difference.

Multiple cooling and heating experiments were run using the same pilot tower that was used in previous MQP's. For cooling runs, heated air was passed through the packed bed at various flow rates while cooling water flowed through the jacket of the tower. The temperature profile of the air was measured 5 millimeters above the packing. For heating experiments, room temperature air was sent through the column at various flow rates while steam was passed through the tower jacket. The air absorbed heat and the temperature profile was measured above the packing. The collected data was run through a computer model to determine the various heat transfer parameters. These parameters were compared for both the heating and cooling experiments and used to determine the different in the heat transfer.

# Background

## Heat Transfer

Heat transfer occurs through three main mechanisms: conduction, convection, and radiation. In a packed bed, heat can be transferred in many different ways using these mechanisms. For both heating and cooling experiments, heat transfer occurs by convection when the fluid flows past the particles (Adeyanju & Manohar, 2009). The velocity of the fluid and the type of particle can affect the rate of heat transfer. Heat is also transferred by conduction between particles since they are in contact. Fourier's Law governs this type of heat transfer:

Equation 1: Fourier's Law

$$q_r = -k_r \frac{\delta T}{\delta r}$$

The type of particles and temperature gradient between the fluid and the particles determines the rate of conduction. Conduction also occurs between the particles and the tower wall. Heat transfer can occur by radiation, although this is often neglected at low temperatures.
In a cylindrical packed bed, heat is transferred in both the axial and radial directions. Convection is the dominating mechanism for heat transfer in each direction.

## Dimensionless Numbers

When modeling heat transfer in packed beds, various parameters are determined. The Reynolds number is a dimensional number used when analyzing fluid dynamics. The Reynolds number is a measure of the ratio of inertial forces to the viscous forces, and is used to characterize fluid flow as laminar or turbulent (Batchelor, 1967). Since the particle diameter and fluid viscosity/density are all constants, the Reynolds number increases proportional to the superficial velocity of the air.

Equation 2: Reynolds Number

$$Re = \frac{\rho v d_p}{\mu}$$

Where ρ is the density of the fluid, v is the fluid velocity, $d_p$ is particle diameter, and μ is the viscosity of the fluid. For this research, the Reynolds number was varied by changing the velocity of the air, since the physical properties of air are constant.

The Biot number is a ratio of the heat transfer resistances inside of and at the surface of a body. For heat transfer in a packed bed, the wall Biot number is used. This looks at the ratio of heat transfer resistance at the wall to the resistance of the particles in the bed:

**Equation 3: Biot Number**

$$Bi = \frac{h_w R}{k_r}$$

Where $h_w$ is the wall heat transfer coefficient, R is the tower's radius, and $k_r$ is the effective radial thermal conductivity. In packed bed heat transfer experiments, the Biot number is expected to decrease as the fluid flow rate increases (DeWitt, 2007).

The Peclet number is the ratio of the rate of advection to the rate of diffusion. Advection is the movement of a fluid due to its bulk motion, while diffusion is the movement of particles without requiring bulk motion. This ratio is expected to increase in packed bed heat transfer experiments, which means bulk motion is having more of an effect (Batchelor, 1967). For packed beds the radial Peclet number is generally used.

**Equation 4: Peclet Number**

$$Pe_r = \frac{\rho v c_p d_p}{k_r}$$

Where ρ is the fluid density, v is the fluid velocity, $c_p$ is fluid heat capacity, $d_p$ is the diameter of the particles, and $k_r$ is the effective radial thermal conductivity (Patankar, 1980).

The Nusselt number is the ratio of the rate of convection to the rate of conduction. As the Reynolds number increases, the rate of convection increases, which increases the Nusselt

number. In packed bed experiments, the Nusselt number at the wall of the tower is often calculated (DeWitt, 2007).

**Equation 5: Nusselt Number**

$$Nu_w = \frac{h_w R}{k_f}$$

These and other heat transfer parameters are used to analyze the heat transfer that occurs in packed beds (Dixon & van Dongeren, 1998). These parameters are found using various models. Along with these models, the experimental setup can alter the heat transfer parameters. One of the most important parameters that affects heat transfer is the tube to particle diameter ratio, N. The tower diameter can vary, along with the particle shape and size. In order to adequately study the effects of varying N, the particle size cannot solely be varied since bed scale velocity depends on N, while pellet scale mixing depends on the diameter of the particles. Therefore, Dixon and van Dongeren (1998) ran experiments with fixed N by varying both diameters and with two different values of N to compare between the two. This noticed that the effective radial thermal conductivity and values of the Nusselt number change as the tube to particle diameter ratio changes. However, these parameters do not vary as much when the tube diameter or particle diameter are changed independently.

## Experimental Techniques

In determining heat transfer parameters, experimental technique has been found to strongly impact the accuracy of results. A variety of research has been performed to determine which experimental setups and sampling techniques collect the most reliable data. As a result, there has been much controversy over which techniques provide the best representation of the heat transfer phenomena in packed beds. This has furthermore created doubt in experimental data in the literature. It is therefore necessary to discuss common approaches to heat transfer experimentation in packed beds and the advantages and disadvantages of alternative methods.

The typical experimental setup for measuring both the effective thermal conductivity, $k_r/k_f$, and wall heat transfer coefficient, $h_w$, parameters simultaneously involves a vertical column packed

with catalyst carriers, or other packing material. The column itself is composed of a heated or cooled test section downstream of a non-heated or cooled calming section. The purpose of the test section is to provide a constant temperature wall to heat or cool the bed as fluid is passed through the packing. The calming section is used to develop the velocity profile of the fluid before entering the test section to avoid entrance effects. It has been shown in heating experiments that heat is transferred via conduction from the test section into the calming section, thus preheating the fluid and changing entrance conditions ( (Dixon A. G., 1985), (Freiwald & Paterson, 1992)). It is recommended therefore that low thermal conductive materials such as nylon be used for the calming section since reliable parameters cannot be fitted for setups with metal calming sections (Dixon A. G., 1985).

In the test section, axial and radial temperature measurements are needed to fit parameters. The equipment used for such measurements has caused the most controversy, for there are advantages and disadvantages to each. Common methods include ladder frames, axial thermowells, radial thermowells imbedded in the packing and crosses or rings of thermocouples suspended above the bed ( (Thomeo, Rouiller, & Freire, 2004), (Dixon A. G., 2012 b)). A ladder frame is a ladder that supports thermocouples inside the packing at different axial and radial positions. An axial thermowell is similar, but instead of a ladder, it is a long tube inserted down the center of the bed. Radial thermowells are pushed radially through the test section at many axial positions. Borkink & Westerterp (1992a, 1992b) uses a device similar to this with a low thermal conductivity shaft.

Advantages to using embedded measuring devices are that many axial and radial positions can be measured simultaneously (Thomeo, Rouiller, & Freire, 2004). Suspended thermocouples, on the other hand, measure the radial positions above the packing, and therefore multiple packing heights are needed to obtain axial temperature profiles. Embedded devices, however, disturb the packing structure of the column, which could affect temperature profiles and measured parameters. It is also possible that conduction can occur through these devices, which alter temperature readings especially when highly conductive materials such as metals are used.

For devices that measure temperatures above the bed, there is some debate over whether these measurements are representative of temperatures inside the packing since flow patterns are expected to change after leaving the packing (Thomeo, Rouiller, & Freire, 2004). Additionally, there is controversy over the specific type of device to use, how far above the packing it should be placed, and how long it should be immersed in the test section to obtain the best results. Some authors used a cross containing thermocouples at many radial positions and replicas. Dixon (1985), for example, used an eight armed cross that could measure four angular replicas of six radial positions. Crosses with multiple arms show scatter in the temperature measurements at differing angular positions. This can be attributed to changes in airflow patterns in the heterogeneous packing. To eliminate this, some authors used a device containing concentric metal rings welded to thermocouples at different radial positions, which averaged the readings along the ring. This showed smoother temperature profiles without scatter (Kwong & Smith, 1957). Dixon (2012b) criticized this method, since important statistical information about the variability in the bed is lost. Thomeo, Rouiller, and Feire (2004) conducted a study where they compared a ring sensor to an aligned thermocouple sensor which measured two replicas of four radial positions 180 degrees apart. In this study, differences were found using the two different devices, where the ring sensors were compared to the aligned thermocouples averaged over 72 angular positions. These authors attributed the differences to the amount of area the comprising the two devices. They estimated that the ring sensor takes up 20% of the cross sectional area in the column whereas the aligned thermocouples take up less than 1%. It was theorized that sensors with greater areas alter the flow of air leaving the packing, which therefore skew the measurements obtained. They hypothesized that even point thermocouple devices with a large number of arms such as Dixon's cover approximately 19% of the area and would produce the same results as the ring sensors. These suggestions, however, are only speculations as no solid evidence was presented to support this theory.

In addition to the type of device, the material of construction has also been shown to be significant in obtaining good results. Dixon (1985) was the first to show that materials with low thermal conductivity were necessary in preventing conduction from the wall through the

thermocouple cross. In comparing a metal cross with a nylon cross, he showed that length effects for estimated parameters were less significant using the nylon cross. Freiwald and Patterson (1992) confirmed the need for low thermal conductive materials. They compared measurements of $k_r$ with a metal cross and a low conductivity cross to the Zehner and Bauer correlation as an unbiased source, since the equipment used in establishing this correlation was different. It was found that the low conductivity cross was in good agreement with the correlation and that the measurements made with the metal cross gave $k_r$ values that were much higher.

While the main criticism of suspended sensors is that temperature readings above the bed may not be representative of the inside, there has been little agreement as to how far above the packing the cross should be placed. Dixon and van Dongeren (1998) typically used 3-5 millimeters. Freiwald and Paterson (1992) argued that the best position should be directly on the packing, since that should best reflect phenomena in the bed. Dixon, however, obtained scattered results if the thermocouples touched the surface of the packing. Thomeo, Rouiller, and Feire (2004) conducted a study where they found the most optimal position to be five millimeters. This, however, was recommended taking into account a restraining screen they used at the bed's surface to prevent fluidization of the bed. Positions closer than five millimeters appeared to decrease the measured temperature, for heat was conducted from the metal screen to the cooling wall.

An additional experiment performed by Freiwald and Patterson (1992) was to determine the appropriate immersion time of the thermocouple cross in the column when taking measurements. This is important because conduction through the cross can still occur even for materials with a low thermal conductivity. For this experiment a two-hour immersion time was compared with 0.75 minutes. It was found that there were differences between the two and that the shorter time was more comparable to the Zehner and Bauer correlation. The differences were greater at low Reynolds numbers but became less significant at higher flow rates. This showed that conducted heat is removed when the air is at a higher flow rate. To find an optimal immersion time, temperature readings were taken overtime at a low Reynolds

number, with the hope of observing an obvious point in the curve where a steady temperature was met before conduction effects started to occur. This point was not observed and it was concluded that there was a large relaxation time for the thermocouples and that conduction starts occurring before a steady state is reached. With these results, Freiwald and Patterson (1992) developed a temperature recovery model to find the correct temperature; however, the process is quite tedious.

Another area of difficulty in temperature measurements has been the entrance temperature. In the literature the inlet temperature has been measured using a radial thermocouple at z=0, the point where the test section meets the calming section with the assumption that the entrance temperature profile is flat. For this technique, however, conduction was found to occur radially through the thermocouples. Since preheating in the calming section was found to occur, some measurements were taken before the calming section and the warm up in the calming section was incorporated into the model (Dixon A. G., 1985). Another idea developed by Borkink and Westerterp (1992a) was to use an entrance temperature above z=0 and to fit it as a parabolic profile. This technique was found to eliminate length effects. Thomeo, Rouiller, and Feire (2004), however, argued that this method would lose information in an important region for estimating parameters. Dixon (2012a) also found that using the first bed height as the inlet temperature profile eliminated length effects by eliminating pre-heating in the calming section.

The only mentionable difference in heating and cooling in literature was observed by Leva in the 1940s and 1950s. Leva ( (1947), (1950)) found different correlations for the overall Nusselt number varied between heating and cooling. The columns used had a diameter of less than three inches and the temperatures in the beds were measured using a thermometer a fraction of an inch above the packing. When plotting the Reynolds number against the overall Nusselt number, Leva found different trends for heating versus cooling. Also Leva based the Nusselt number off of the tube diameter, not the particle number. For the newer research, the wall Nusselt number is usually found. The correlation between the overall and wall Nusselt number is:

Equation 6: Overall Wall Nusselt Number

$$\frac{1}{Nu_o} = \frac{1}{Nu_w} + \frac{N/6}{\frac{k_r}{k_f}} * \frac{Bi+3}{Bi+4}$$

Leva found for heating when the $D_p/D_T$ ratio is less than 0.35:

Equation 7: Heating Leva Nusselt Number

$$Nu_o = 0.813 * \exp\left(-6\frac{D_p}{D_T}\right) * Re^{0.9}$$

Leva found for cooling when the $D_p/D_T$ ratio is less than 0.35:

Equation 8: Cooling Leva Nusselt Number

$$Nu_o = 3.50 * \exp\left(-4.6\frac{D_p}{D_T}\right) * Re^{0.7}$$

## MODELING

When modeling heat transfer in a packed bed, heat transfer can be thought to occur in one or two dimensions. One dimension only examines heat transfer in the axial direction, so therefore an average temperature is used for all radial positions (Dixon & van Dongeren, 1998). This average is found using the mean-cup average and by using this and the wall temperature, the overall heat-transfer coefficient, U, coefficient can be found.

The problem with assuming an average temperature across the bed is that the true radial mean temperature can vary significantly from this value (de Wasch & Froment, 1972). This resulted in the development of a two dimensional model which allows for temperature changes in both the axial and radial direction (Dixon & van Dongeren, 1998). Another reason the one-dimensional model is not often used is because the value of U can be easily found from two-dimensional model using the following correlation (Borkink & Westerterp, 1992 b):

Equation 9: Overall Heat Transfer

$$\frac{1}{U} = \frac{1}{h_w} + \frac{N}{\beta k_r}$$

Where U is defined as the overall heat-transfer coefficient, $h_w$ is the wall heat-transfer coefficient, N is the ratio of the tube diameter to the particle diameter, $k_r$ is the effective radial heat conductivity, and β is a lump parameter that combines all the other heat transfer parameters. In order to find the value of β, the above equation can be fitted with the experimentally found values for the other parameters. The Borkink and Westerterp (1992a) study found that a value of 7.4 is the best-fit value for β.

For situations where there is a negligible temperature difference between the bulk fluid phase and the packing material, a pseudo-homogenous model is assumed (Wen & Ding, 2006). This allows for the packing and the air to be considered to be a homogenous medium, which makes modeling easier since the packing of the material does not need to be modeled. This is assumed to be the case for most steady state systems that have no reaction taking place (Dixon A. G., 2012 b). For systems where a reaction or dynamic changes are occurring, it is necessary to use a heterogeneous model.

The velocity profile of the gas can be modeled in two common ways, with a constant unidirectional plug flow model or with a radial dependence model (Winterberg, Tsotsas, Krischke, & Vortmeyer, 2000). Using the plug flow model accounts for the axial convection of heat in the packing (Dixon A. G., 2012 a). However, this model also results in a constant effective radial thermal conductivity, $k_r$, which lumps together all the mechanisms for radial heat transfer (Dixon A. G., 2012 b). Since a sharp decrease in conductivity has been observed at the column wall, a wall heat-transfer coefficient, $h_w$, was introduced. This accounts for the observed temperature jump at the wall, resulting from a thin film of air that greatly increases the resistance to heat transfer.

Using a radial dependence of velocity allows the model to account for changes resulting from channeling effects and differences in the packing material (Borkink & Westerterp, 1992 b). This consequently yields a radial thermal conductivity that is dependent on radial position, $k_r(r)$. Since the conductivity is not assumed to be constant and allowed to vary, this eliminates the need for $h_w$ by using the boundary condition of $T=T_w$ in conjunction with the $k_r(r)$ model (Winterberg, Tsotsas, Krischke, & Vortmeyer, 2000). For experimental set-ups that use a low

ratio of tube diameter to particle diameter, N, this effect is more important, since it makes up a larger percentage of the bed. However, this requires the bed porosity to be known in order to derive a velocity profile, so for simplicity a plug flow model was used for this research.

For some experiments, it has been observed that the parameters $h_w$ and $k_r$ vary with increasing bed heights ( (Dixon A. G., 2012 b), (Borkink & Westerterp, 1992 b)). Specifically, it was found that $k_r$ would decrease with increasing bed length reaching an asymptotic value, as well as $h_w$, but to a lesser degree. It is generally agreed that to obtain good results, length effects must be eliminated. It was first proposed that length effects were a result of not including the axial dispersion term into the model. This led to the development of the Axially Dispersed Plug Flow Two-dimensional Model, ADPF2D, which includes three parameters, $k_r$, $h_w$ and $k_a$. While this addition did remove length effects, reproducible values for this parameter could not be obtained ( (Freiwald & Paterson, 1992), (Dixon A. G., 1985)). In later experimentation, difficulties were found in measuring inlet temperature. In order to eliminate these length effects, the correct inlet temperature must be used. It was found that assuming a radially flat inlet profile results in lengths effects. These length effects were eliminated by assuming a parabolic profile. Also, Dixon (1985) found that heat loss in the calming section also led to length effects. By using the first bed height as the inlet temperature profile length, effects because of pre-heating or heat loss in the calming section were eliminated. In addition to heat losses in the calming sections, assuming the first bed height as the initial temperature profile eliminates any heat loss due to conduction of the metal grates in the calming section (Thomeo, Rouiller, & Freire, 2004). These metal grates are used to hold the calming section particle in the calming section and to keep the bed particles out of the calming section.

When studying heat transfer in a packed bed, choices must be made in terms of modeling the heat transfer. These choices effect what parameters are found and different assumptions in modeling can result in some errors being more significant. For this research, Dixon's Generalized Initial Profile Plug Flow, GIPPF, model was used, which includes the following assumptions: two dimensional, steady state, no reaction, constant physical properties, plug flow velocity, no pressure drop, constant wall temperature, pseudo-homogenous, no axial

dispersion of heat, no free convection of heat, and no radiation. To model heat transfer with these assumptions, first an energy balance is on a disc shaped region on the tower is performed to give the following equation (Dixon A. G., 2012 a):

**Equation 10: Axial Heat Transfer Equation**

$$0 = -\frac{1}{r}\frac{\delta}{\delta r}(rq_r) - \frac{\delta q_z}{\delta z}$$

It is assumed the velocity field is unidirectional in the axial direction, constant, and accounts for axial convection of heat. This allows all other heat transfer to be lumped into an effective conduction terms, $k_r$ and $k_a$ that are constant and follow Fourier's law. For the model used in this research:

**Equation 11: Fourier's Law**

$$q_r = -k_r\frac{\delta T}{\delta r}$$

$$q_z = v\rho c_p(T - T_{ref})$$

Since our model neglects axial conduction compared to convection the following formula is found by plugging the above equations into equation 10:

**Equation 12: Modified Axial Heat Transfer Equation**

$$v\rho c_p\frac{\delta T}{\delta z} = k_r\frac{1}{r}\frac{\delta}{\delta r}(r\frac{\delta T}{\delta r}) = k_r(\frac{\delta^2 T}{\delta r^2} + \frac{1}{r}\frac{\delta T}{\delta r})$$

Since the column is assumed to be axisymmetric, the temperature gradient at the center of the bed is zero. Then to account for the temperature increase found at the column wall, the wall heat transfer coefficient, $h_w$, which used in conjunction with the observed temperature at the wall yields:

**Equation 13: Boundary Condition at the Wall**

$$-k_r\frac{\delta T}{\delta r}_R = h_W(T_R - T_W)$$

To make the following equations dimensionless the following parameters were defined:

Equation 14: Dimensionless Parameters

$$y = \frac{r}{R}$$

$$x = \frac{z}{R}$$

$$\Theta = \frac{T - T_w}{T_o - T_W}$$

The resulting dimensionless equation is found:

Equation 15: Dimensionless Equation

$$\frac{\delta\Theta}{\delta x} = \frac{k_r}{v\rho c_p R}\left(\frac{\delta^2\Theta}{\delta y^2} + \frac{1}{y}\frac{\delta\Theta}{\delta y}\right)$$

With the following boundary conditions:

Equation 16: Boundary Conditions

$$\frac{\delta\Theta}{\delta y} = 0 \quad at\ y = 0$$

$$\frac{\delta\Theta}{\delta y} + \frac{h_w R}{k_r}\Theta = 0 \quad at\ y = 1$$

The solution is found using separation of variables for partial differential variables, which is beyond the scope of this paper so the final result, will be given:

Equation 17: GIPPF Model

$$\Theta(y,x) = 2\sum_{i=1}^{\infty}\frac{\lambda_i^2 J_o(\lambda_{ij})}{\{J_o(\lambda_{ij})\}^2}\exp\left(\frac{-\lambda_i^2(x - x_o)}{Pe_r\frac{R}{d_p}}\right)x\int_0^1 \Theta_o(y)J_o\,(\lambda_{ij})ydy$$

Dixon termed this model the generalized initial profile plug flow, GIPPF, model. The initial dimensionless profile, $\Theta_o(y)$, is taken to be the initial bed height. This initial profile is found by taking the measured data and fitting a cubic spline interpolation to it. Unlike other models, this creates a generalized profile and not one that is restricted to a certain geometry. Once the model was derived, computer software was used in order obtain the desired heat transfer parameters.

## History of Cooling Experiments at Worcester Polytechnic Institute

The two most recent studies at Worcester Polytechnic Institute that examined cooling in packed beds were Alexander, Ledwith, and Linskey (2011) and Ashman, Rybak, and Skene (2009). These two groups have found systematic differences in cooling and heating experiments, where cooling trended higher than heating when comparing their own data to heating data from the same column taken in the 1990s.

The first relevant MQP group that conducted cooling studies in the packed bed columns was the Ashman et al. (2009). Ashman et al. (2009) examined a variety of packing materials in the two-inch and four-inch column for applications in steam reforming technology. Heat transfer parameters were calculated using the Inlet Profile Plug Flow, IPPF, model, which varies slightly from the GIPPF model used in this research, in that the inlet profile is assumed to be parabolic and is not interpolated. To collect data, Ashman et al. (2009) used Procedure B, which is defined in the Methods section as the procedure where all Reynolds numbers are collected at one bed height per day.

For the group's raschig ring study, they found their experimental data for effective conductivity correlated very well with Borkink (Borkink, Borman, & Westerterp, 1993), an author in the literature who has done extensive studies on wall-cooled packed beds. Ashman et al. (2009) also conducted some experiments with one half-inch ceramic spheres in the four-inch column making a tube to particle ratio of eight and compared the results to heating experiments performed in the same column with the same packing by former studies, van Dongeren (1998) and Pollica (1996). The cooling data from Ashman et al. (2009) showed a much higher trend for effective conductivity compared to both studies, suggesting that cooling experiments provide

more effective heat transfer than heating experiments. For the Nusselt number, the intercept of the tread line was higher than the other two studies, however, the slope was identical to Pollica (1996) and smaller than van Dongeren (1998). It should be noted again that this parameter is very scattered and linear least squared fit lines are highly influenced by this scatter, making it difficult to compare correlations. The proximity of the data was comparable across the three studies.

Alexander et al. (2011) used raschig rings in the two-inch and four-inch columns to attempt to resolve discrepancies found between heating and cooling from past experiments at WPI such as in the Ashman et al. (2009) half-inch spheres study. In contrast to Ashman et al (2009) and past work on the column, experiments were conducted so that one Reynolds number was run for one day at all bed heights, which is defined as Procedure A in the Methods section. This was done so that changes in the day-to-day air would not skew temperature profiles, as they claimed to observe nonsensical trends using Ashman et al. (2009) and other previous researcher's collection method. Alexander et al. (2011) made another alteration to the methodology by multiplying the calculated Reynolds number by 1.2 to correct for air expansion as it was passed through the heater.

Alexander et al. (2011) compared the rashig ring results in the four-inch column to Ashman et al. (2009) and Borkink (1992 a). In comparing these results, Alexander et al. (2011) multiplied the Reynolds numbers of Ashman et al. (2009) by 1.2 as was done in their own experiments. The resulting graph illustrated that their data agreed better with Borkink (1992 a) than with Ashman et al. (2009) and attributed that to the difference in experimental procedures, A and B. The data from the Ashman et al. (2009) study was slightly lower than the other two. This is in contrast to the Ashman et al. (2009) finding that the group agreed well with Borkink et al, (1993) before the additional 1.2 factor in the Reynolds number. Also, the claim that the method of collection would account for differences observed appears unsupported. Other than showing strange temperature profiles using Procedure B, no evidence is shown which would imply that a different correlation would be generated by the two procedures. Furthermore, Ashman et al. (2009) did not find any problems with temperature profiles using Procedure B. For the Nusselt

number, Alexander et al. (2011) found that both their study and Ashman et al. (2009) showed a much higher trend in the data than Borkink. The data was comparable up to a Reynolds number of about 200, but then departed from the values found by Borkink. These differences were considered to be a result of the different equipment used between the column and Borkink's, particularly the placement of the thermocouple nearest to the wall, which would affect near wall parameters such as the Nusselt.

Alexander et al. (2011) results in the two-inch column were compared to Ashman et al.'s cooling experiments and the heating data from Dixon (1997). They found that the effective conductivity compared very well to Dixon (1997) and Alexander et al. (2011) data were both higher than Ashman et al. (2009) for that parameter. Again, the 1.2 factor on the Reynolds number influenced the results to appear shifted so that the data is comparable. For the Nusselt number, all three sets of data were comparable, because of scatter in the data; however, the cooling studies were slightly higher than the Dixon (1997) heating.

# METHODOLOGY

## EQUIPMENT

The column used had a two-inch inner diameter and an inner height 18 $^{5}/_{8}$ inches. This column consisted of two concentric brass tubes with differing diameters. The tubes were welded together with a brass circular plate on the top and bottom. The space left between the two tubes allowed cooling water or steam to pass through to either cool or heat the column walls. The column was placed on top of a nylon calming section. Nylon was used because it has a very low thermal conductivity, which minimizes heat transfer from the air or column. This reduces any preheating or cooling of the air. There were four screws that attached the column and the calming section together. The calming section was filled with ¼-inch steel spheres. The purpose of the calming section was to allow the airflow to become uniform before entering the packed bed. Additionally, insulation was used on the column for heating experiments.

To collect temperatures, three thermocouples were placed throughout the walls of the column, five in the calming section, and twenty-five on a cross that was inserted into the column. The thermocouple cross has six thermocouples across in eight angular positions with an addition thermocouple in the center, to see a drawing of the cross please see Figure 1. The cross was inserted into the column and placed five millimeters above the packing. The temperature readings were collected using ExceLINX, which will be discussed later.

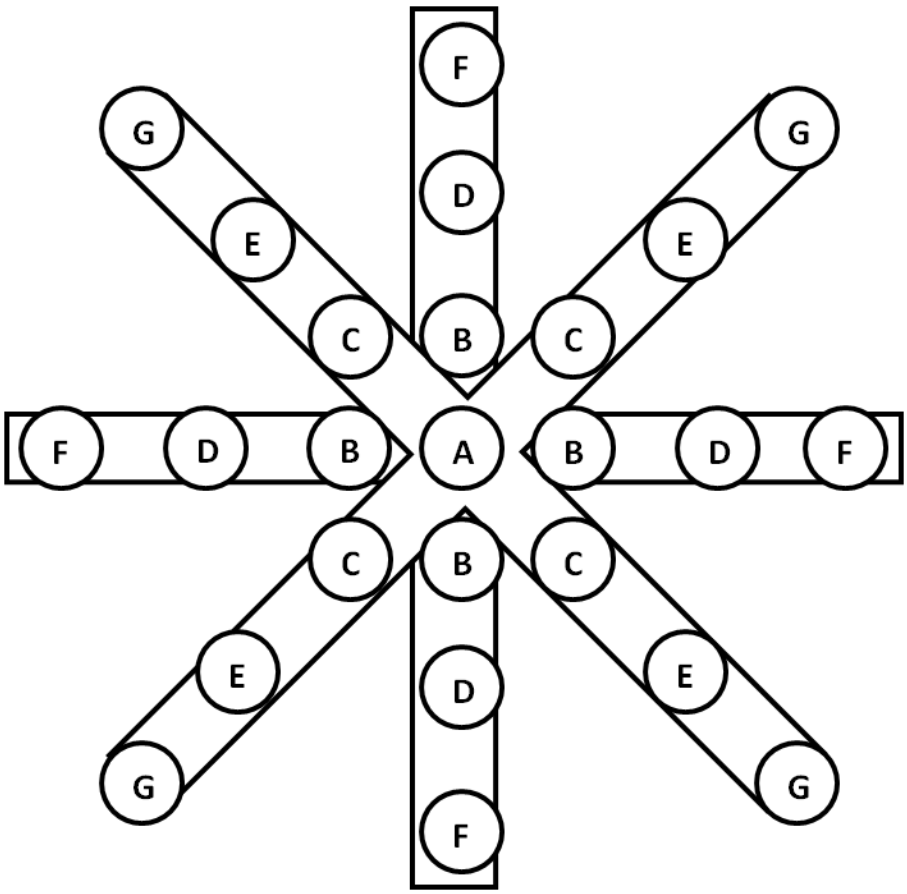


Figure 1: Diagram of Thermocouple Cross

For both heating and cooling experiments, air was passed upwards through a packed bed, which was either cooled with water or heated with steam. For cooling, air was passed through an AV1, an air filter, AV 2, a rotameter and a heater before entering the calming section. Cooling water passed through WV 1, WV 2, and a rotameter before entering the tower. To see a diagram for the cooling setup, please refer to Figure 2. For the initial set-up, the water flow was countercurrent, with the air entering the bottom of the column and water entering the top of column.

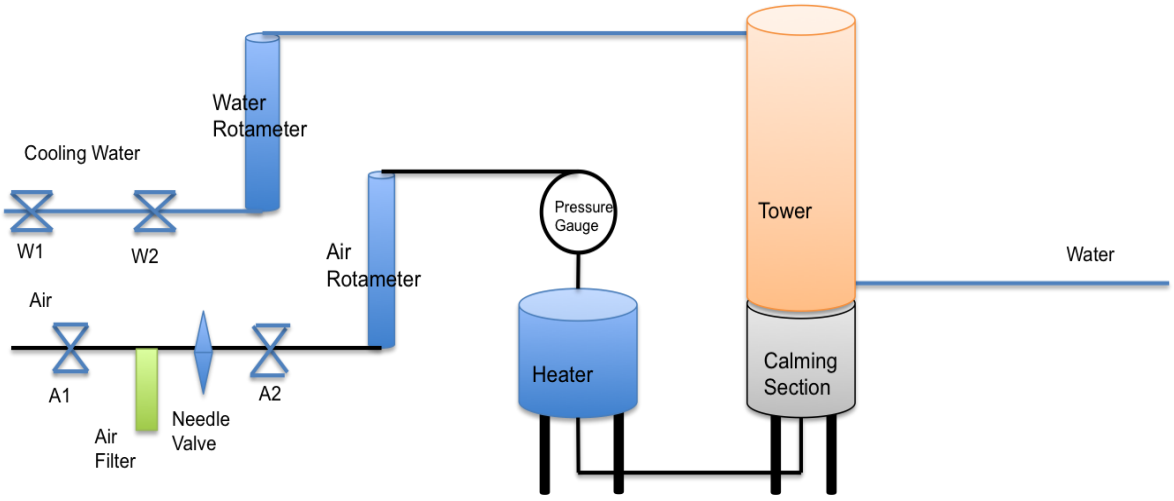


Figure 2: Cooling Setup Sketch

For heating experiments, steam passed through S1, a steam regulator, S2 and into the jacket of the column. When the steam condensed on the tower, it could drain from the bottom while vapor rose out through a tube and into a condenser. The cooling water entered W1, W2, and then a rotameter before entering the condenser. The air was passed through AV1, an air filter, AV 2, a rotameter and a heater before entering the calming section. For heating experiments the heater was not turned on. To see the set up for heating, please refer to Figure 3.

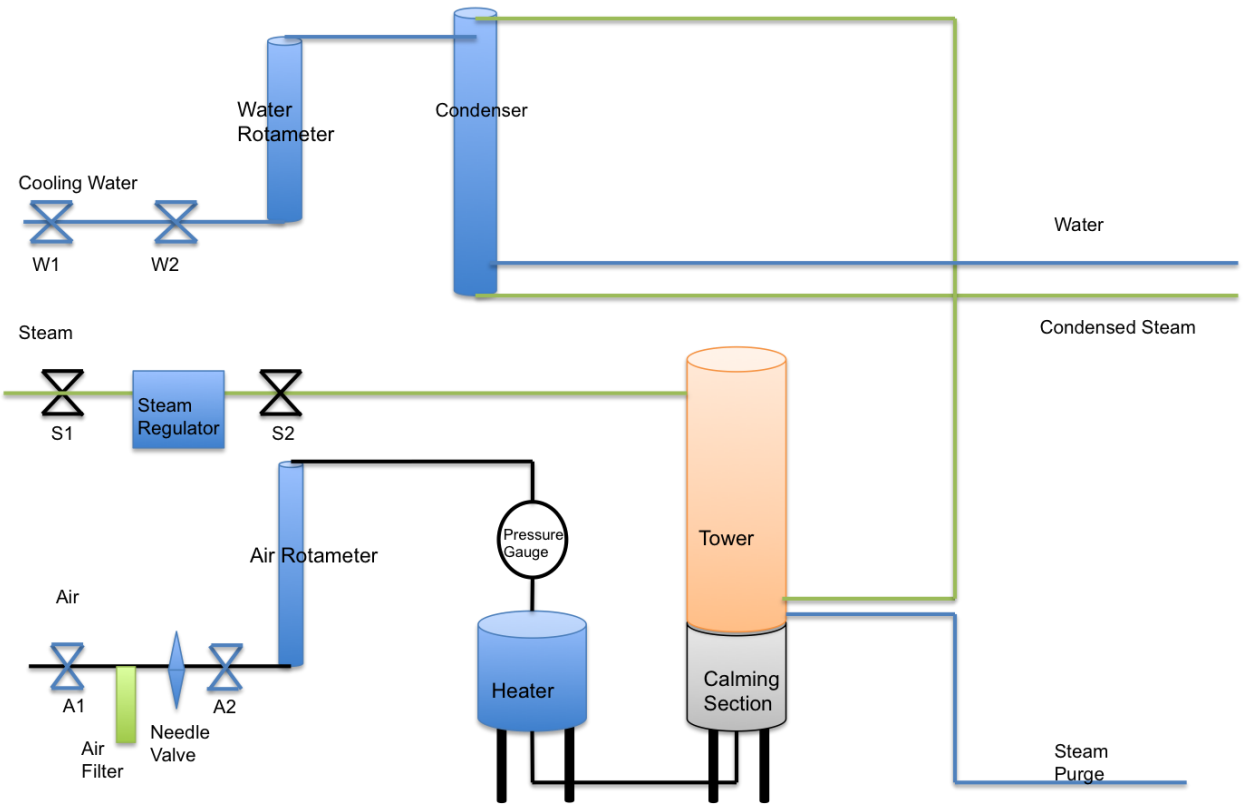


Figure 3: Heating Setup Sketch

After several cooling runs, it was observed that during most of the cooling runs the wall temperature varied by 1°C and for some runs a difference up to 5°C was seen. To see the detailed wall temperatures, please refer to Appendices L-M. The column was originally set up to operate in a countercurrent configuration, with air flowing up through the bed and water flowing down the jacket. In an attempt to get more uniform wall temperatures, the water flow was increased after two runs. Higher flow could potentially result in more uniform temperatures. However, this also did not fix the non-uniformity in the wall temperatures. After one more run, it was considered that in countercurrent operation the water was not completely covering the inside jacket, which may result in hot spots and non-uniform wall temperatures.

In a second attempt to fix the wall temperatures, the column was switched to a co-current operation, with both the air and water entering the bottom of the column. It was believed that the water would be forced up through the column and would completely cover the outside. After running ten runs in co-current configuration, the problem of non-uniform wall

temperatures was still observed. For comparison, the column was switched back to countercurrent configuration and ten similar Reynolds numbers were tested. After reviewing previous research, it was found that the problem of non-uniform wall temperatures was evident in previous experiments using a countercurrent operation.

During the early cooling runs, it was noticed that the temperature of inlet air decreased due to heat loss in the calming section. Therefore, several runs were conducted with the calming section removed. The thought was that the air was losing heat in the calming section, so it was removed for several runs. However temperatures in the bed were still lower than the inlet air, so the calming section was put back on. The calming section is important since it establishes the velocity profile for the bed, so the two runs conducted without it were not used for the research.

### LAB SAFETY

The main safety concern for both heating and cooling experiments was the high temperatures. In performing experiments, touching hot objects was avoided. These objects included the heater, any metal near the heater, the steam lines, and the column jacket when operating with steam. Protective heat gloves and eye protection were worn when working with steam. In addition, general lab safety was practiced. This included wearing long pants with closed toe shoes and tying back long hair.

To prevent damage to the equipment during cooling experiments, the flow-rate of air for cooling experiments did not exceed 55% or drop below 25% for the air rotameter. At flow rates below the lower boundary, there was not enough air to absorb heat from the heater, causing it to overheat. At flow rates above 55%, the particles fluidized, which could cause damage to the thermocouple cross.

## PROCEDURE A

The column was packed with ¼-inch ceramic particles at bed heights of four, six, eight, and ten inches (Alexander, Ledwith, & Linskey, 2011). Since it was previously found that changes in day to day air quality affects temperature readings for cooling experiments each day a different

Reynolds number was run at all bed heights to attain physically reasonable temperature profiles per Reynolds number.

To begin the experimental run, the packing from the previous experiment was removed from the column. This was done by unscrewing the column from the calming section and carefully moving the column over a box to collect the packing. The column was then reattached to the calming section. Since the column was insulated for heating runs and the screws were obstructed, the column was tipped over and the packing was poured out into the container. Care was taken not to put tension on thermocouple wires.

As it was being added, the packing was compressed several times using a metal to ensure a tight packing arrangement. The thermocouple cross was adjusted so that the tips of the thermocouples would be five millimeters above the surface of the packing. The cooling water or steam was run through the wall of the column. The cooling water was operated at maximum flow. The air filter was first purged to remove any collected moisture. After the air was purged, AV2 was opened to run air through the column. A needle valve was used to adjust the flow rate of the air. For cooling experiments, a heater was used to raise the air temperature to about 95 °C. A Keithley Series 20007 Datalogger was used with the ExceLINX add on to measure the radial temperature profile of the air measured by thermocouple cross.

After startup, the column was run for two hours to ensure steady state was reached before data collection. The rotameter, air gages, steam/water gages, and heated gage were read and recorded at this point. Data collection was then stopped, the cross was rotated $45^{o}$ and a new sheet was made in Excel. After ten minutes, the same measurements were taken. For cooling experiments the heater was shut off and air was run through for a period of time to decrease the temperature of the heater, then the air was turned off and the airline was purged of collected water. The bed was then raised to the next height, taking care to pack the bed. After initial set up, steady state was achieved in one hour instead of two. This procedure was repeated for bed heights of eight inches and ten inches. After the final experimental run was completed, the air, cooling water/steam, and heater were shut off and the data was saved. For cooling experiments air was run through the heater for ten minutes after the heater had been

shut off to ensure that it did not overheat. For heating experiments, room temperature air was run through the column after the steam had been turned off to help cool down the packing and the column.

### PROCEDURE B

In addition to the procedure described above, it was also desired to perform the experiment using the procedure used in past research at WPI. For this method, one bed height was used per day for all Reynolds numbers. To begin the experiment, the column was packed as described previously to the desired bed height, four, six, eight, or ten inches. The startup procedures for both cooling and heating runs were the same as described previously, setting the air flow to the first Reynolds number. After startup, the column was run for two hours to ensure steady state was reached before data collection. The rotameter, air gages, steam/water gages, and heated gage were read and recorded at this point. Data collection was then stopped, the cross was rotated $45^{o}$ and a new sheet was made in Excel to record the rotated position of data. The same measurements were taken and the data collection was allowed to run until reaching about row 70 on the excel sheet. After stopping the data collection, the air line and stream condensate line were purged of collected water and the air flow was set to the next Reynolds number. From this point, about an hour or at least 500 rows were allowed for the column to reach the next steady state and the steps described above were repeated. Shutdown procedure was the same as described previously.

### DATA COLLECTION

The temperature data was acquired using thermocouples placed in the column and collected using a Keithley Series 20007 Datalogger. The Datalogger was capable of collecting data from 200 channels at a time, but this experiment only utilized 34 of them. The data was recorded using a Microsoft Excel add-in called ExceLINX. In order to do this, go to Excel, click on Tools → 'Add In' and select 'ExceLINX.xla'. ExceLINX was then available in the dropdown menu bar in Excel.

#### EXCELINX

Since ExceLINX uses macros, it was highly suggested to turn the security settings for macros off. This ensured that the program was able to run correctly every time. In order to start collecting

data the ExceLINX first had to be configured. To do this, a blank Excel spreadsheet was opened and Select ExceLINX→ 'Create' → 'DMM Config' was clicked.

In order for the Keithley instrument to be configured correctly the following selections were made:

In the drop down menu, 'Device' Ke2700_COM1 was selected and MM7700 was selected for both 'Slot 1 Module' and 'Slot 2 Module'. The drop down for 'Front Panel Lockout' should be 'off'. The remaining dropdowns were left as their defaults.

Below the drop down menus, there is a section titled Channel Scan List. Under the first column 'Channel', the 'List' was set as '101-120, 201-214' to make sure all of the data from the channels in use was being collected. Under the column labeled 'Measurement' under the 'Function' drop down 'TEMP' was selected. Without selecting this option, the wrong data would be collected and that run would be useless. Under the 'Range' dropdown, 'K' was selected and under 'Options' the 'Opt 1' dropdown 'INT' was selected, as illustrated in Figure 4.

ExceLINX — KEITHLEY — A Greater Measure of Confidence

**Task: Configure Scanning DMM Channels**

| | | |
|---|---|---|
| Task | Name | DMM Config |
| | Description | |
| | Created By | kjudge |
| | Company | Worcester Polytechnic Institute |
| | Date Created | 1/29/13 |
| | Date Modified | 1/29/13 |
| | Status/Cmds | Task stopped successfully |
| Instrument | Device | KE2700_COM1 |
| | Password | |
| | Slot 1 Module | M7700 |
| | Slot 2 Module | M7700 |
| | Slot 3 Module | |
| | Slot 4 Module | |
| | Slot 5 Module | |
| | Front Panel Lockout | On |
| Setup | Line Sync | Off |
| | Autozero | On |
| | Display Digits | 5½ |
| | DCV Input Divider | Off |
| | Open TC Detection | On |
| | Temp Scale | °C |
| Limits | Digital Outputs | Off |
| | Pulse Output | Off |
| | Polarity | High |
| | Duration | 0.02 sec |
| | Master Latch | Off |

**Channel Scan List**

| Channel | | | Measurement | | Scaling | | | | | Alarm Limits | | | | | | Rep Filter | | Sampling | | Options | | | |
|---|---|---|---|---|---|---|---|---|---|---|---|---|---|---|---|---|---|---|---|---|---|---|---|
| Enb | List | Tag | Function | Range | Rel | Math | m/reb | b | U | En1 | Hi1 | Lo1 | En2 | Hi2 | Lo2 | Enb | Count | Rate | AC BW | Opt 1 | Opt 2 | Opt 3 | Opt 4 |
| On | 101-120,201-214 | | TEMP | K | Off | None | | | | Off | | | Off | | | Off | | SLOW | | INT | | | |

Figure 4: DMM Configuration Setup

After the correct selections had been made, the ‘start’ option was selected from the status/commands menu. The enter key must be hit to register the selection and to start the configuration of the Datalogger.

After the Datalogger was configured, a new tab was selected in the spreadsheet and ExceLINX→ ‘Create’→ ‘DMM Scan’ was selected from the toolbar. Data for different runs was stored in the same spreadsheet by opening different scan tabs for each run. To ensure the data was collected properly, only one scan was run at a time.

To properly set up the data sheet the following options were chosen:

For the ‘Reading Count’ dropdown ‘INF’ was selected. This changed the number of data points to infinite to ensure the data was collected until steady state is achieved. Under the dropdowns for ‘Add Channel Tags’ and ‘Add Channels’, yes was selected. The update interval should be 100msec and all other options were left at their default, as illustrated in Figure 5.

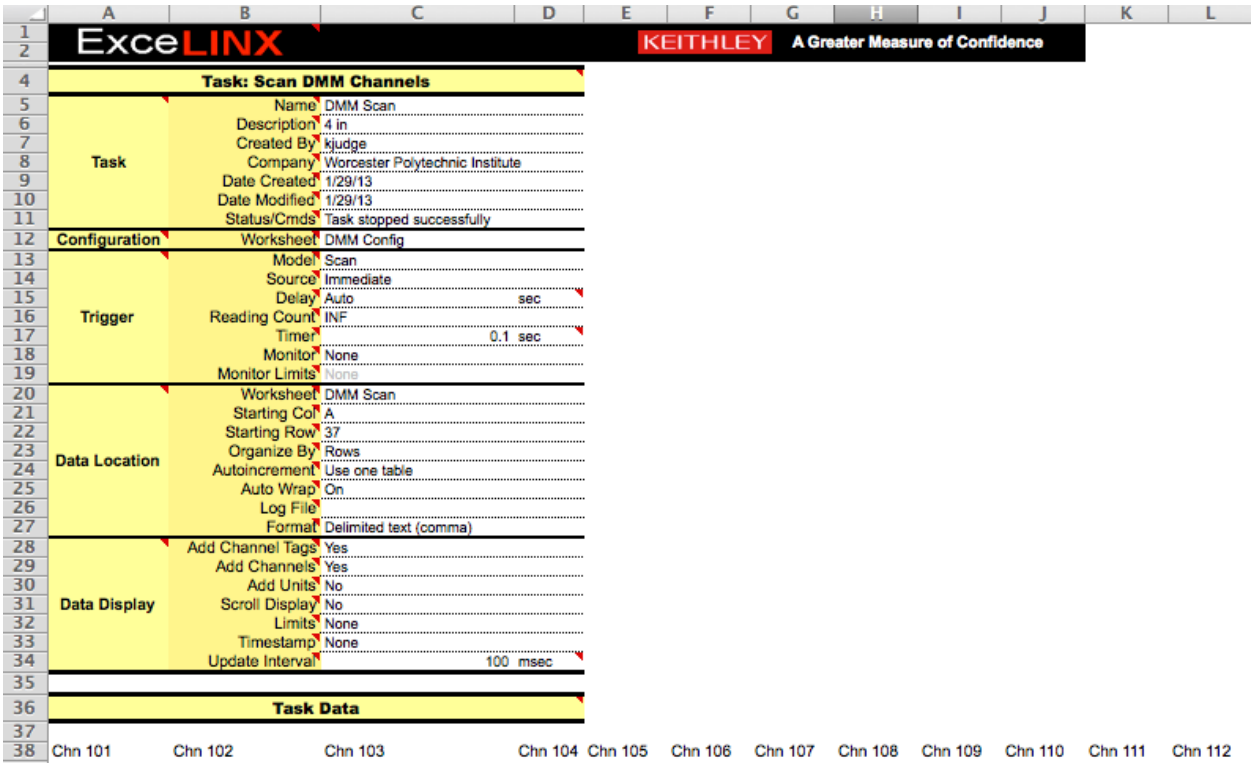

ExceLINX KEITHLEY A Greater Measure of Confidence

| Task: Scan DMM Channels | | | |
|---|---|---|---|
| Task | Name | DMM Scan | |
| | Description | 4 in | |
| | Created By | kjudge | |
| | Company | Worcester Polytechnic Institute | |
| | Date Created | 1/29/13 | |
| | Date Modified | 1/29/13 | |
| | Status/Cmds | Task stopped successfully | |
| Configuration | Worksheet | DMM Config | |
| Trigger | Mode | Scan | |
| | Source | Immediate | |
| | Delay | Auto | sec |
| | Reading Count | INF | |
| | Timer | 0.1 | sec |
| | Monitor | None | |
| | Monitor Limits | None | |
| Data Location | Worksheet | DMM Scan | |
| | Starting Col | A | |
| | Starting Row | 37 | |
| | Organize By | Rows | |
| | Autoincrement | Use one table | |
| | Auto Wrap | On | |
| | Log File | | |
| | Format | Delimited text (comma) | |
| Data Display | Add Channel Tags | Yes | |
| | Add Channels | Yes | |
| | Add Units | No | |
| | Scroll Display | No | |
| | Limits | None | |
| | Timestamp | None | |
| | Update Interval | 100 | msec |

Task Data

| Chn 101 | Chn 102 | Chn 103 | Chn 104 | Chn 105 | Chn 106 | Chn 107 | Chn 108 | Chn 109 | Chn 110 | Chn 111 | Chn 112 |
|---|---|---|---|---|---|---|---|---|---|---|---|

Figure 5: DMM Scan Setup

After the column set up was complete, the heater was turned on for cooling experiments and the thermocouple cross was put in the proper position, 'Start' was selected from the Status/Commands menu. In order to start the data collection, the enter key had to be hit. To stop data collection, the stop command was selected and the enter key hit at the same time.

## Data Analysis

Once the data was collected it was analyzed in two ways. First, dimensionless graphs were made. This was done to ensure that the profiles made physical sense and followed the expected trends. The second way used a FORTRAN program in Microsoft Developer Studio that fit heat transfer parameters to the data.

### Reynolds Number

The Reynolds Number had to be calculated from the measure flow rate measurements. The maximum flow rate was determined using a data table. The maximum flow rate was calculated by the specific rotameter in the lab as well as the air pressure. A higher pressure would result in a lower maximum flow rate. The flow rate in Standard Cubic Feet per Minute (SCFM) was found:

Equation 18: Air Flow Calculation

$$SCFM = (Air\ \%)(MAX)\frac{(14.7 + PRESSURE)}{14.7}$$

This value was then converted to the superficial velocity using the cross sectional area of our column.

Equation 19: Superficial Velocity Calculation

$$v = \frac{SCFM}{\pi(.083)^2}\frac{1\ min}{60\ sec}$$

This velocity was multiplied by the particle diameter (ft) and air density, and then divided by the viscosity of the air.

Equation 20: Reynolds Number Calculation

$$Re = \frac{(.0023769)(.02083)v}{.000000394}$$

### Dimensionless Temperature Plots

After the data was collected the dimensionless temperature was plotted against the dimensionless radial position. The dimensionless temperature was defined as:

**Equation 21: Dimensionless Temperature**

$$\theta = \frac{T - T_w}{T_o - T_w}$$

The dimensionless radial position was defined as:

**Equation 22: Dimensionless Radial Position**

$$y = r/R$$

To make the graphs, lines approximately ten rows from the bottom were copied and pasted from the ExceLINX Data sheets into a pre-made Excel spreadsheet. It was important that these lines were chosen from the data obtained during steady state, or else the resulting parameters would be incorrect. This spreadsheet was labeled to identify which column correlated to which thermocouple. All of the temperatures for one thermocouple position were then averaged together. This was done for the zero degree and the forty-five degree thermocouple cross rotation. This average was used as the temperature for that radial position. The wall temperature for the dimensionless equation was found by averaging the three wall thermocouples. The plots were created by taking this temperature profile for all four bed heights and plotting them on the same graph.

### Data Files for GIPPF Program

In order to analyze the data, it had to be entered in a certain format that the program could read. This was done by entering the information in the following format and saving the test file with a .cdat extension in Notepad:

**Table 1: GIPPF Format**

| | | | | | | |
|---|---|---|---|---|---|---|
| Number of Profiles | Number of Radial Positions | Number of Wall Readings | Number of Angles | | | |
| Column Diameter | Particle Diameter | | | | | |
| Radius 1 | Radius 2 | Radius 3 | Radius 4 | R5 | R6 | R7 |
| Reynolds Number | Bed Depth | Angle of Rotation | | | | |
| Inlet Temperature | | | | | | |
| R1 TC1 | -1 | -1 | -1 | | | |
| R2 TC 1 | R2 TC 2 | R2 TC 3 | R2 TC 4 | | | |
| R3 TC 1 | R3 TC 2 | R3 TC 3 | R3 TC 4 | | | |
| R4 TC 1 | R4 TC 2 | R4 TC 3 | R4 TC 4 | | | |
| R5 TC 1 | R5 TC 2 | R5 TC 3 | R5 TC 4 | | | |
| R6 TC 1 | R6 TC 2 | R6 TC 3 | R6 TC 4 | | | |
| R7 TC 1 | R7 TC 2 | R7 TC 3 | R7 TC 4 | | | |
| Wall TC 1 | Wall TC 2 | Wall TC | | | | |
| -1 | -1 | -1 | | | | |

When including the center thermocouple at radius r=0, since there was only one thermocouple reading, -1 was inserted for the remaining thermocouple positions. Once all of the profiles were entered in this format, a new line of -1 -1 -1 had to be entered to in order for the computer program to recognize the end of the file being analyzed. Also the temperatures are in degrees Celsius to two decimal points and the lengths in millimeters. To run the program the following steps were taken:

1. Open Microsoft Developer Studio
2. Open the workplace “GIPPF_FIT.for” found under the Working folder
3. Click on Build → Click on All
4. Click on Build on Bui GIPPF_FIT.exe
5. The following screen appears (See Figure 6)
6. Input the file name including the extension and hit enter

7. Enter the range of Reynolds number to be analyzed. One Reynolds number can be analyzed at a time and the model requires a symmetric input with the actual value between the two extremes (Example Min=410, Max=414, actual Re=412)

8. Enter the bed depths to be analyzed. To analyze all input 0.0 for minimum and 1000.0 for the maximum.

9. Enter a guess for Peclet number ($Pe_r$) and the Biot number (Bi). Starting guesses of 5.0 and 10.0 respectively generally give results. Name output will an extension of .res

10. Run analysis

11. After the analysis is complete the file can be opened and temperature profiles may be viewed.

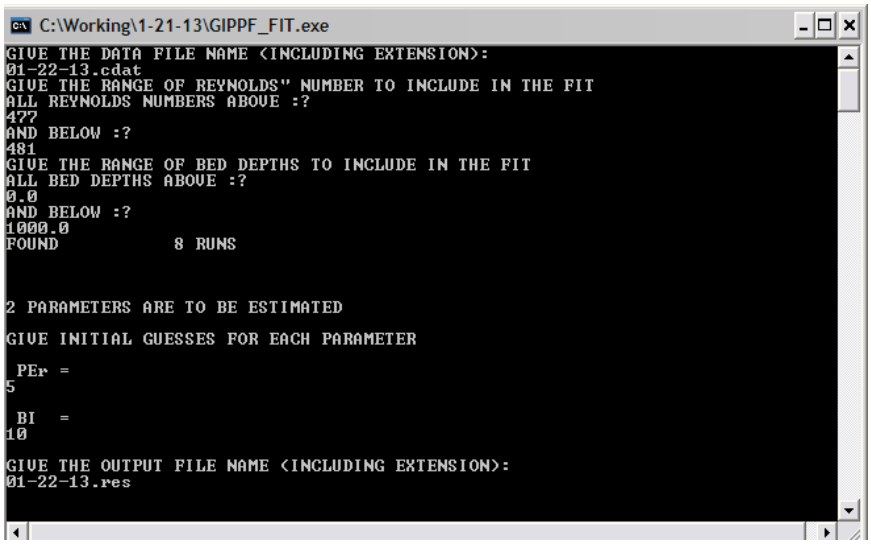


Figure 6: Screen Before Building the GIPPF Model

After the run was completed, the results were opened in Notepad. The program used the first bed depth as the inlet, so results for three heights are given. For these three heights, the dimensionless radial position and the correlating dimensionless temperature were given. For the heat transfer parameters the Peclet number, Biot number, $K_r/K_f$, and Nusselt number were given, along with a 95% confidence interval and F-test critical values for that interval. From this information, graphs were made comparing the heat transfer parameters with the Reynolds number to determine the patterns. These patterns were then compared to observed patterns in literature.

## Results and Discussion

Both heating and cooling experiments were performed using both Procedure A and Procedure B. For Procedure A the bed height was varied during a given day and the air flow remained constant. For Procedure B the air flow was varied during a given day with the bed height remaining constant. For cooling experiments using Procedure A, co-current and countercurrent flows were utilized to compare differences in maintaining a constant wall temperature. Results obtained from heating and cooling experiments were compared to sources in the literature as well as data taken from the same laboratory in past MQP and graduate studies. Recommendations were made to improve the representation of the inlet profile in the GIPPF model and an evaluation was made to determine the most reliable procedure.

## Procedure A

### Cooling Results

Cooling water was run through the cooling jacket of the column in both co-current and countercurrent configurations. The error bars on the graphs represent 95% confidence intervals. These error bars illustrate that out of all possible data points for each of these Reynolds numbers, ninety-five percent will fall within that confidence interval. Since the effective thermal conductivity and Nusselt numbers are the most relevant to the discussion of heat transfer in the bed they will be presented and discussed. Correlations for the Biot and Peclet numbers with respect to Reynolds number can be found in Appendix O.

#### *Countercurrent Cooling*

A typical dimensionless temperature profile using the countercurrent water flow is shown in Figure 7. This graph shows expected trends in temperature, where at increasing radial distance the temperature in the bed approaches the wall temperature in a parabolic trend, shown by lower values of the dimensionless temperature. Also as expected, increases in bed height also show values that are closer to the wall temperature. Temperature profile graphs for the rest of the data collected can be viewed in Appendix C.

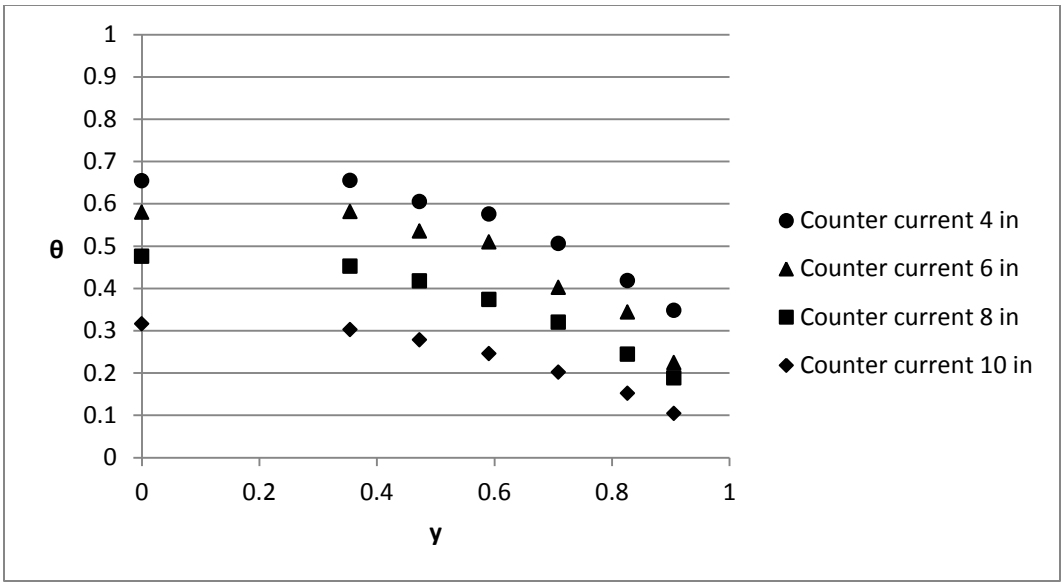


Figure 7: Dimensional Temperature Profile for Countercurrent Cooling (Re = 420)

Once it was clear our temperature profiles made physical sense, the data could be analyzed. For countercurrent cooling, it was found that there was a good correlation between the effective thermal conductivity and Reynolds number, as shown in Figure 8. The intercept, which represents the effective thermal conductivity in a stagnant fluid, is expected to range between 8 and 10 for ceramic spheres (Dixon & van Dongeren, 1998). For this research an intercept of 11.051 was observed. This shows our data is reasonable and fits into expected literature values. The data fits a general linear trend, although there are a few points that deviate from this trend.

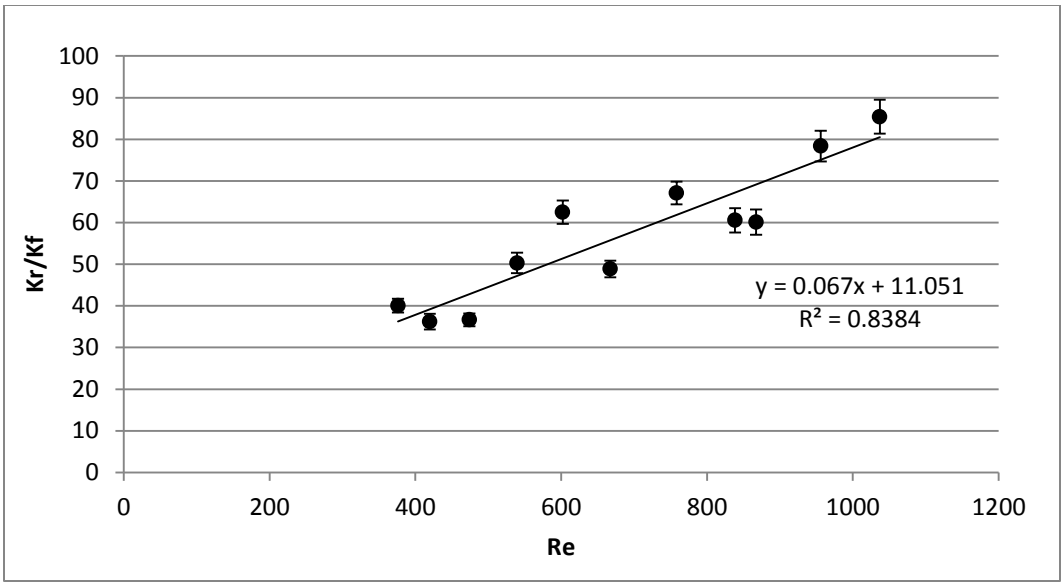


Figure 8: Effective Thermal Conductivity versus Reynolds Number for Countercurrent Cooling

Nusselt number versus the Reynolds is illustrated in Figure 9 below. As with the effective thermal conductivity, the intercept represents heat transfer at the wall for stagnant fluid conditions. The data does not show as strong of a linear trend as was observed for the effective thermal conductivity. This is expected however since the Nusselt number is known to have more variability.

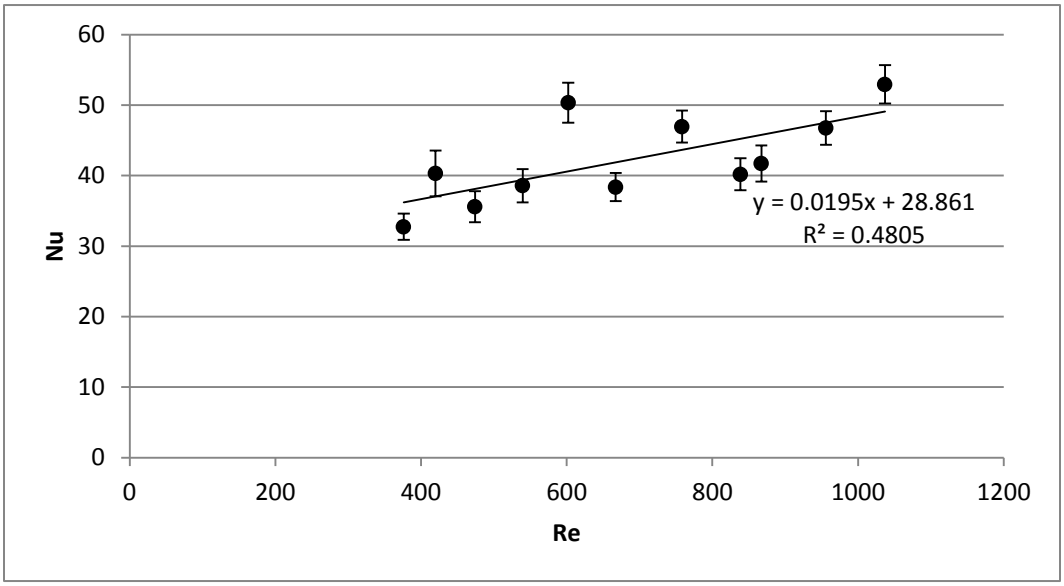


Figure 9: Nusselt Number versus Reynolds for Countercurrent Cooling

### *Co-Current Cooling*

A typical co-current dimensionless temperature profile is shown in Figure 10. As with the countercurrent flow, the trends seen in the data also make physical sense. The profiles for the rest of the data can be found in Appendix D.

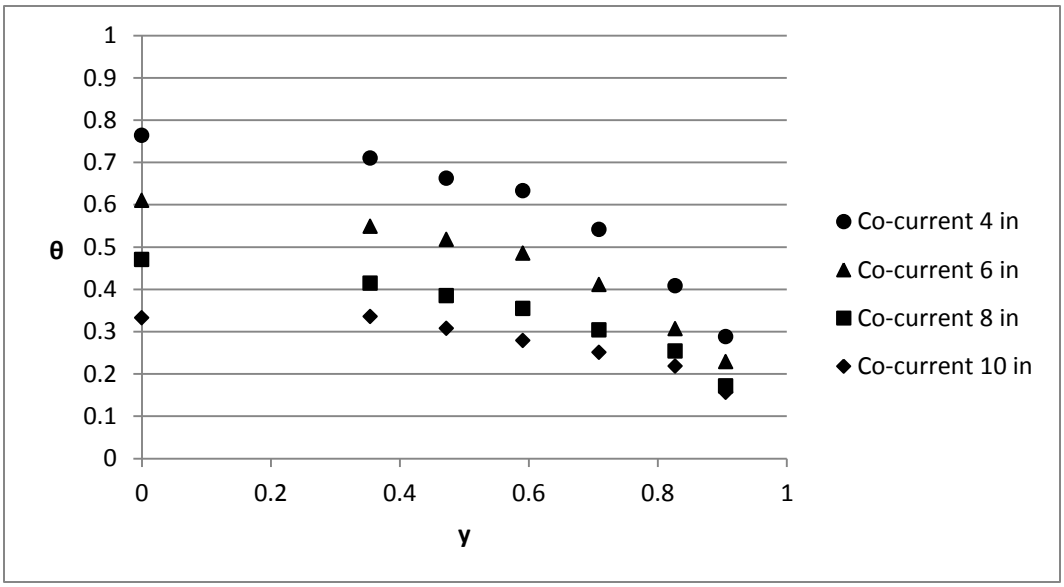


Figure 10: Dimensionless Radial Temperature Profile for Co-Current Cooling

Once again, once the dimensionless profiles showed our data made physical sense, it could be analyzed. For co-current cooling, it was found that there was a weaker correlation between the effective thermal conductivity and Reynolds number, as shown in Figure 11. The intercept was observed to be 25.8, which falls well outside the expected range of 8 and 10. The linear trend observed for this data has a weaker linear trend than for the countercurrent cooling.

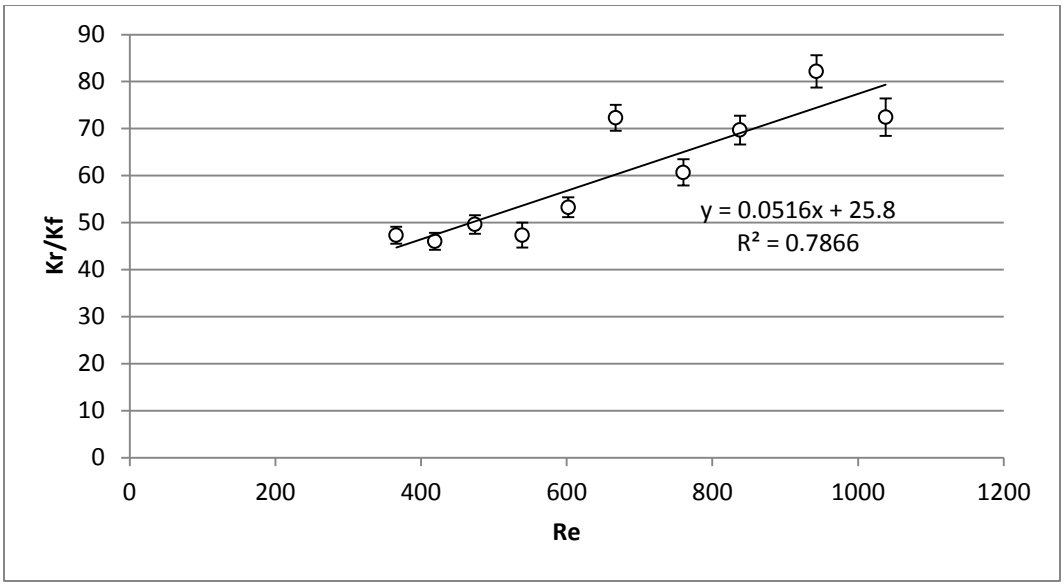


Figure 11: Effective Thermal Conductivity versus Reynolds Number for Co-Current Cooling

Figure 12 below illustrates the correlation of the dimensionless Nusselt number to the Reynolds number for co-current cooling. This graph shows almost no linear relationship between Nusselt number and the Reynolds number.

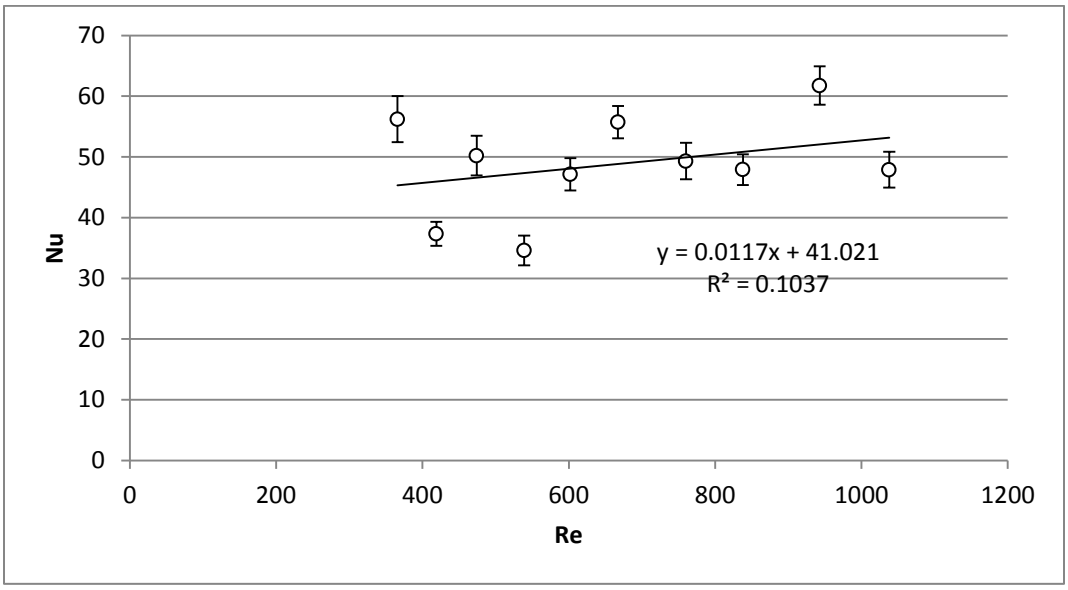


Figure 12: Nusselt Number versus Reynolds for Co-Current Cooling

### *Co-Current versus Countercurrent Operation*

The heat transfer parameters for both co-current and countercurrent cooling were graphed together for comparisons to see if any significant differences could be observed between the

two configurations. When the effective thermal conductivity was graphed, it was found that there was little difference between the co-current and countercurrent data. There was no observable pattern of countercurrent or co-current being higher, except for the three lowest points. These seem to skew the general linear trend for co-current being higher.

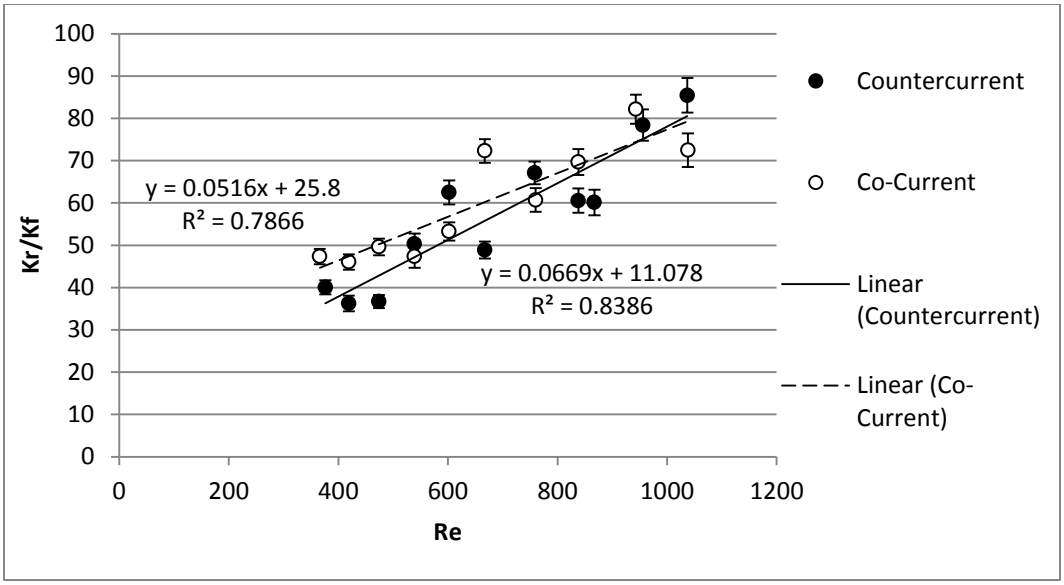


Figure 13: Effective Thermal Conductivity for Co-Current and Countercurrent

This suggests that co-current removes more heat from the column, which is generally supported by the temperature profiles illustrated in Figure 14. To see all of the comparisons, refer to Appendix E. The lower values for dimensionless temperature show co-current has lower bed temperatures than countercurrent. Another possible explanation for this finding could be the initial larger driving force in the colder water entering at the bottom of the column. However, the results are not distinct enough to draw a definite conclusion.

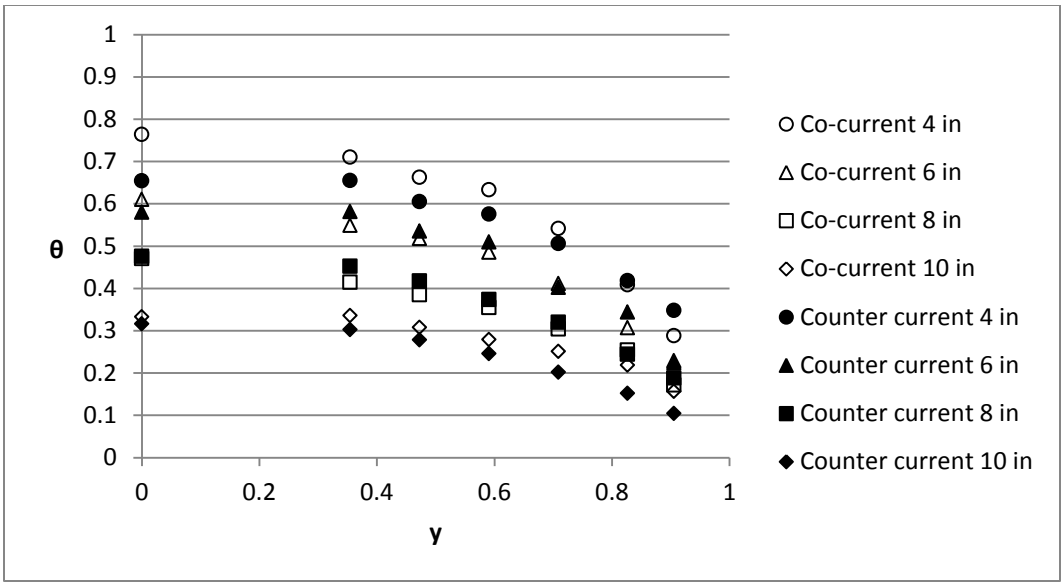


Figure 14: Dimensionless Temperature Graph for Co-Current (Re=420) and Countercurrent (Re=420)

This may be a result of varying wall temperatures, which can be seen in Table 2.

Table 2: Wall Temperatures for Re = 420

| Bed Height | Countercurrent (11/30/12) | | | Co-Current (11/14/12) | | |
|---|---|---|---|---|---|---|
| | TC 1 | TC 2 | TC 3 | TC 1 | TC 2 | TC 3 |
| **4 in, 0** | 12.510 | 12.750 | 13.431 | 11.072 | 12.015 | 11.894 |
| **4 in, 45** | 12.452 | 12.720 | 13.407 | 11.003 | 11.923 | 11.761 |
| **6 in, 0** | 10.003 | 10.313 | 11.009 | 11.414 | 12.356 | 12.396 |
| **6 in, 45** | 9.490 | 9.903 | 10.652 | 12.211 | 13.158 | 13.335 |
| **8 in, 0** | 8.343 | 8.818 | 10.293 | 12.762 | 13.797 | 14.047 |
| **8 in, 45** | 8.653 | 8.902 | 10.209 | 13.270 | 14.282 | 14.864 |
| **10 in, 0** | 9.081 | 9.538 | 10.917 | 13.594 | 14.790 | 15.191 |
| **10 in, 45** | 9.467 | 10.003 | 11.322 | 13.768 | 14.967 | 15.425 |

When comparing the Nusselt number, more scatter in the data is observed than the effective thermal conductivity, which is to be expected. For the Nusselt number, co-current has a more apparent higher linear trend.

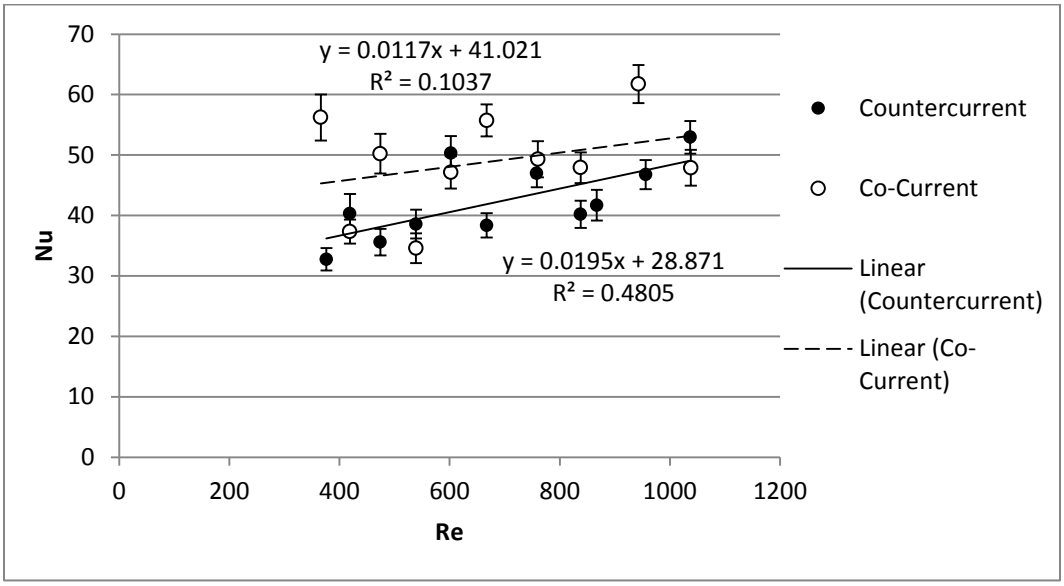


Figure 15: Nusselt Number versus Reynolds Number for Co-Current and Countercurrent

After comparing the resulting parameters, it was found that the data was comparable when accounting for scatter; however, countercurrent was chosen as the better method because there was less scatter found when using that configuration. Also the purpose of running co-current operation was to attempt to create more uniform temperatures, which did not occur. To see this please refer to Table 2. Since all the past experiments used the countercurrent configuration, this research will use the countercurrent data for cooling to eliminate variables during comparison to past data.

### *Wall Temperature Sensitivity*

Since the GIPPF assumes uniform wall temperatures, the effect of non-uniform wall temperatures was studied. To determine the effect of the non-uniform wall temperature on cooling experiments, the computer model was run using the highest and lowest temperature values of the three wall temperatures. The model was first run with the highest value of the wall temperatures inputted for each respective bed height and Reynolds number and then again with the lowest wall temperatures.

The resulting parameters effective thermal conductivity and Nusselt number are shown in Figures 16 and 17 below. The Peclet and Biot number plots can be found in Appendix O.

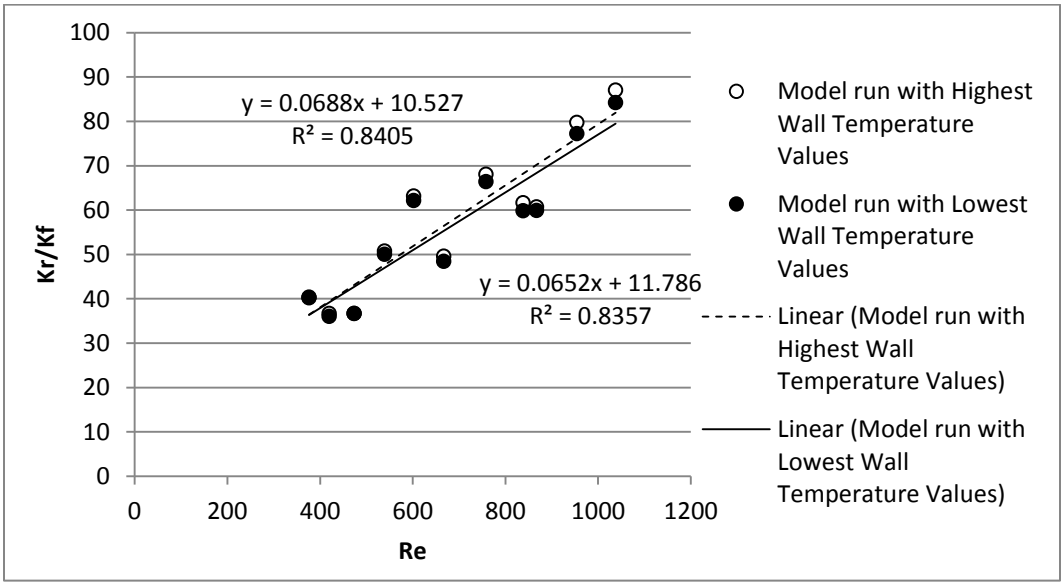


Figure 16: Effective Thermal Conductivity for High and Low Wall Temperatures for Countercurrent Cooling

As can be seen from the figure above, the effective thermal conductivity is not significantly affected by changing the wall temperature thermocouple readings.

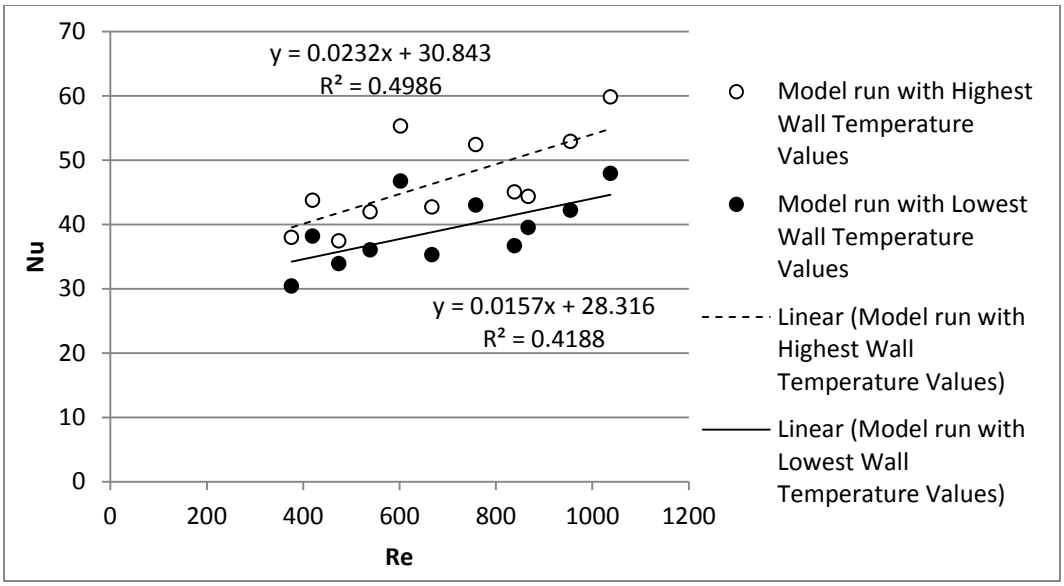


Figure 17: Nusselt for High and Low Wall Temperatures for Countercurrent Cooling

The high wall temperature generates a greater Nusselt number than the low wall temperature. For the higher wall temperature there is a small difference in temperature, using the rate of heat transfer equation below:

Equation 23: Rate of Heat Transfer

$$q_r = h_W(T_R - T_W)$$

Therefore, when the wall temperature is lower there is a higher estimate of the wall heat transfer coefficient. This result suggests that the differences in temperature along the walls of the column could be contributing to the scatter in this parameter observed for the cooling data. Since the differences in temperature along the column vary from run to run, this could alter the value of the Nusselt number at each Reynolds number creating scatter.

### *Cooling Comparisons*

To verify that the cooling results were consistent with data taken in the past from the same column and that the results were reasonable with respect to the literature, data was compared to the Ashman et al. (2009) MQP group and the Borkink and Westerterp (1992b) paper. The results could not be compared to the Alexander et al. (2011) MQP, since different packing was used.

The major differences between experimentation from this study and the Ashman et al. (2009) were column and particle diameter sizes and the use of the center thermocouple reading in the present model. The Ashman et al. (2009) used a four-inch column, whereas this study used a two-inch column. The Ashman et al. (2009) study also used ceramics spheres with a diameter of one half inch. However, since the tube to particle diameter ratio is the same as in this study, the cooling results can be compared. Lastly, this study also introduced the center thermocouple reading to the GIPPF model, which was not included in the IPPF model used by the Ashman et al. (2009). Figure 18 below shows the compared cooling results for $k_r/k_f$ from the Ashman et al. (2009) and this study.

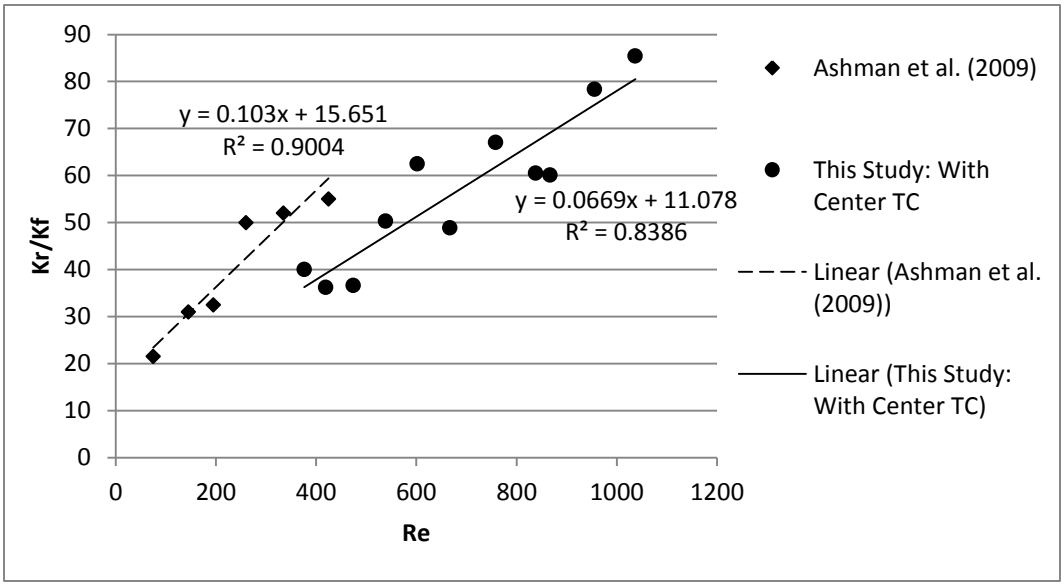


**Figure 18: Effective Conductivity Comparison of Countercurrent Cooling in Two-Inch Tube with 1/4-Inch Ceramic Spheres with the Ashman et al. (2009) Study in Four-Inch Column with 1/2-Inch Ceramic Spheres**

It can be concluded from the figure that the slope for Ashman et al. (2009) is higher than the results found in this study. Because the larger diameter of the column created air flow limitations, Ashman et al. (2009) was only able to measure a low set of Reynolds numbers. It is possible that the data in this study would be comparable to Ashman et al. (2009) in the 75-200 range; however, the data set as a whole is higher. Some differences can be attributed to the differences between experiments mentioned, the most significant of these being the addition of the center thermocouple for this study. As will be discussed further in a later section, the addition of the center thermocouple shifted the entire data set down by a significant amount,

which could help to account for the difference seen in Figure 18. Figure 19 below shows the comparison of the model without the center thermocouple with Ashman et al. (2009) data.

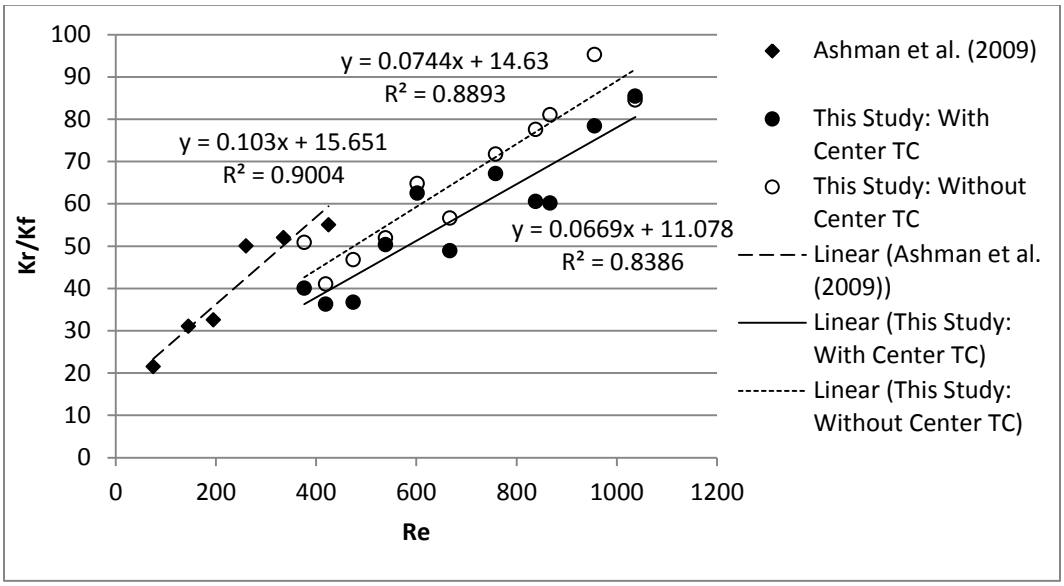


**Figure 19: Comparison of Effective Thermal Conductivity for Countercurrent Cooling for Both Models with and Without the Center Thermocouple to the Ashman et al. (2009) Study in Four-Inch Column with 1/2-Inch Ceramic Spheres**

The data sets are more comparable. Some differences remain in the slopes of the lines, but this could be because of the narrow set of Reynolds numbers used in the Ashman et al. (2009) study and the other minor alterations in experimentation.

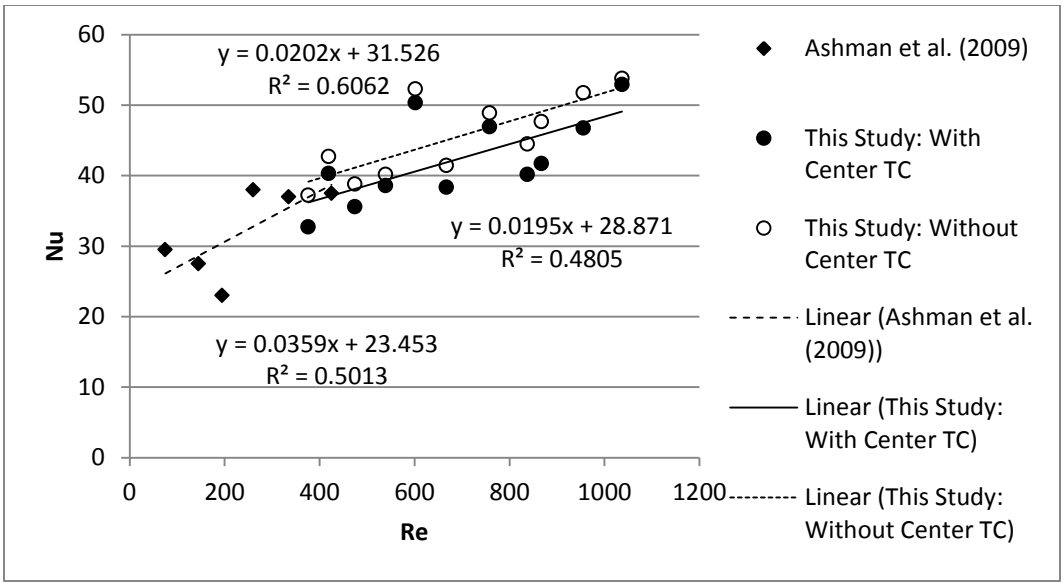


**Figure 20: Nusselt Number Comparison of countercurrent cooling with the Ashman et al. (2009) study in four inch column with 1/2 inch ceramic spheres**

For the Nusselt number, there are again differences between this study and the Ashman et al. (2009). These differences are less apparent when comparing to the model that excludes the center thermocouple. Since the Nusselt number is a more scattered parameter, many points are important in establishing a reliable trend. The small window of data collected and few points could be a key factor in differences seen between this study and Ashman et al. (2009).

Results from this study were also compared to the literature. Figure 21 below shows the results for countercurrent cooling data for $k_r/k_f$ against the Borkink and Westerterp (1992b) correlation for 7.2 mm glass spheres.

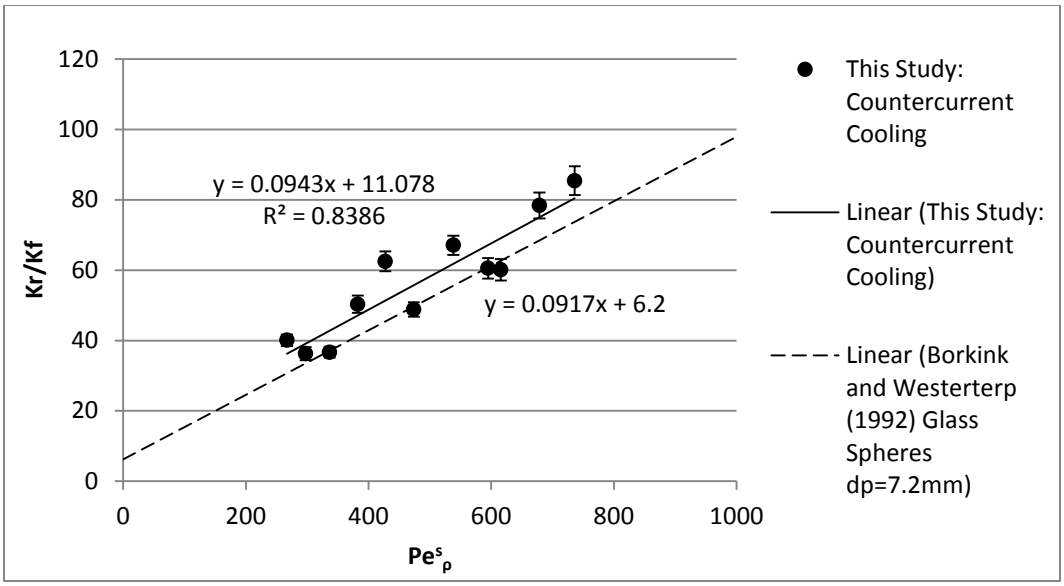


**Figure 21: Countercurrent Cooling Data from This Study in Comparison to the Borkink and Westerterp (1992b) Correlation for 7.2 mm Glass Spheres**

As illustrated in Figure 21, the experimental data from this study matches the Borkink and Westerterp (1992b) correlation reasonably well. The linear trend line for this study has a similar trend, although it trends slightly higher. Ceramic has a higher conductivity than glass, so the higher trend is expected and it can be seen that the experimental data from this study is in good agreement with the Borkink and Westerterp (1992b) correlation.

The comparison with the Borkink and Westerterp (1992b) correlation for the Nusselt number is shown in Figure 22 below.

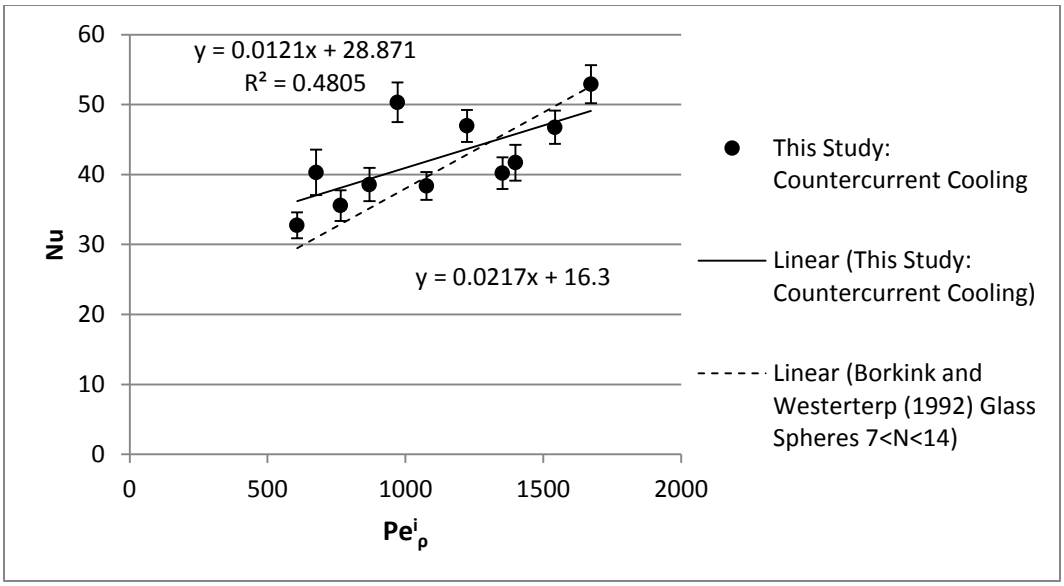


**Figure 22: Countercurrent Cooling Data from This Study in Comparison to the Borkink and Westerterp (1992b) Correlation for Glass Spheres**

It can be seen from Figure 22, that the measurements taken in this study are comparable in proximity to the Borkink and Westerterp (1992b) correlation. The least squares fit for the data in this study shows a different correlation; however, the data is so scattered that the trend line is very sensitive and easily influenced by points that may not be accurate.

From these comparative studies, it was determined that the collected data from this study are comparable to literature and differences between past cooling experiments can be explained by changes implemented by this study.

### HEATING RESULTS

The effective thermal conductivity, $k_r/k_f$, versus Reynolds number graph is shown in Figure 23 below. There is a strong linear correlation in the data. The intercept was a value of 13.819, which is reasonably close to the literature range of 8 to 10. The outlier shown in Figure 23 was removed from the data set contributing to the trendline since the F-value ratio from that data point was high at a value of 7.86, showing the model did not fit the data well. This point is represented as an unfilled triangle.

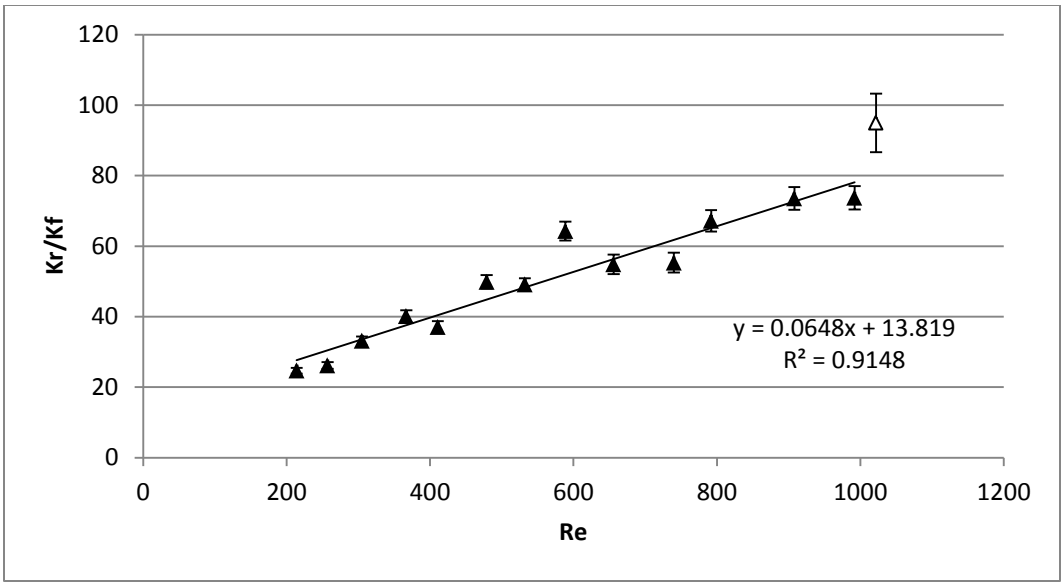


Figure 23: Effective Thermal Conductivity versus Reynolds Number for Heating

The Nusselt number for the heating data shows a reasonable linear trend, as shown in Figure 24. The outliers are again shown as open triangles. The same 1022 Reynolds number was removed for the same reasons as in the Figure 24. The 586 Reynolds number was removed for being more than twice the standard deviation of the Nusselt number from the correlation, as is discussed in a later section.

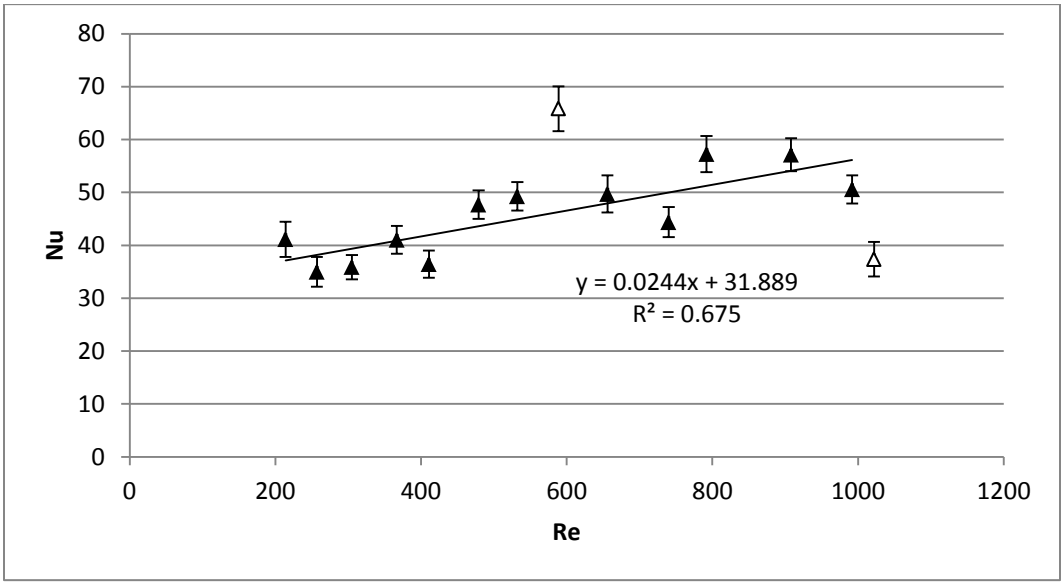


Figure 24: Nusselt Number verses Reynolds Number for Heating

### *HEATING COMPARISONS*

This experiment has been the first experiment since Pollica (1996) that has examined heating in the lab at Worcester Polytechnic Institute. The current research revisited heating to see if similar trends were observed as were found in previous research. In order to compare our research to past research, the tube to particle diameter ratio, N, and particle shape needed to be the same. The research conducted by Chubb (1991), Pollica (1996), and van Dongeren (1998) met these requirements, so they will be the focus of our comparisons.

Even with the same packing and tube to particle ratio, each of the past researches used a different model to analyze their data. Chubb (1991) used the Axially Dispersed Plug Flow, ADPF, model which included axial dispersion of heat and is the least comparable to our GIPPF model. However the difference is not enough to exclude it from comparison. Pollica (1996) used both a Wall Cooled Plug Flow, WCPF, model that included the wall temperature in the model and an Inlet Profile Plug Flow, IPPF, model that assumed a parabolic inlet profile. Van Dongeren (1998) assumed a Wall Cooled, WC, model that included the wall temperature. The model that most closely resembles the GIPPF model is the IPPF model, the main difference being for the GIPPF model the initial dimensionless profile is found by using a cubic spline interpolation to the measured data. Despite the differences in each model used by the other studies, the resulting data can be compared as long as the slight differences are considered. In order to compare the data more clearly, the current research will be compared to the Pollica (1996) and van Dongeren (1998) research and then all the research will be plotted together.

Since Pollica (1996) used the two models, which most closely resembled the model used in this research, their results will be compared first. The only data available for comparison was the effective thermal conductivity, $k_r/k_f$, and the Nusselt number, Nu. When comparing $k_r/k_f$, it can be seen that for Reynolds numbers under 600, there is a good comparison between the current research and Pollica (1996). However for higher Reynolds numbers, Pollica (1996) did not have any data. However if the trend is extended, it appears the current research is more scattered and has several points that are higher.

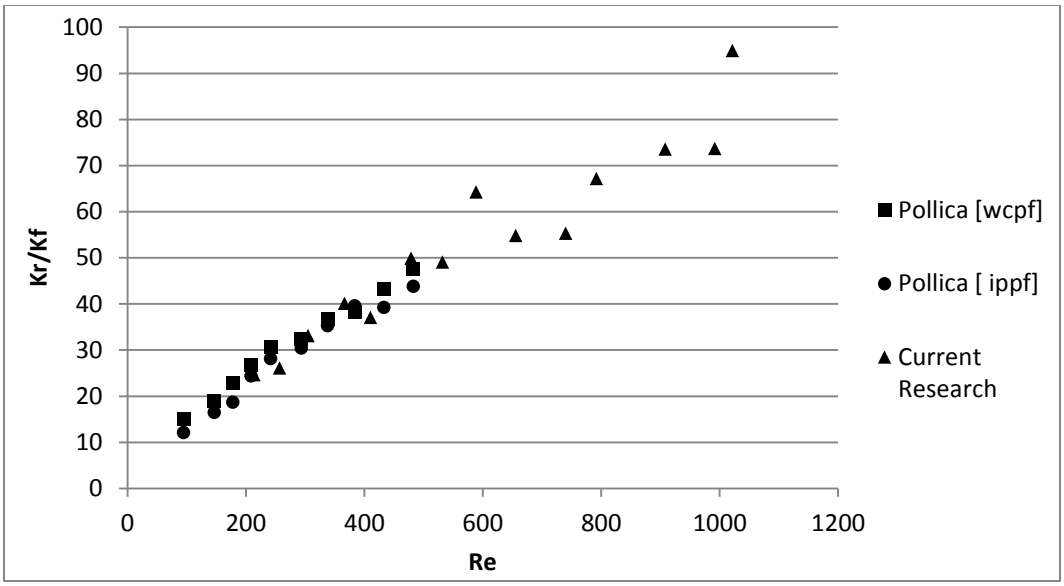


Figure 25: Comparison of Effective Thermal Conductivity for Pollica (1996) and Current Research

When the Nusselt number was compared, the current research was found to have a considerably larger amount of scatter then Pollica (1996). Also, the current research trended higher than what was observed in previous research.

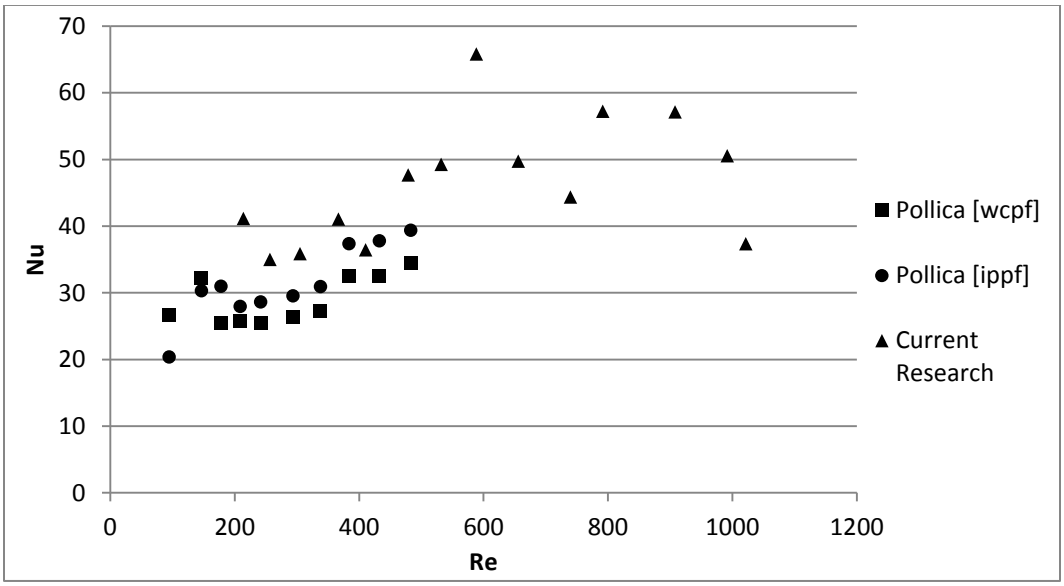


Figure 26: Comparison of Nusselt Number for Pollica (1996) and Current Research

The experiments conducted by van Dongeren (1998) were repeated two times in order to gain an understanding of repeatability. The repeats showed good agreement between the data obtained from different runs. There also were runs with higher Reynolds numbers that allowed

for more comparison to the current research. The same trends were observed as when comparison was done to Pollica (1996). There is much more scatter in the current research, which is more obvious considering the two repeating experiments. The general trend in the current research also appears to be higher than the trend in the van Dongeren (1998) data. This was also the case with the Chubb (1991) data, which will not be shown individually since the models are the most different and Chubb (1991) only has one experiment to compare to. Those graphs however can be seen in Appendix N.

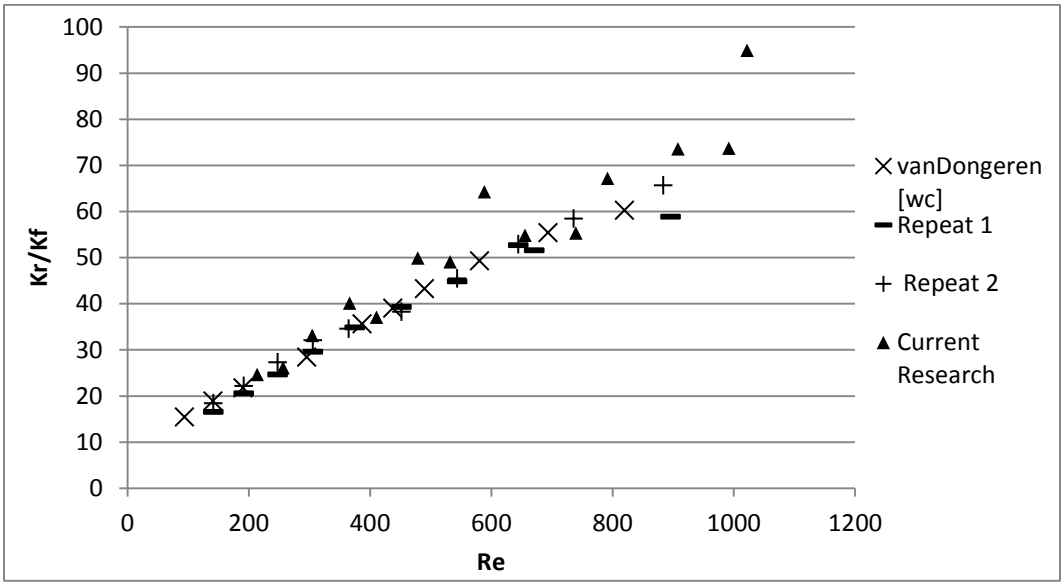


Figure 27: Comparison of Effective Thermal Conductivity for van Dongeren (1998) and Current Research

When the Nusselt number data for van Dongeren (1998) was compared to the current data, there was an obvious higher trend in the current data. There was also a much higher level of scatter, as was observed when the Nusselt number was compared for the Pollica (1996) data. Once again this trend was also observed in the Chubb (1991) comparison, which also can be found in Appendix N.

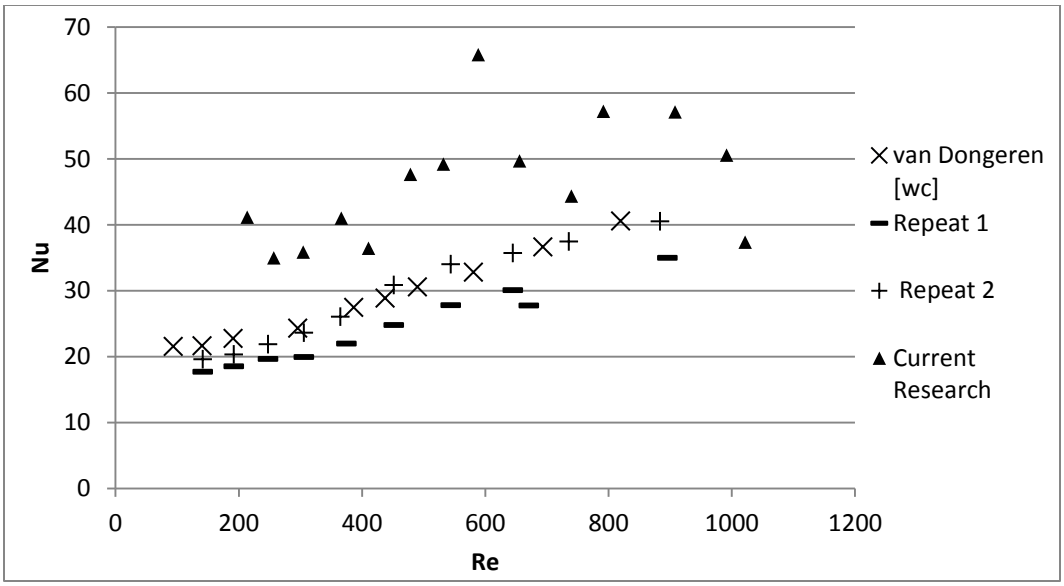


Figure 28: Comparison of Wall Nusselt for van Dongeren (1998) and Current Research

To see the overall trend in the parameters, all of the previous and current data was plotted together. For the overall comparison of effective thermal conductivity, the trends seen in the individual comparisons were confirmed. The data collected by Procedure A has more scatter than the previous heating data. Also, a few points of the current research are higher than the trend. When possible reasons for the seemingly new introduction of scatter were examined, a possible explanation in Procedure A data was the change in the experimental procedure. During the period of only cooling experiments, the procedure was changed to keep a constant airflow during one day and vary the bed heights. The older research varied the airflow on one day with a constant bed height. The newer experimental procedure could introduce more scatter based on daily variation in air quality and packing structure.

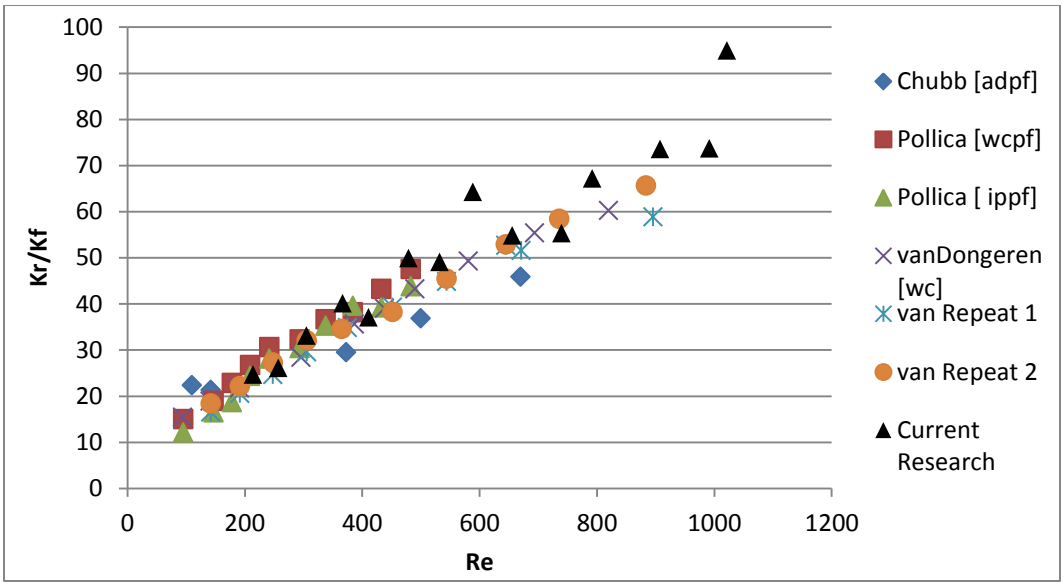


Figure 29: Comparison of Effective Thermal Conductivity for Previous Research to Current Research

The same trends of more scatter and higher values were also observed for the Wall Nusselt number.

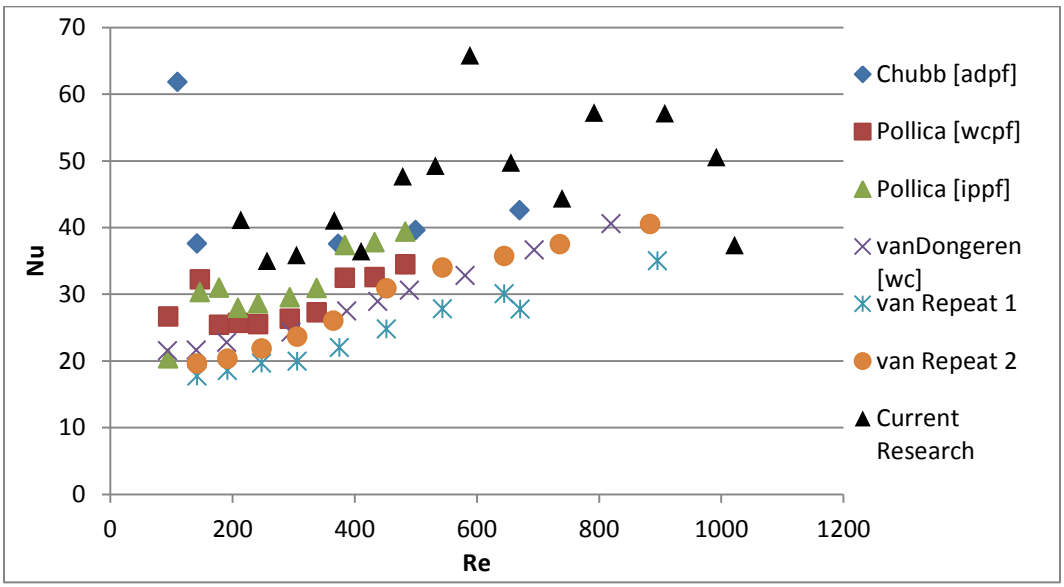


Figure 30: Comparison of Wall Nusselt for Previous Research to Current Research

### *Quantification of Scatter for Parameters*

The fitted parameters collected in past heating experiments in the column generally had a very good linear correlation. The data obtained from this study for both heating and cooling show a greater amount of scatter than what used to be present. This suggests that something must

have changed in the experimentation method between then and now. As discussed in the background, one of the biggest changes implemented since the past heating experiments was the shift from Procedure B to Procedure A. This was done by Alexander et al. (2011) because it was thought that the change in air quality from day to day was making the collection of data from one bed height to another inconsistent. While the collection of data using Procedure A would make conditions consistent for the bed heights of individual data points, it would introduce inconsistencies in conditions over a whole set of Reynolds numbers. This could generate more scatter in the resulting correlation.

Since water in the air supply was considered to be a source of experimental error for Alexander et al. (2011), this study evaluated the effect of ambient humidity and temperature on the resulting parameters. This was done by running the same flow over five different days to keep all other variables the same. The bed was re-packed each day since all four bed heights were used on a given day.

Table 3: Results for Repeating Five Runs at 38% Air Flow

| Date | Temperature (F) | Humidity | Dew Point | Re | Pe | Bi | $K_r/K_f$ | Nu |
|---|---|---|---|---|---|---|---|---|
| **1/24/2013** | 0 | NR | NR | 588.7 | 6.596 | 4.095 | 64.297 | 65.822 |
| **2/5/2013** | 25 | 50% | 12 | 582.7 | 6.836 | 3.15 | 61.297 | 48.273 |
| **2/6/2013** | 31 | 54% | 19 | 586 | 8.363 | 4.16 | 50.45 | 52.472 |
| **2/7/2013** | 22 | 33% | 1 | 582.7 | 8.672 | 3.448 | 48.319 | 41.656 |
| **2/11/2013** | 42 | 95% | 41 | 585.5 | 9.251 | 3.874 | 45.531 | 44.094 |

As seen in Table 3 above, there are no observable trends in the parameters with temperature, humidity, or dew point. These results illustrate that there is either no correlating trend with air quality or the air quality measured outside does not directly affect the air quality used in the lab.

Although ambient conditions were not found to directly affect the data, there was still scatter observed. The data points for the repeated runs compared to the rest of the data are shown in Figures 31-32 below. The graphs of the Biot number and Peclet number can be found in Appendix O.

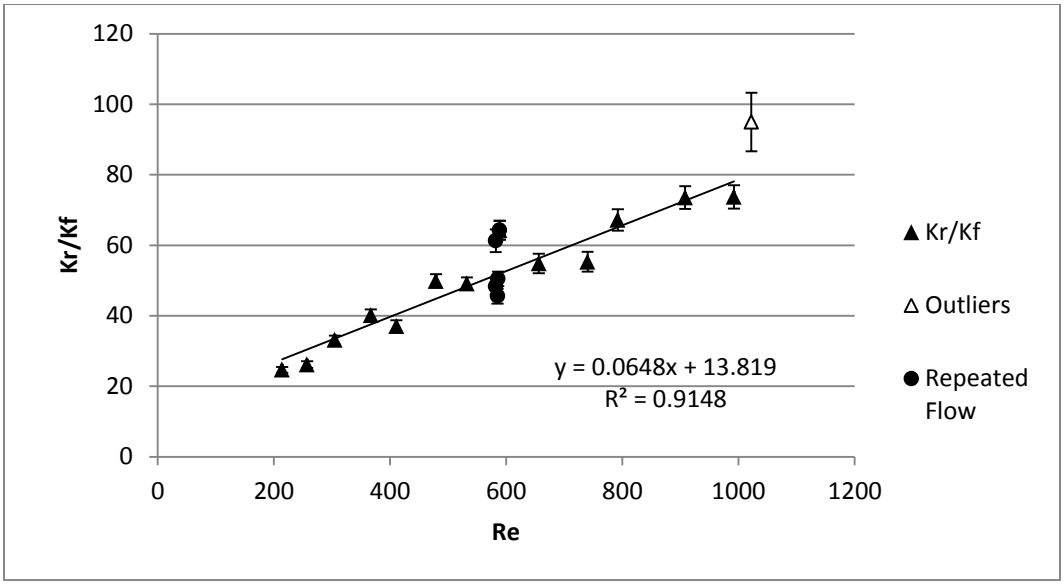


Figure 31: Repeated Flow Compared to Collected Effective Thermal Conductivity Parameters

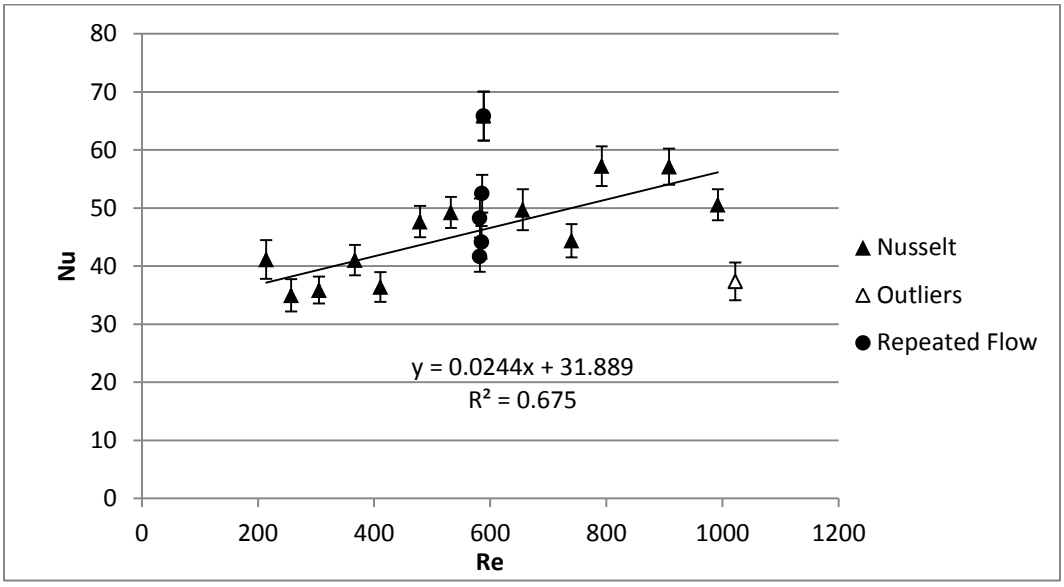


Figure 32: Repeated Flow Compared to Collected Nusselt Parameters

As demonstrated from the figures above, there is quite a bit of difference from day to day that appears to account for most of the scatter. Since humidity and temperature were not found to

affect the data, another source of error must have been introduced in past work to create this difference from older heating data. One of the big things that could not be kept similar between runs using Procedure A was the packing structure, sine the bed had to be repacked for each run. Packing structure was found to have a significant effect on resulting parameters in the literature (Wijngaarden & Westerterp, 1992). In order to find whether keeping the packing structure consistent removed the scatter from the data, Procedure B was performed, which will be discussed further in a later section.

To quantify the amount of scatter across the different packing structures using Procedure A, the average and standard deviation was calculated for the five runs. The results are shown in Table 4 below.

**Table 4: Average and standard deviation of 38% airflow heating parameters**

| | Pe | Bi | $K_r/K_f$ | Nu |
|---|---|---|---|---|
| **Ave** | 7.94 | 3.75 | 53.98 | 50.46 |
| **STDEV** | 1.17 | 0.43 | 8.30 | 9.52 |

This data was used to identify outliers on the parameter graphs to help reduce the scatter to make more reliable correlations. Points further than two standard deviations away from the least squares curve were removed from the fitted data. The point at the Reynolds number of 1022 was taken out of all parameter fits because the $F/F_{Critical}$ value for the F-test was over 7.86 showing that the model fit the experimental data very poorly for that run.

### *Conduction in Thermocouple Cross*

Once the data collected was compared to past heating data, it was found that past heating had lower trends in heat transfer parameters. A possible explanation that was considered was conduction in the nylon thermocouple cross, even though nylon was used because it has a low thermal conductivity. The idea was that this conduction was resulting in artificially high temperature readings in the thermocouples, which was presented in previous literature by Freiwald and Paterson (1992). In order to test this idea, the column was packed to four inches and run for two hours without the thermocouple cross in place to allow the system to come to steady state. After steady state had been achieved, the cross was put in place and the column

was run for another two hours. It was noted which lines in the data file corresponded to the cross first being placed in, an hour later, and two hours later. The experiment was repeated for six inches of packing.

To observe if the temperature readings increased with time, the temperature for each thermocouple at the initial time, one hour, and two hours were compared. It was found the thermocouple cross took some time to accurately read the temperature in the column, so for the initial time the temperature line was taken after 30 rows of data had been collected, which is about two minutes. When these three temperatures were compared, it was found that they varied by less than a degree for all thermocouples, with the standard deviation usually being about 0.3 degrees. To see the complete temperature readings and averages, please refer to Appendix K. Therefore, it was concluded that the experimental procedure of leaving the thermocouple cross in place while the column was coming to steady state was not causing artificially high temperature readings.

### Heating and Cooling Comparison

Once data was collected for both heating and cooling, the resulting parameters were graphed together to see how heating and cooling compared. As discussed in previous sections, using standard deviations the heating outliers are shown on the graph but not included in the linear correlation. For the effective thermal conductivity once the outliers are removed, heating and cooling seem to have comparable data. However, it is difficult to make a definite conclusion because of the scatter in the data and the fact outliers needed to be removed. Heating seems to generally have a higher trend than cooling, implying that during heating experiments more heat is being transferred across the bed.

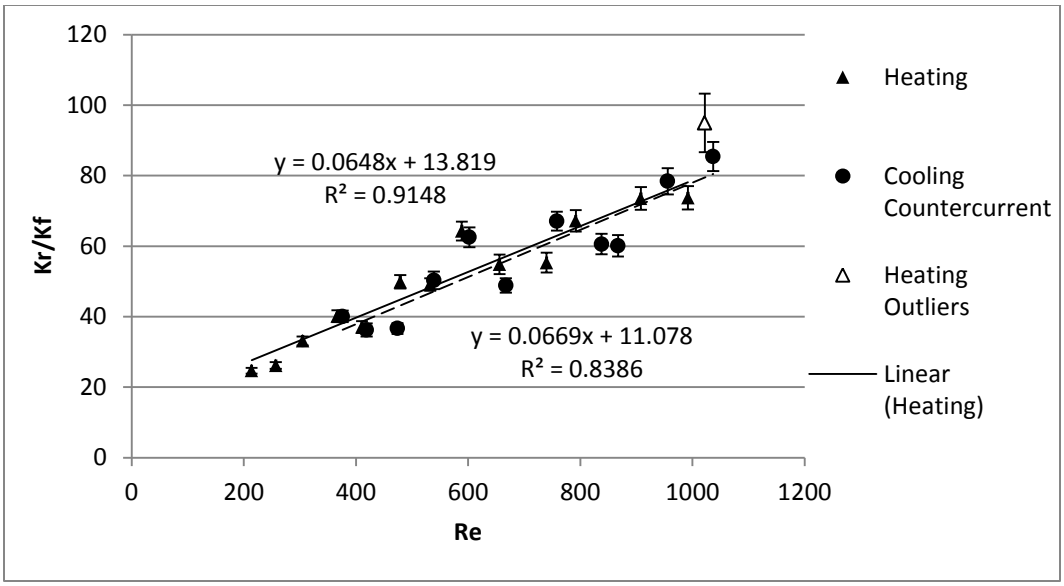


Figure 33: Effective Thermal Conductivity for Heating versus Cooling

Heating also had a higher general trend for the Nusselt number. The discrepancy between the heating and cooling however has increased for the Nusselt number. Once again, the outliers were shown on the graphs, but were not included in the trendline.

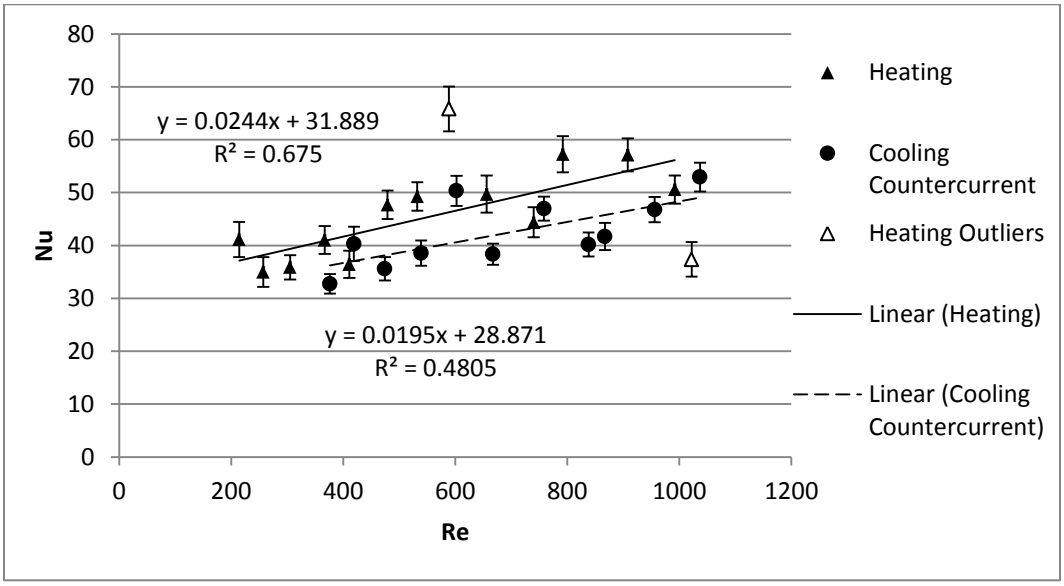


Figure 34: Nusselt Number for Heating versus Cooling

For the Peclet number, a straight trendline did not fit the data or what was physically occurring, so the curves were fitted to the following equation:

Equation 24: Peclet Number Trendline

$$\frac{1}{Pe} = \frac{1}{Pe_{\infty}} + \frac{\frac{k_r}{k_f}}{Pr * Re}$$

The resulting curves were too similar when scatter was considered in order to draw any solid conclusions about the relationship between heating and cooling. Once again, the heating outliers were included on the graph but not the curve.

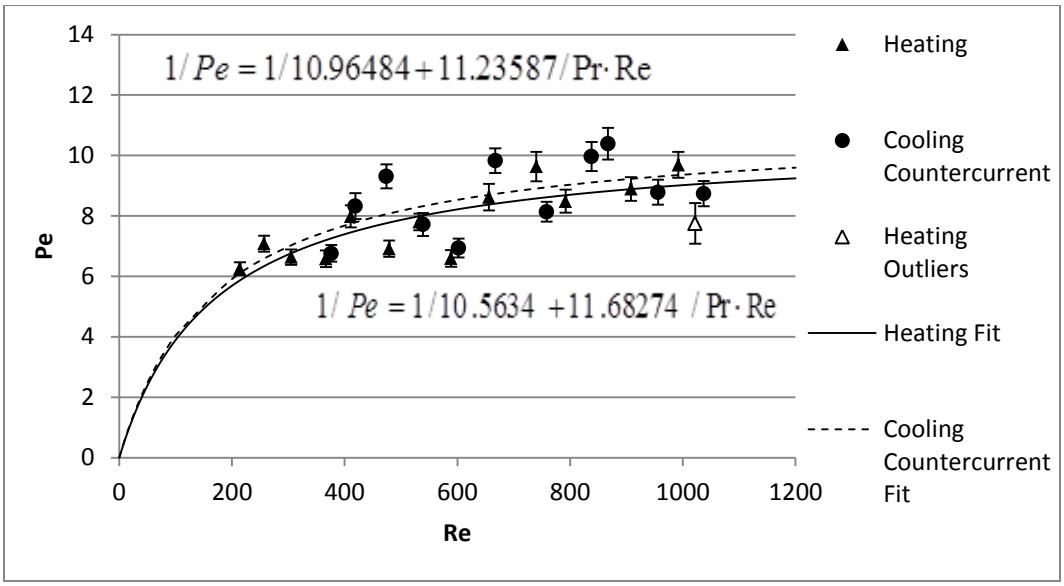


Figure 35: Peclet Number for Heating versus Cooling

For the Biot number, heating once again had a higher trend than the cooling data. This supports the trends observed by the other data that heating has more efficient heat transfer at the wall.

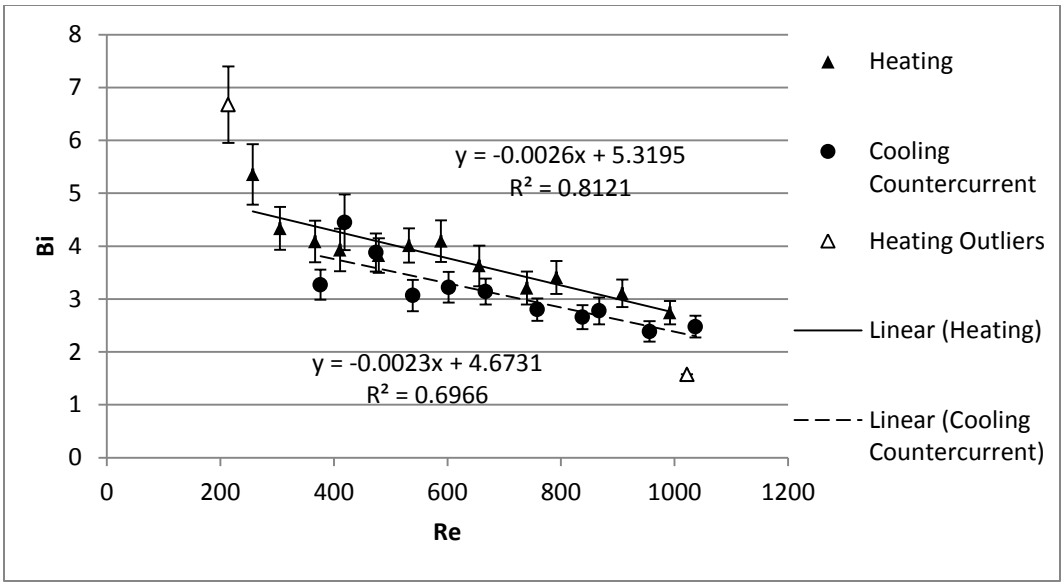


Figure 36: Biot Number for Heating versus Cooling

Although the trends in the data collected with Procedure A seem to indicate that heating has higher values of parameters because of more effective heat transfer, the scatter prevents any definite conclusions from being made. The outliers in the heating data tend to be lower than the cooling and not all of the heating points lie above the cooling. Because of this uncertainty and the results found when heating was collected with Procedure A was compared to past heating, the study also decided to collect data the way it was done in the past. This method required keeping the bed height constant during the day and varying the air flow rate.

### Including the Center Thermocouple in the GIPPF Model

The GIPPF model yields values for various heat transfer parameters. The model uses the first bed height as the inlet profile. It also gives dimensionless temperature profiles for all bed heights with respect to radial position. In order to ensure the correct inlet profile was being used, the interpolated temperature profile of the first bed height was compared to the experimental temperature profiles. Since the model did not produce a physically reasonable temperature profile, it was shown that the model was not calculating the heat transfer parameters correctly.

The interpolated temperature profile was comparable to the observed profile for dimensionless radial positions above approximately 0.35 and then it continued linearly to a value above one at the center of the tube, as can be seen in Figure 37.

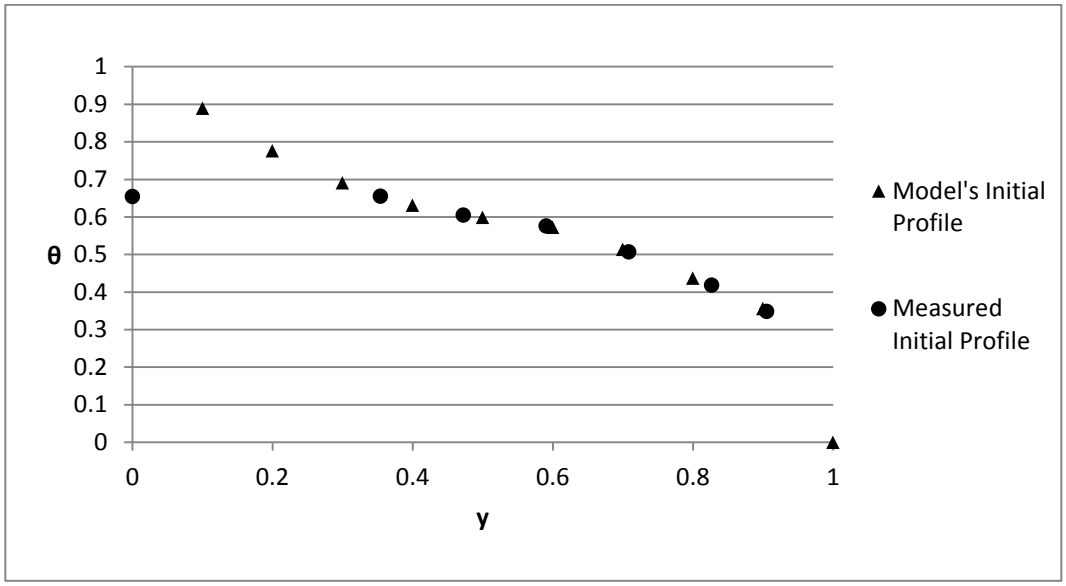


Figure 37: Original Interpolated Dimensionless Temperature Profile

This does not match the known dimensionless temperature profiles because the known profiles reach a parabolic maximum as the radial position approaches zero. Due to the definition of dimensionless temperature, having a value that was larger than one at the center of the bed did not make physical sense as well.

The reason for this was the center thermocouple was not included in the model. The model was only using measured values of y larger than 0.35 to create the plot and then using a cubic spline to interpolate values from there to the center of the bed. This would sometimes lead to values that showed appropriate paths to the center, but also could interpolate values, which did not make physical sense. In order to correct this, the center thermocouple was added by inputting the center reading four times. This was consistent with the way the other thermocouples were inputted. This gave more reasonable temperature profiles as shown in Figure 38.

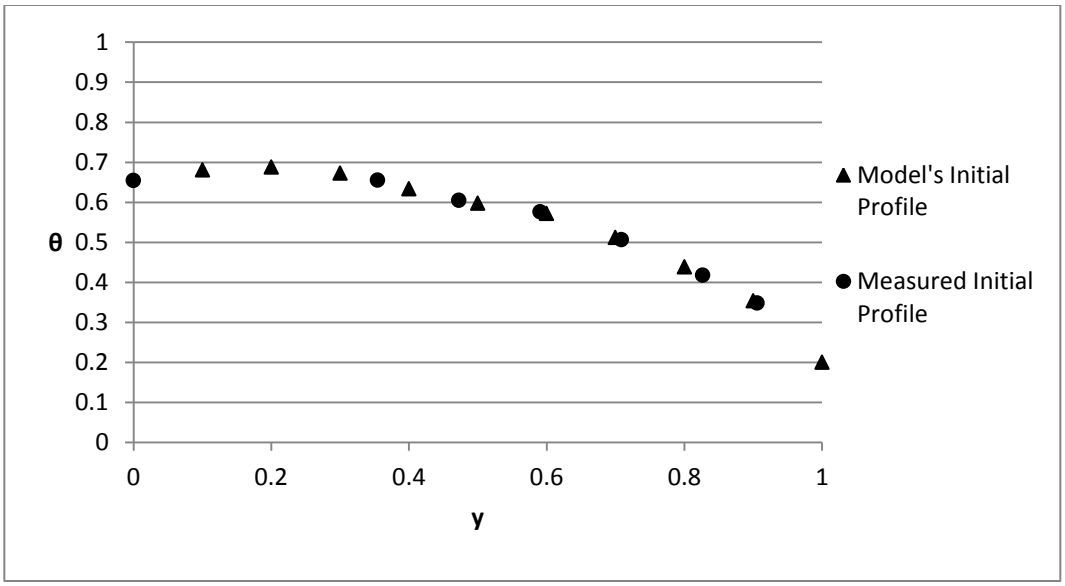


Figure 38: Interpolated Profile with Four Center Thermocouple Measurements

However, by inputting the same value four times there were concerns about having an overly accurate center reading since there is only one reading at the center position.

To account for this, a value of -1 was put into the model signifying no measurement. Using this method, the model yielded interpolated graphs with dimensionless temperatures that were parabolic.

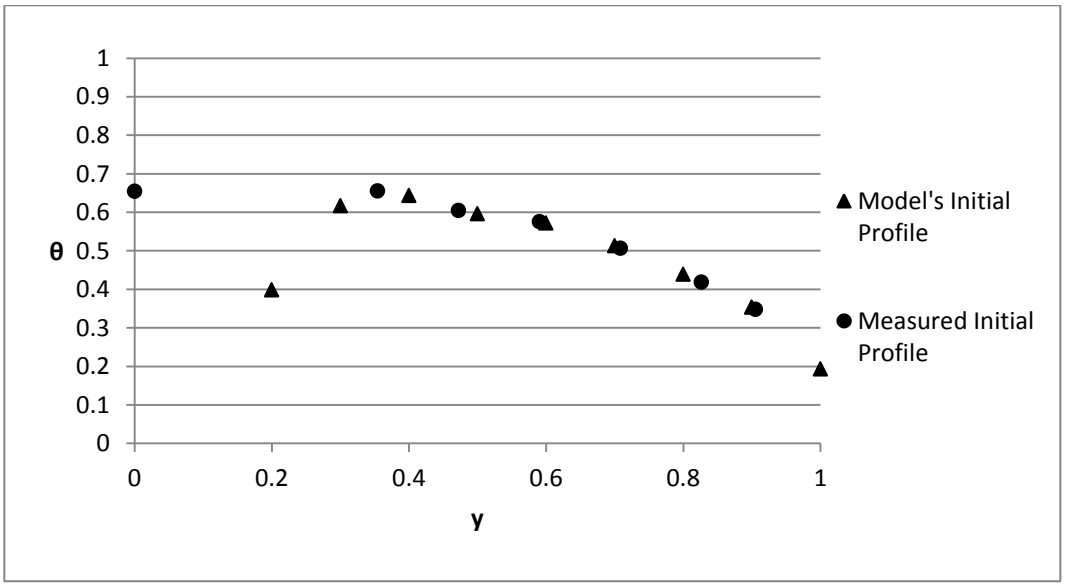


Figure 39: Interpolated Profile with Center Thermocouple and -1 Values

These results showed that the model was taking the values of -1 to be actual values. In order to improve the model further, the computer program had to be altered so that -1 would signify no measurement instead of an actual measurement of -1. The resulting temperature profiles after

the model change were more closely related to known dimensionless temperature values, as shown in Figure 40.

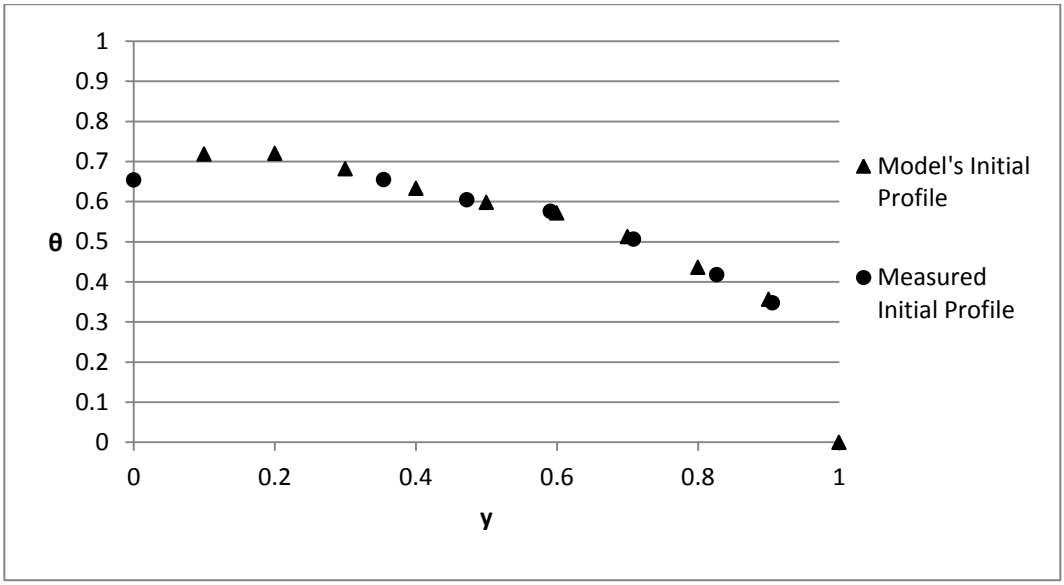


Figure 40: Interpolated Profiles using Improved Model

### *The Effect on Heat Transfer Parameters*

All of the cooling and heating runs were analyzed using both the original model that excluded the center thermocouple and the model that included the center thermocouple. The heat transfer parameter graphs were studied in order to see the effect of including the center thermocouple in the model.

When looking at the effective thermal conductivity for cooling, including the center thermocouple slightly decreased the intercept from 11.143 to 10.871. This brings the cooling data closer to the expected range, which supports the thought that including the center thermocouple couple is a better model. Also, by including the center thermocouple the scatter in the data decreases.

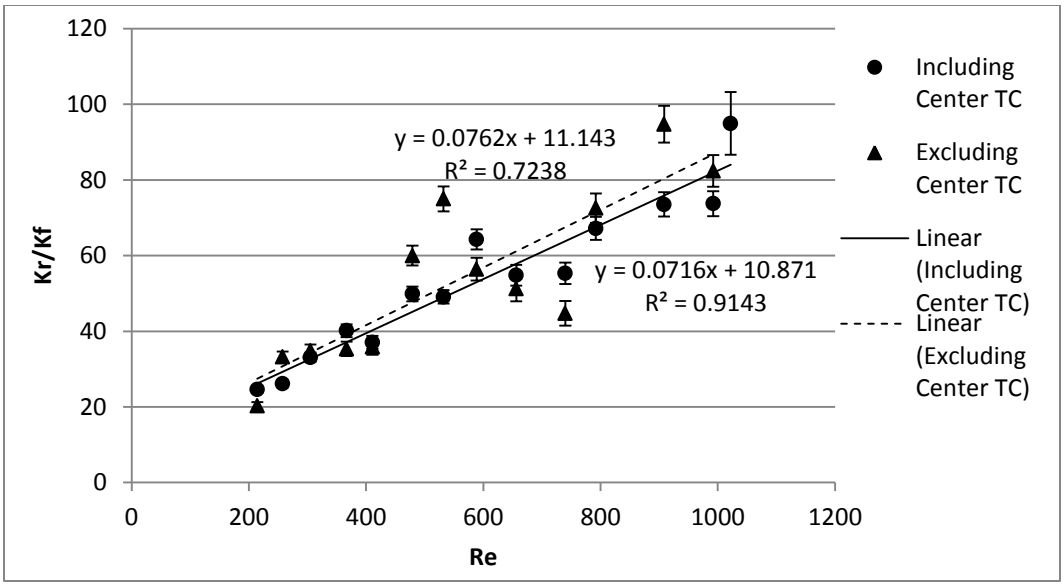


Figure 41: Effective Thermal Conductivity for Cooling Runs Including and Excluding the Center Thermocouple

The wall Nusselt number was also looked at and can be seen in Figure 42. The same type of change was observed. There was a systematic shift downwards for the Nusselt Number, although the data did become more scattered.

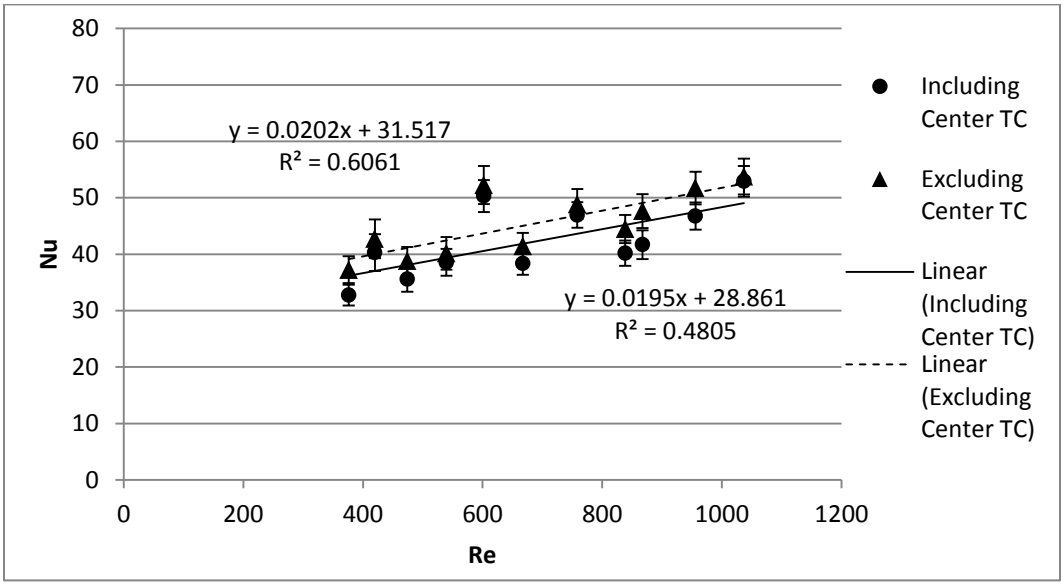


Figure 42: Nusselt Number for Cooling Runs Including and Excluding the Center Thermocouple

When looking at the data for heating, it was found there was less of a change between data analyzed with and without the center thermocouple. One possible reason for this is the initial graphs were more accurate than cooling without the use of the center thermocouple.

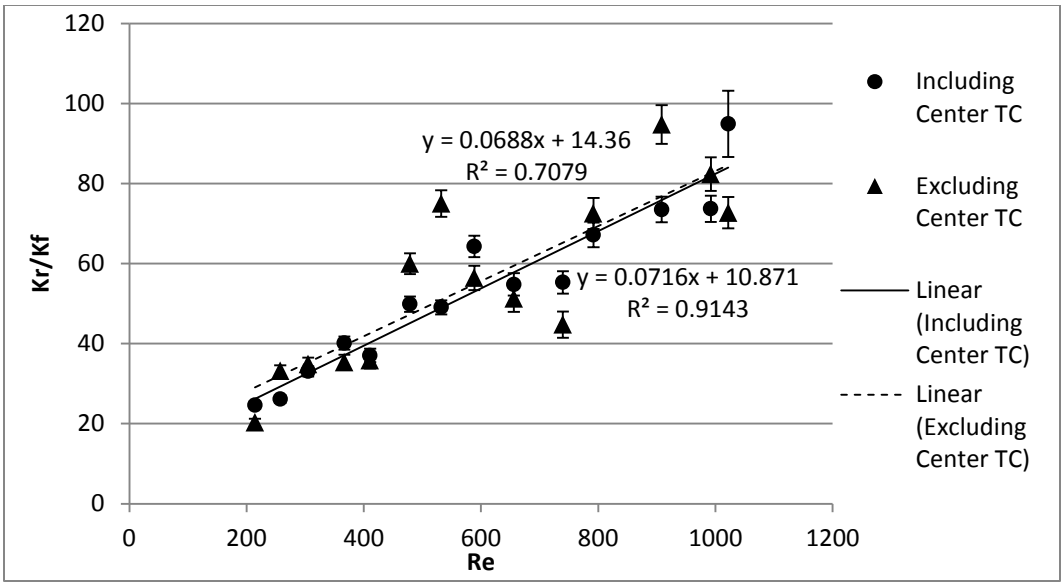


Figure 43: Effective Thermal Conductivity for Heating Runs Before and After the Model Change

However, when looking at the Nusselt number, there was a change between the two models, as shown in Figure 44. This suggests that by including the center thermocouple the model assumes less heat is being transferred in the bed. This makes sense if some of the profiles had the issue where the center position was interpolated as larger than one. There was also an increase in the amount of scatter for this change as well.

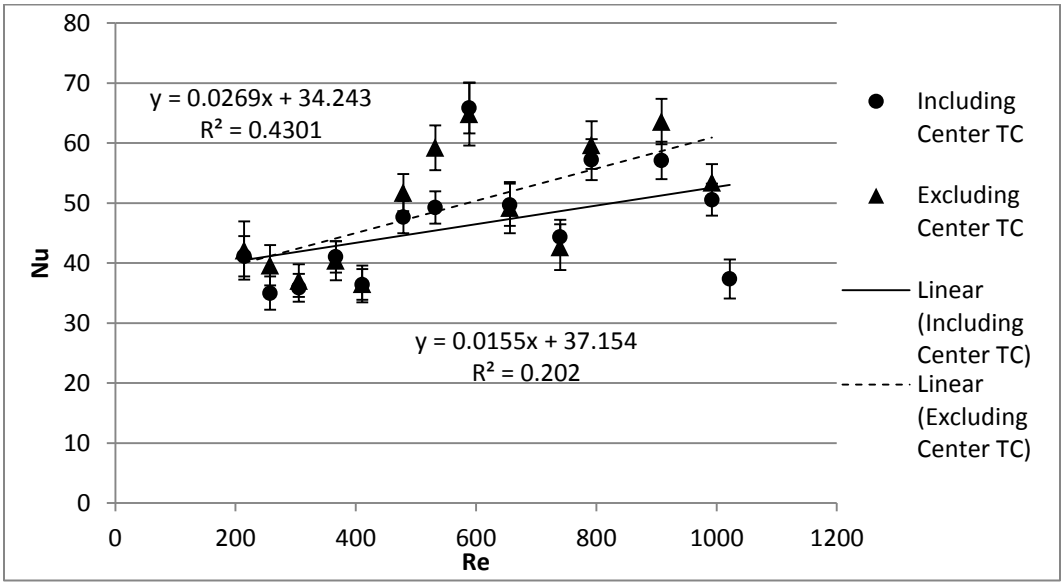


Figure 44: Nusselt Number for Heating Runs Before and After the Model Change

After comparisons were made between cooling and heating individually, heating and cooling were compared to see if there was any major difference between including and excluding the

center thermocouple. Graphs the comparison for Peclet and Biot numbers can be found in Appendix O.

When the effective thermal conductivity was compared, it was found that including the center thermocouple lowered the values for both heating and cooling, as can be seen in Figures 45-46. Also, cooling was originally above heating, showing more effective cooling, but after the inclusion of the center thermocouple it was lower. This makes sense since including the center thermocouple had a more profound effect on cooling rather than heating.

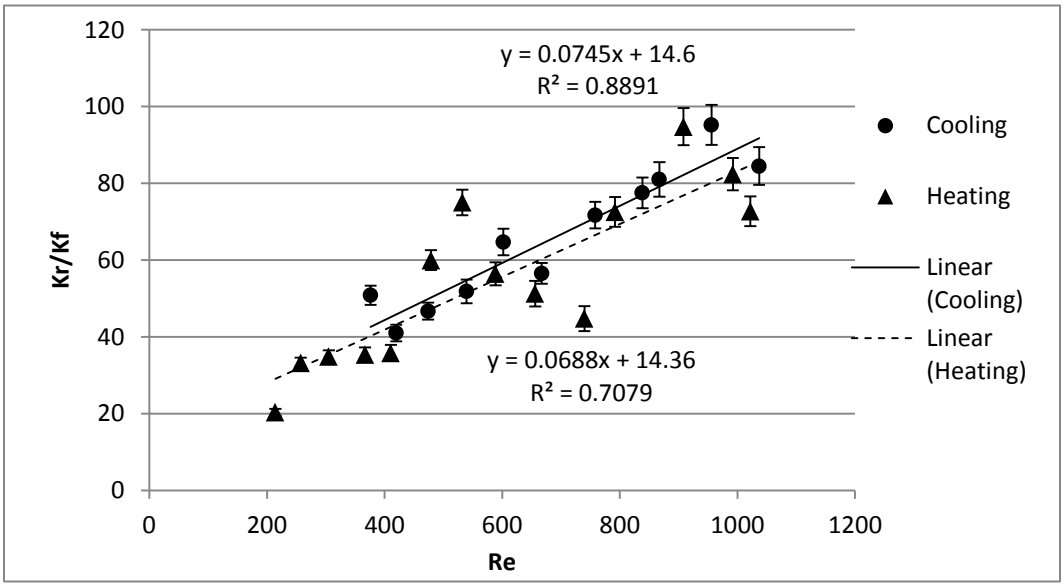


Figure 45: Heating versus Cooling Effective Thermal Conductivity Excluding the Center Thermocouple

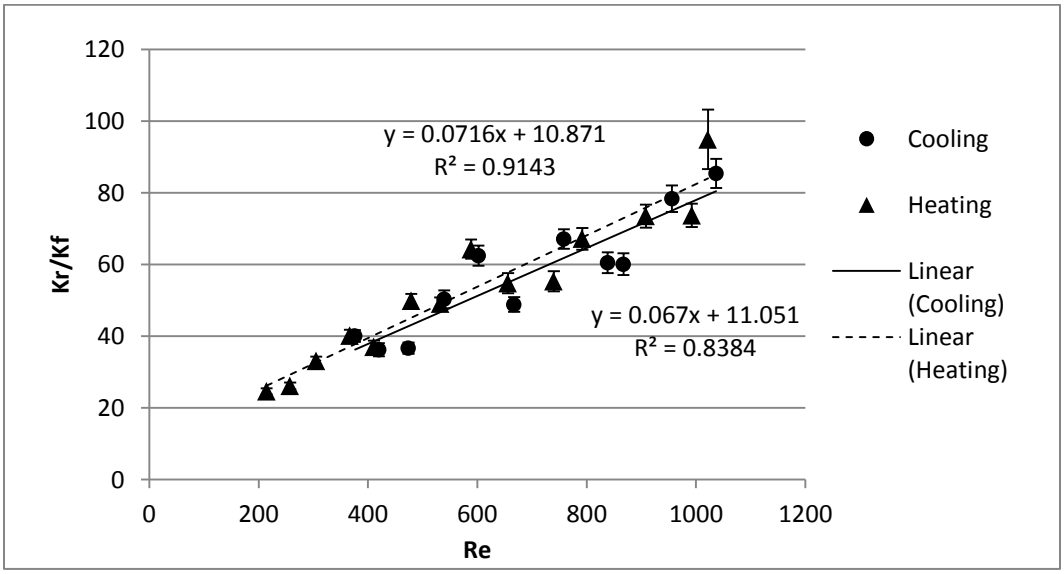


Figure 46: Heating versus Cooling Effective Thermal Conductivity Including the Center Thermocouple

For the Nusselt number, once again the inclusion of the center thermocouple lowered the parameters for both heating and cooling. However, heating was higher than cooling for both models, although the discrepancy between heating and cooling decreased by adding the center thermocouple.

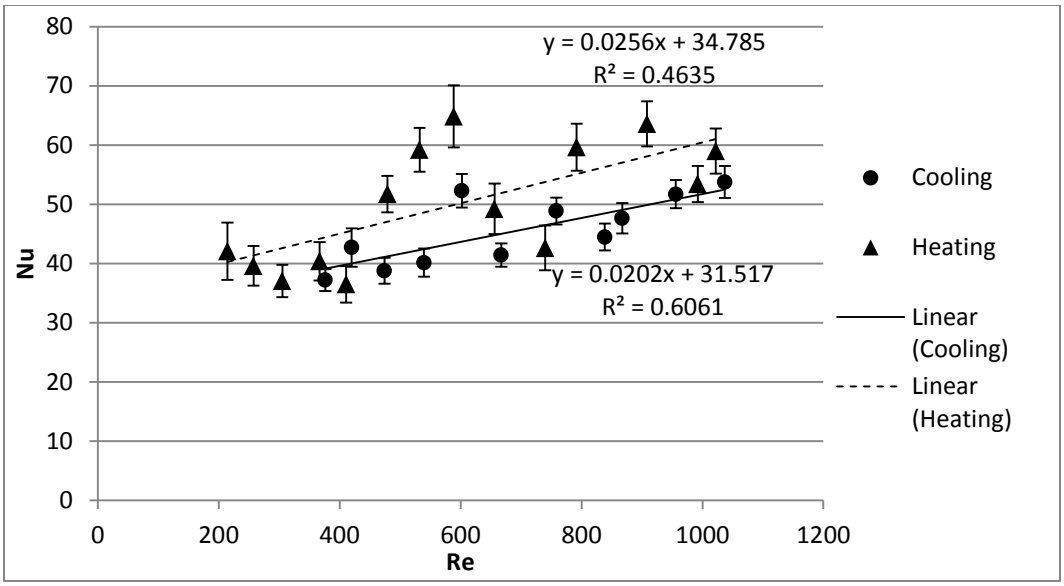


Figure 47: Heating versus Cooling Nusselt Number Excluding the Center Thermocouple

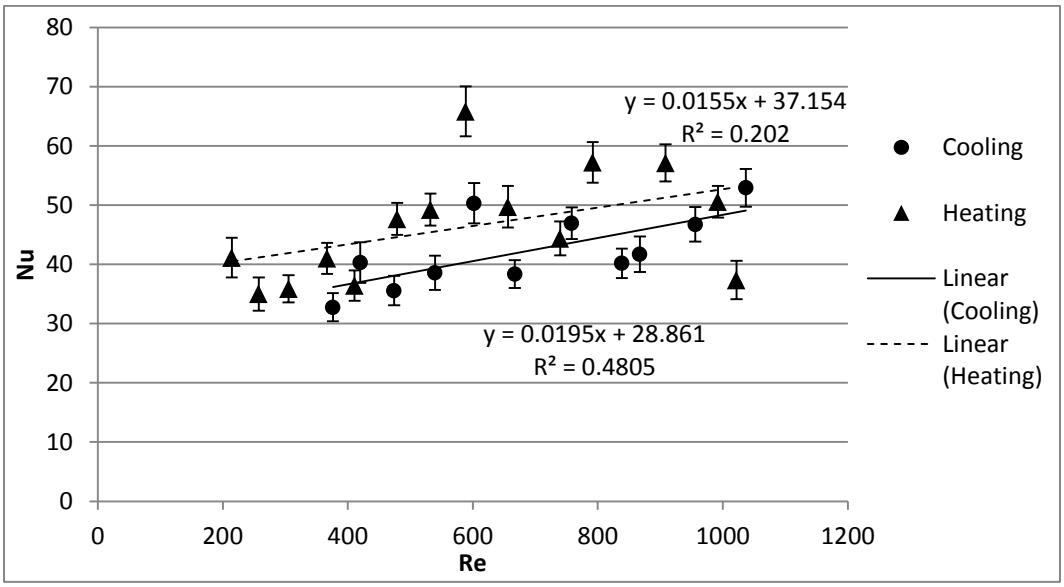


Figure 48: Heating versus Cooling Nusselt Number Including the Center Thermocouple

## PROCEDURE B

### COOLING RESULTS

For Procedure B the effective thermal conductivity has a very strong linear trend as seen in Figure 49. The intercept was 22.922, which was higher than the expected range of 8-10, but still reasonable.

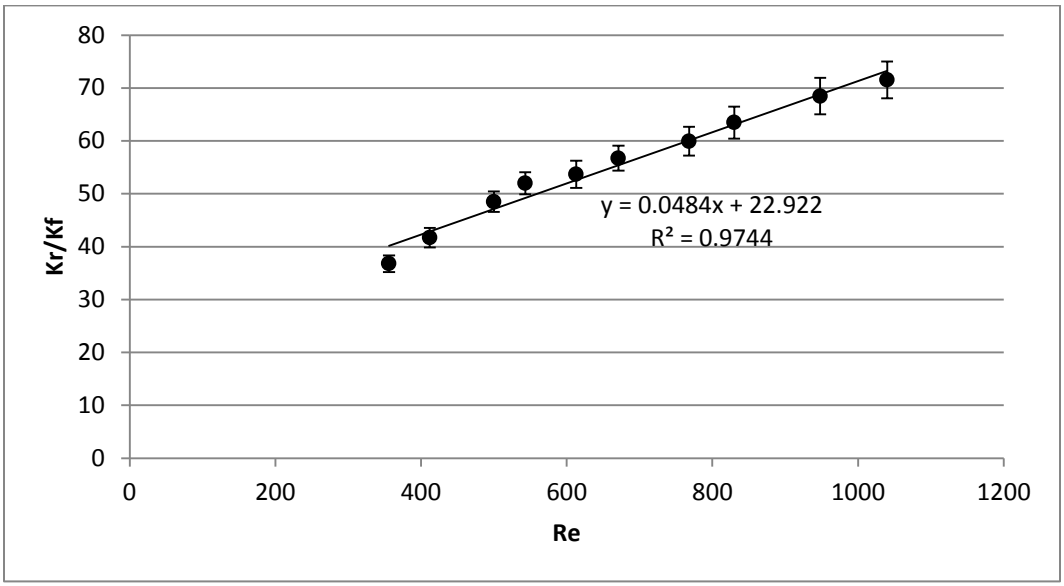


Figure 49: Effective Thermal Conductivity versus Reynolds Number for Cooling Procedure B

For the Nusselt number versus the Reynolds number, the data was more scattered as expected but still had a strong linear trend.

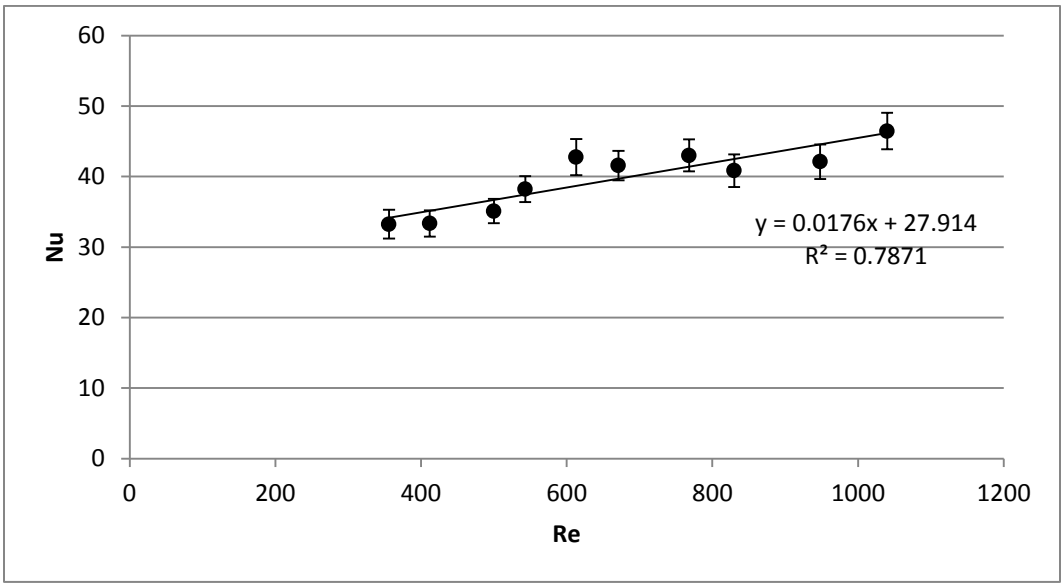


Figure 50: Nusselt Number versus Reynolds Number for Cooling Procedure B

### *Procedure B Comparison With Cooling Past MQPs*

The data obtained from re-running the cooling experiments using procedure B was compared to the results from Ashman et al. (2009). The effective thermal conductivity can be seen in Figure 51 and the Nusselt number can be seen in Figure 52. By returning to procedure B, the only differences between the two experiments are the tube diameter and particle size as discussed previously.

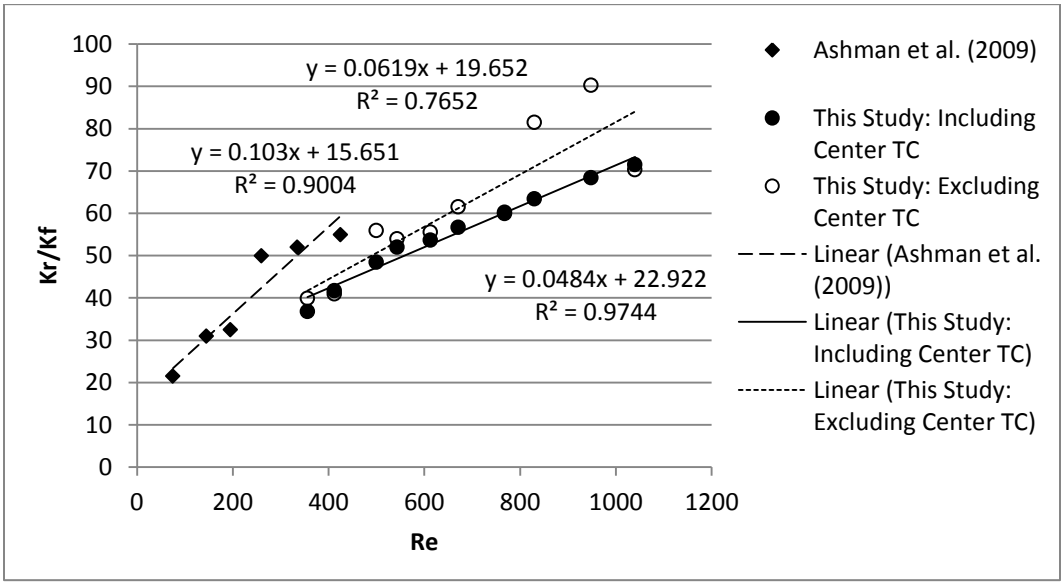


Figure 51: Comparison of Effective Thermal Conductivity Using Procedure B to Ashman et al. (2009)

There are still differences between this study and Ashman et al. (2009). Even when using the same experimental procedure, this study does not find the thermal conductivity in cooling experiments to be as high as Ashman et al. (2009). This may be attributed in part to the different dimensions of the column; however, further studies would be needed to support this. The range of Reynolds numbers used may also be an important factor in the differences seen, especially given the higher scatter when using the model without the center thermocouple, which is the model Ashman used. Ashman et al. (2009) collected fewer Reynolds numbers over a smaller range, which may not be as good a representation of the thermal conductivity.

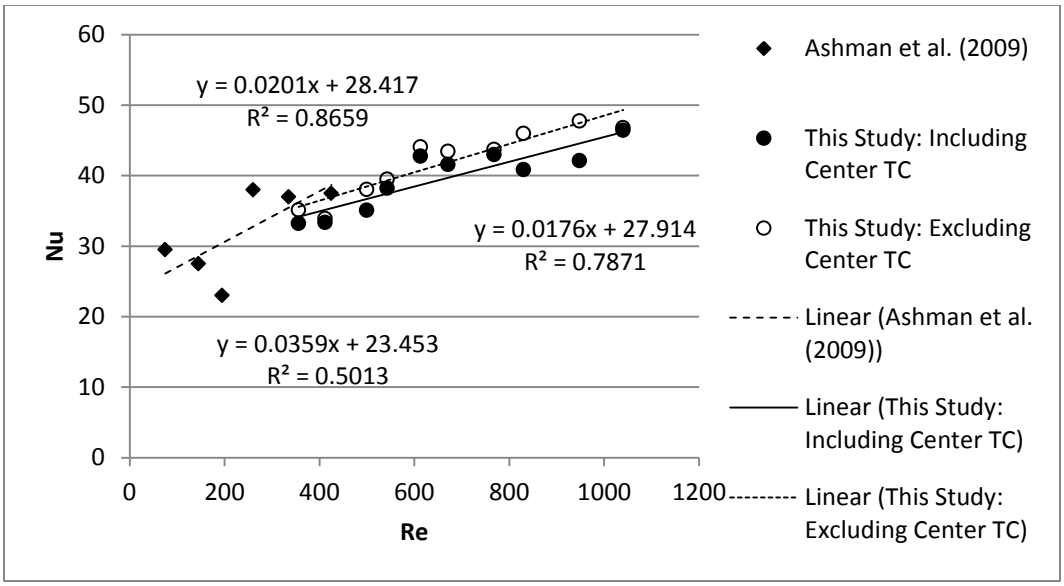


Figure 52: Comparison of Nusselt Number Using Procedure B to Ashman et al. (2009)

For the Nusselt number, the data seems to be comparable, expect for the two data points for Ashman et al. (2009) around a Reynolds number of 200.

### *Procedure B Comparison with Literature*

The procedure B data was also compared to Borkink and Westerterp (1992b). The effective thermal conductivity is shown in Figure 53 and the Nusselt number is shown in Figure 54.

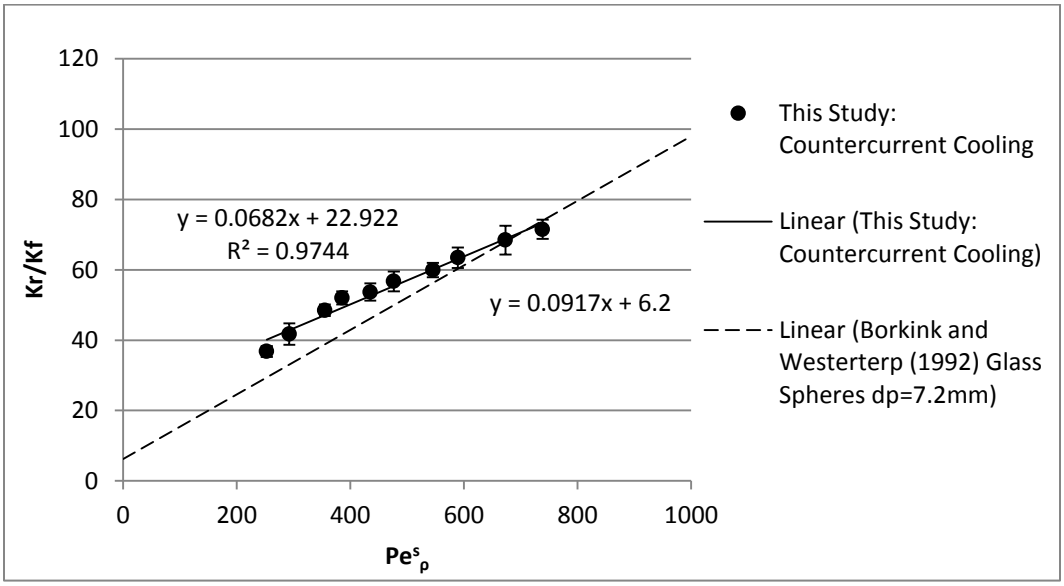


Figure 53: Procedure B Cooling Effective Thermal Conductivity Compared to Borkink and Westerterp (1992b)

The data from procedure B is a bit different in comparison to the new procedure. The stagnant effective conductivity is much more removed from the value Borkink and Westerterp (1992b)

found and the slope of the correlation is slightly lower instead of parallel as it was with the old procedure data. Given that Borkink and Westerterp (1992b) used a slightly different material, particle, and tube sizes, the results are fairly comparable. The conductivity of ceramic is higher than glass, so the differences shown here make physical sense. The differences between the Procedure A and B's comparison could be due to the amount of times the column was packed. In procedure A, the column was repacked more frequently creating a trend that represents more of a statistical average than Procedure B. Procedure B represents one packing. It is possible that if Procedure B was repeated multiple times, the average would lie parallel to Borkink and Westerterp (1992b)'s data, as was shown in comparing Procedure A.

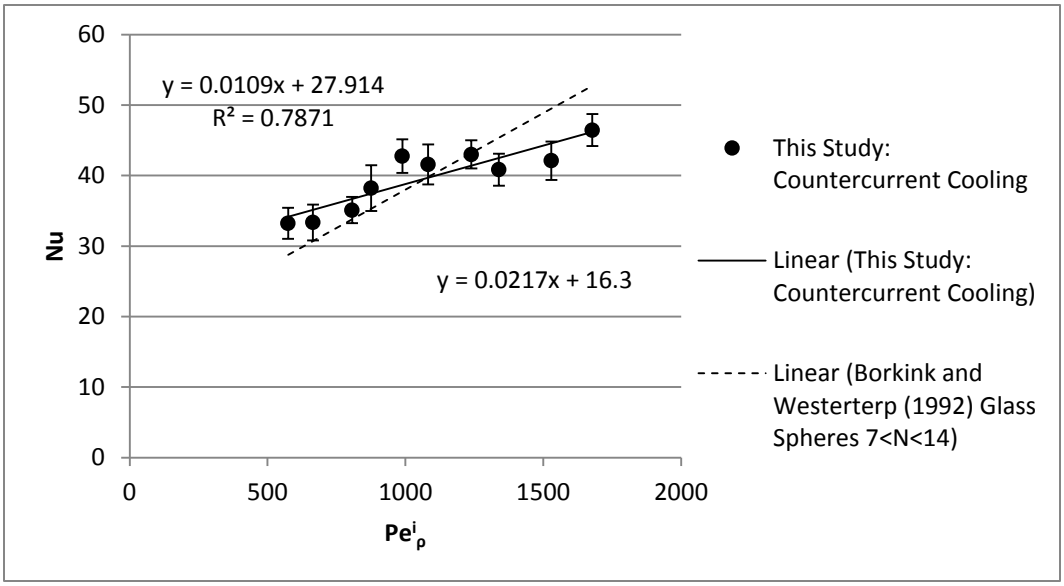


Figure 54: Procedure B Cooling Nusselt Number Compared to Borkink and Westerterp (1992b)

For the Nusselt number, the correlations intersect. As with the effective thermal conductivity, the intercept for this study is much higher and the slope is lower. This can also be because of the packing structure used for this experimental run. Overall the data is fairly comparable.

### Heating Results

Below are the results for the heating runs with Procedure B. The effective conductivity versus the Reynolds number is illustrated in Figure 55 below. There is a strong linear trend and the intercept of 14.536 falls near the expected range of 8-10. Graphs containing the Biot numbers and the Peclet numbers are located in Appendix O.

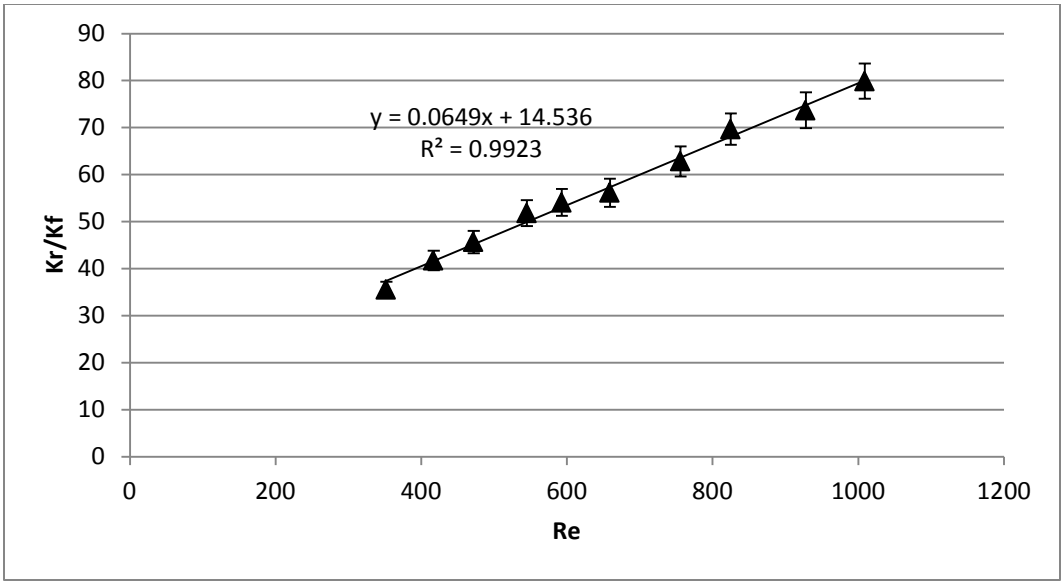


Figure 55: Effective Thermal Conductivity versus Reynolds Number for Heating Procedure B

Below is the graph of the Nusselt number versus the Reynolds number. There is a strong linear trend between the Nusselt number and the Reynolds number.

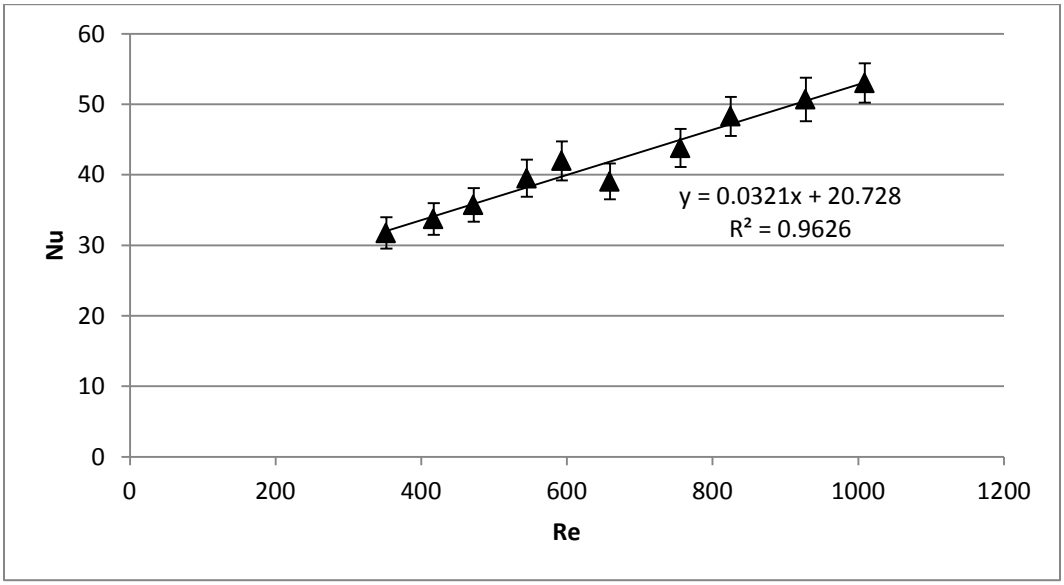


Figure 56: Nusselt Number versus Reynolds Number for Heating Procedure B

### *Comparison of Procedure B to Past Heating*

Procedure B was compared to past data from Pollica (1996), van Dongeren (1998), and Chubb (1991) to verify that it was consistent with prior data from the same column. When the effective thermal conductivity was plotted against the Pollica (1996) data, it was found that the trends were closely followed.

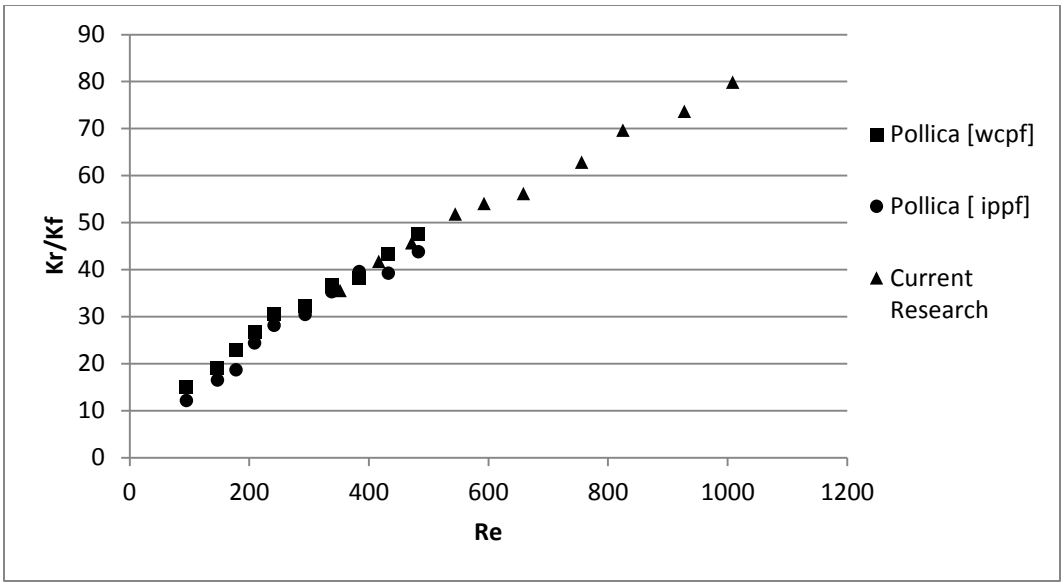


Figure 57: Pollica (1996) Data for Effective Conductivity Compared to Procedure B

This shows a much more consistent trend with less scatter with the effective conductivity. A similar trend was also observed for the Nusselt number.

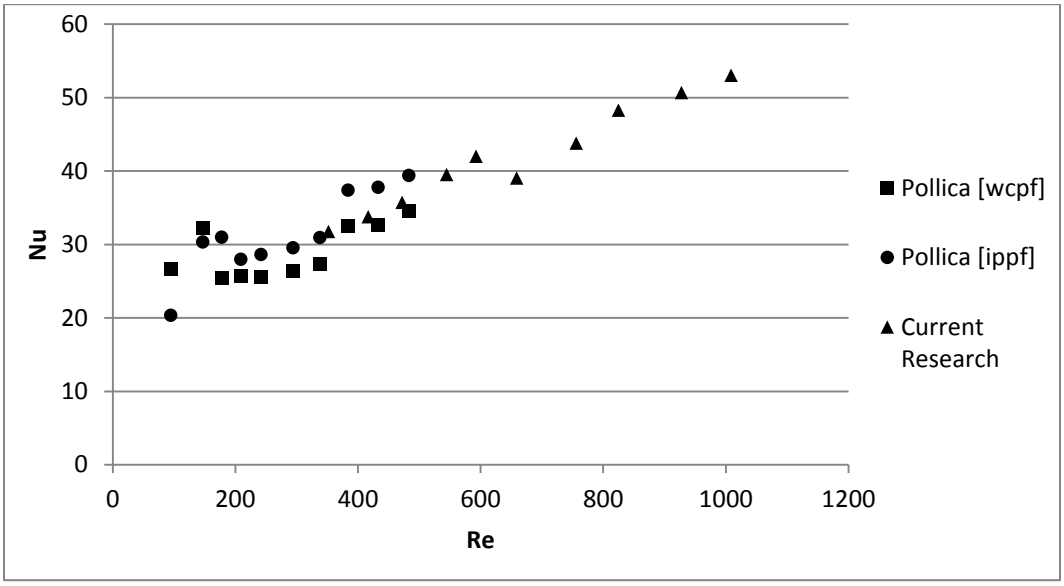


Figure 58: Pollica (1996) Data for Nusselt Number Compared to Procedure B

When all the data for Pollica (1996), van Dongeren (1998), Chubb (1991), and the current data were plotted together, it was found that the effective thermal conductivity for all the experiments followed a similar trend. There also was a low amount of scatter. This supports the idea that using the procedure of keeping one bed height per day and varying the air flow gives

better results. The comparisons to Chubb (1991) and van Dongeren (1998) can be found in Appendix N.

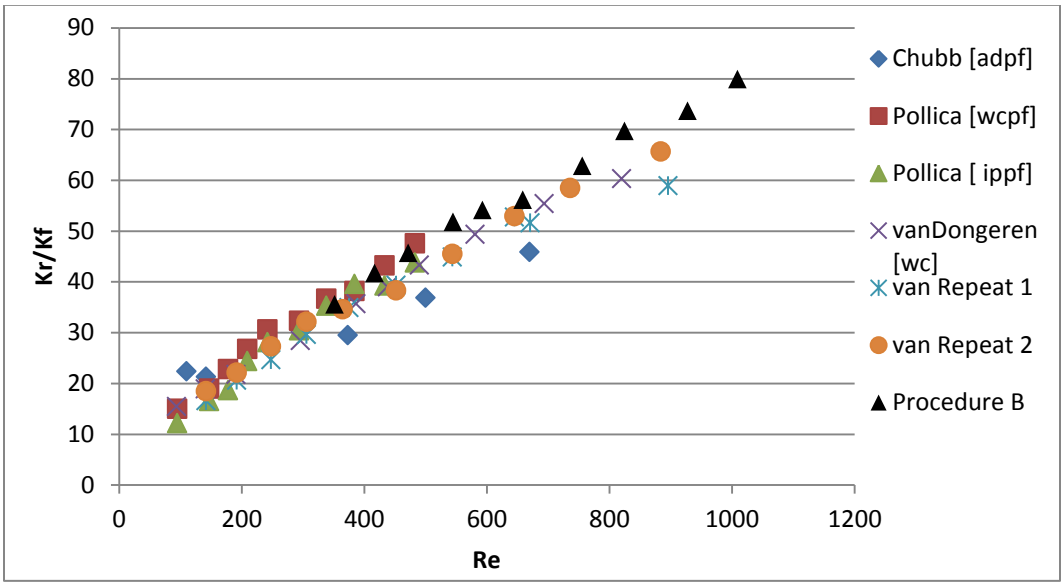


Figure 59: Comparison of Effective Conductivity for Previous Research to Current Research

The same trend was observed for the Nusselt number as the effective conductivity. All of the data seemed to follow a general trend. There was more scatter observed for the Nusselt number than the effective thermal conductivity, but that is usually observed.

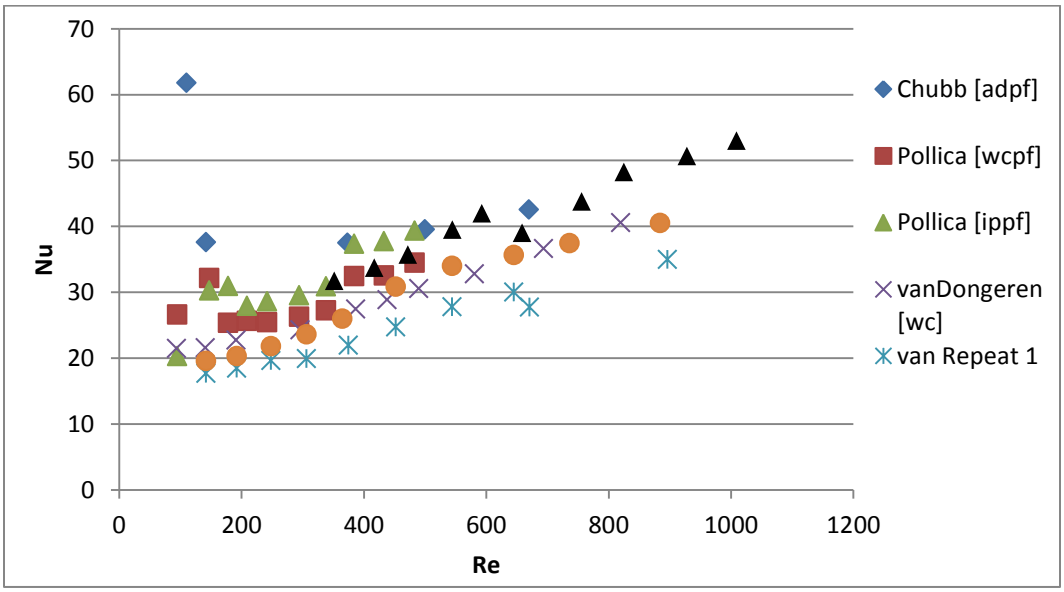


Figure 60: Comparison of Wall Nusselt for Previous Research to Current Research

### Heating and Cooling Comparisons

After data was collected for both heating and cooling for procedure B, the resulting parameters were compared to see if any there was any difference in the heat transfer between heating and cooling. These parameters appear to be much more comparable than for procedure A. For the effective thermal conductivity, the values for heating and cooling are closer than what has been observed in the past. In fact, cooling is higher than heating at lower Reynolds numbers and then around a Reynolds number of approximately 500 intersects the heating data. For Reynolds numbers between 500 and 600 the points match up and then cooling has lower values. The data collected using procedure B gives data with much less scatter, which allows for a stronger trend to be observed than with procedure A. Based on this data, it appears any difference between heating and cooling is small. If there is any difference, cooling seems to be more effective at Reynolds numbers below 500 and for Reynolds numbers above 600 heating is more effective. However, to draw a definite conclusion, more data would have to be collected under more conditions.

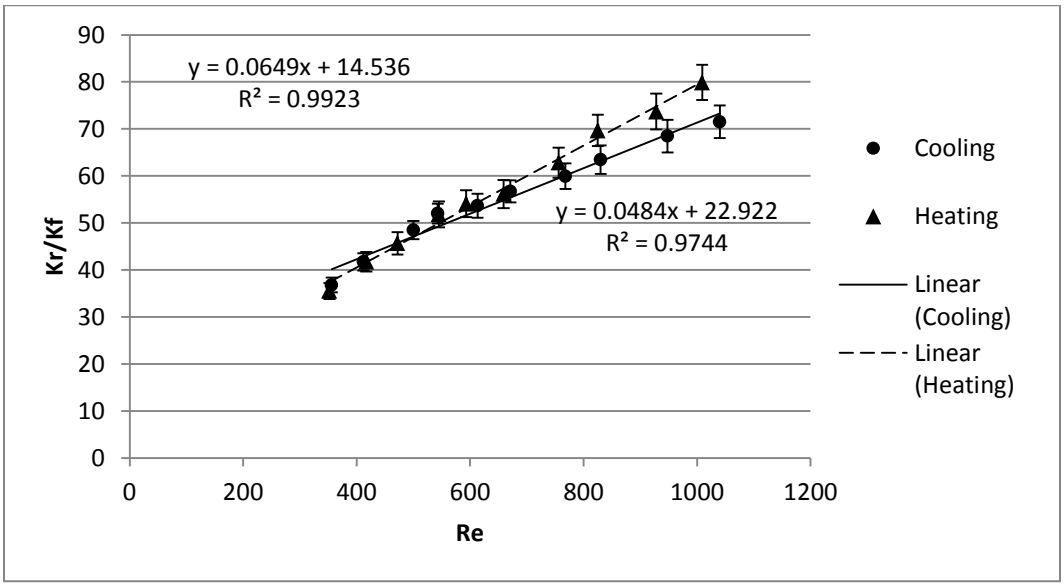


Figure 61: Effective Thermal Conductivity Comparison for Procedure B Heating and Cooling

For the Nusselt number, the same general trend was observed as the effective thermal conductivity. The difference between heating and cooling is slightly more pronounced and there is more scatter in the cooling data. This makes sense with past data, which finds there is generally more scatter in the Nusselt number, especially for cooling.

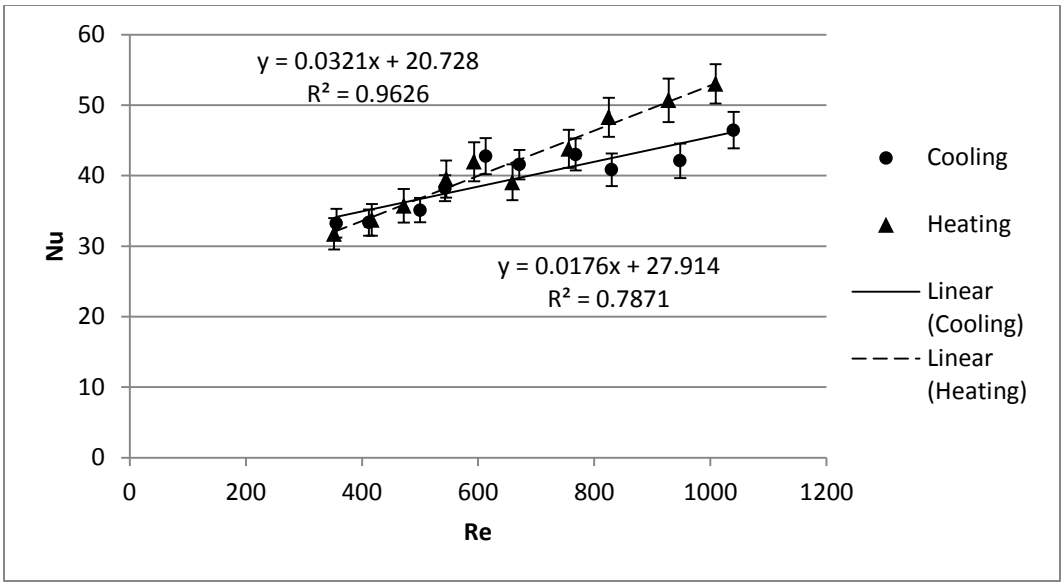


Figure 62: Nusselt Number Comparison for Procedure B Heating and Cooling

### *LEVA CORRELATIONS*

In order to investigate any difference between heating and cooling, this study's data was inputted into the correlations Leva found in 1947 and 1950. Since Leva used the overall Nusselt number, the following equation was used to find what the overall Nusselt number would be for this research's data:

Equation 25: Overall Nusselt Number

$$\frac{1}{Nu_o} = \frac{1}{Nu_w} + \frac{\frac{N}{6}}{\frac{k_r}{k_f}} * \frac{Bi + 3}{Bi + 4}$$

Since Leva used the Nusselt number based on the tube diameter and this research used the particle diameter, the predicted Nusselt number using Leva's correlations was divided by N, the ratio of the tube to particle diameter. When entering the Reynolds numbers used for this research, the following values of overall Nusselt number were predicted.

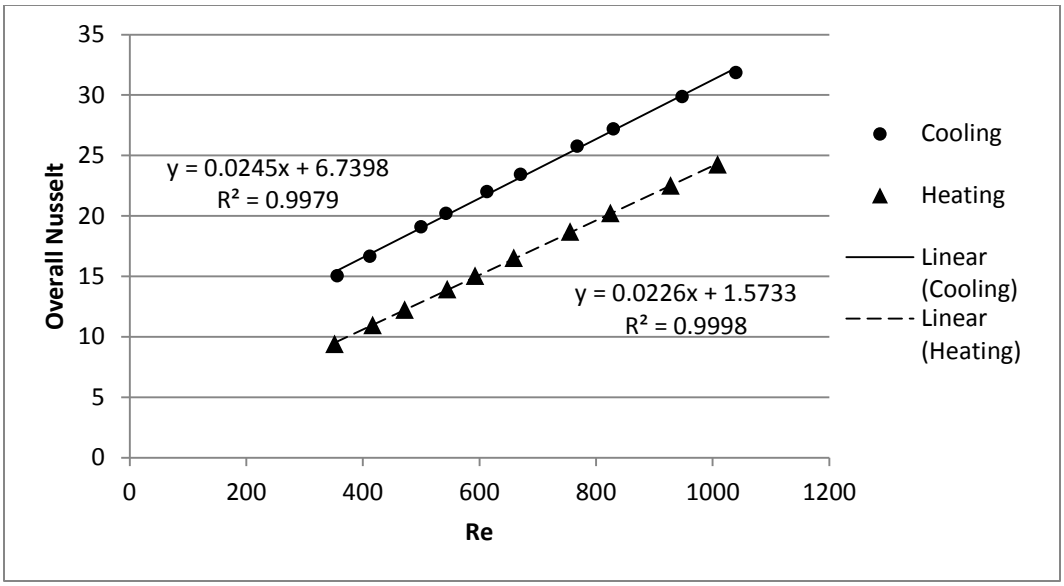


Figure 63: Predicated Values of Overall Nusselt Number Using Leva Correlations

From the Leva correlations, cooling should have a higher value for the Nusselt number. However, when the experimental values were plotted, it was found that cooling was slightly higher than heating at low Reynolds numbers and then for Reynolds numbers above 500 cooling was lower than heating, as shown in Figure 64. This shows that this study's data does not follow the correlations found by Leva, or the general trend Leva observed.

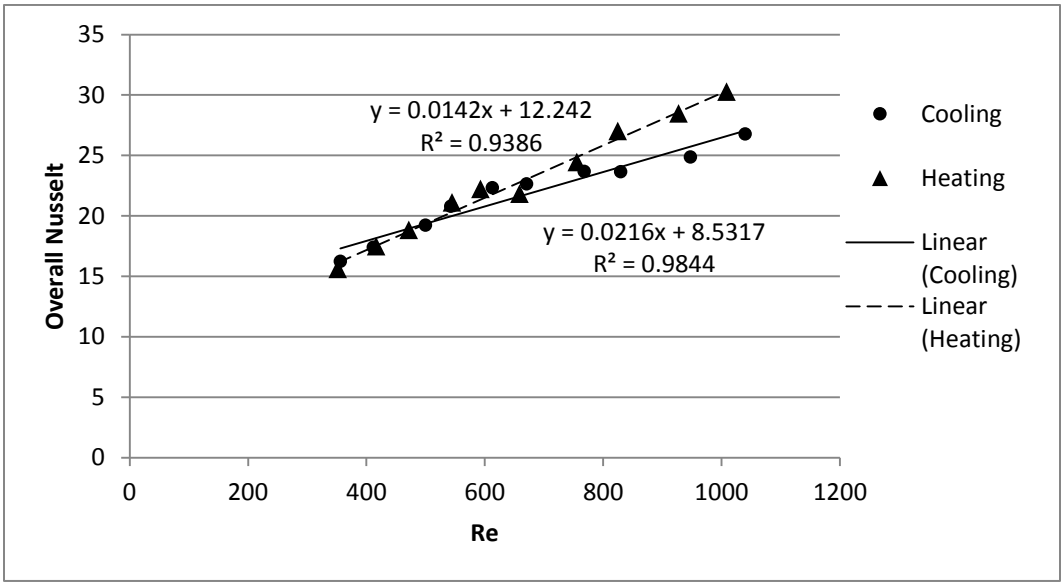


Figure 64: Experimental Values of Overall Nusselt Number

After comparing procedure B results for heating and cooling for this experiment and also the predicated values found with the Leva correlations, there is evidence to support heating and

cooling are similar or have a small difference. The difference says that cooling is slightly more effective for Reynolds numbers below 500 and for Reynolds numbers above 600 heating is slightly more effective. However, since the data was only collected for procedure B for two weeks, there is not enough data to make a definite conclusion on whether or not heating and cooling are similar.

### Including the Center Thermocouple in the GIPPF Model

After obtaining less scattered results using Procedure B, a difference was observed between this study and past studies. This could be attributed to the change in the model. All of the models run using Procedure B were re-run using the version of the model which excluded the center thermocouple measurement.

### *The Effect on the Heat Transfer Parameters*

The heat transfer parameter graphs were studied in order to see the effect of including the center thermocouple in the model. Including the center thermocouple decreased the effective radial thermal conductivity for the cooling runs, but increased the intercept. The main finding was the decrease in scatter when the center thermocouple was included.

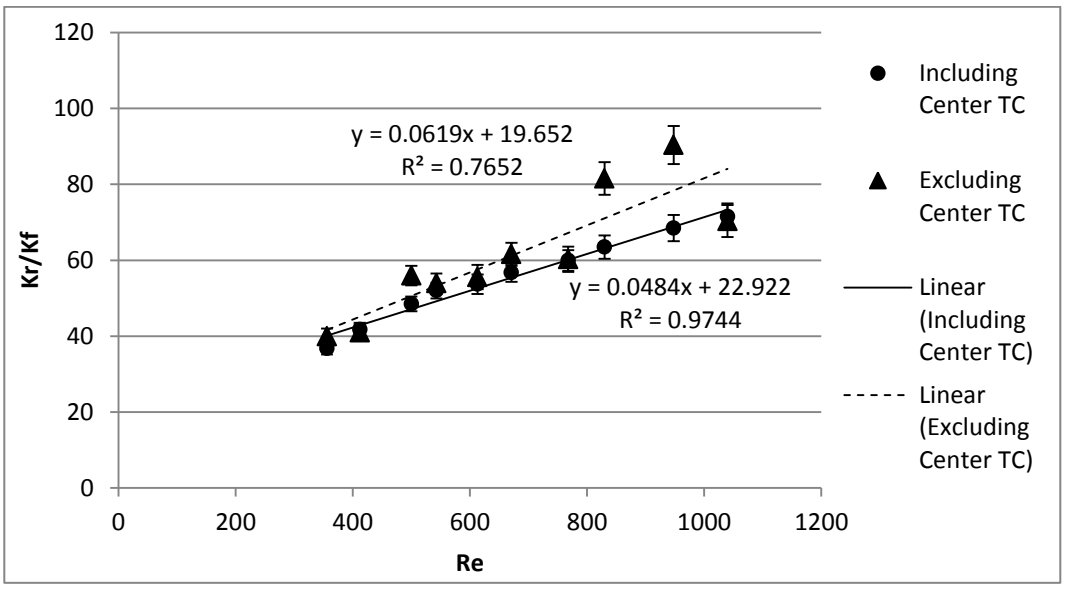


Figure 65: Effective Thermal Conductivity for Cooling Runs Including and Excluding the Center Thermocouple

For the Nusselt number, both the general trend and intercept decreased with the inclusion of the center thermocouple. The change in the model reduced the amount of scatter observed as well, which greatly increases the confidence in the data.

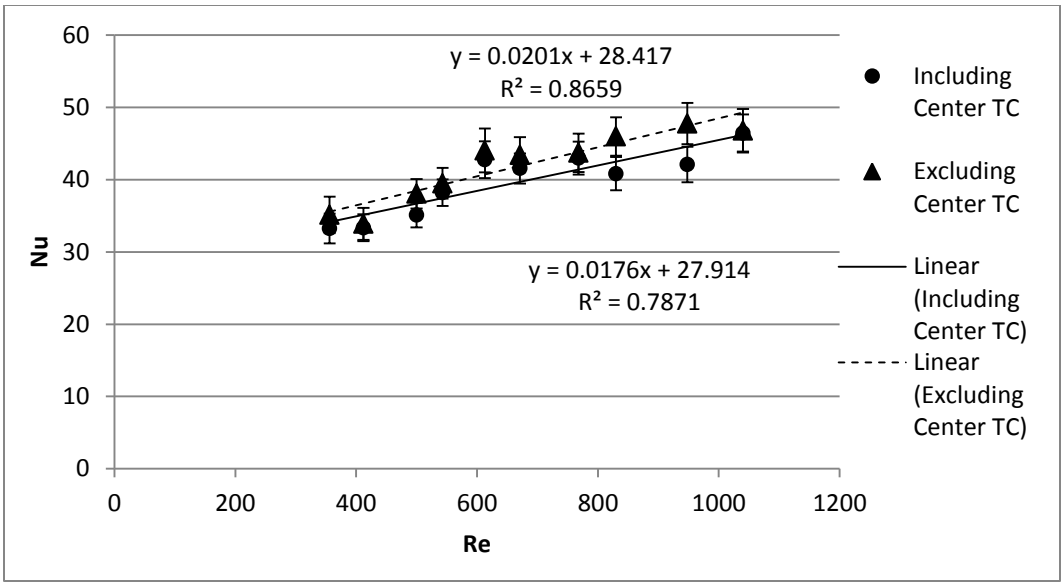


Figure 66: Nusselt Number for Cooling Runs Including and Excluding the Center Thermocouple

When the effect of including the center thermocouple for heating was reviewed, it was found that the effective thermal conductivity decreased when the center thermocouple was added. Also, the linear trend is more apparent when including the center thermocouple in the model.

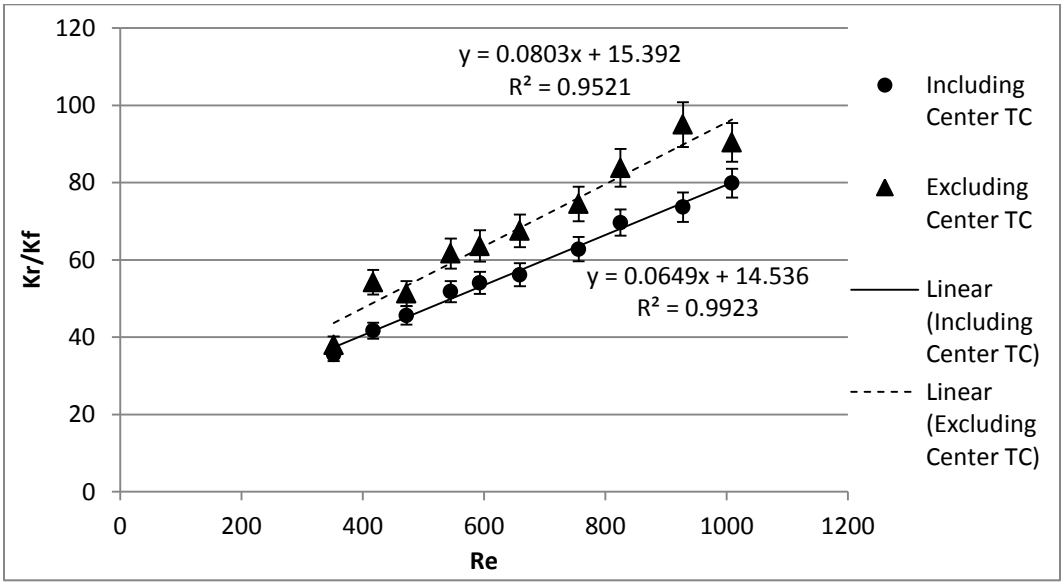


Figure 67: Effective Thermal Conductivity for Heating Runs Including and Excluding the Center Thermocouple

For the Nusselt number, the values decreased with the inclusion of the center thermocouple. The scatter increased for the inclusion of the center thermocouple, but not by a considerable degree.

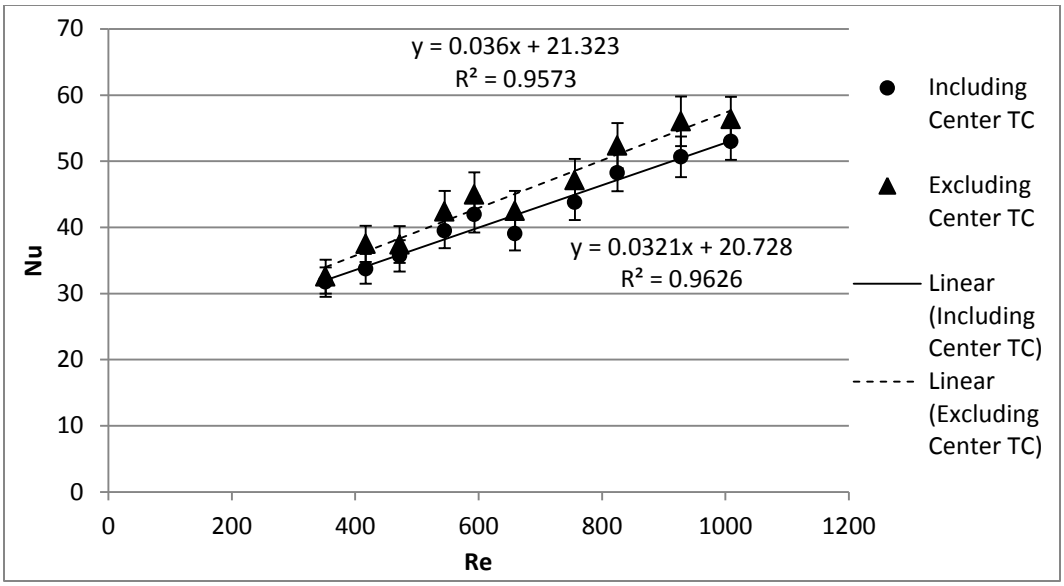


Figure 68: Nusselt Number for Heating Runs Including and Excluding the Center Thermocouple

After heating and cooling were individually compared, they were compared together to see the change between them including and excluding the center thermocouple. When the thermocouple was excluded, heating was found to be higher than cooling, as shown in Figure 69. However, when the center thermocouple is included, they cross over at a Reynolds number of about 500, as shown in Figure 70. Also, the inclusion of the thermocouple lowered the values for both heating and cooling.

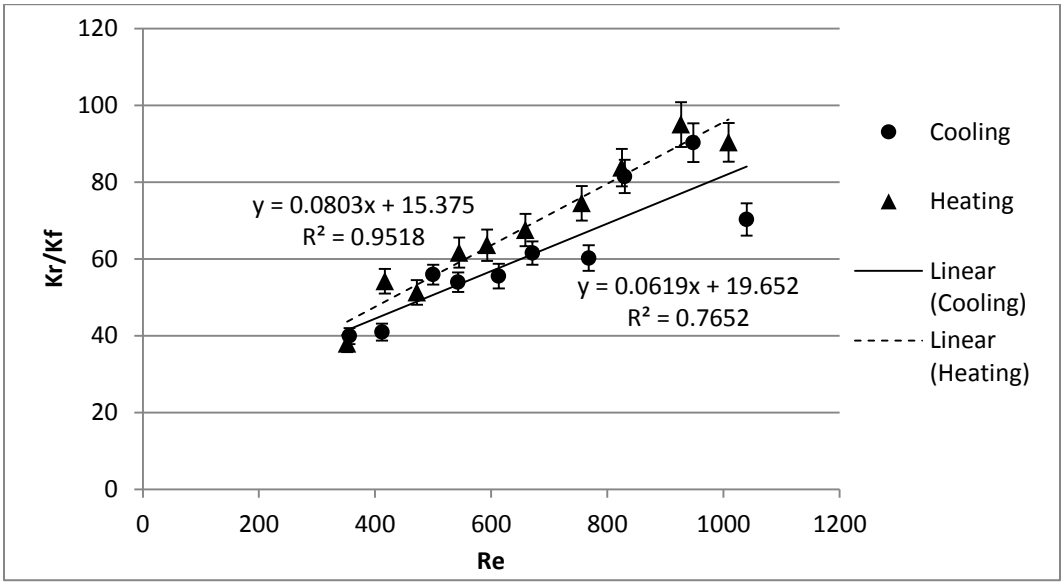


Figure 69: Effective Thermal Conductivity for Heating versus Cooling Excluding the Center Thermocouple

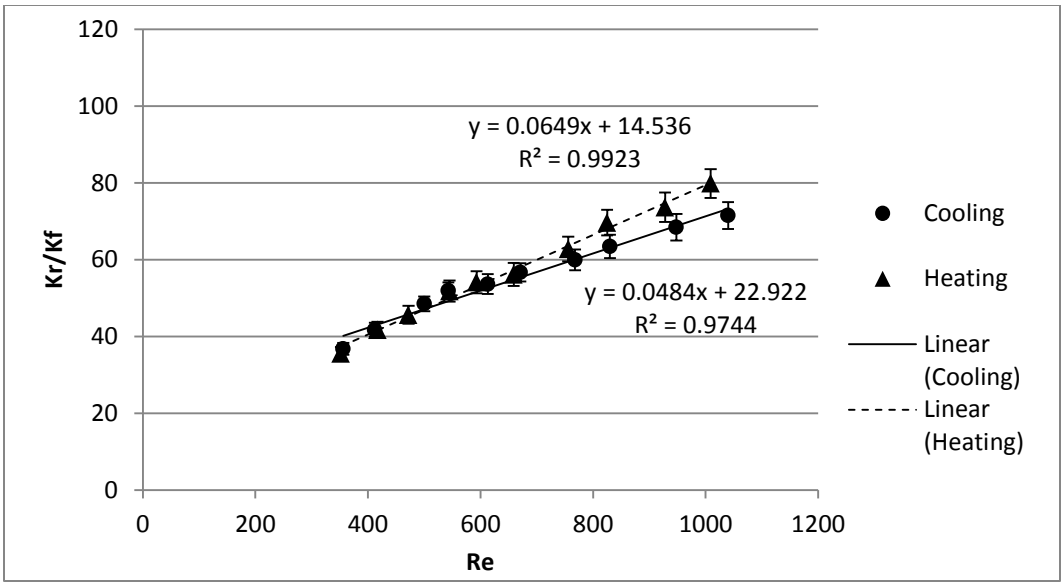


Figure 70: Effective Thermal Conductivity for Heating versus Cooling Including the Center Thermocouple

For the Nusselt number, the crossover of heating and cooling was seen for both including and excluding the center thermocouple, as shown in Figures 71-72. However, as with $k_r/k_f$, including the center thermocouple lowered the values.

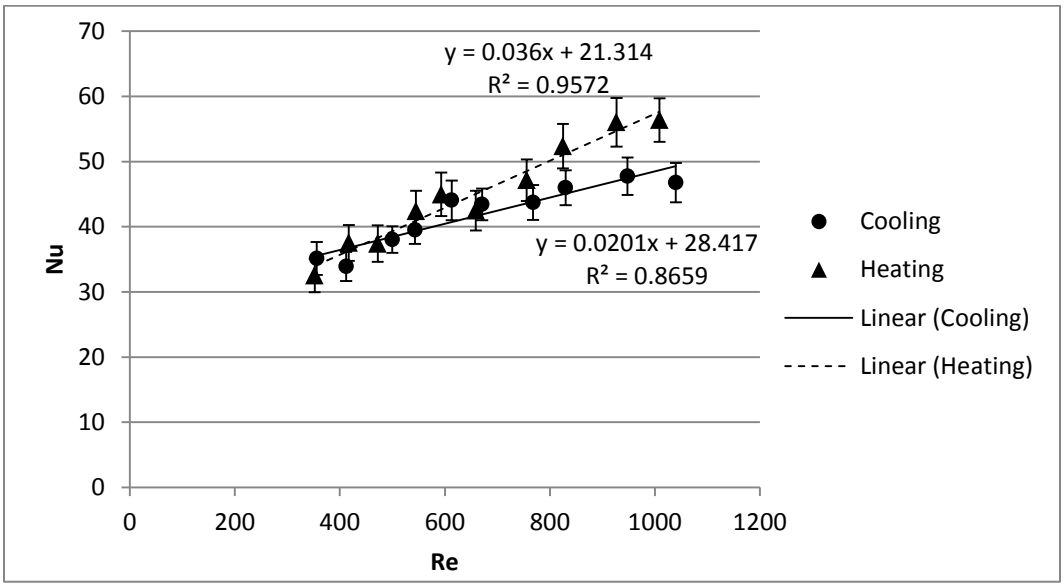


Figure 71: Nusselt Number for Heating versus Cooling Excluding the Center Thermocouple

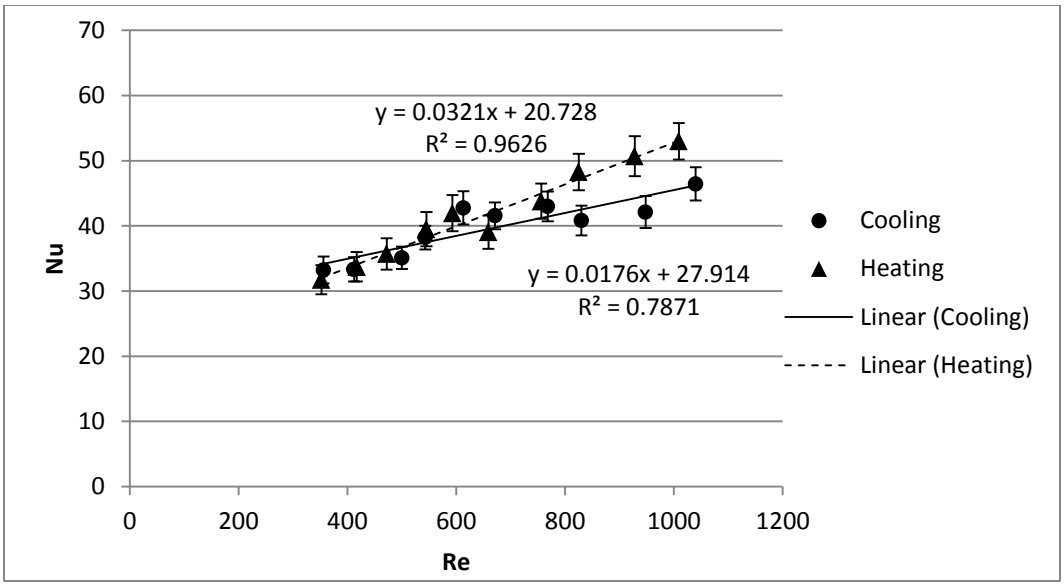


Figure 72: Nusselt Number for Heating versus Cooling Including the Center Thermocouple

The model including the center thermocouple shows heating and cooling data that is more comparable than what has been observed in the past. Also, heating is found to now be higher than cooling. Since the inclusion of the center thermocouple shifts the cooling data more than heating, this makes sense. The past data was analyzed without the center thermocouple, creating a discrepancy for a direct comparison.

## CONCLUSIONS AND RECOMMENDATIONS

This research is one of the first which conducted both heating and cooling experiments in the same column, with the same packing, with the same operators and analyzed this data using the same model. The limited number of variables allowed for more definite comparison to be made between heating and cooling in a packed bed. During the research however, changes needed to be made to the model and procedure in order to obtain reliable data that could be compared. These changes were thought of due to problems that arose during the research.

The first problem that was investigated was non-uniform wall temperatures observed during cooling experiments. The first attempt to fix this problem was to turn up the water flow rate in hopes that a higher flow would have a more constant temperature. When this did not fix the problem, it was thought in a countercurrent configuration the water was not fully covering the jacket and forming channels. These channels could have resulted in hot spots on the column. In order to test this, the column was run in a co-current configuration. When it was observed co-current did not create more uniform wall temperatures, the resulting parameters were compared for both configurations. There was not a strong enough difference between the two parameters, although countercurrent yielded results with slightly less scatter. Since the wall temperatures were not different to support a change in the experimental procedure, the original configuration of countercurrent was chosen.

The next problem that arose had to do with the interpolated inlet profile for the computer model. In the original GIPPF model, the center thermocouple was excluded and instead was found using a cubic spline interpolation. It was found that this resulted in dimensionless temperature profiles where the bed center had values larger than one for some Reynolds numbers. Due to the definition of the dimensionless temperature, this did not make physical sense. To fix this, the center thermocouple was added into the original computer model in two ways. The first way was to input the temperature value four times. The concern with this method was that since there was only one temperature reading for the center, this gave a value that was too consistent. This led to inputting -1 for the other three readings, which was supposed to indicate no reading. However when looking at the interpolated temperature profiles, it was obvious the model was reading the -1 as temperature values. This led to the

model being modified to eliminate the boundary condition at the bed center and instead including the center thermocouple reading, with the -1 values being set to mean no reading. The resulting interpolated temperature profiles made physical sense and also compared well with the experimental profiles. The recommendation is that the modified model which includes the center thermocouple and recognized -1 as no reading, be used.

Once the best model was chosen and the current research was compared to past research conducted in the same laboratory, it was found that for heating data there was more scatter in the current research. Historically, it has been observed that there was some scatter in the cooling, but not in heating. When reasons for this introduction of scatter were looked into, the only significant change was in the experimental procedure. When heating experiments were conducted, all of the Reynolds numbers were collected on one day with a constant bed height, termed Procedure B. During the Alexander et al. (2011) MQP this was changed to all four bed heights being collected on one day for a constant bed height, termed Procedure A. Therefore, heating and cooling was re-run using Procedure B. Procedure B was found to decrease the observed scatter and brought heating more in line with past heating data. The reason for this decrease in scatter is thought to be because of less re-packing of the bed and reducing on the day to day changes in air quality.

From these observations and trials, the recommended procedure for studying heat transfer in a packed bed is using countercurrent flow for cooling and using the procedure of keeping a constant bed height during the day and varying the air flow. Once this data is collected, it is recommended to analyze it using the GIPPF model that includes the center thermocouple in the dimensionless temperature profiles and recognizes an input of -1 as no reading. If possible, cooling should be modified in a way that yields more uniform wall temperatures, since heating has almost no variation in wall temperatures during runs.

When this procedure and model were decided upon, heating and cooling were able to be compared. It was found that heating and cooling appear be similar, or have very small differences. The differences found showed cooing was more effective at Reynolds numbers below 500 and heating was more effective above 600. However, since the most accurate

procedure and model were only run for two weeks, definite conclusions cannot be drawn. In order to answer this question of similarities or differences in heating and cooling, it is recommended that more data be collected using the recommended procedure and model. Also, it is recommended that several re-runs of both heating and cooling in the two-inch column with ¼-inch ceramic spheres be conducted. After several data collections have occurred, a more concise picture will be available. Also, once a conclusion is drawn for those experiential conditions, different packing and columns should be tested to see if an overall correlation between heating and cooling can be made.

## NOMENCLATURE

| | |
|---|---|
| β | Lump Parameter |
| $\theta = \frac{T-T_w}{T_o-T_w}$ | Dimensionless Temperature |
| $y = r/R$ | Dimensionless Radial Position |
| M | Viscosity of the Fluid |
| ρ | Density of Fluid |
| $Bi = \frac{h_w R}{k_r}$ | Biot Number |
| $d_p$ | Particle Diameter |
| $d_T$ | Tower Diameter |
| $h_w$ | Apparent wall heat transfer coefficient |
| $k_r$ | Effective radial thermal conductivity |
| $k_f$ | Thermal conductivity of the fluid |
| $\frac{k_r}{k_f} = \frac{RePr}{Pe_r}$ | Effective Conductivity |
| $N = \frac{d_T}{d_P}$ | Tube to Particle Diameter Ratio |
| $Nu_w = \frac{h_w d_p}{k_f}$ | Wall Nusselt Number |
| $Pe_r = \frac{\rho v c_p d_p}{k_r}$ | Radial Peclet Number |
| $Pe_\rho^s = Re \cdot Pr$ | Molecular Superficial Peclet Number |
| $Pe_\rho^i = \frac{\rho_f Cp_f v d_p}{\epsilon k_f} = \frac{Re \cdot Pr}{\epsilon}$ | Molecular Interstitial Peclet Number |
| R | Tower Radius |
| $Re = \frac{\rho v d_p}{\mu}$ | Reynolds Number |
| U | Overall Heat-Transfer Coefficient |
| v | Fluid Velocity |

## WORKS CITED


Adeyanju, A. A., & Manohar, K. (2009). Theoretical and Experimental Investigation of Heat Transfer in Packed Beds . *Research Journal of Applied Sciences, 4*(5), 166-177.

Alexander, T. E., Ledwith, B. C., & Linskey, M. M. (2011, April 27). Heat Transfer in Packed Bed Reactors -- Heating vs. Cooling.

Ashman, M., Rybak, D., & Skene, W. (2009). Heat Transfer Parameters of Cylindrical Catalyst Particles with Internal Voids in Fixed Bed Reactor Tubes. *Worcester Polytechnic Institute*.

Batchelor, G. K. (1967). *An Introduction to Fluid Dynamics.* Cambridge University Press.

Borkink, J. G., & Westerterp, K. R. (1992 a). Determination of Effective Heat Transport Coefficents for Wall-Cooled Packed Beds. *Chemical Engineering Science, 47*(9-11), 2337-2342.

Borkink, J. G., & Westerterp, K. R. (1992 b, May). Influence of Tube and Particle Diameter on Heat Transfer in Packed Beds. *AIChE Journal, 38*(5), 703-715.

Borkink, J., Borman, P., & Westerterp, K. (1993). Modeling of the Radial Heat Transport of Wall-Cooled Packed Beds. *Chemical Engineering Communications*, 121,135-155.

Chubb, C. (1991). (WPI, Ed.)

de Wasch, A. P., & Froment, G. F. (1972). Heat Transfer in Packed Beds. *Chemical Engineering Science, 27*(3), 567-576.

DeWitt, B. L. (2007). *Fundamentals of Heat and Mass Transfer (6th Edition).* New York: John Wiley & Sons.

Dixon, A. G. (1985, December). The Length Effect on Packed Bed Effective Heat Transfer Parameters. *Chemical Engineering Journal, 31*(3), 163–173.

Dixon, A. G. (2012 a, November 16). Heat Transfer Modelings. (A. DiNino, E. Hartzel, K. Judge, & A. Morgan, Interviewers)

Dixon, A. G. (2012 b, June). Fixed Bed Catalytic Reactor Modelling—the Radial Heat Transfer Problem. *The Canadian Journal of Chemical Engineering, 90*(3), 507-527.

Dixon, A. G., & van Dongeren, J. H. (1998). The influence of the tube and particle diameters at constant ratio on heat transfer on packed beds . *Chemical Engineering and Processing, 37*, 23-32.

Freiwald, M. G., & Paterson, W. (1992). Accuracy of Model Predictions and Reliability of Experimental Data for Heat Transfer in Packed Beds. *Chemical Engineering Science, 47*(7), 1545-1560.

Kwong, S. S., & Smith, J. M. (1957, May). Radial Heat Transfer in Packed Beds. *Industrial & Engineering Chemistry, 49*(5), 894-903.

Leva, M. (1947). Heat Transfer to Gases through Packed Tubes. *Industrial and Engineering Chemistry*, 857-862.

Leva, M. (1950). Packed-Tube Heat Transfer. *Industrial and Engineering Chemistry*, 2498-2501.

Patankar, S. V. (1980). *Numerical Heat Transfer and Fluid Flow.* New York: McGraw-Hill.

Pollica, D. (1996). (WPI, Ed.)

Thomeo, J. C., Rouiller, C. O., & Freire, J. T. (2004, June 11). Experimental Analysis of Heat Transfer in Packed Beds with Air Flow. *Industrial and Engineering Chemistry Research, 43*(15), 4140-4148.

Wen, D., & Ding, Y. (2006, Feburary 15). Heat transfer of gas flow through a packed bed. *Chemical Engineering Science, 61*, 3532-3542.

Wijngaarden, R., & Westerterp, K. R. (1992, December 6). The Statistical Character of Packed-bed Heat Transport Properties. *Chemical Engineering Science, 47*(12), 3125-3129.

Winterberg, M., Tsotsas, E., Krischke, A., & Vortmeyer, D. (2000). A simple and coherent set of coefficients for modelling of heat and mass transport with and without chemical reaction in tubes filled with spheres. *Chemical Engineering Science, 55*(5), 967-979.

# APPENDIX

## APPENDIX A: SUMMARY OF RUNS PROCEDURE A

**Table 5: Procedure A Summary of Runs**

| Date of Run | Co or Counter Water? | Reynolds Number | Air % | Pe | Bi | Kr/Kf | Nu | F | F/Fcrit |
|---|---|---|---|---|---|---|---|---|---|
| 9/14/12 | Counter Cooling | 474.1 | 31.5 | 9.309 | 3.88 | 36.661 | 35.564 | 3.95135 | 2.399134178 |
| 9/21/12 | Counter Cooling | 867.3 | 52 | 10.387 | 2.775 | 60.101 | 41.699 | 2.88203 | 1.749877048 |
| 9/26/12 | Counter Cooling | 376.2 | 25 | 6.759 | 3.27 | 40.052 | 32.743 | 3.30596 | 2.007273875 |
| 11/30/12 | Counter Cooling | 419.9 | 28 | 8.327 | 4.449 | 36.23 | 40.298 | 8.2005 | 4.979083055 |
| 12/3/12 | Counter Cooling | 539.5 | 35 | 7.716 | 3.066 | 50.297 | 38.557 | 4.16753 | 2.530391806 |
| 12/5/12 | Counter Cooling | 602.1 | 38 | 6.935 | 3.221 | 62.499 | 50.321 | 1.22891 | 0.746155107 |
| 12/6/12 | Counter Cooling | 667.3 | 41 | 9.83 | 3.141 | 48.857 | 38.36 | 1.84908 | 1.122702627 |
| 12/7/12 | Counter Cooling | 838.5 | 48 | 9.964 | 2.655 | 60.551 | 40.184 | 5.42334 | 3.292879738 |
| 12/10/12 | Counter Cooling | 1037.8 | 55 | 8.741 | 2.478 | 85.422 | 52.928 | 3.86225 | 2.345035489 |
| 12/12/12 | Counter Cooling | 758.3 | 45 | 8.135 | 2.799 | 67.09 | 46.947 | 2.516 | 1.527635262 |
| 12/13/12 | Counter Cooling | 954.7 | 52 | 8.781 | 2.386 | 78.384 | 46.751 | 2.46917 | 1.499201574 |
| 11/5/12 | Co-Current Cooling | 366.5 | 25 | 5.569 | 4.752 | 47.319 | 56.211 | 2.57138 | 1.561260238 |
| 11/7/12 | Co-Current Cooling | 474.1 | 31.5 | 6.881 | 4.049 | 49.598 | 50.202 | 4.89722 | 2.97343639 |
| 11/8/12 | Co-Current Cooling | 760.2 | 45 | 9.019 | 3.251 | 60.673 | 49.308 | 3.43274 | 2.084250663 |
| 11/9/12 | Co-Current Cooling | 943.6 | 52 | 8.264 | 3.006 | 82.162 | 61.753 | 1.9594 | 1.189685426 |
| 11/12/12 | Co-Current Cooling | 602.1 | 38 | 8.137 | 3.538 | 53.268 | 47.122 | 1.99681 | 1.21239959 |
| 11/14/12 | Co-Current Cooling | 419.9 | 28 | 6.553 | 3.243 | 46.036 | 37.329 | 3.89943 | 2.367610004 |
| 11/15/12 | Co-Current Cooling | 539.5 | 35 | 8.198 | 2.924 | 47.339 | 34.601 | 2.13561 | 1.29667454 |
| 11/19/12 | Co-Current Cooling | 667.3 | 41 | 6.664 | 3.083 | 72.28 | 55.718 | 5.0813 | 3.085203917 |
| 11/26/12 | Co-Current Cooling | 838.5 | 48 | 8.659 | 2.75 | 69.681 | 47.909 | 2.35528 | 1.430051184 |

| | | | | | | | | | |
|---|---|---|---|---|---|---|---|---|---|
| 11/29/12 | Co-Current Cooling | 1038.7 | 55 | 10.314 | 2.644 | 72.462 | 47.893 | 3.17539 | 1.92799592 |
| 1/16/13 | Heating | 366.8 | 25 | 6.582 | 4.087 | 40.146 | 41.017 | 1.9467 | 1.18 |
| 1/17/13 | Heating | 410.8 | 28 | 7.983 | 3.93 | 37.068 | 36.416 | 3.71412 | 2.26 |
| 1/22/13 | Heating | 479 | 31.5 | 6.914 | 3.822 | 49.878 | 47.665 | 1.76764 | 1.07 |
| 1/23/13 | Heating | 532.2 | 35 | 7.802 | 4.012 | 49.092 | 49.235 | 1.67657 | 1.02 |
| 1/24/13 | Heating | 588.7 | 38 | 6.596 | 4.095 | 64.297 | 65.822 | 1.92687 | 1.17 |
| 1/28/13 | Heating | 656.2 | 41 | 8.618 | 3.628 | 54.808 | 49.709 | 1.4938 | 0.91 |
| 1/29/13 | Heating | 739.9 | 45 | 9.634 | 3.209 | 55.306 | 44.372 | 2.68523 | 1.63 |
| 1/30/13 | Heating | 792 | 48 | 8.488 | 3.407 | 67.186 | 57.222 | 2 | 1.21 |
| 1/31/13 | Heating | 908.4 | 52 | 8.891 | 3.107 | 73.533 | 57.118 | 2.31714 | 4.41 |
| 2/4/13 | Heating | 1022 | 55 | 7.752 | 1.574 | 94.925 | 37.35 | 12.95259 | 7.86440112 |
| 2/5/13 | Heating | 582.7 | 38 | 6.836 | 3.15 | 61.297 | 48.273 | 2.96065 | 1.797612615 |
| 2/6/13 | Heating | 586 | 38 | 8.363 | 4.16 | 50.45 | 52.472 | 1.78219 | 1.082089144 |
| 2/7/13 | Heating | 582.7 | 38 | 8.672 | 3.448 | 48.319 | 41.656 | 1.36059 | 0.826107019 |
| 2/11/13 | Heating | 585.5 | 38 | 9.251 | 3.874 | 45.531 | 44.094 | 1.99353 | 1.210408078 |
| 2/12/13 | Heating | 305.2 | 21 | 6.637 | 4.336 | 33.089 | 35.866 | 2.60849 | 1.583792251 |
| 2/13/13 | Heating | 257.5 | 18 | 7.081 | 5.355 | 26.132 | 34.986 | 1.91693 | 1.163898991 |
| 2/15/13 | Heating | 214.4 | 15 | 6.25 | 6.673 | 24.653 | 41.13 | 0.94518 | 0.573883266 |
| 2/20/13 | Heating | 992.3 | 55 | 9.689 | 2.744 | 73.716 | 50.562 | 2.71519 | 1.648577101 |

## APPENDIX B: SUMMARY OF RUNS PROCEDURE B

**Table 6: Procedure B Summary of Runs**

| Date | Heating of Cooling? | Reynolds Number | Air % | Pe | Bi | Kr/Kf | Nu | F | F/Fcrit |
|---|---|---|---|---|---|---|---|---|---|
| 3/11-15/2013 | Heating | 325.1 | 25% | 7.136 | 3.575 | 35.516 | 31.744 | 2.37184 | 1.44010589 |
| 3/11-15/2013 | Heating | 417 | 28% | 7.197 | 3.234 | 41.719 | 33.728 | 2.24446 | 1.362764801 |
| 3/11-15/2013 | Heating | 472.4 | 31% | 7.443 | 3.128 | 45.659 | 35.701 | 1.49394 | 0.907072903 |
| 3/11-15/2013 | Heating | 545.8 | 35% | 7.574 | 3.05 | 51.808 | 39.5 | 1.36288 | 0.827497435 |
| 3/11-15/2013 | Heating | 593 | 38% | 7.894 | 3.104 | 54.085 | 41.974 | 1.93971 | 1.177730284 |
| 3/11-15/2013 | Heating | 659.6 | 41% | 8.45 | 2.781 | 56.155 | 39.043 | 1.63679 | 0.993806884 |
| 3/11-15/2013 | Heating | 756.9 | 45% | 8.667 | 2.789 | 62.805 | 43.788 | 1.80412 | 1.095404344 |
| 3/11-15/2013 | Heating | 825.1 | 48% | 8.525 | 2.771 | 69.675 | 48.269 | 2.51612 | 1.527708122 |
| 3/11-15/2013 | Heating | 927.9 | 52% | 9.069 | 2.751 | 73.672 | 50.676 | 2.57903 | 1.565905075 |
| 3/11-15/2013 | Heating | 1009.1 | 55% | 9.096 | 2.654 | 79.872 | 52.993 | 3.41021 | 2.070571163 |
| 3/18-22/2013 | Cooling | 356.4 | 25% | 6.968 | 3.615 | 36.784 | 33.24 | 4.54837 | 2.761625754 |
| 3/18-22/2013 | Cooling | 412.9 | 28% | 7.112 | 3.197 | 41.711 | 33.341 | 2.42097 | 1.469936065 |
| 3/18-22/2013 | Cooling | 500.7 | 31% | 7.423 | 2.895 | 48.498 | 35.104 | 2.68832 | 1.632262491 |
| 3/18-22/2013 | Cooling | 543.9 | 35% | 7.52 | 2.94 | 51.986 | 38.215 | 2.89613 | 1.75843812 |
| 3/18-22/2013 | Cooling | 613.9 | 38% | 8.225 | 3.187 | 53.662 | 42.754 | 2.61213 | 1.586002344 |
| 3/18-22/2013 | Cooling | 671.4 | 41% | 8.519 | 2.931 | 56.713 | 41.555 | 1.72333 | 1.046351223 |
| 3/18-22/2013 | Cooling | 768.2 | 45% | 9.227 | 2.869 | 59.931 | 42.99 | 1.72191 | 1.045489044 |
| 3/18-22/2013 | Cooling | 830.2 | 48% | 9.418 | 2.574 | 63.453 | 40.828 | 2.5986 | 1.577787358 |
| 3/18-22/2013 | Cooling | 948.5 | 52% | 9.97 | 2.46 | 68.465 | 42.107 | 2.85532 | 1.733659585 |
| 3/18-22/2013 | Cooling | 1040.5 | 55% | 10.471 | 2.598 | 71.514 | 46.449 | 4.51395 | 2.740727023 |

## APPENDIX C: COUNTER COOLING TEMPERATURE PROFILE GRAPHS PROCEDURE A

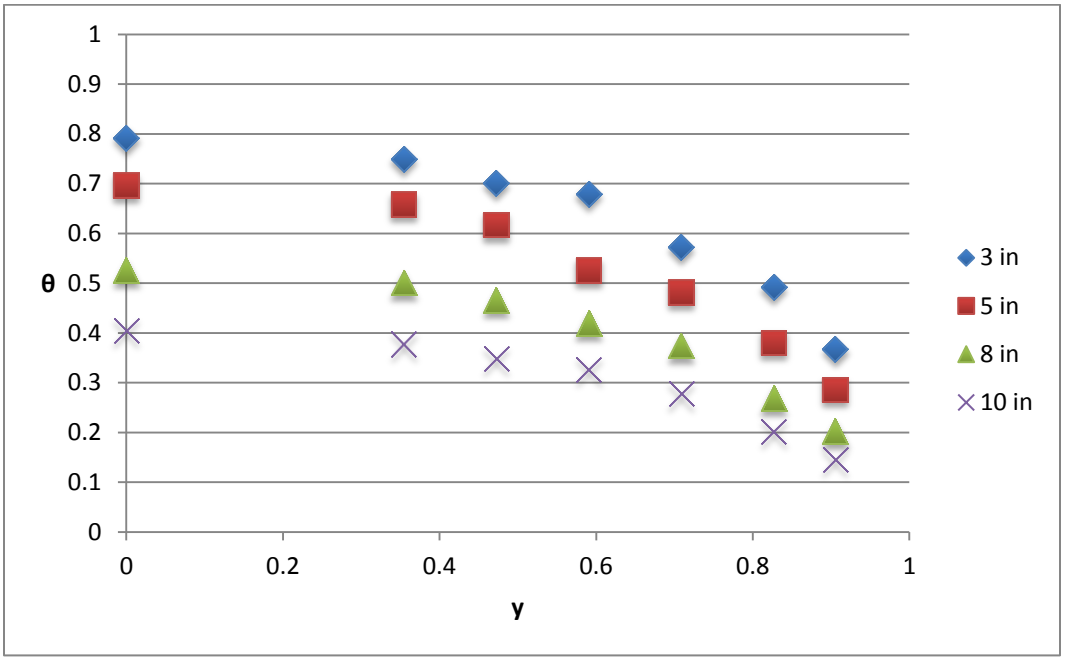


Figure 73: Countercurrent Cooling Temperature Profile for Re=474 Procedure A

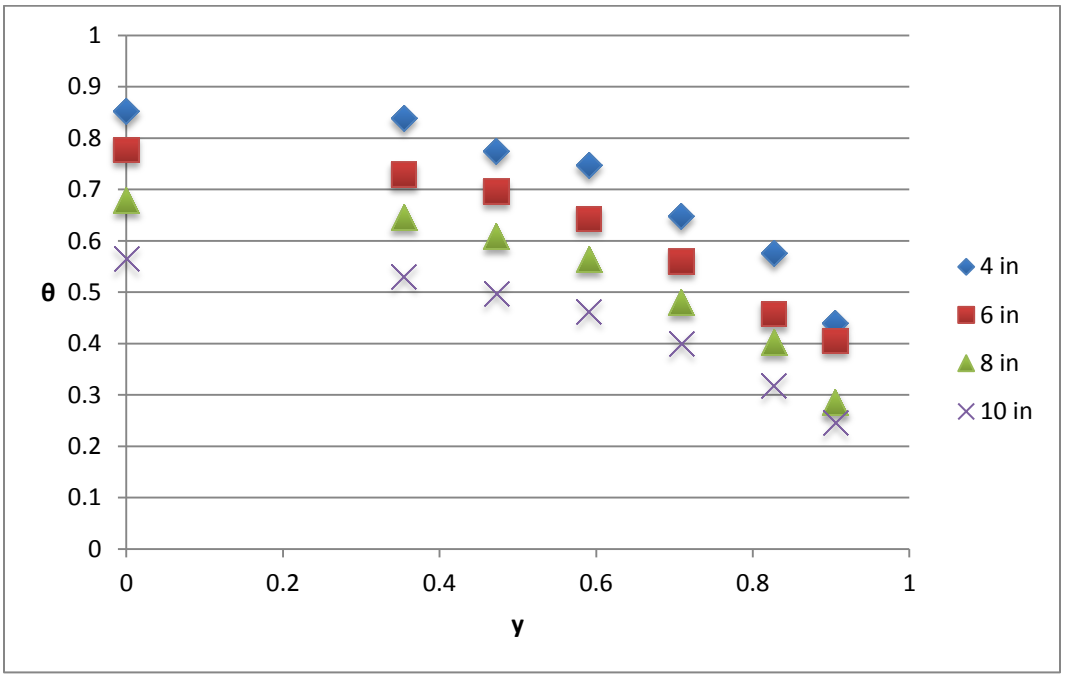


Figure 74: Countercurrent Cooling Temperature Profile for Re=867 Procedure A

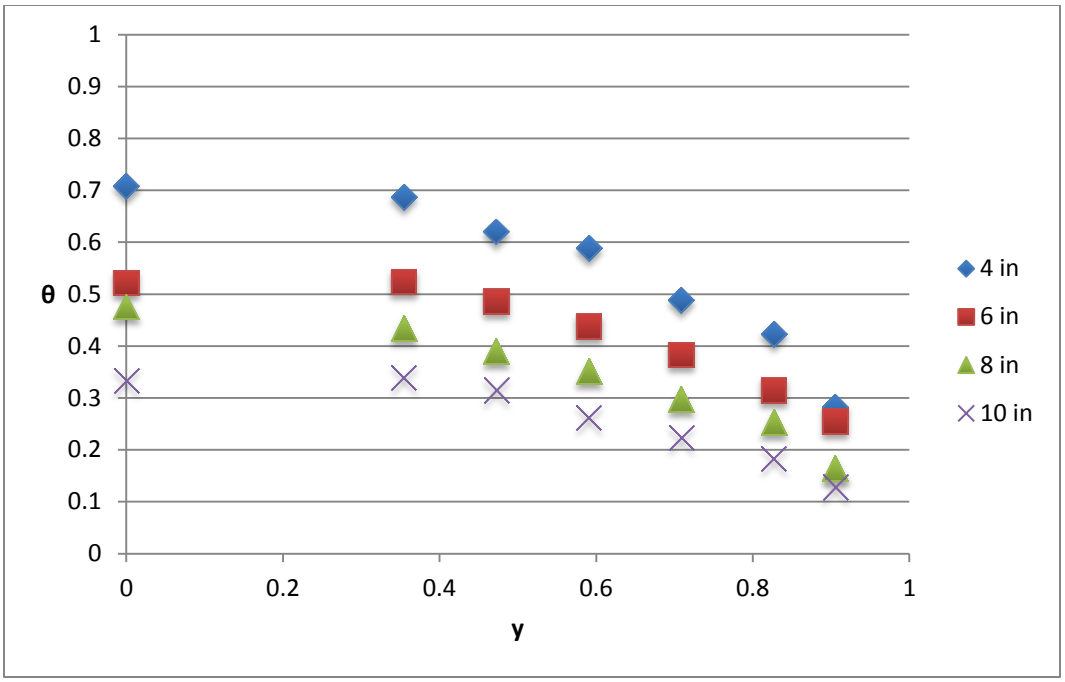


Figure 75: Countercurrent Cooling Temperature Profile for Re=376 Procedure A

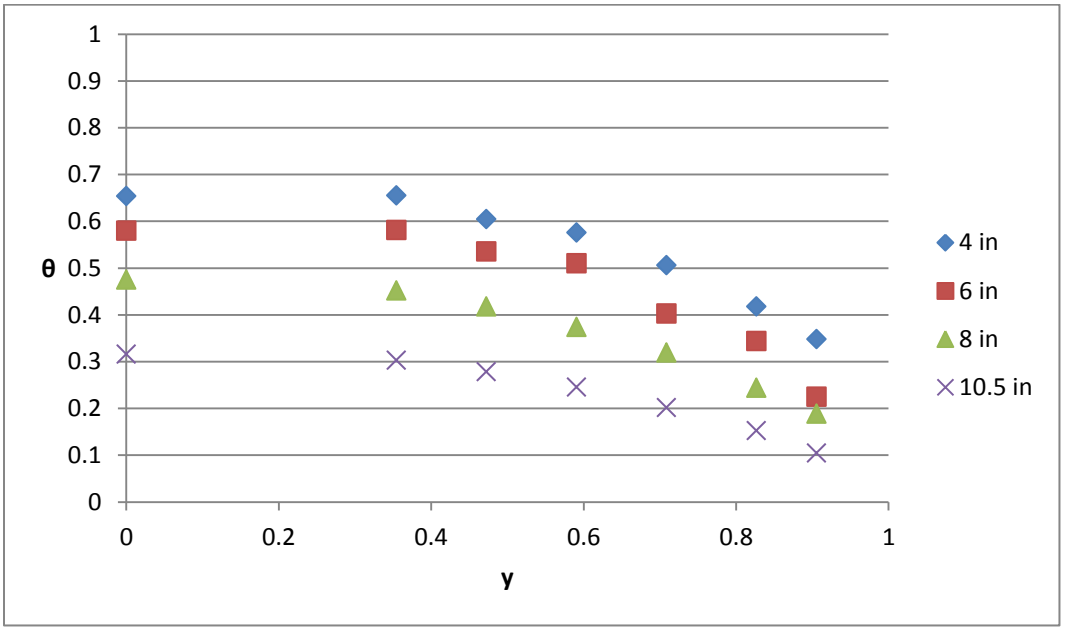


Figure 76: Countercurrent Cooling Temperature Profile for Re=420 Procedure A

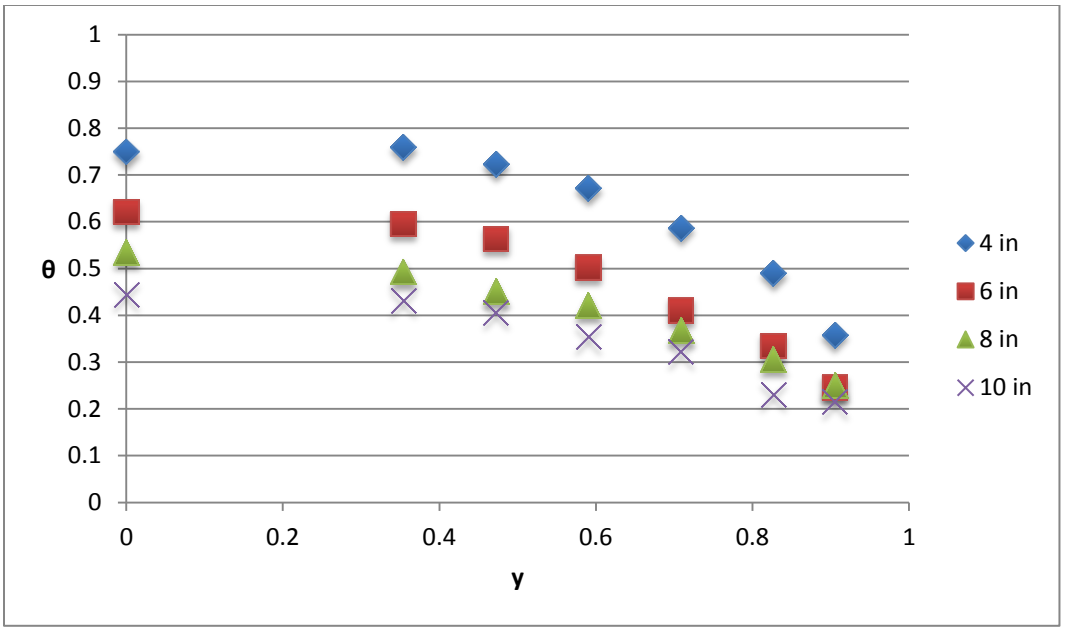


Figure 77: Countercurrent Cooling Temperature Profile for Re=540 Procedure A

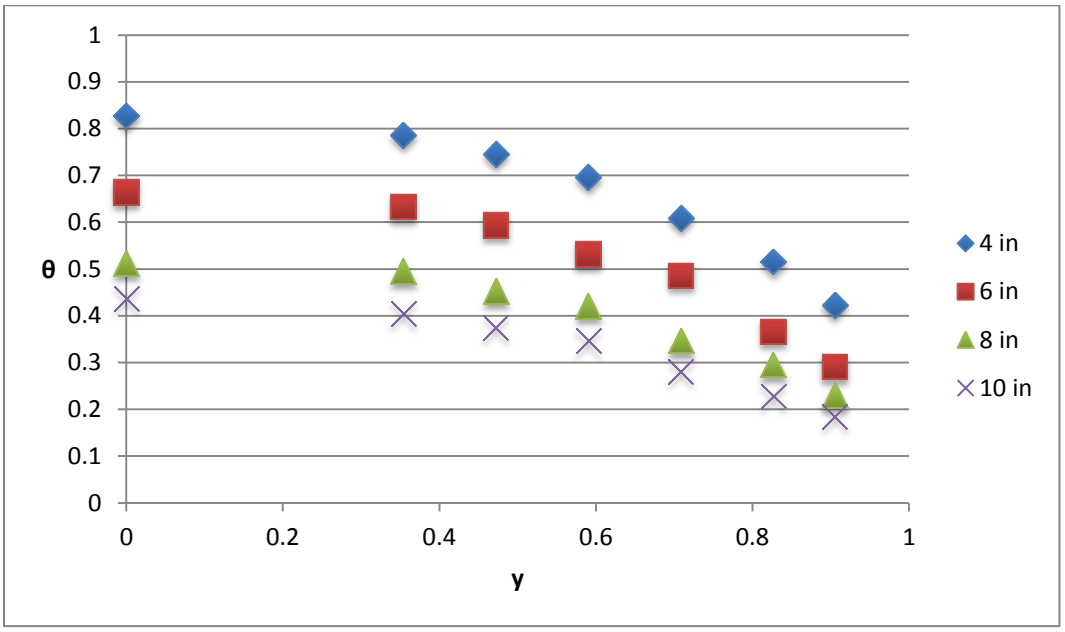


Figure 78: Countercurrent Cooling Temperature Profile for Re=602 Procedure A

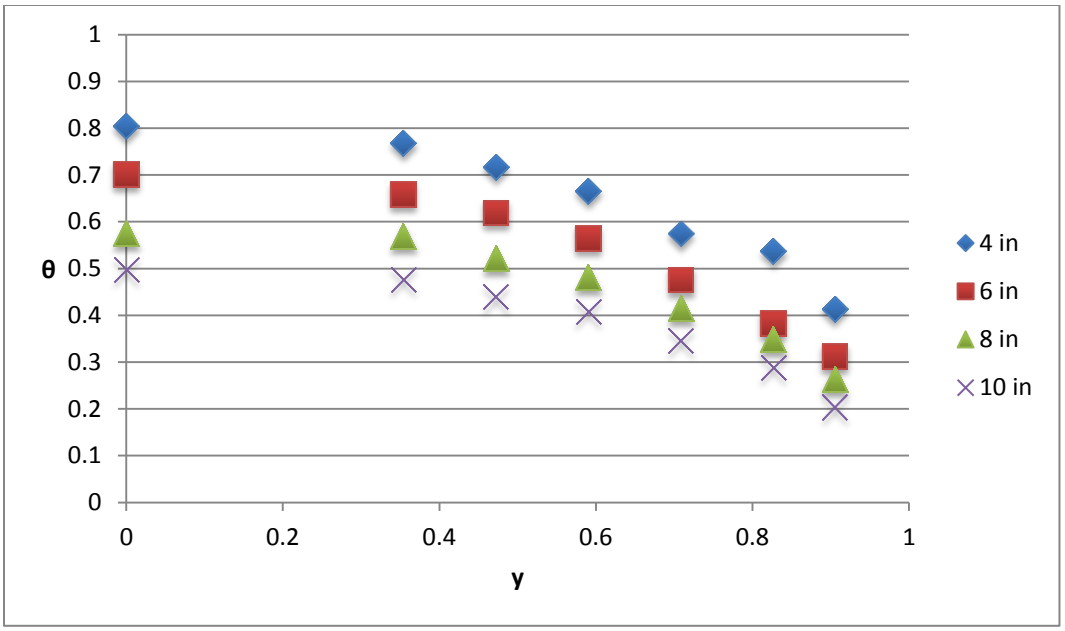


Figure 79: Countercurrent Cooling Temperature Profile for Re=667 Procedure A

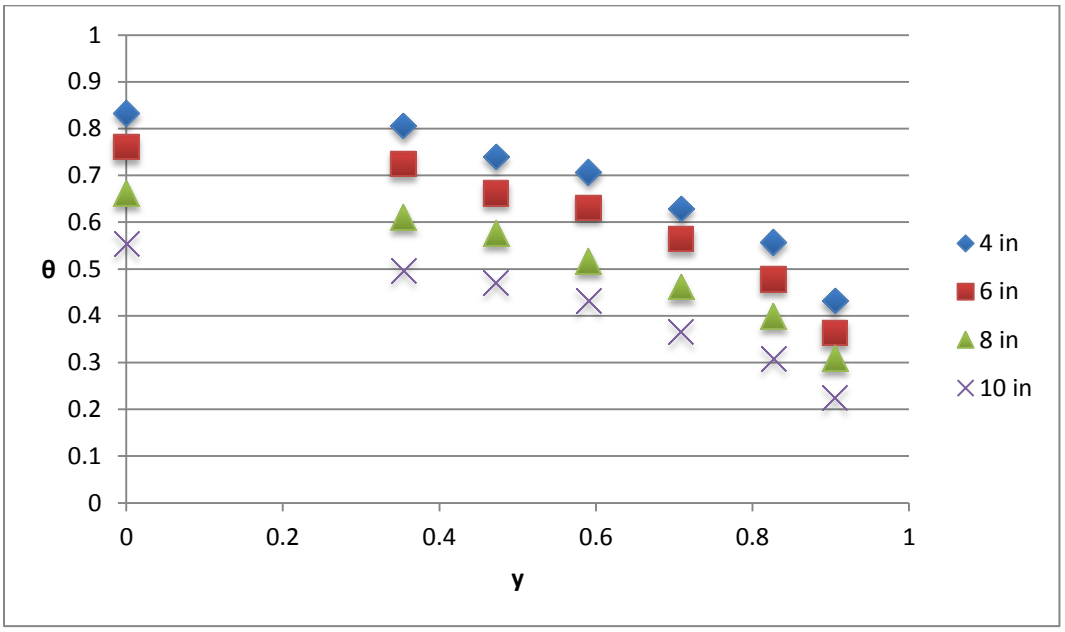


Figure 80: Countercurrent Cooling Temperature Profile for Re=839 Procedure A

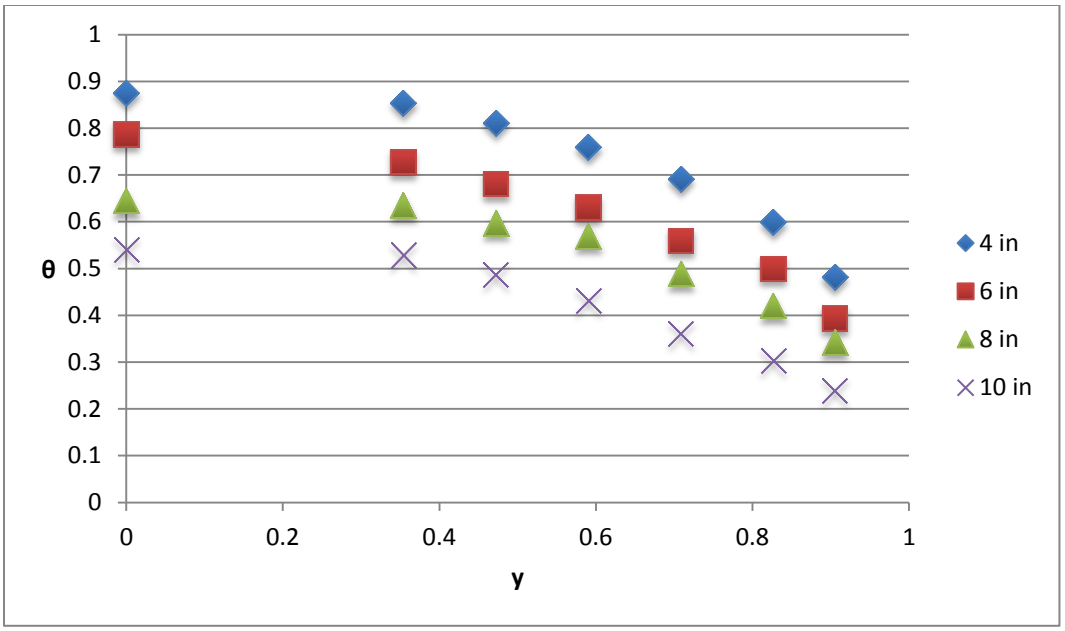


Figure 81: Countercurrent Cooling Temperature Profile for Re=1038 Procedure A

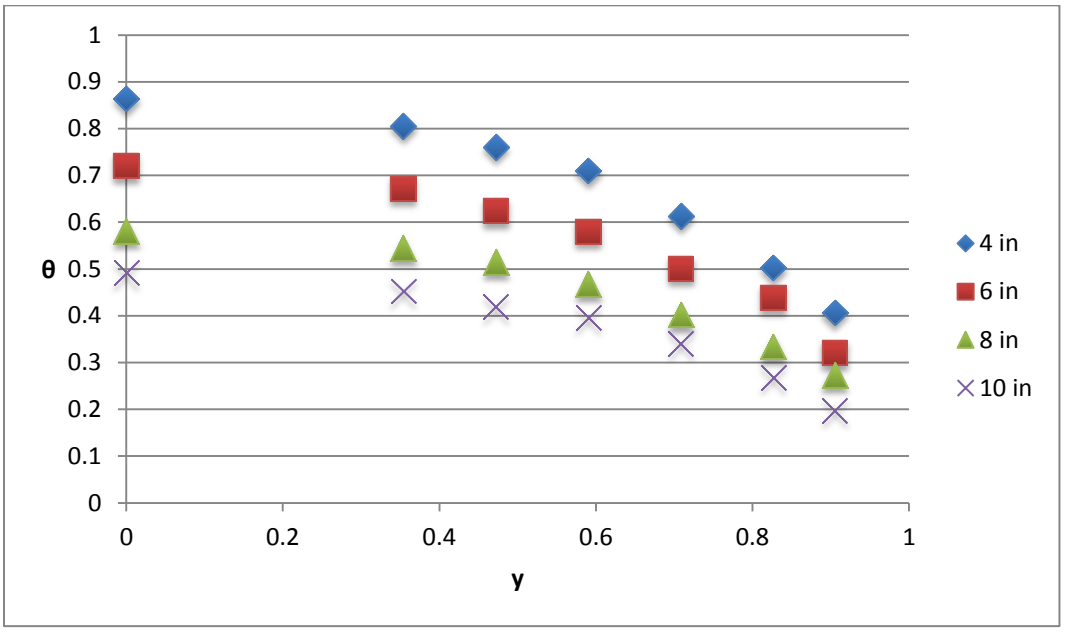


Figure 82: Countercurrent Cooling Temperature Profile for Re=758 Procedure A

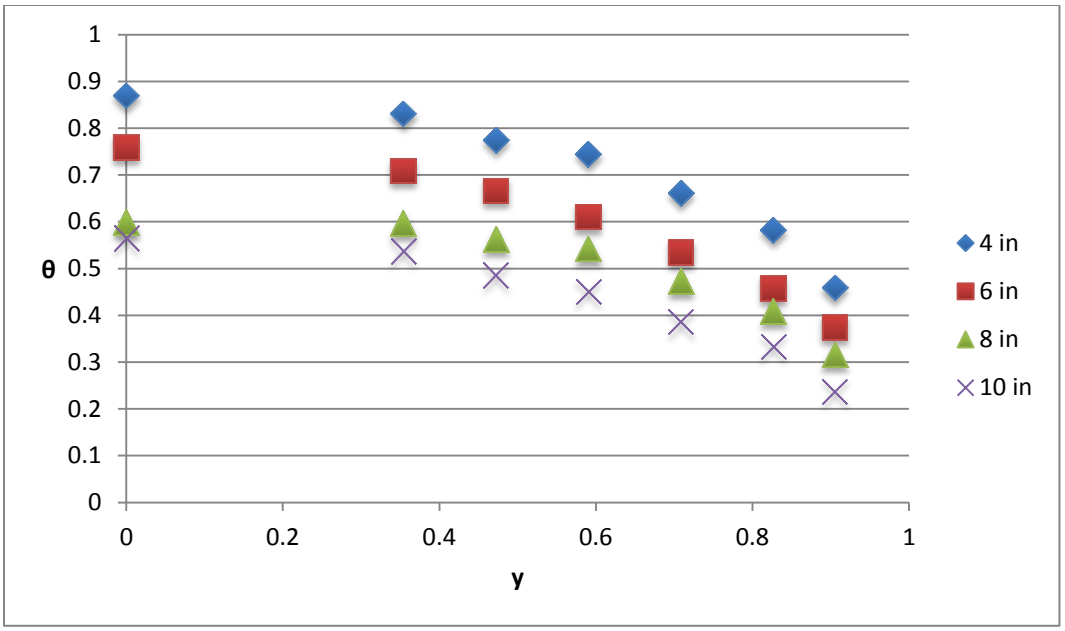


Figure 83: Countercurrent Cooling Temperature Profile for Re=954.7 Procedure A

## APPENDIX D: CO-CURRENT COOLING TEMPERATURE PROFILE GRAPHS PROCEDURE A

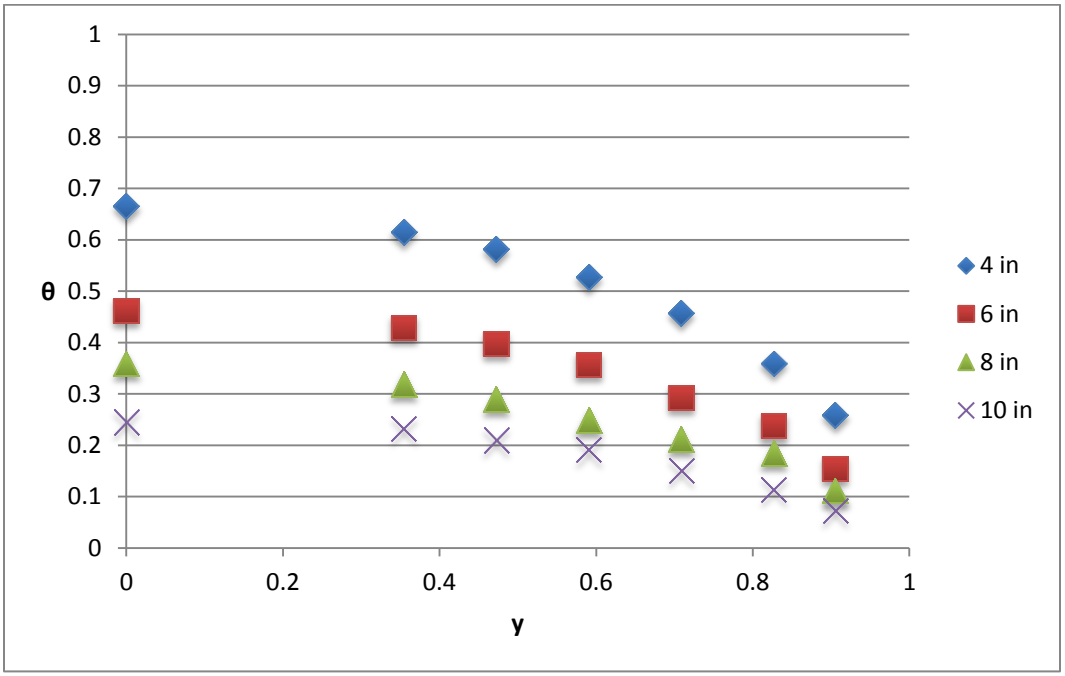


Figure 84: Co-current Cooling Temperature Profile for Re=367 Procedure A

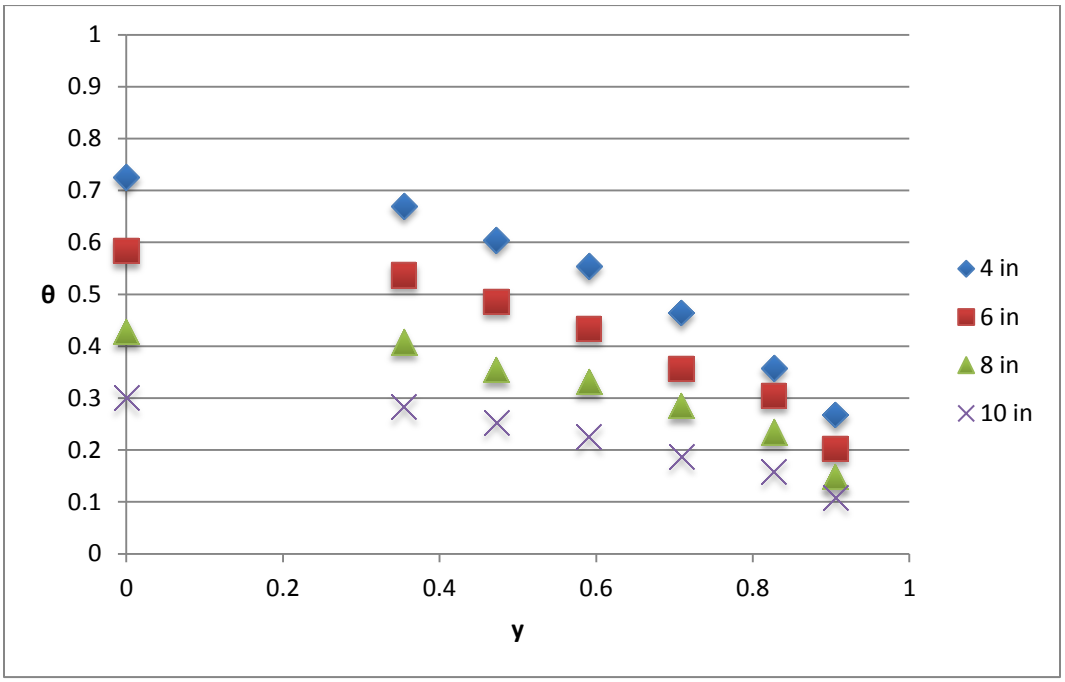


Figure 85: Co-current Cooling Temperature Profile for Re=474 Procedure A

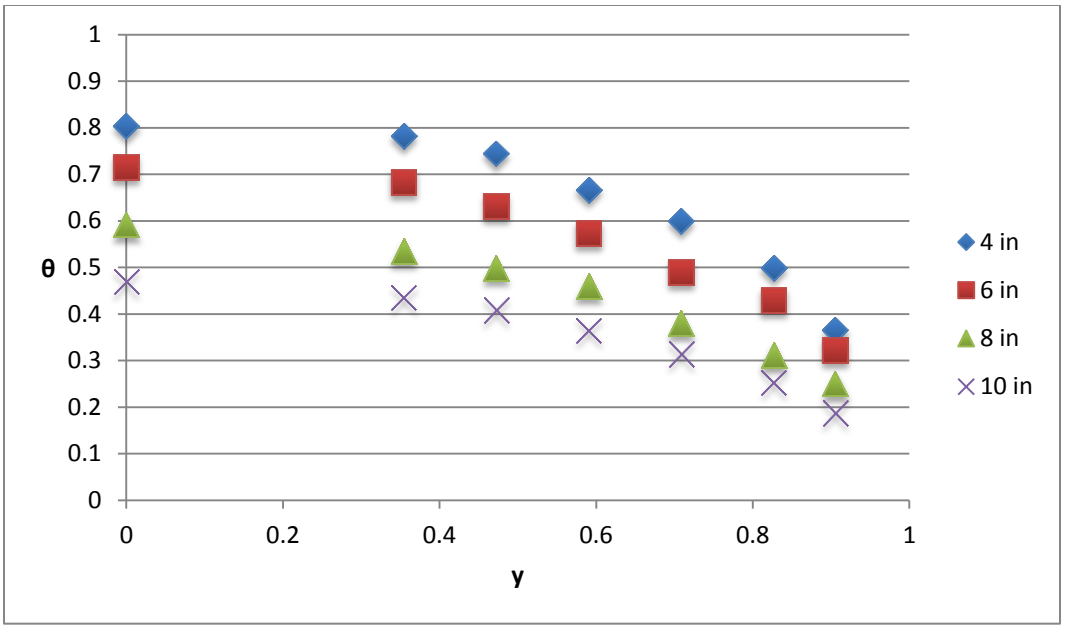


Figure 86: Co-current Cooling Temperature Profile for Re=760 Procedure A

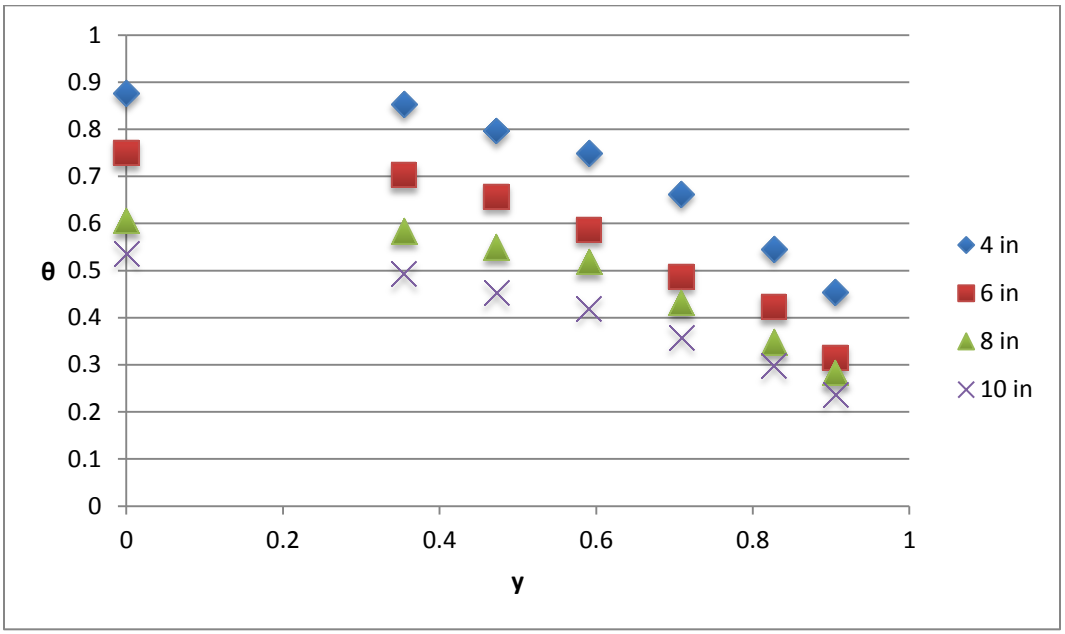


Figure 87: Co-current Cooling Temperature Profile for Re=944 Procedure A

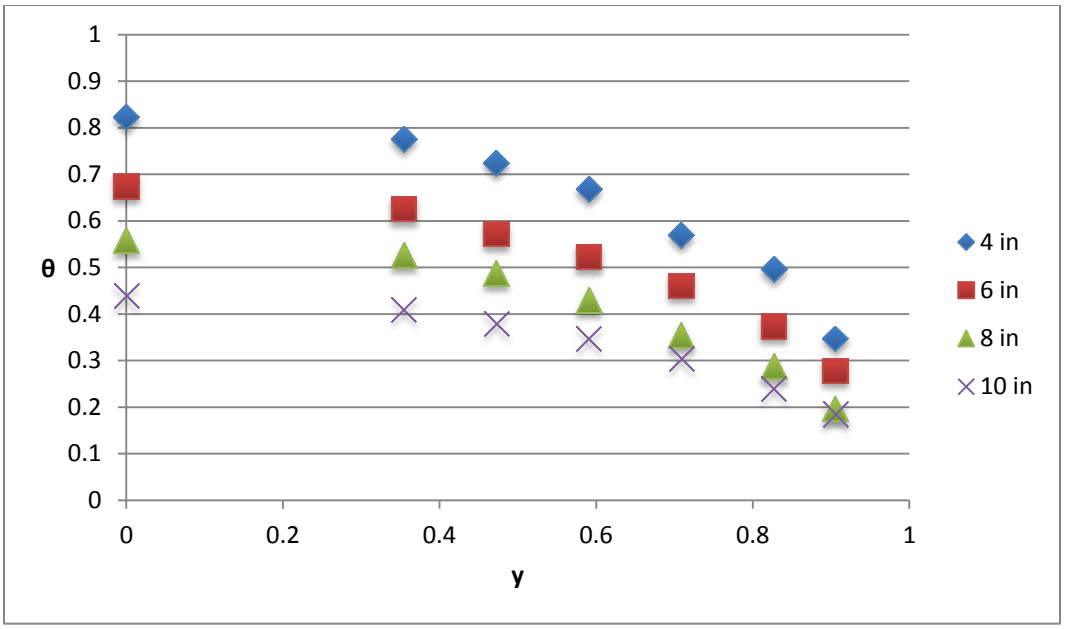


Figure 88: Co-current Cooling Temperature Profile for Re=602 Procedure A

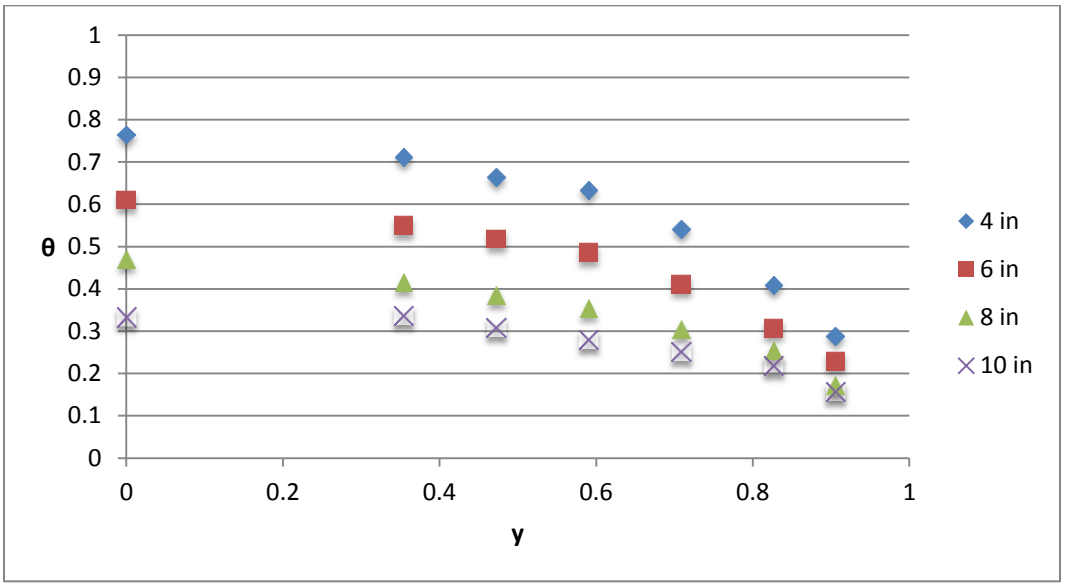


Figure 89: Co-current Cooling Temperature Profile for Re=420 Procedure A

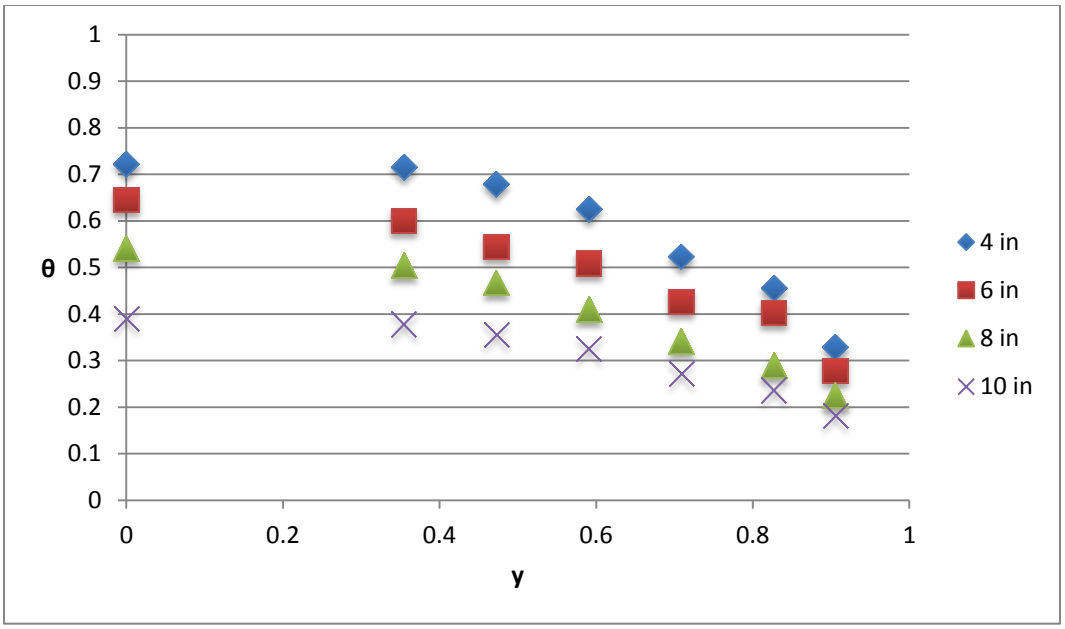


Figure 90: Co-current Cooling Temperature Profile for Re=540 Procedure A

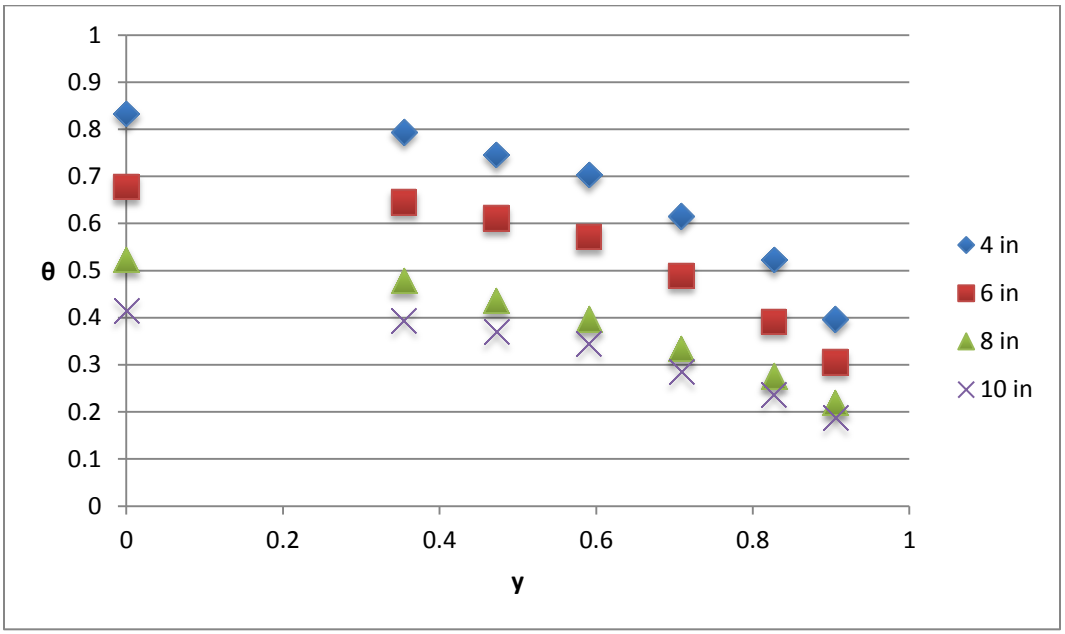


Figure 91: Co-current Cooling Temperature Profile for Re=667 Procedure A

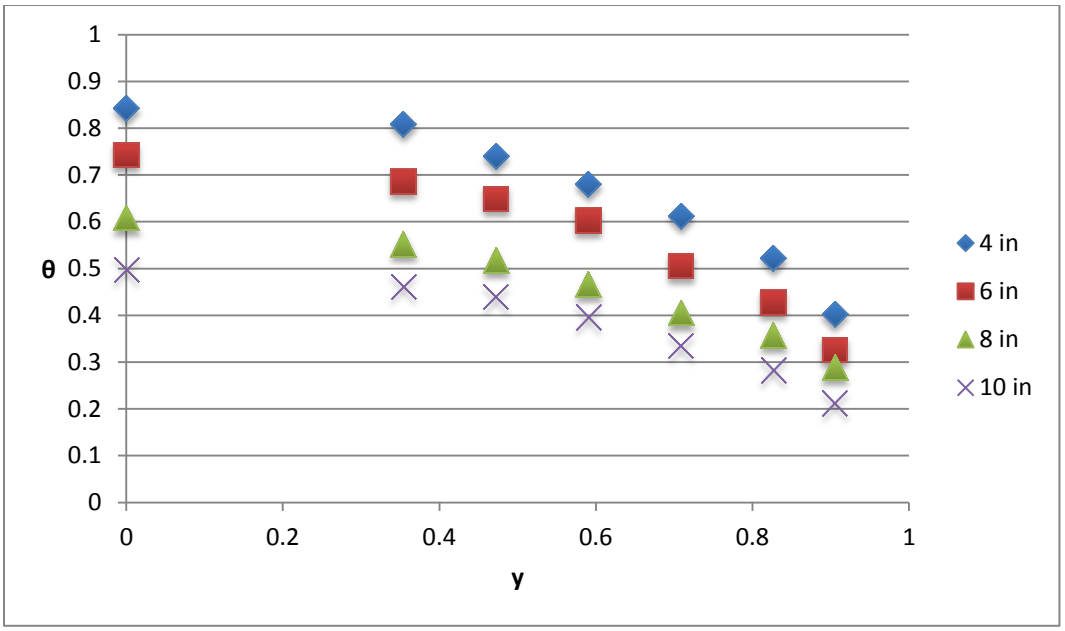


Figure 92: Co-current Cooling Temperature Profile for Re=839 Procedure A

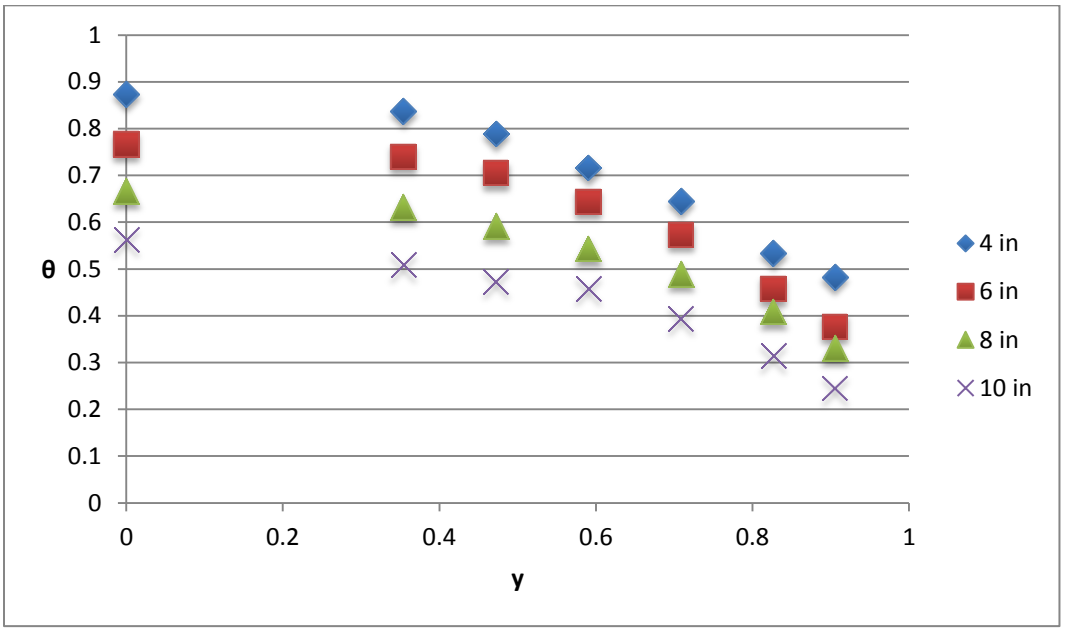


Figure 93: Co-current Cooling Temperature Profile for Re=1039 Procedure A

## Appendix E: Co-current versus Countercurrent Temperature Profiles for Procedure A

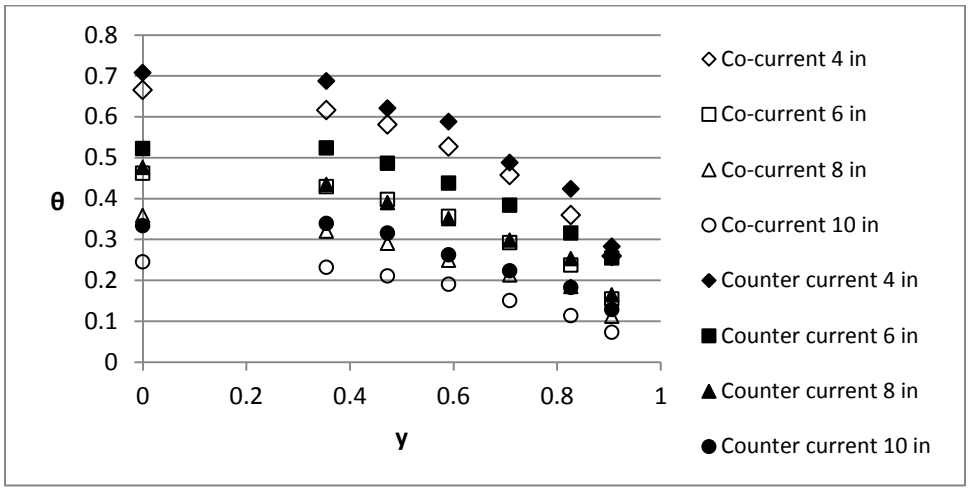


Figure 94: Countercurrent (Re=376.2) versus Co-current (Re=366.5)

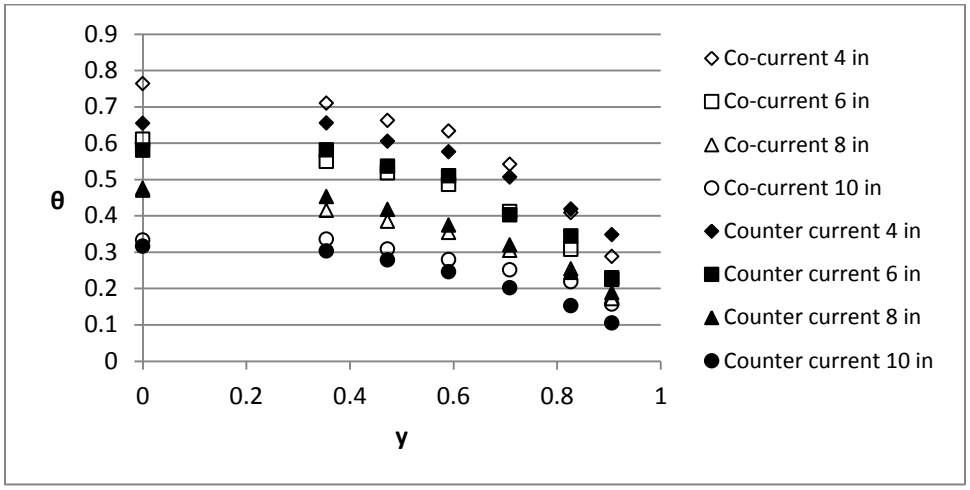


Figure 95: Countercurrent (Re=419.9) versus Co-current (Re=419.9)

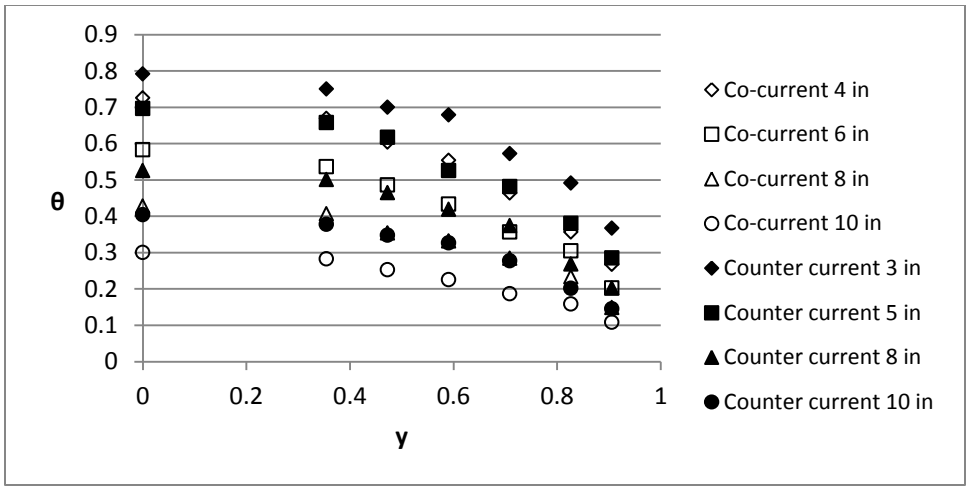


Figure 96: Countercurrent (Re=474.1) versus Co-current (Re=474.1)

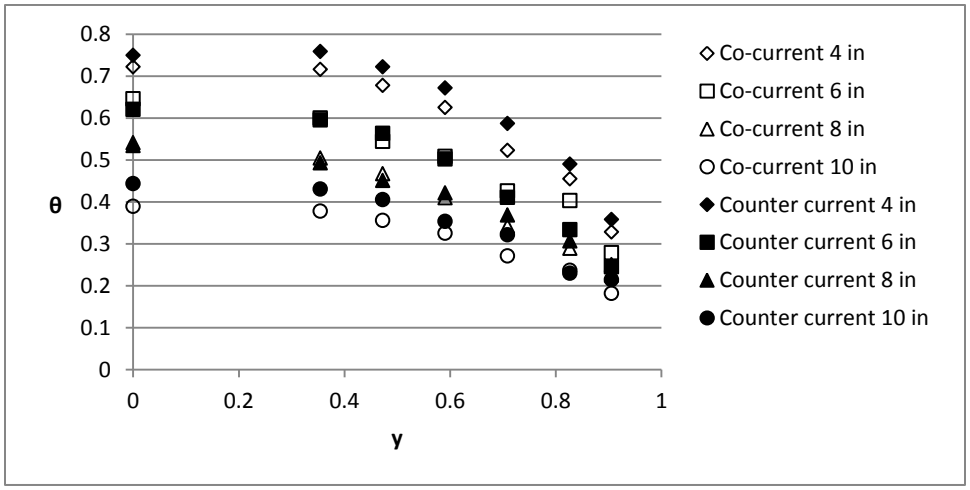


Figure 97: Countercurrent (Re=540) versus Co-current (Re=540)

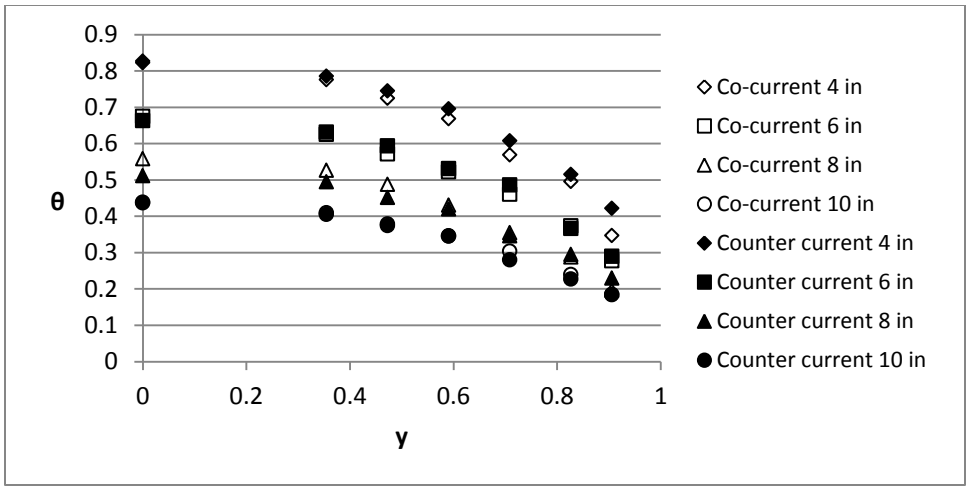


Figure 98: Countercurrent (Re=602.1) versus Co-current (Re=602.1)

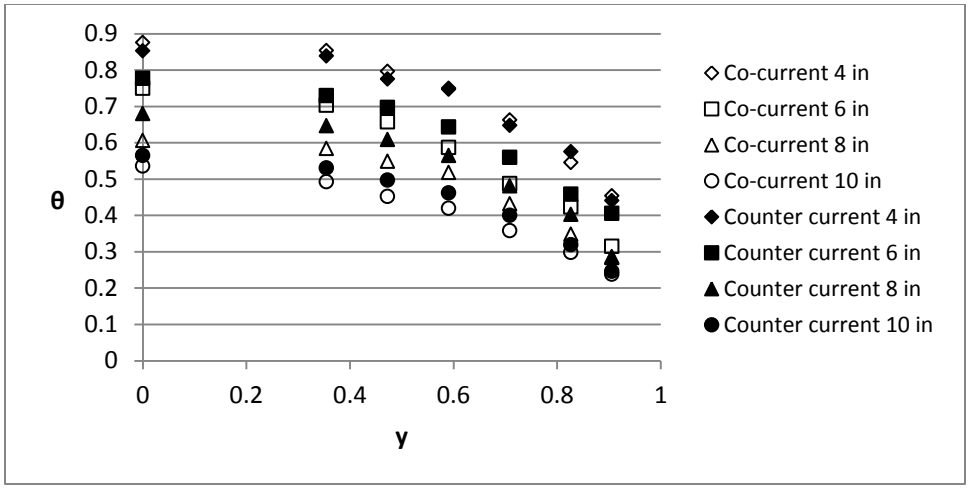


Figure 99: Countercurrent (Re=867.3) versus Co-current (Re=943.6)

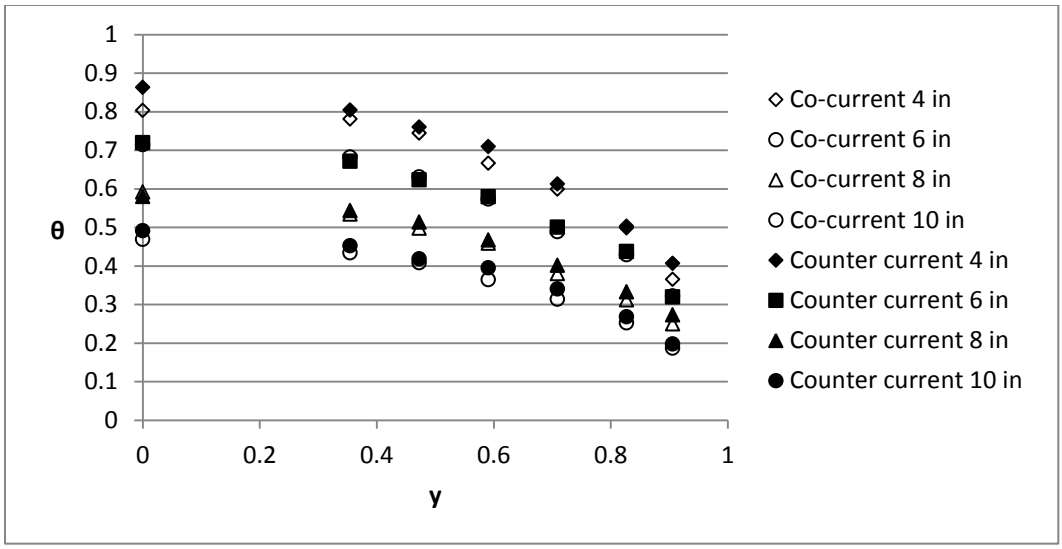


Figure 100: Countercurrent (Re=758.3) versus Co-current (Re=760.2)

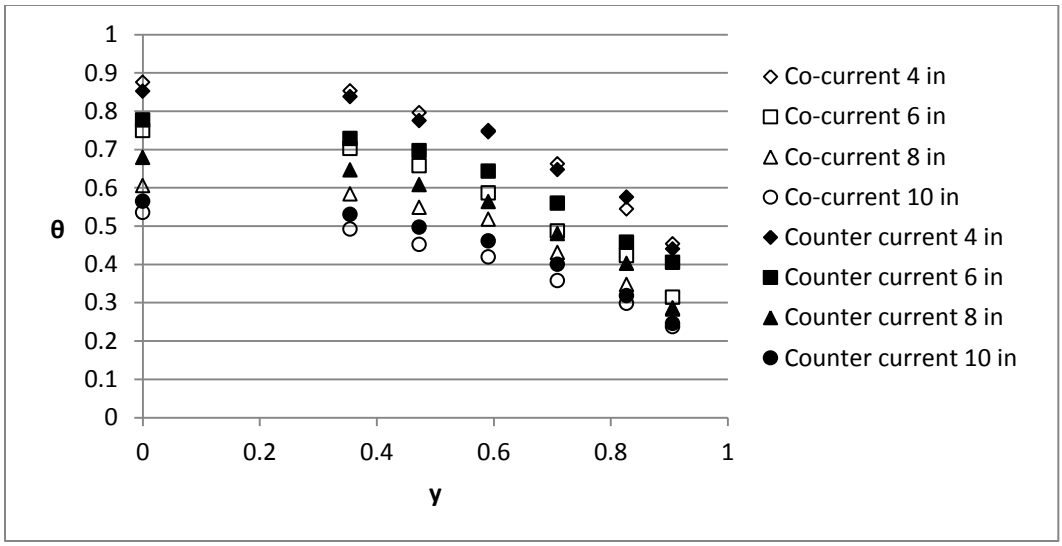


Figure 101: Countercurrent (Re=867.3) versus Co-current (Re=943.6)

## APPENDIX F: HEATING TEMPERATURE PROFILE GRAPHS PROCEDURE A

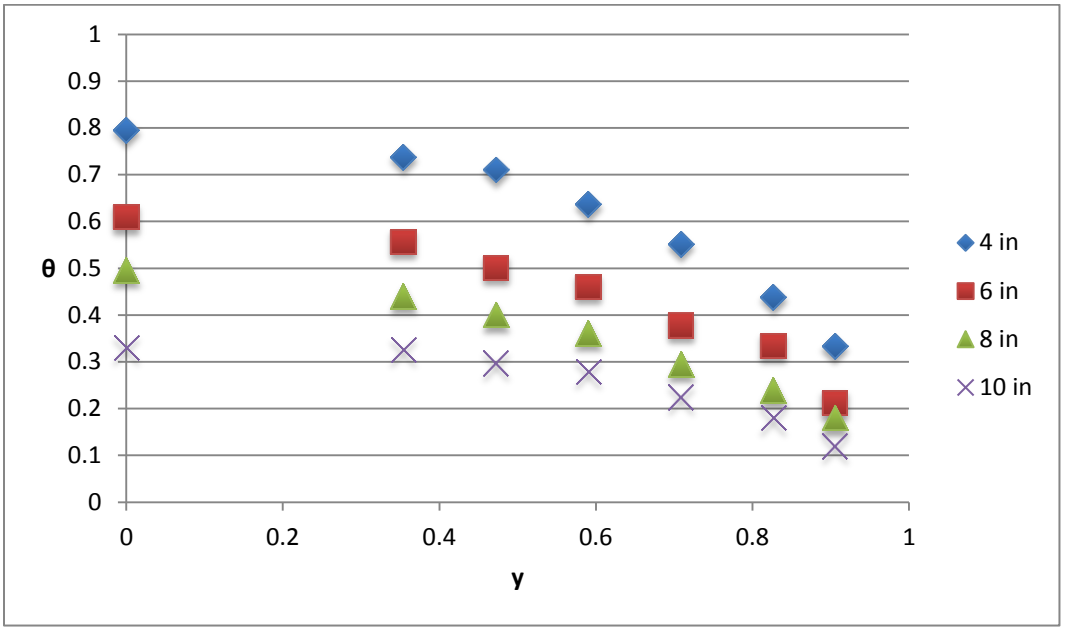


Figure 102: Heating Temperature Profile Re=366.8 Procedure A

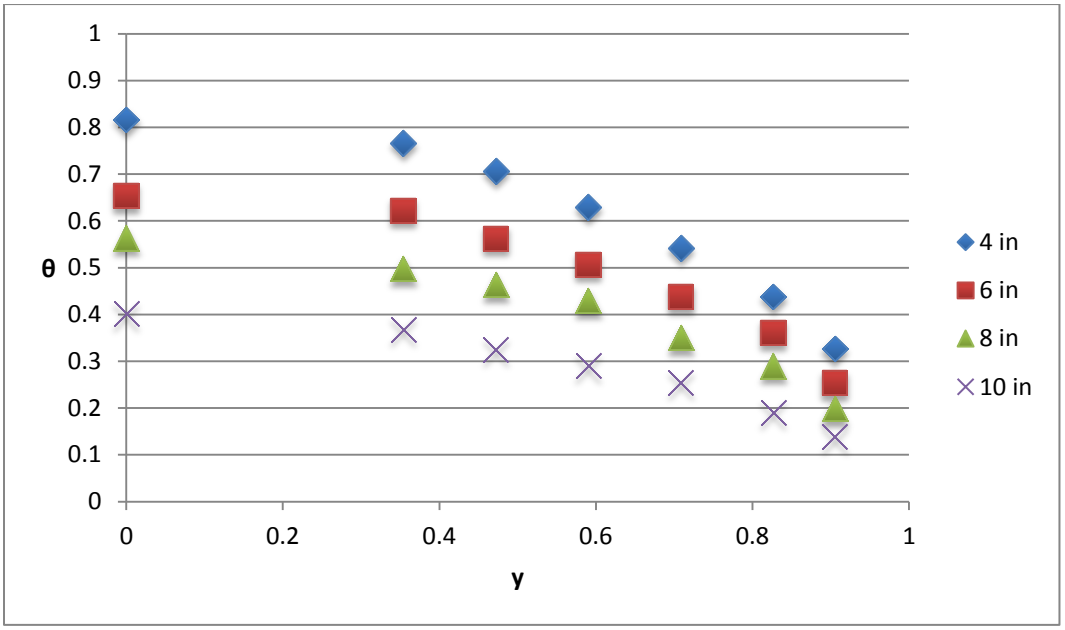


Figure 103: Heating Temperature Profile Re=410.8 Procedure A

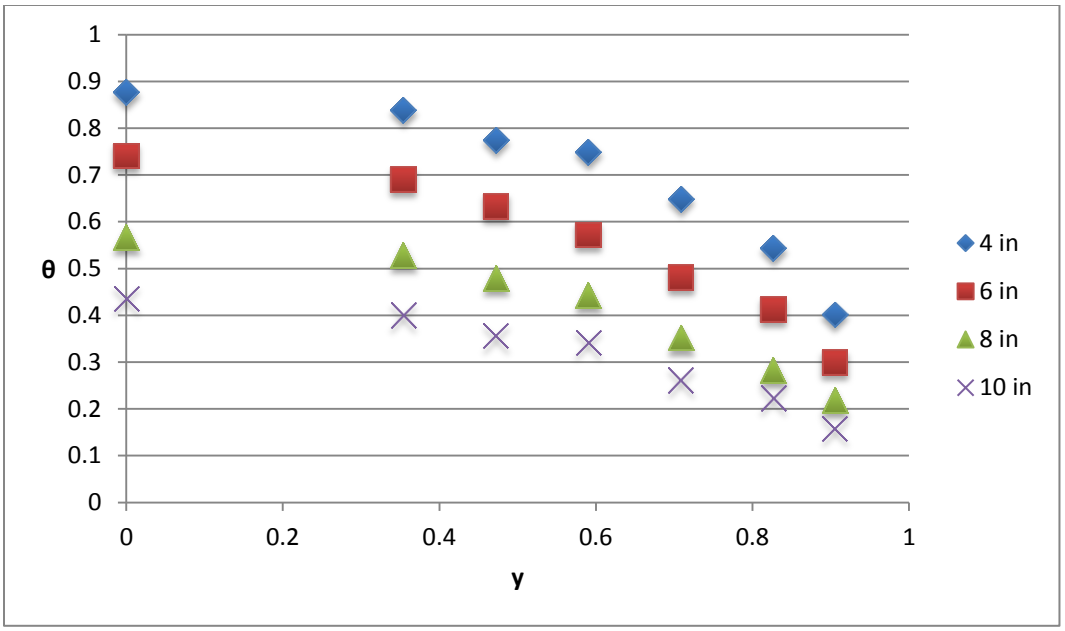


Figure 104: Heating Temperature Profile Re=686 Procedure A

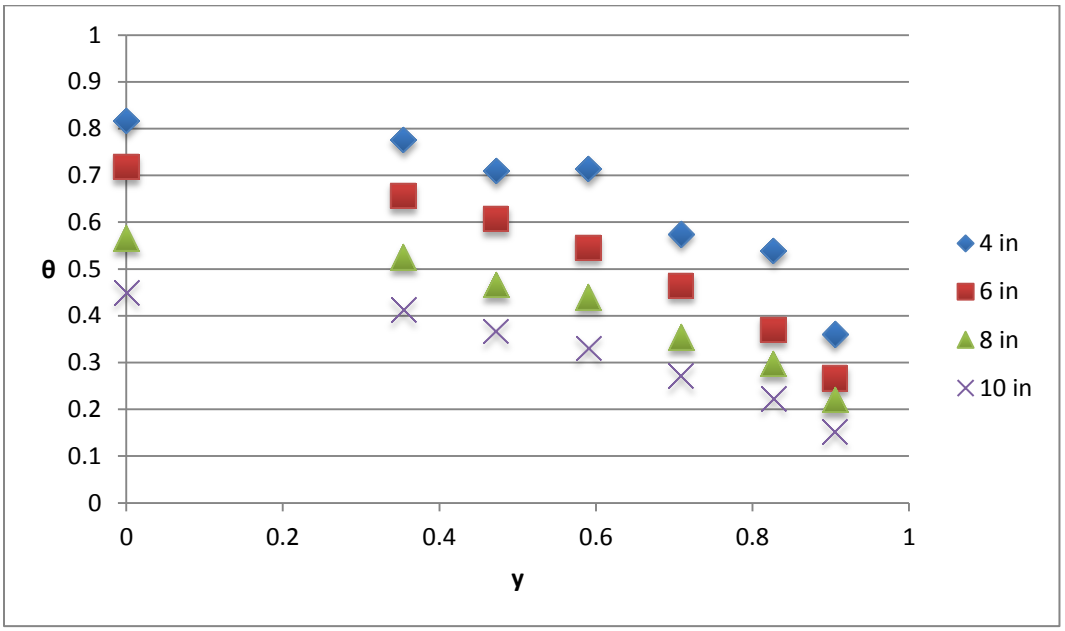


Figure 105: Heating Temperature Profile Re=532.2 Procedure A

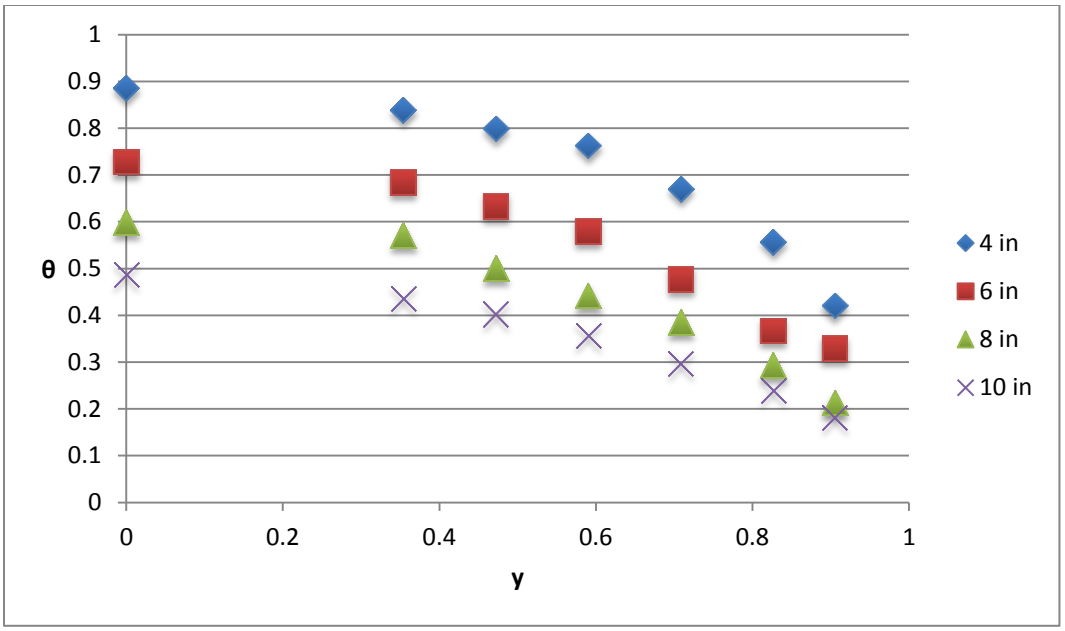


Figure 106: Heating Temperature Profile Re=588.7 Procedure A

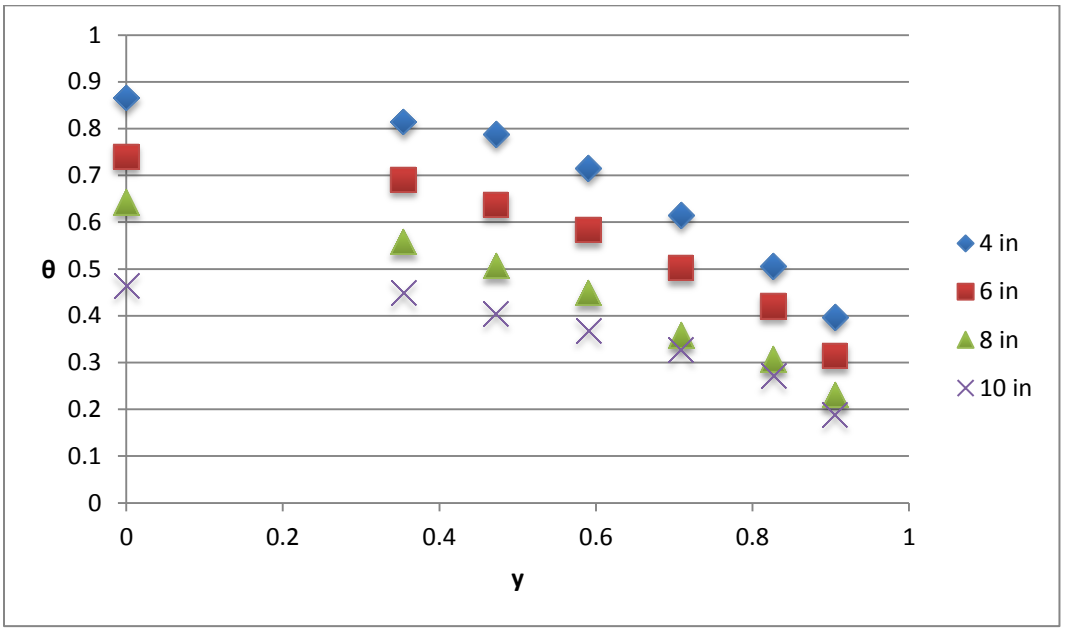


Figure 107: Heating Temperature Profile Re=656 Procedure A

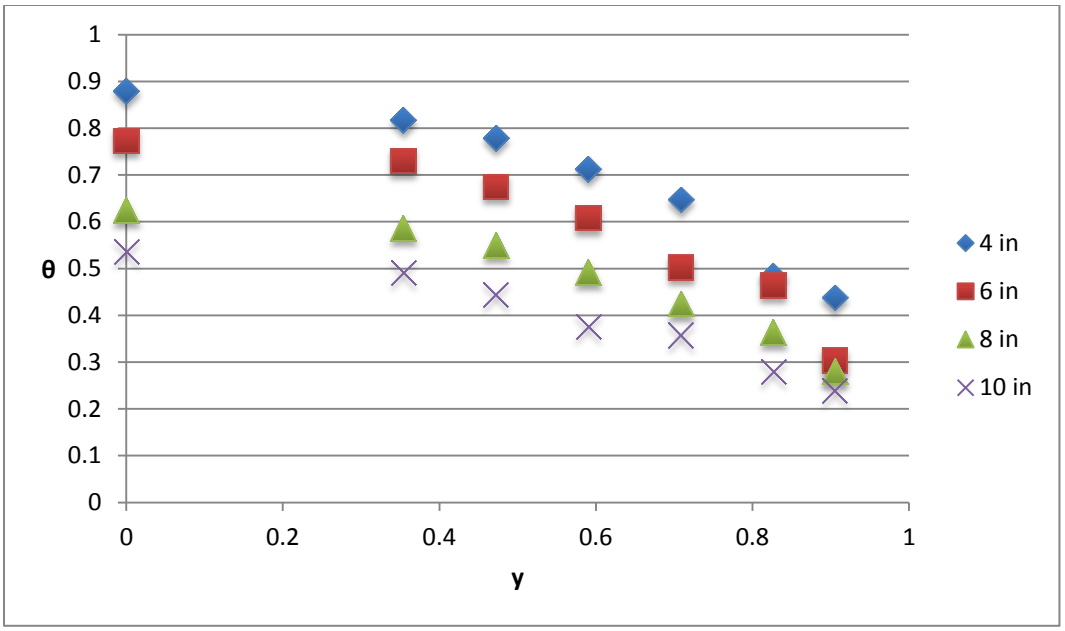


Figure 108: Heating Temperature Profile Re=738 Procedure A

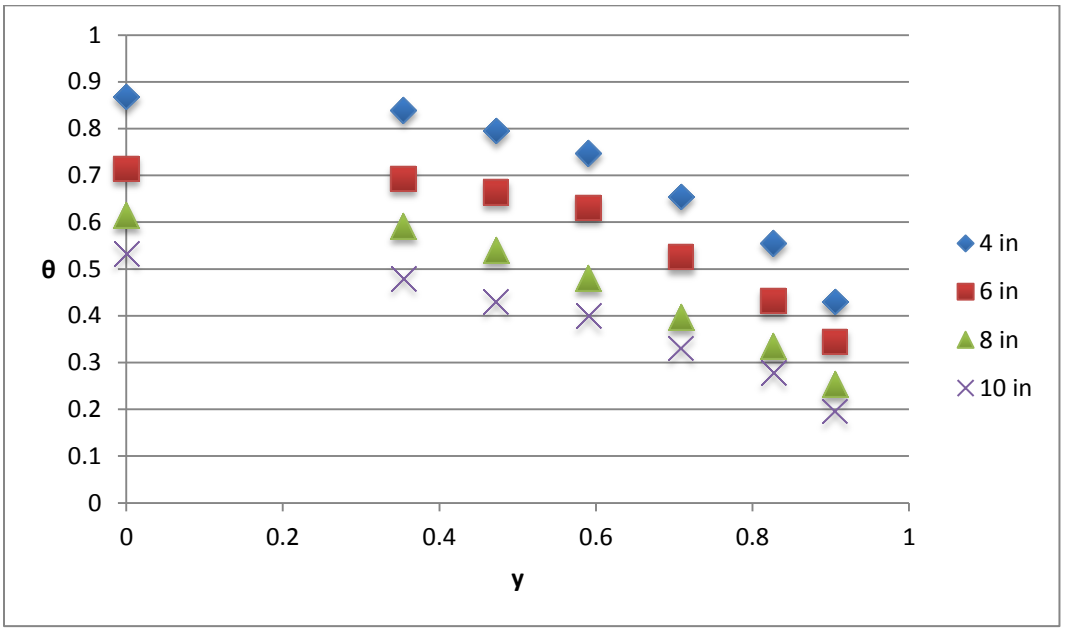


Figure 109: Heating Temperature Profile Re=792 Procedure A

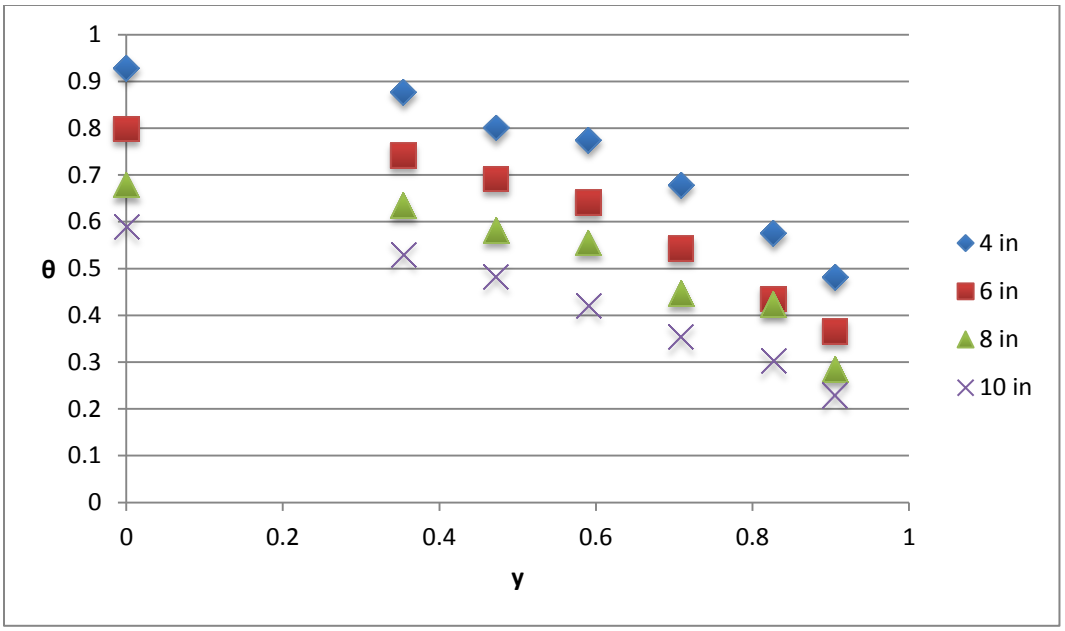


Figure 110: Heating Temperature Profile Re=908 Procedure A

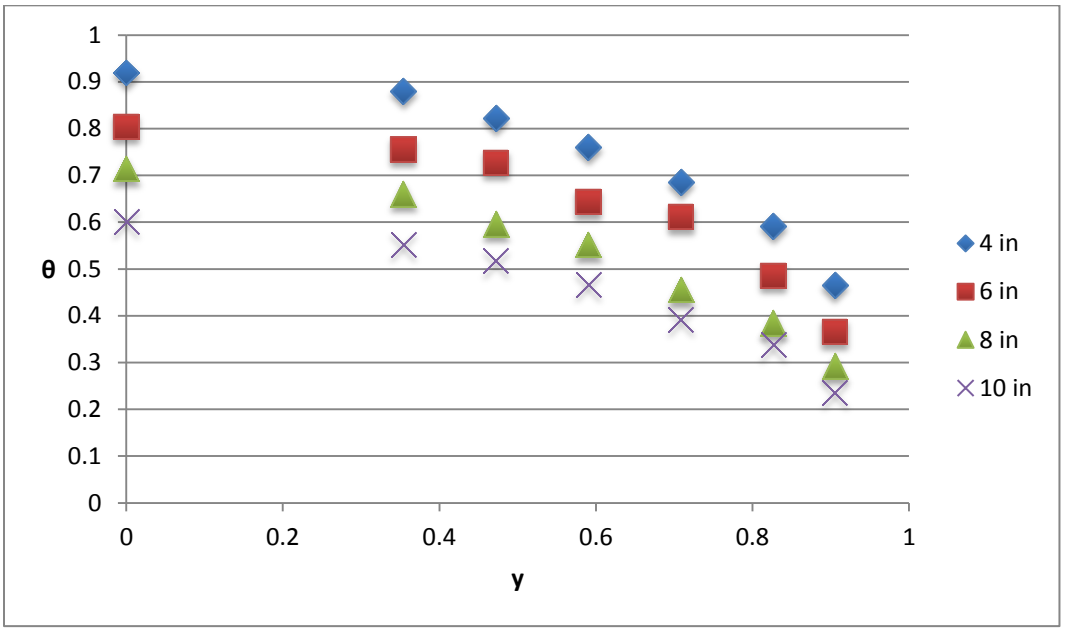


Figure 111: Heating Temperature Profile Re=1022 Procedure A

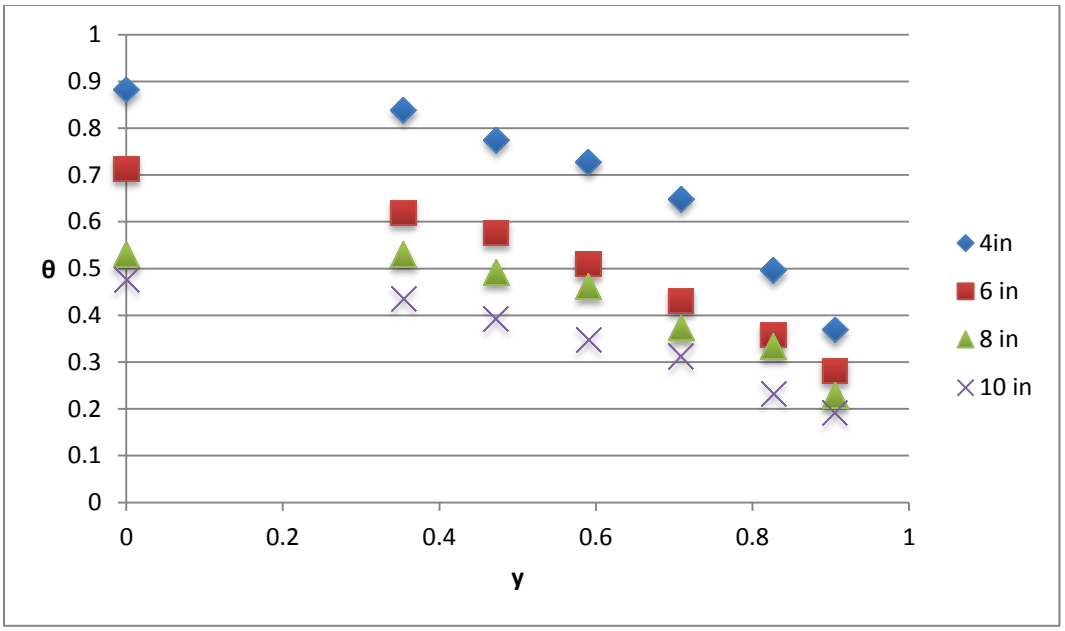


Figure 112: Heating Temperature Profile Re=583 Procedure A

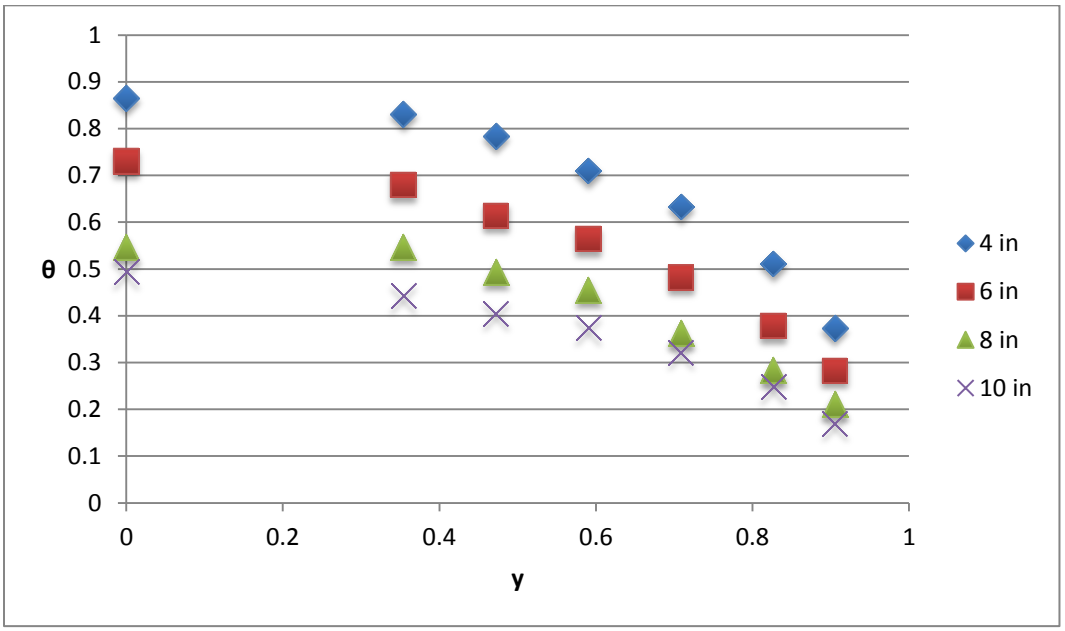


Figure 113: Heating Temperature Profile Re=586 Procedure A

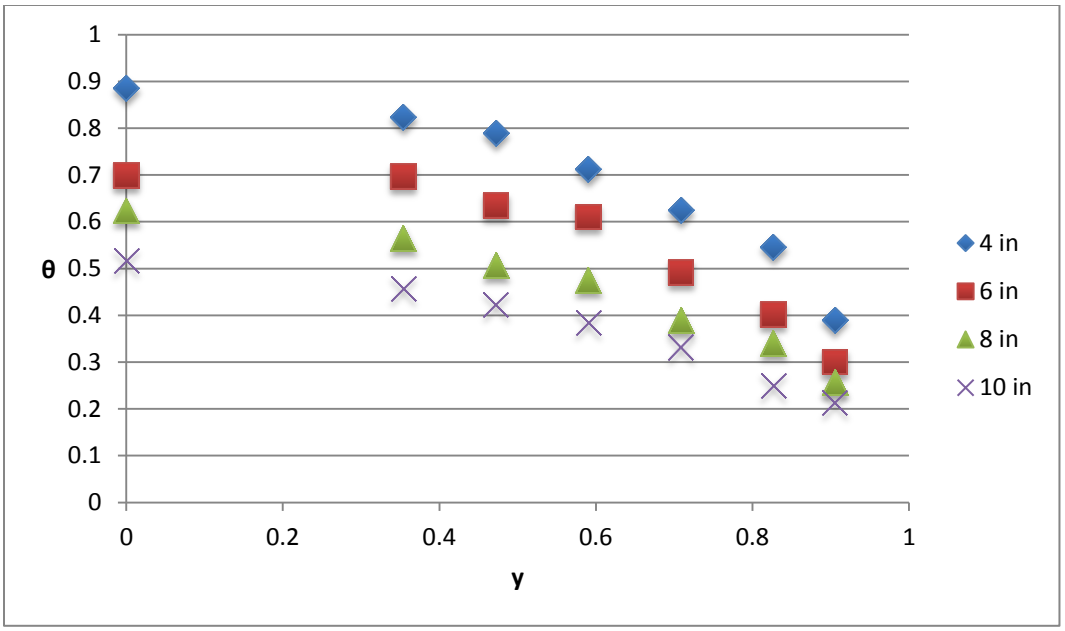


Figure 114: Heating Temperature Profile Re=583 Procedure A

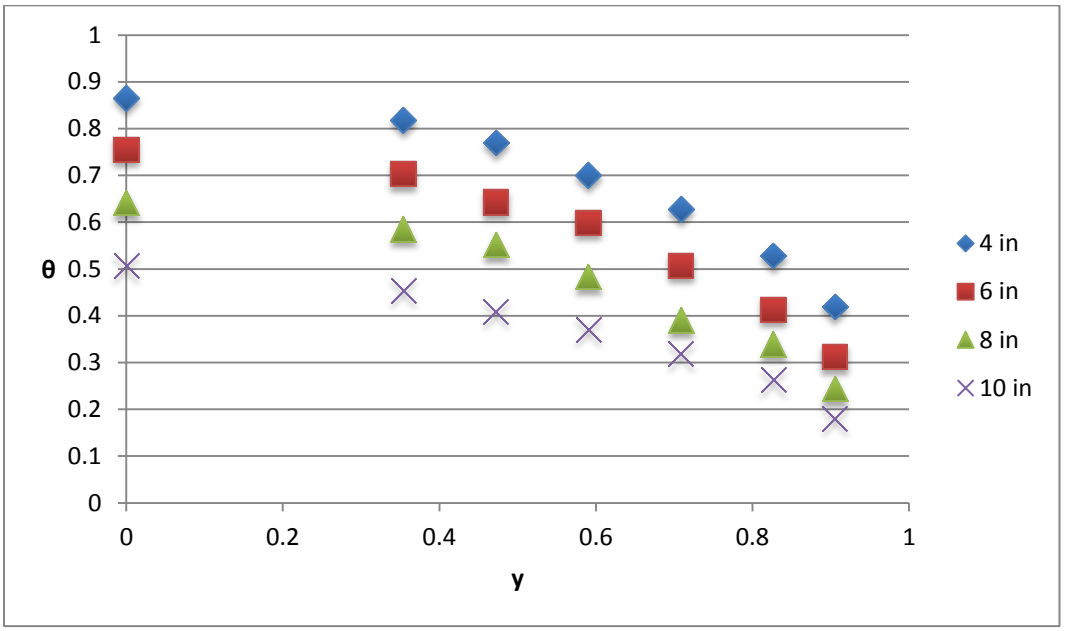


Figure 115: Heating Temperature Profile Re=586 Procedure A

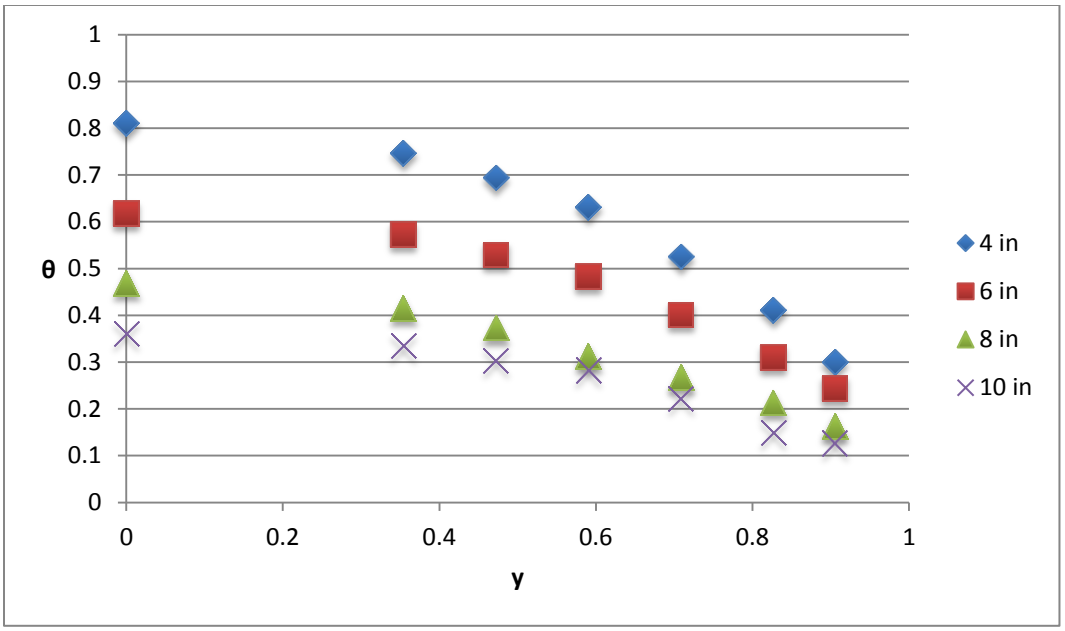


Figure 116: Heating Temperature Profile Re=305 Procedure A

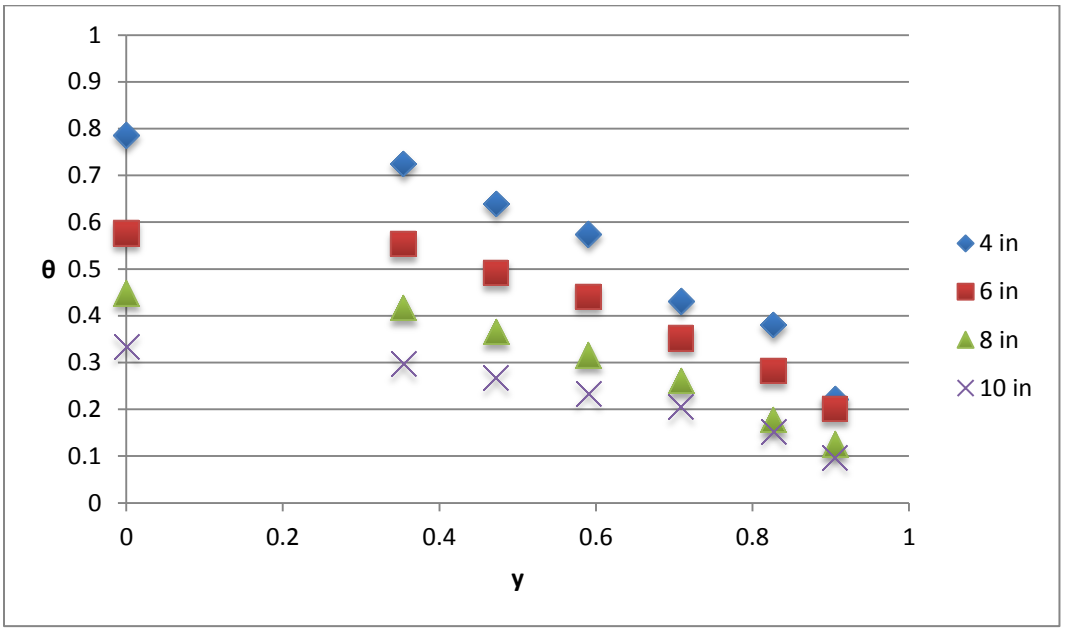


Figure 117: Heating Temperature Profile Re=258 Procedure A

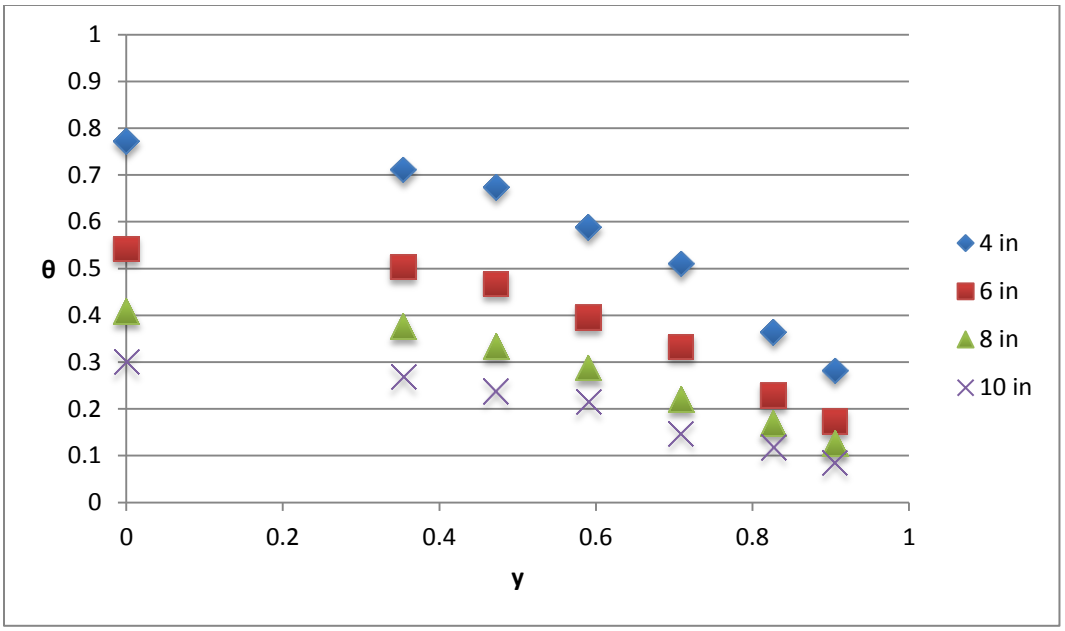


Figure 118: Heating Temperature Profile Re=214 Procedure A

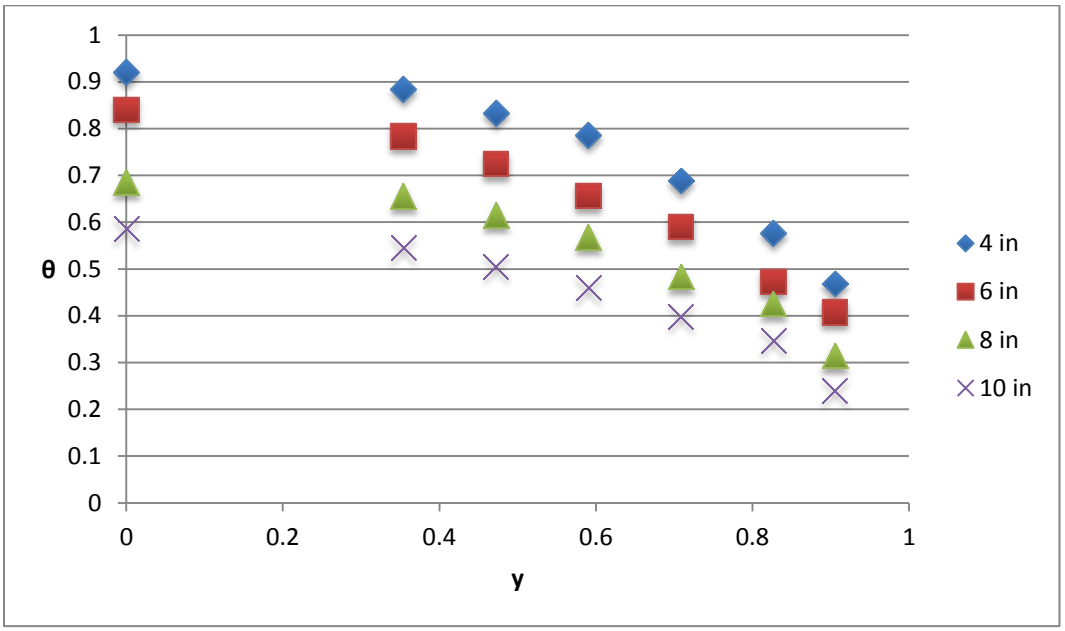


Figure 119: Heating Temperature Profile Re=992 Procedure A

## Appendix G: Countercurrent Cooling Temperature Profile Graphs Procedure B

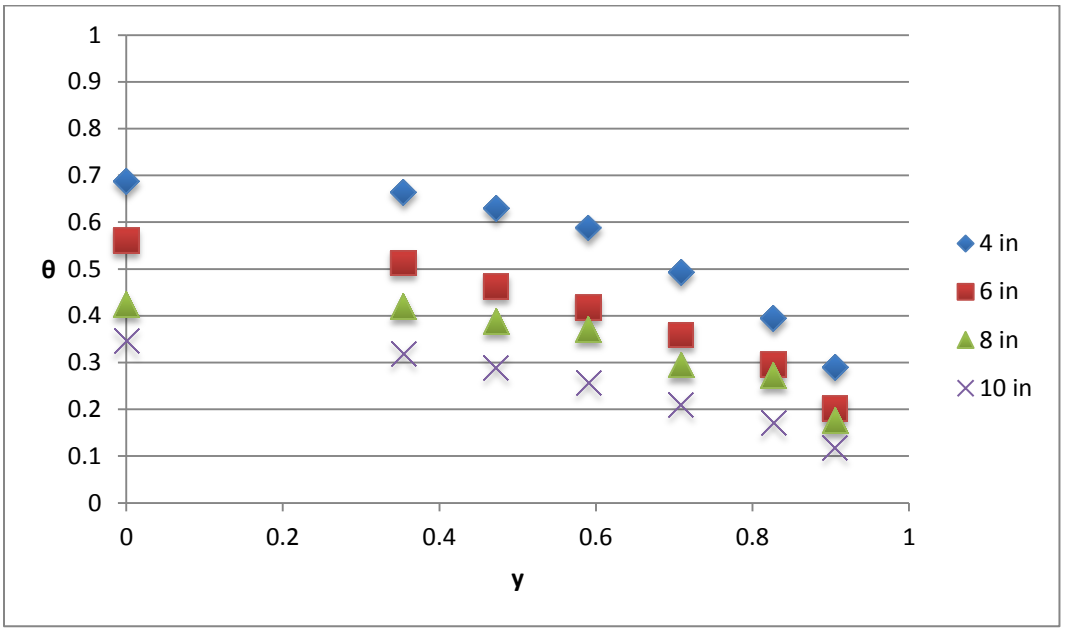


Figure 120: Countercurrent Cooling Temperature Profile Procedure B Re=325

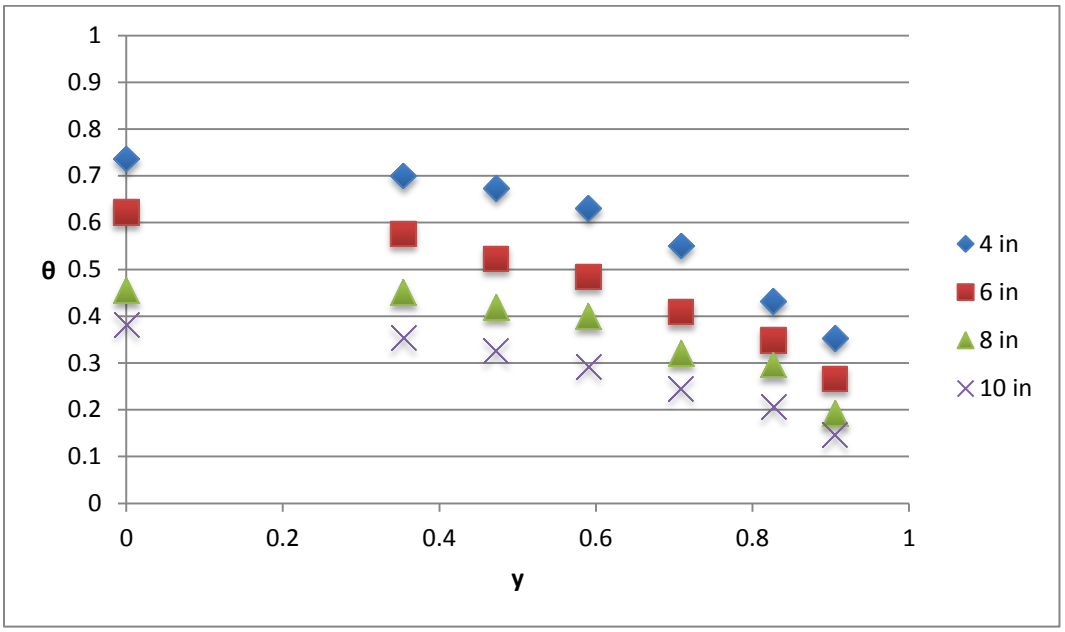


Figure 121: Countercurrent Cooling Temperature Profile Procedure B Re=413

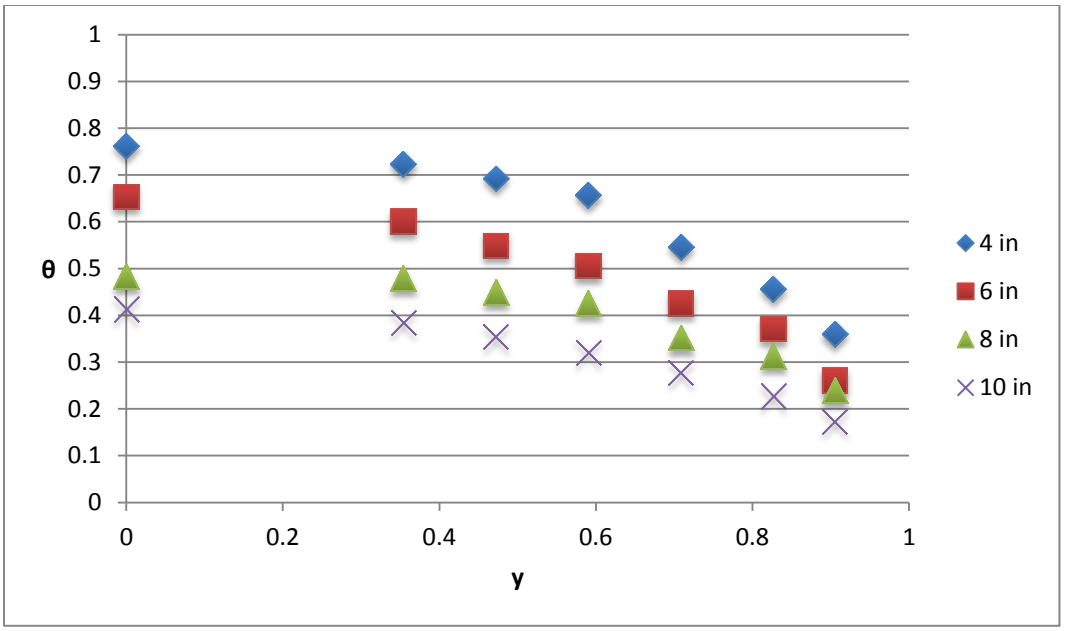


Figure 122: Countercurrent Cooling Temperature Profile Procedure B Re=501

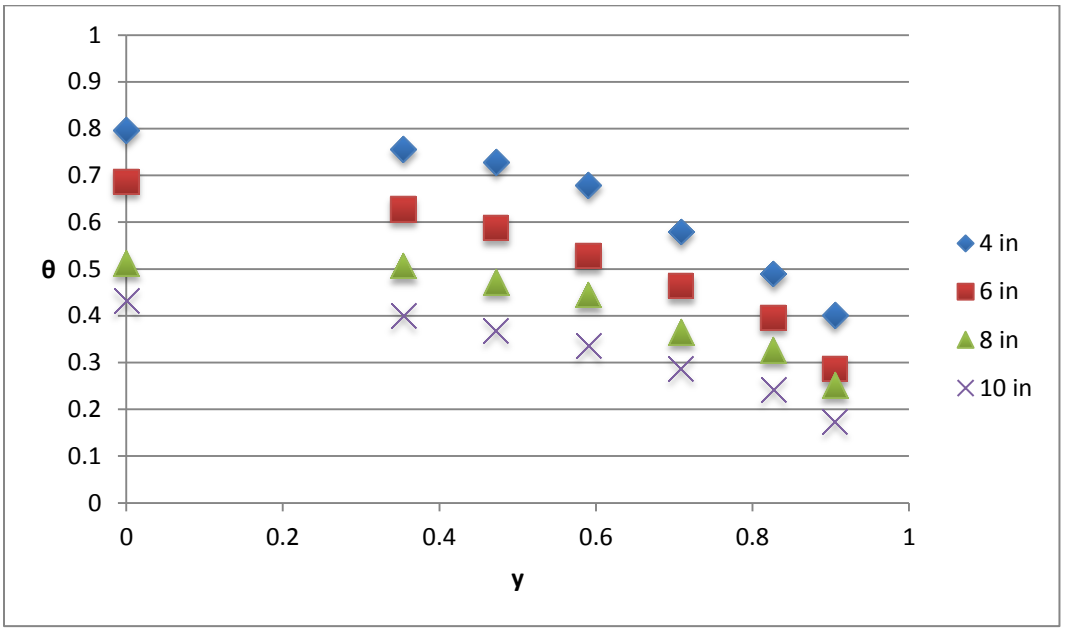


Figure 123: Countercurrent Cooling Temperature Profile Procedure B Re=544

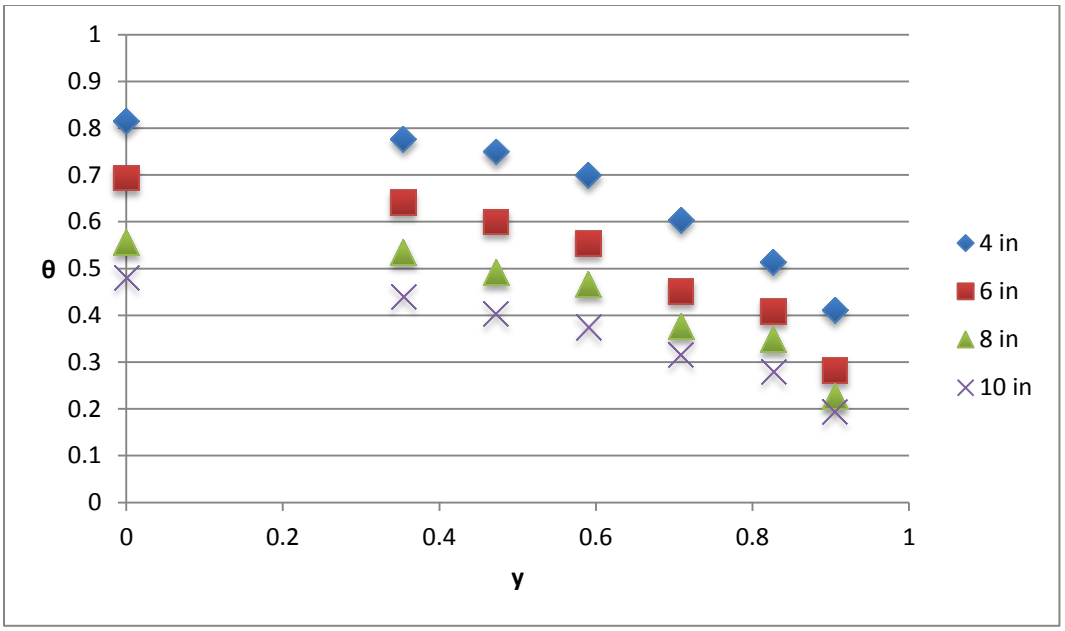


Figure 124: Countercurrent Cooling Temperature Profile Procedure B Re=614

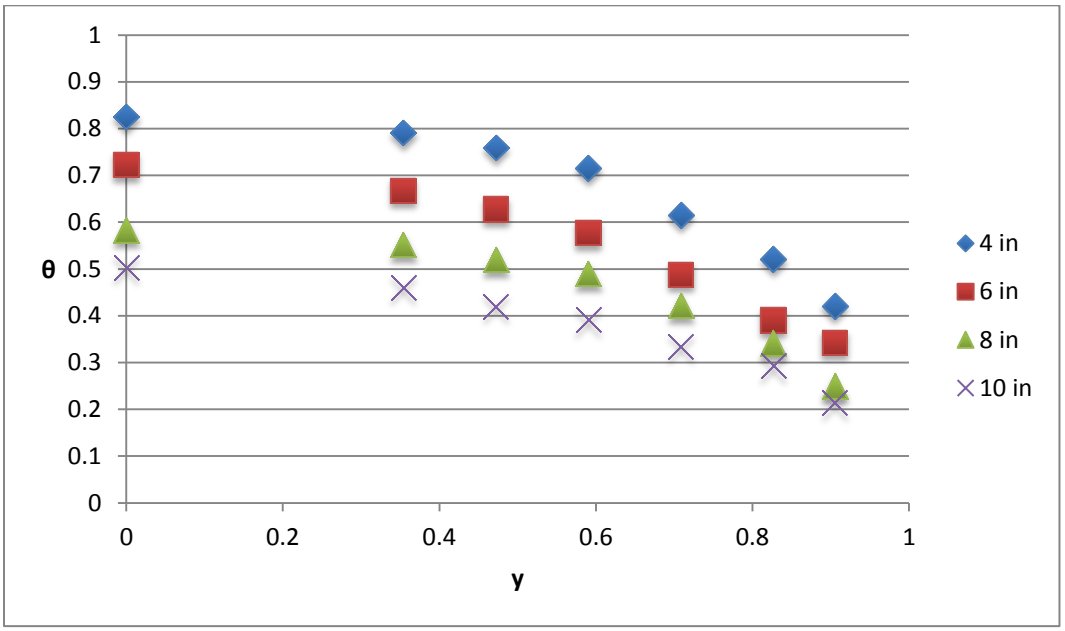


Figure 125: Countercurrent Cooling Temperature Profile Procedure B Re=671

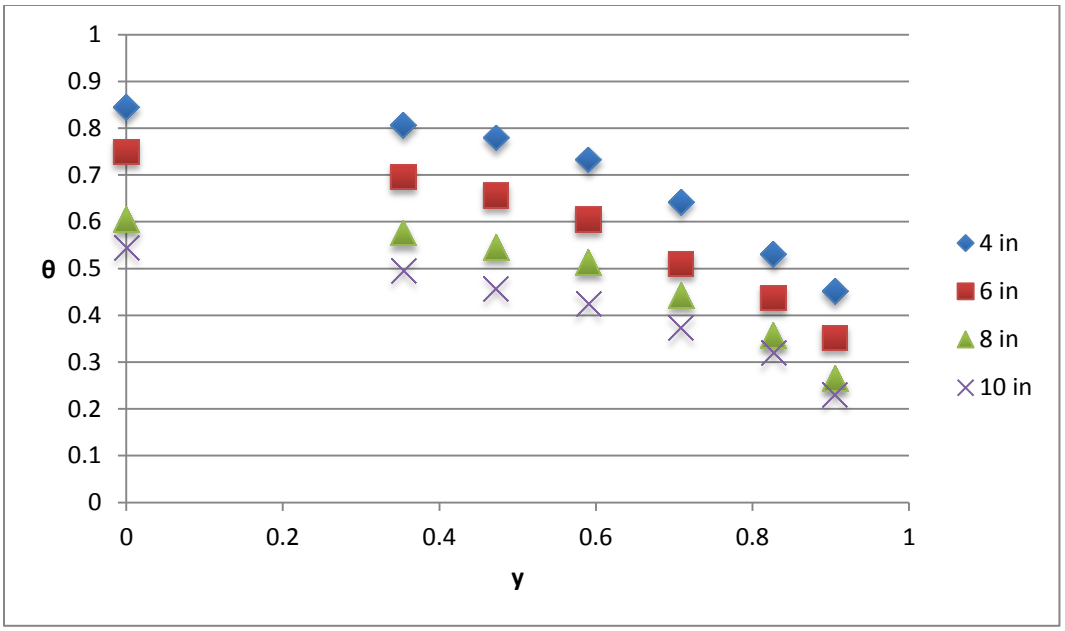


Figure 126: Countercurrent Cooling Temperature Profile Procedure B Re=768

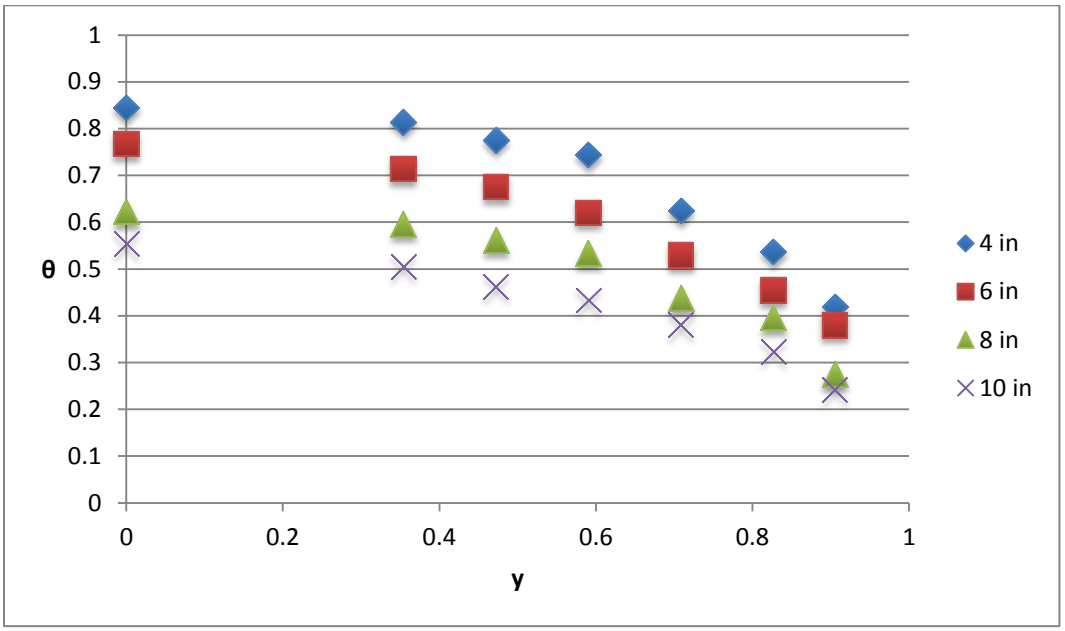


Figure 127: Countercurrent Cooling Temperature Profile Procedure B Re=830

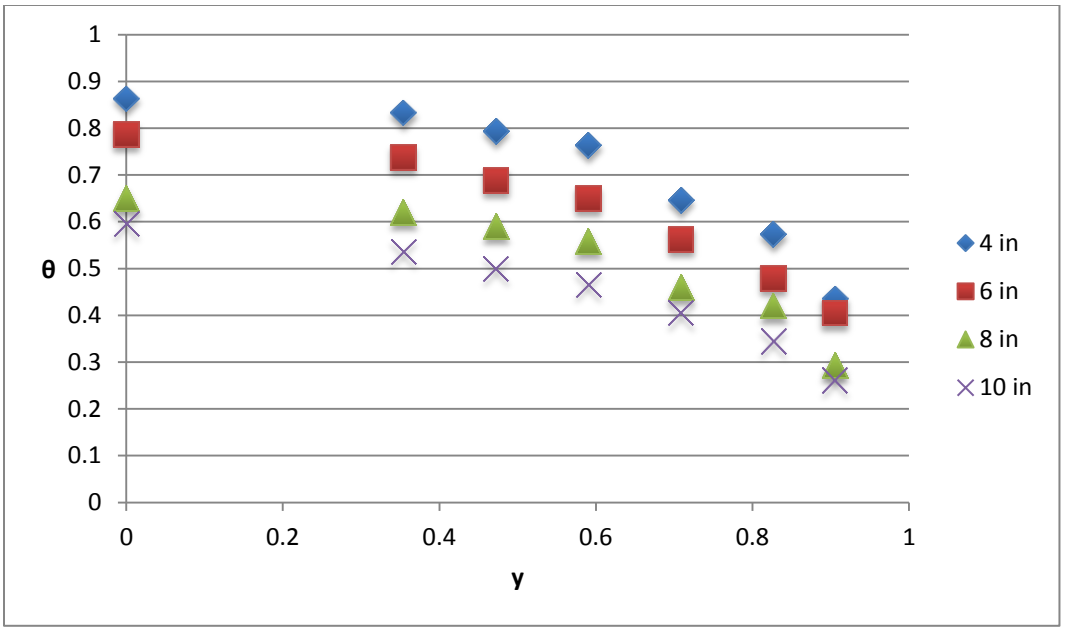


Figure 128: Countercurrent Cooling Temperature Profile Procedure B Re=949

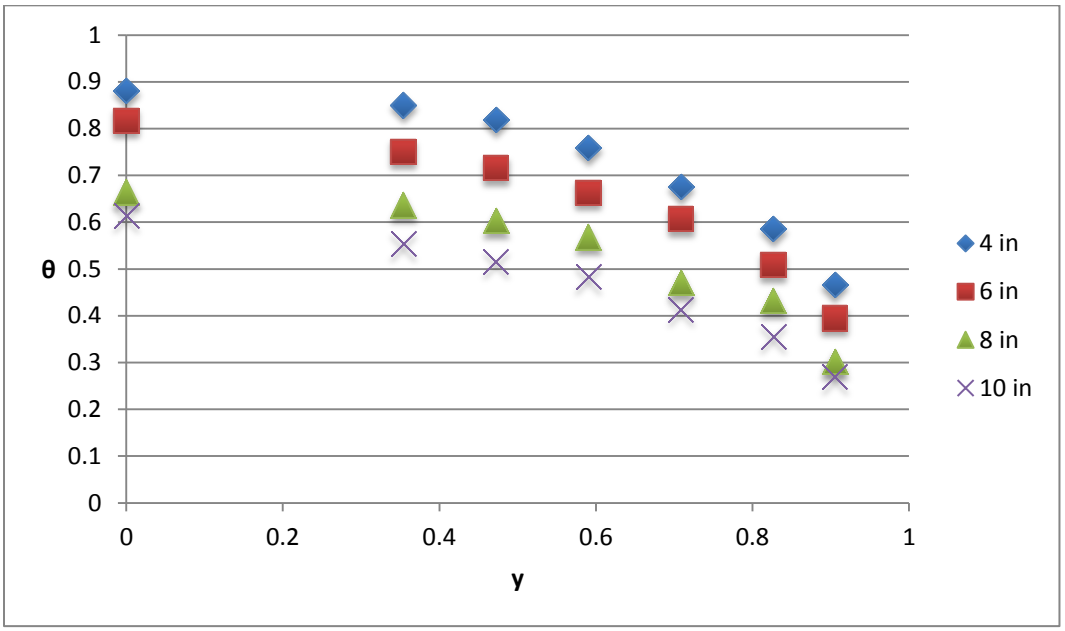


Figure 129: Countercurrent Cooling Temperature Profile Procedure B Re=1041

## APPENDIX H: HEATING TEMPERATURE PROFILE GRAPHS PROCEDURE B

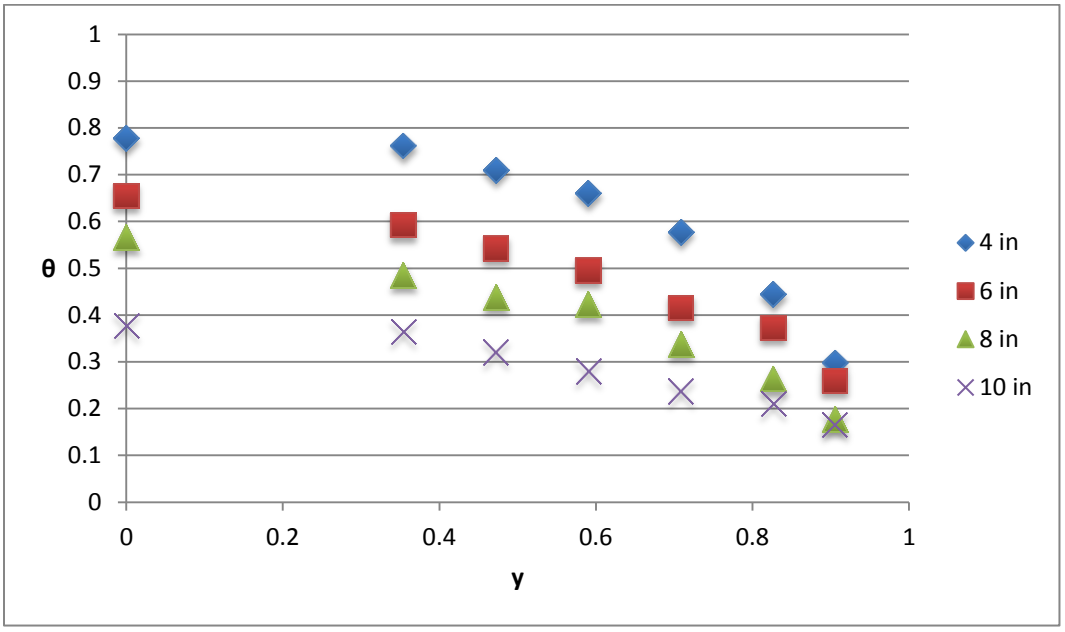


Figure 130: Heating Temperature Profile Procedure B Re=325

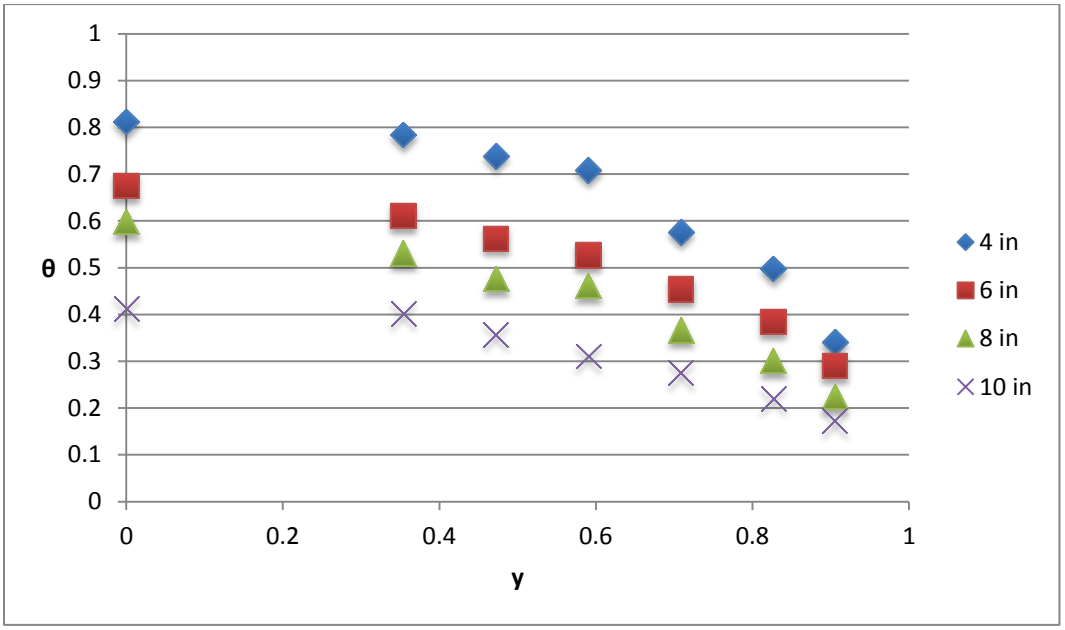


Figure 131: Heating Temperature Profile Procedure B Re=417

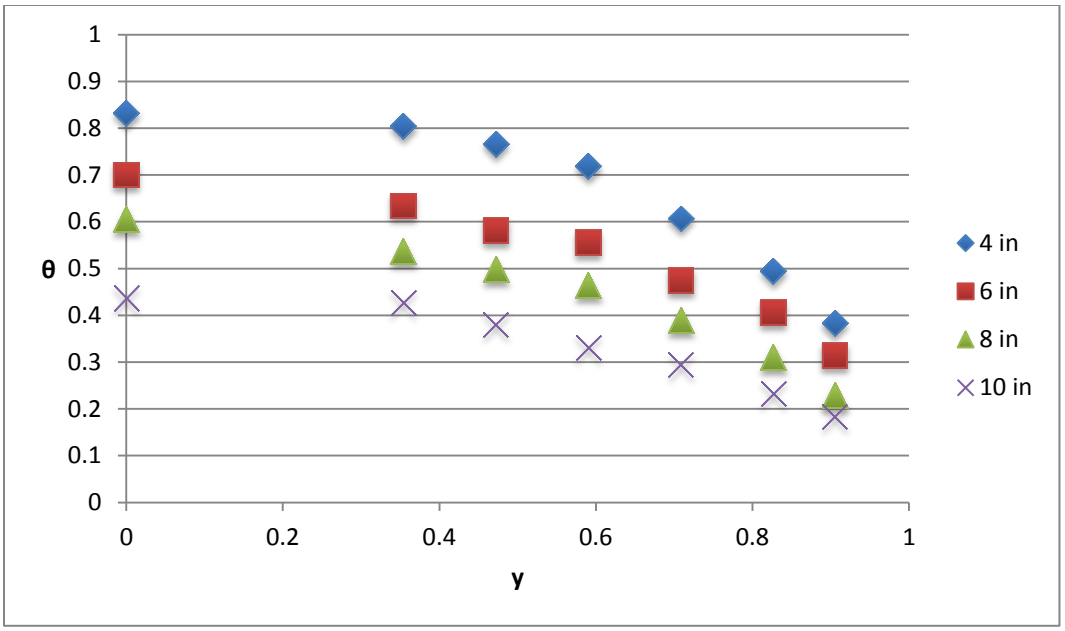


Figure 132: Heating Temperature Profile Procedure B Re=472

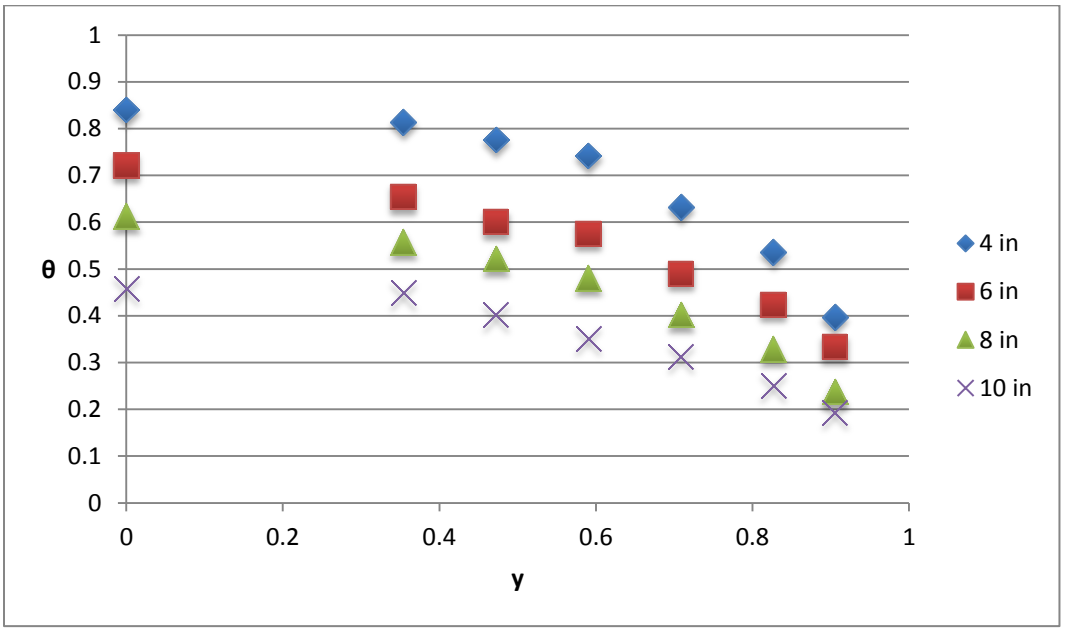


Figure 133: Heating Temperature Profile Procedure B Re=546

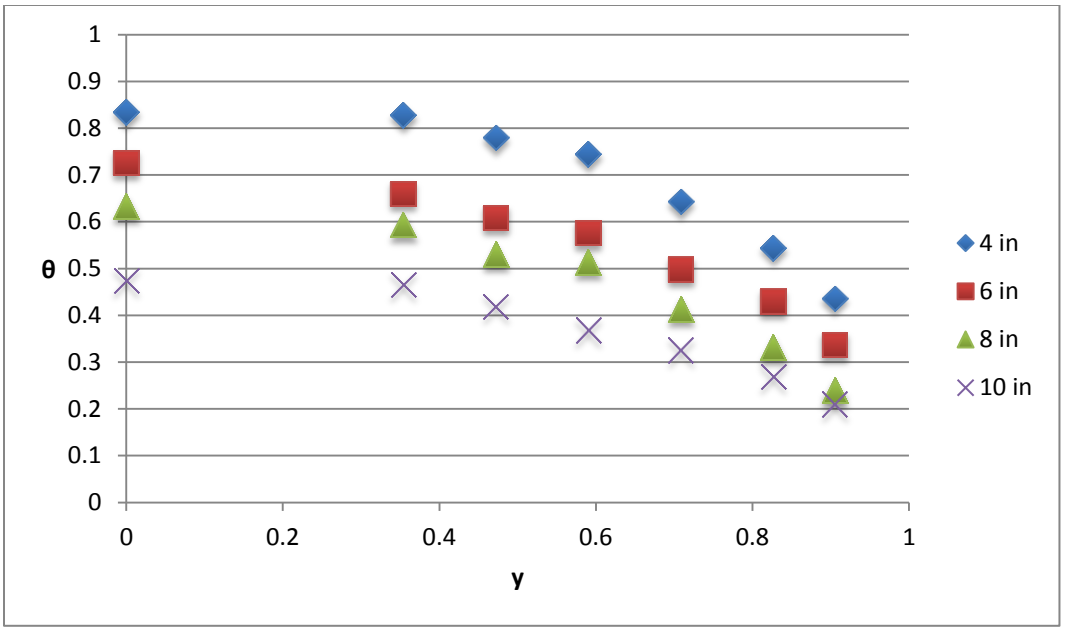


Figure 134: Heating Temperature Profile Procedure B Re=593

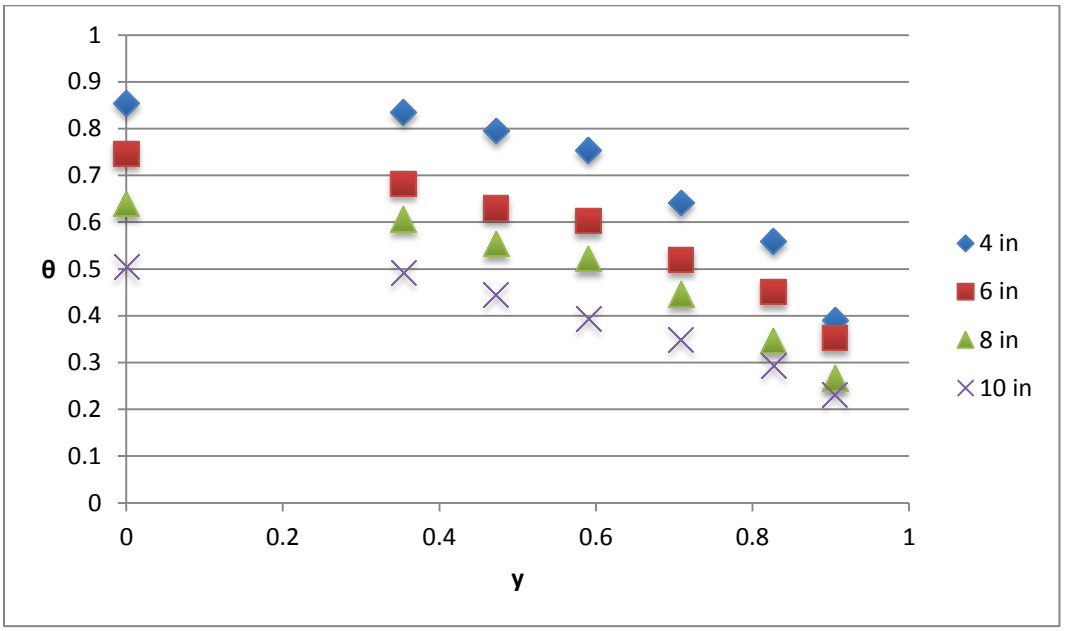


Figure 135: Heating Temperature Profile Procedure B Re=660

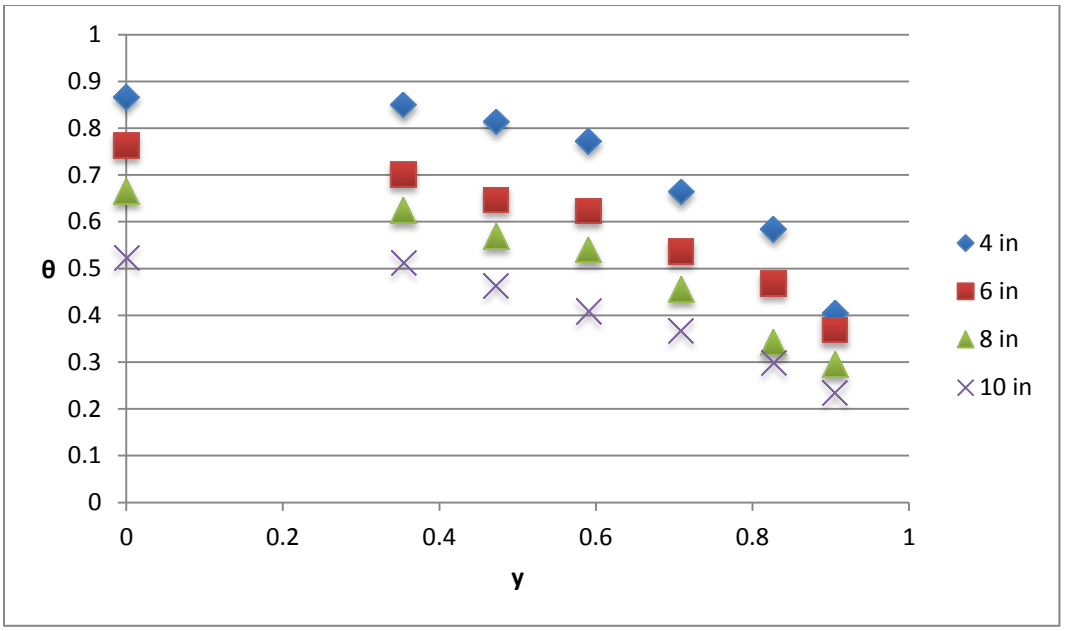


Figure 136: Heating Temperature Profile Procedure B Re=757

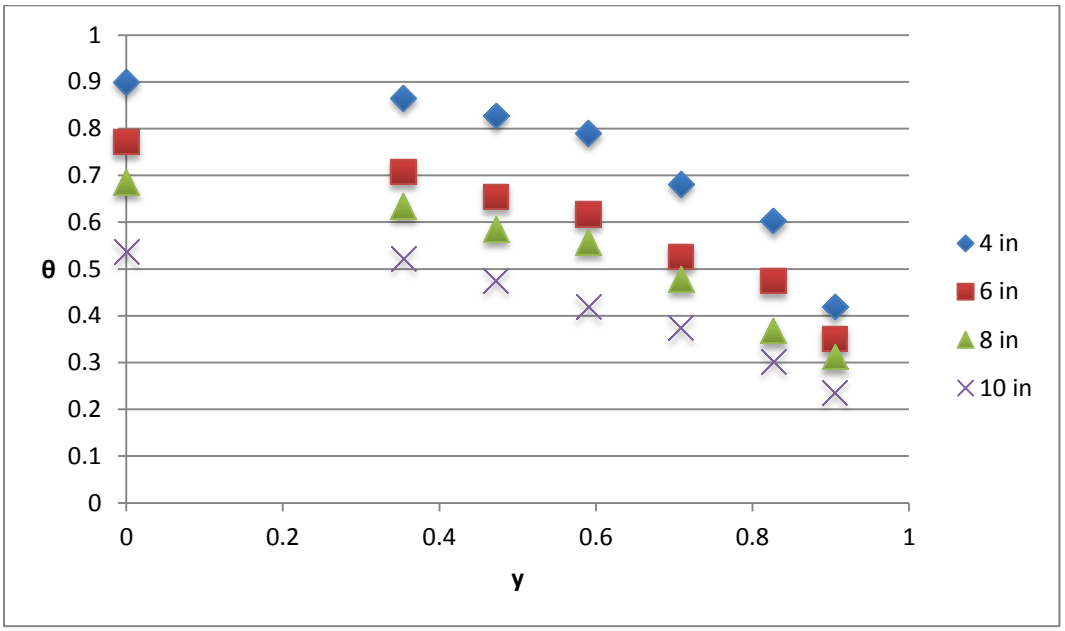


Figure 137: Heating Temperature Profile Procedure B Re=825

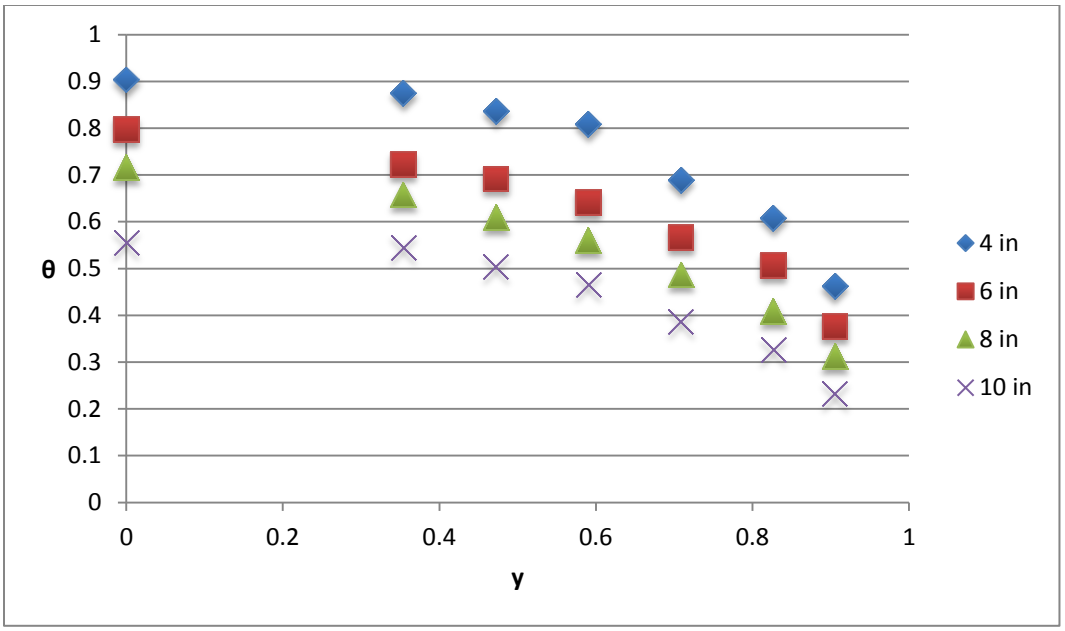


Figure 138: Heating Temperature Profile Procedure B Re=928

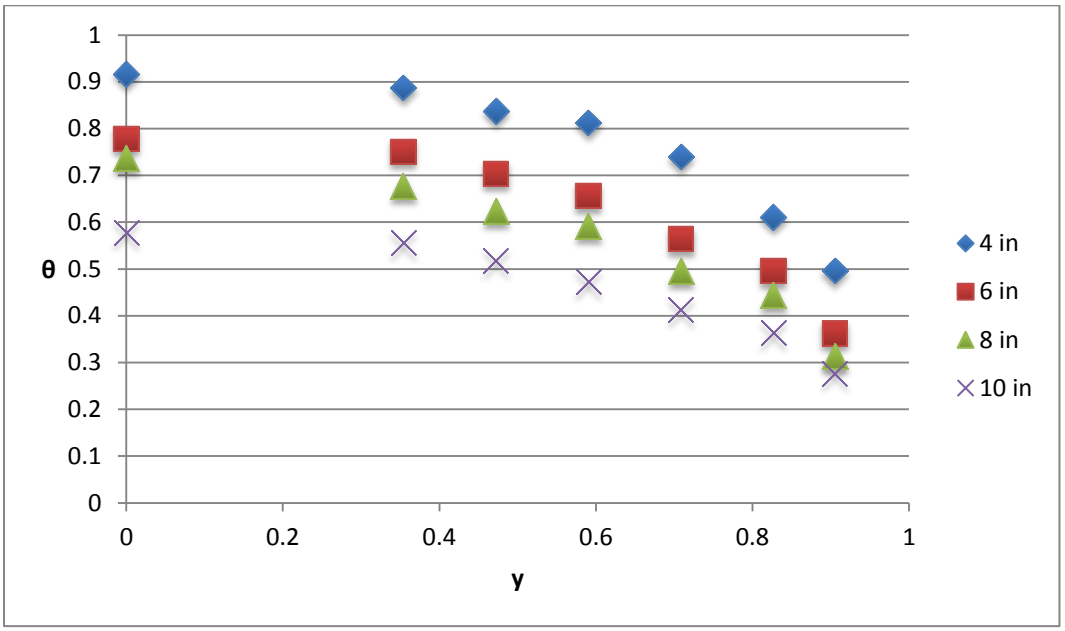


Figure 139: Heating Temperature Profile Procedure B Re=1009

# APPENDIX I: AIR FLOW RATE

**Table 7:Air Flow Rate to Gauge Pressure**

| Gauge Pressure | Maximum Flow-rate |
|---|---|
| 0 | 14.54 |
| 1 | 14.05 |
| 2 | 13.64 |
| 3 | 13.23 |
| 4 | 12.87 |
| 5 | 12.55 |
| 6 | 12.24 |
| 7 | 11.97 |
| 8 | 11.69 |
| 9 | 11.44 |
| 10 | 11.21 |
| 11 | 10.99 |
| 12 | 10.79 |
| 13 | 10.59 |
| 14 | 10.41 |
| 15 | 10.24 |
| 16 | 10.06 |
| 17 | 9.9 |
| 18 | 9.74 |
| 19 | 9.6 |
| 20 | 9.47 |
| 21 | 9.33 |
| 22 | 9.2 |
| 23 | 9.07 |
| 24 | 8.96 |
| 25 | 8.85 |

## APPENDIX J: COMPARISON OF OLD HEATING TO PROCEDURE B

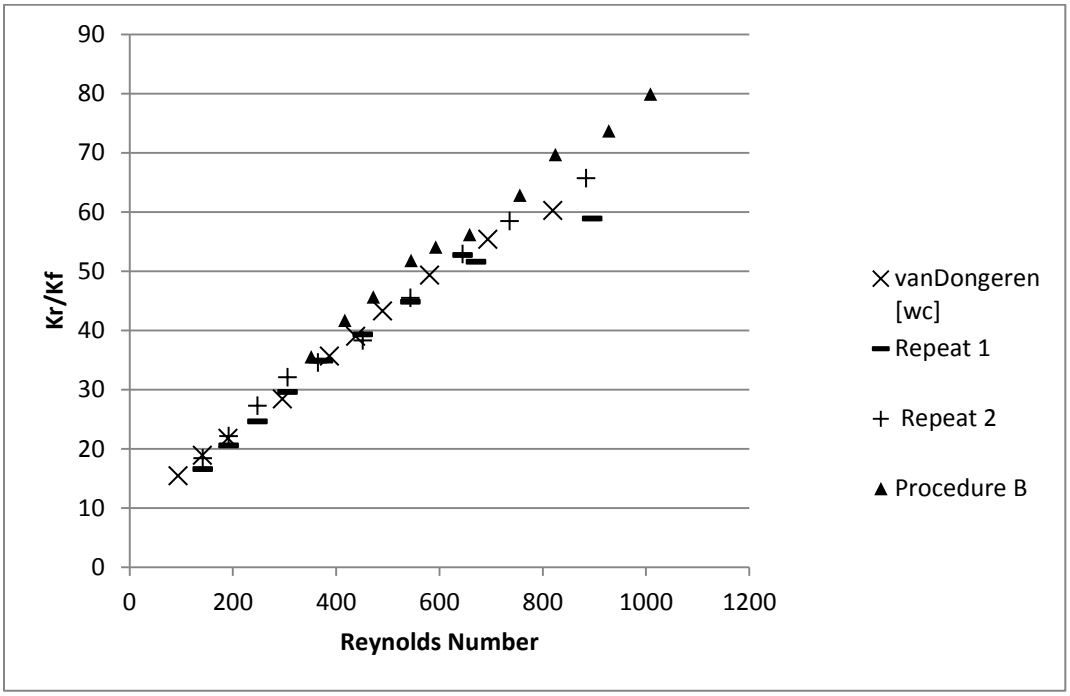


Figure 140: Effective Thermal Conductivity of Procedure B Compared to van Dongeren

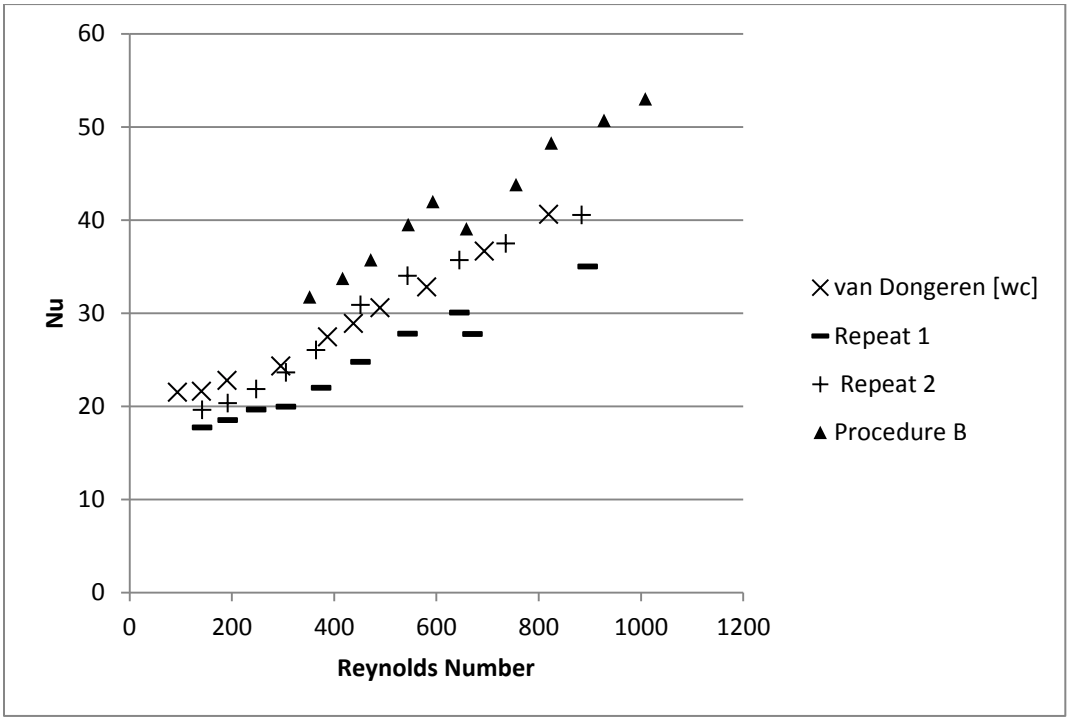


Figure 141: Nusselt Number of Procedure B Compared to van Dongeren

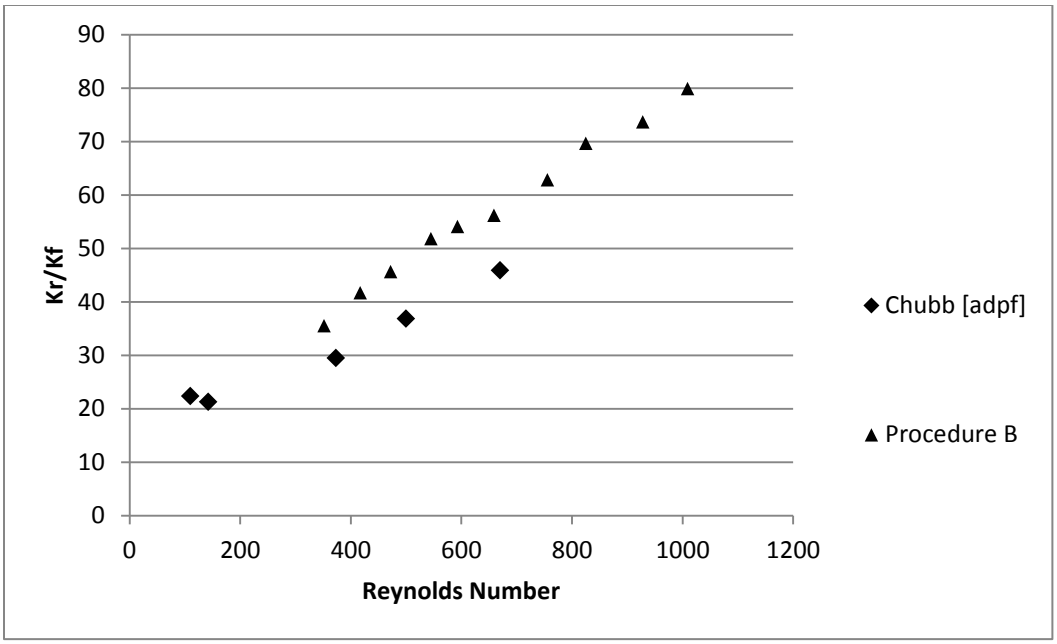


Figure 142: Effective Thermal Conductivity of Procedure B Compared to Chubb

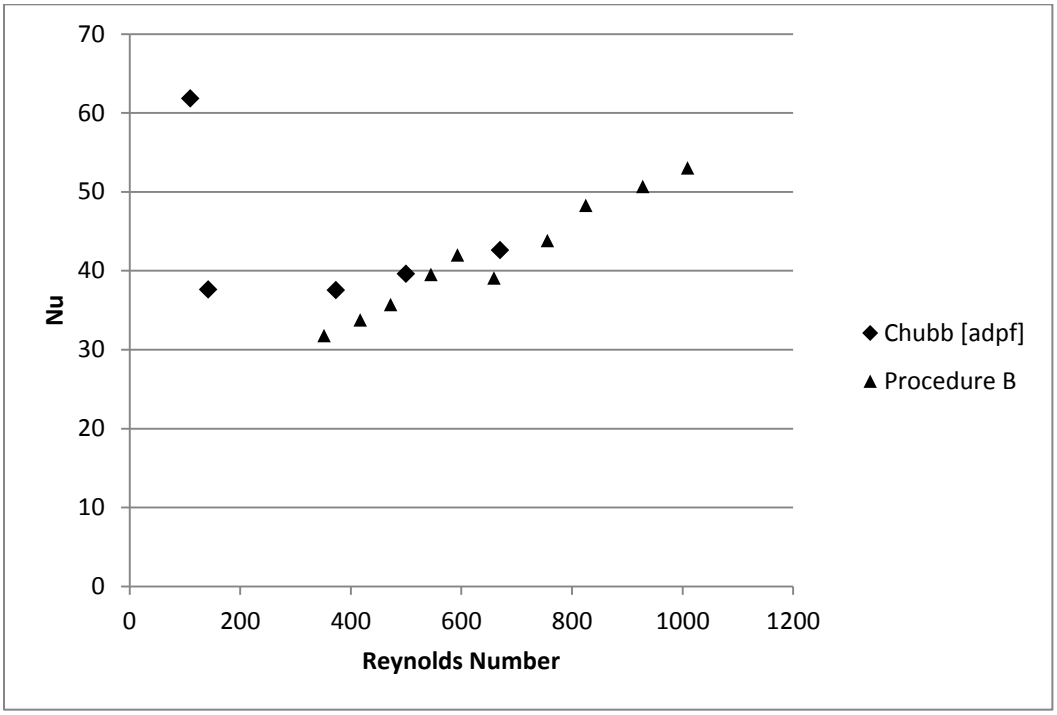


Figure 143: Nusselt Number of Procedure B Compared to Chubb

## APPENDIX K: TEMPERATURE VARIATIONS WITH TIME IN THERMOCOUPLES

**Four Inches**

| Thermocouple | A | F | F | F | F | G | G | G | G | D | D |
|---|---|---|---|---|---|---|---|---|---|---|---|
| Initial Time | 34.55 | 81.16 | 68.83 | 70.10 | 74.94 | 63.53 | 65.52 | 59.80 | 66.15 | 63.93 | 45.09 |
| One Hour | 35.10 | 82.81 | 68.51 | 69.37 | 75.49 | 64.45 | 65.40 | 59.13 | 66.59 | 65.37 | 45.08 |
| Two Hours | 35.11 | 83.08 | 68.63 | 69.47 | 75.53 | 64.78 | 65.57 | 59.13 | 66.68 | 65.76 | 45.13 |
| **Average** | **34.92** | **82.35** | **68.65** | **69.64** | **75.32** | **64.26** | **65.50** | **59.35** | **66.48** | **65.02** | **45.10** |
| **Standard Deviation** | **0.32** | **1.04** | **0.16** | **0.40** | **0.33** | **0.65** | **0.09** | **0.38** | **0.28** | **0.96** | **0.03** |

| Thermocouple | E | E | E | E | B | B | B | B | C | C | C |
|---|---|---|---|---|---|---|---|---|---|---|---|
| Initial Time | 49.47 | 47.77 | 52.59 | 47.69 | 50.07 | 40.96 | 41.63 | 47.72 | 40.94 | 38.88 | 41.80 |
| One Hour | 49.78 | 48.15 | 52.41 | 47.96 | 50.70 | 40.79 | 41.30 | 47.62 | 41.31 | 39.27 | 41.23 |
| Two Hours | 50.06 | 48.20 | 52.60 | 47.97 | 50.89 | 40.74 | 41.29 | 47.69 | 41.43 | 39.25 | 41.29 |
| **Average** | **49.77** | **48.04** | **52.53** | **47.87** | **50.56** | **40.83** | **41.41** | **47.68** | **41.23** | **39.14** | **41.44** |
| **Standard Deviation** | **0.29** | **0.24** | **0.10** | **0.16** | **0.43** | **0.11** | **0.20** | **0.05** | **0.26** | **0.22** | **0.31** |

| Thermocouple | C | D | D |
|---|---|---|---|
| Initial Time | 44.50 | 59.66 | 56.83 |
| One Hour | 43.95 | 58.47 | 56.41 |
| Two Hours | 43.93 | 58.49 | 56.54 |
| **Average** | **44.13** | **58.87** | **56.60** |
| **Standard Deviation** | **0.33** | **0.68** | **0.22** |

**Six Inches**

| Thermocouple | A | F | F | F | F | G | G | G | G | D | D |
|---|---|---|---|---|---|---|---|---|---|---|---|
| Initial Time | 47.66 | 89.68 | 80.46 | 73.92 | 86.54 | 66.16 | 68.51 | 76.14 | 74.27 | 73.48 | 66.83 |
| One Hour | 48.03 | 89.87 | 80.88 | 74.27 | 87.39 | 66.62 | 68.39 | 75.83 | 74.88 | 73.31 | 67.06 |
| Two Hours | 47.84 | 89.88 | 80.79 | 74.25 | 87.40 | 66.47 | 68.09 | 75.55 | 74.86 | 73.28 | 66.90 |
| **Average** | **47.85** | **89.81** | **80.71** | **74.15** | **87.11** | **66.42** | **68.33** | **75.84** | **74.67** | **73.36** | **66.93** |
| **Standard Deviation** | **0.19** | **0.12** | **0.22** | **0.20** | **0.50** | **0.23** | **0.22** | **0.29** | **0.35** | **0.11** | **0.12** |

| Thermocouple | E | E | E | E | B | B | B | B | C | C | C |
|---|---|---|---|---|---|---|---|---|---|---|---|
| Initial Time | 61.77 | 57.71 | 56.24 | 64.25 | 58.01 | 51.34 | 53.61 | 58.60 | 51.34 | 49.35 | 47.10 |
| One Hour | 61.91 | 58.27 | 55.66 | 64.50 | 57.76 | 51.51 | 53.66 | 58.28 | 51.66 | 49.39 | 47.13 |
| Two Hours | 61.65 | 58.04 | 55.56 | 64.20 | 57.61 | 51.33 | 53.54 | 58.10 | 51.50 | 49.23 | 46.96 |
| **Average** | **61.78** | **58.01** | **55.82** | **64.32** | **57.80** | **51.39** | **53.60** | **58.33** | **51.50** | **49.32** | **47.06** |
| **Standard Deviation** | **0.13** | **0.28** | **0.37** | **0.16** | **0.21** | **0.10** | **0.06** | **0.25** | **0.16** | **0.08** | **0.09** |

| Thermocouple | C | D | D |
|---|---|---|---|
| Initial Time | 55.21 | 66.18 | 76.81 |
| One Hour | 55.46 | 66.87 | 77.10 |
| Two Hours | 55.24 | 66.85 | 76.77 |
| **Average** | **55.30** | **66.63** | **76.89** |
| **Standard Deviation** | **0.13** | **0.39** | **0.18** |

## APPENDIX L: WALL TEMPERATURES FOR COUNTERCURRENT CONFIGURATION

| | 9/14/2012* | | | 9/26/2012 | | | 11/30/2012 | | |
|---|---|---|---|---|---|---|---|---|---|
| 4 in | 23.97 | 24.62 | 24.68 | 21.39 | 22.70 | 23.99 | 12.510 | 12.750 | 13.431 |
| 4 in 45 | 23.58 | 24.29 | 24.98 | 20.97 | 22.04 | 23.52 | 12.452 | 12.720 | 13.407 |
| 6 in | 23.60 | 24.62 | 24.39 | 21.25 | 22.16 | 24.04 | 10.003 | 10.313 | 11.009 |
| 6 in 45 | 23.32 | 23.83 | 25.21 | 21.14 | 21.77 | 23.82 | 9.490 | 9.903 | 10.652 |
| 8 in | 23.34 | 23.99 | 25.35 | 20.64 | 21.20 | 23.24 | 8.343 | 8.818 | 10.293 |
| 8 in 45 | 23.05 | 23.61 | 24.10 | 20.60 | 20.78 | 23.22 | 8.653 | 8.902 | 10.209 |
| 10 in | 23.20 | 23.81 | 24.18 | 20.45 | 20.54 | 23.18 | 9.081 | 9.538 | 10.917 |
| 10 in 45 | 23.43 | 24.17 | 24.25 | 20.84 | 21.18 | 23.47 | 9.467 | 10.003 | 11.322 |

*For this run the bed heights are 3 in, 5 in, 8 in, and 10 in

| | 12/3/2012 | | | 12/5/2012 | | | 12/6/2012 | | |
|---|---|---|---|---|---|---|---|---|---|
| 4 in | 12.94 | 13.59 | 14.12 | 8.78 | 9.56 | 10.16 | 10.014 | 11.202 | 11.965 |
| 4 in 45 | 12.78 | 13.45 | 13.94 | 8.82 | 9.70 | 10.46 | 10.395 | 11.482 | 12.307 |
| 6 in | 9.95 | 10.70 | 11.60 | 8.92 | 9.85 | 10.97 | 10.743 | 11.781 | 12.720 |
| 6 in 45 | 9.02 | 9.82 | 10.72 | 9.87 | 10.77 | 11.95 | 10.472 | 11.487 | 12.528 |
| 8 in | 8.06 | 8.95 | 10.39 | 11.18 | 12.10 | 13.74 | 10.470 | 11.631 | 13.462 |
| 8 in 45 | 9.81 | 10.68 | 12.10 | 11.38 | 12.23 | 13.88 | 10.458 | 11.620 | 13.512 |
| 10 in | 11.51 | 12.36 | 13.74 | 11.63 | 12.70 | 14.44 | 9.378 | 10.629 | 12.827 |
| 10 in 45 | 11.56 | 12.38 | 13.98 | 11.61 | 12.63 | 14.58 | 9.603 | 10.805 | 13.041 |

| | 12/7/2012 | | | 12/10/2012 | | | 12/12/2012 | | |
|---|---|---|---|---|---|---|---|---|---|
| 4 in | 8.72 | 9.92 | 11.16 | 10.80 | 12.10 | 13.12 | 11.79 | 12.81 | 13.56 |
| 4 in 45 | 8.77 | 9.92 | 11.10 | 11.12 | 12.22 | 13.26 | 11.31 | 12.38 | 13.23 |
| 6 in | 9.02 | 10.21 | 11.63 | 8.39 | 9.87 | 11.43 | 10.37 | 11.52 | 12.86 |
| 6 in 45 | 8.62 | 9.80 | 11.27 | 8.36 | 9.81 | 11.59 | 10.10 | 11.09 | 12.40 |
| 8 in | 7.95 | 9.47 | 11.78 | 10.92 | 12.50 | 15.13 | 10.37 | 11.69 | 13.72 |
| 8 in 45 | 7.79 | 9.13 | 11.41 | 11.00 | 12.65 | 15.41 | 10.71 | 12.01 | 14.09 |
| 10 in | 7.80 | 9.48 | 12.07 | 11.35 | 13.33 | 16.02 | 11.06 | 12.46 | 14.64 |
| 10 in 45 | 7.72 | 9.34 | 12.02 | 11.58 | 13.36 | 16.17 | 11.32 | 12.66 | 14.81 |

| | 12/13/2012 | | |
|---|---|---|---|
| 4 in | 11.58 | 12.85 | 13.82 |
| 4 in 45 | 11.42 | 12.72 | 13.69 |
| 6 in | 7.84 | 9.30 | 10.93 |
| 6 in 45 | 8.72 | 10.12 | 11.64 |
| 8 in | 8.06 | 9.72 | 12.50 |
| 8 in 45 | 8.06 | 9.66 | 12.34 |
| 10 in | 8.17 | 10.05 | 13.06 |
| 10 in 45 | 8.29 | 10.10 | 12.82 |

## APPENDIX M: WALL TEMPERATURES FOR CO-CURRENT CONFIGURATION

| | 11/5/2012 | | | 11/7/2012 | | | 11/8/2012 | | |
|---|---|---|---|---|---|---|---|---|---|
| 4 in | 15.18 | 15.79 | 15.66 | 12.74 | 13.43 | 13.54 | 13.74 | 15.08 | 15.18 |
| 4 in 45 | 15.88 | 16.52 | 16.40 | 13.24 | 13.91 | 14.00 | 14.29 | 15.50 | 15.68 |
| 6 in | 15.10 | 15.74 | 15.67 | 13.97 | 14.64 | 14.89 | 14.49 | 15.86 | 16.18 |
| 6in 45 | 14.92 | 15.59 | 15.57 | 13.41 | 14.23 | 14.30 | 14.43 | 15.82 | 15.96 |
| 8 in | 15.02 | 15.72 | 15.91 | 14.55 | 15.38 | 15.67 | 13.89 | 15.37 | 16.07 |
| 8 in 45 | 14.70 | 15.39 | 15.51 | 15.18 | 16.02 | 16.32 | 14.67 | 16.01 | 16.91 |
| 10 in | 15.52 | 16.27 | 16.34 | 15.46 | 16.37 | 16.66 | 14.94 | 16.57 | 17.12 |
| 10 in 45 | 16.06 | 16.80 | 16.90 | 15.52 | 16.34 | 16.77 | 14.97 | 16.70 | 17.40 |

| | 11/9/2012 | | | 11/12/2012 | | | 11/14/2012 | | |
|---|---|---|---|---|---|---|---|---|---|
| 4 in | 13.72 | 15.33 | 15.33 | 16.02 | 17.14 | 17.11 | 11.072 | 12.015 | 11.894 |
| 4 in 45 | 13.77 | 15.37 | 15.29 | 13.57 | 14.79 | 14.67 | 11.003 | 11.923 | 11.761 |
| 6 in | 14.31 | 15.98 | 16.22 | 13.82 | 15.01 | 15.21 | 11.414 | 12.356 | 12.396 |
| 6in 45 | 14.53 | 16.23 | 16.44 | 12.19 | 13.53 | 13.67 | 12.211 | 13.158 | 13.335 |
| 8 in | 14.58 | 16.49 | 17.32 | 11.88 | 13.41 | 14.24 | 12.762 | 13.797 | 14.047 |
| 8 in 45 | 13.86 | 15.92 | 16.47 | 11.85 | 13.39 | 14.06 | 13.270 | 14.282 | 14.864 |
| 10 in | 12.81 | 15.22 | 15.89 | 12.45 | 14.31 | 15.03 | 13.594 | 14.790 | 15.191 |
| 10 in 45 | 13.11 | 15.45 | 15.78 | 12.87 | 14.77 | 15.35 | 13.768 | 14.967 | 15.425 |

| | 11/15/2012 | | | 11/19/2012 | | | 11/26/2012 | | |
|---|---|---|---|---|---|---|---|---|---|
| 4 in | 12.63 | 13.74 | 13.75 | 12.40 | 13.68 | 13.63 | 13.68 | 15.19 | 15.11 |
| 4 in 45 | 12.94 | 14.04 | 14.20 | 11.63 | 12.90 | 12.94 | 13.65 | 15.14 | 15.16 |
| 6 in | 12.17 | 13.42 | 13.55 | 11.12 | 12.54 | 12.84 | 13.31 | 14.91 | 15.27 |
| 6in 45 | 12.08 | 13.29 | 13.52 | 11.34 | 12.72 | 13.05 | 12.86 | 14.47 | 14.58 |
| 8 in | 12.61 | 13.99 | 14.56 | 10.75 | 12.39 | 13.18 | 9.39 | 11.37 | 12.14 |
| 8 in 45 | 12.21 | 13.57 | 14.18 | 10.63 | 12.26 | 12.78 | 10.07 | 11.90 | 12.75 |
| 10 in | 12.51 | 14.08 | 14.50 | 11.00 | 12.83 | 13.19 | 11.95 | 14.02 | 14.47 |
| 10 in 45 | 13.38 | 14.87 | 15.23 | 11.33 | 13.28 | 13.87 | 12.52 | 14.49 | 15.09 |

| | 11/29/2012 | | |
|---|---|---|---|
| 4 in | 10.37 | 12.17 | 12.18 |
| 4 in 45 | 10.88 | 12.65 | 12.63 |
| 6 in | 11.19 | 13.18 | 13.47 |
| 6in 45 | 10.16 | 12.18 | 12.60 |
| 8 in | 10.37 | 12.56 | 13.92 |
| 8 in 45 | 9.87 | 12.39 | 13.35 |
| 10 in | 10.48 | 13.17 | 13.95 |
| 10 in 45 | 11.10 | 13.86 | 14.45 |

## APPENDIX N: CHUBB COMPARISON TO CURRENT HEATING

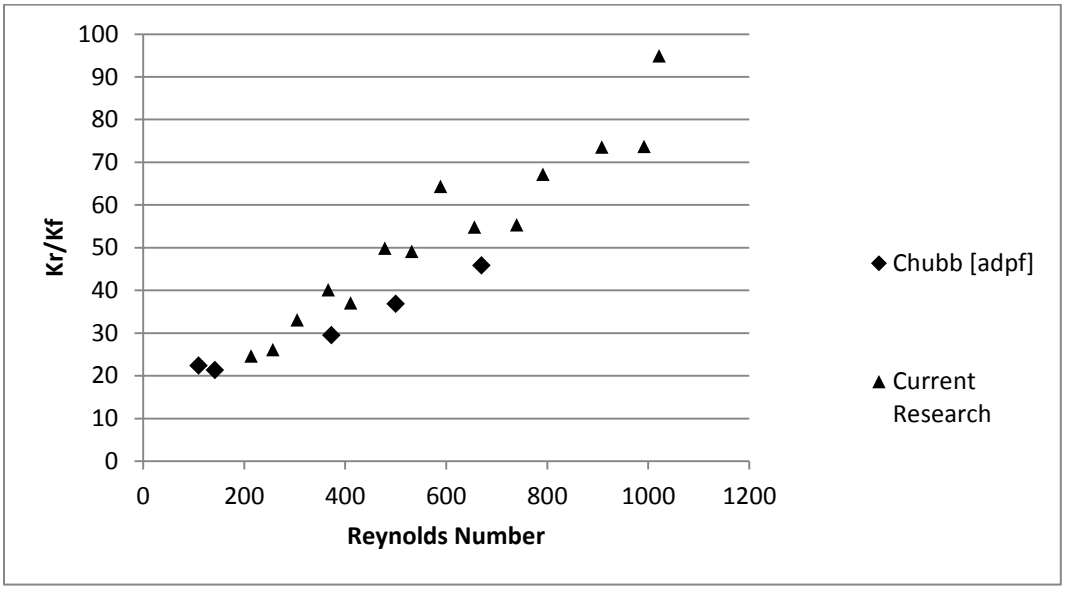


Figure 144: Effective Thermal Conductivity against the Reynolds Number Heating Comparison

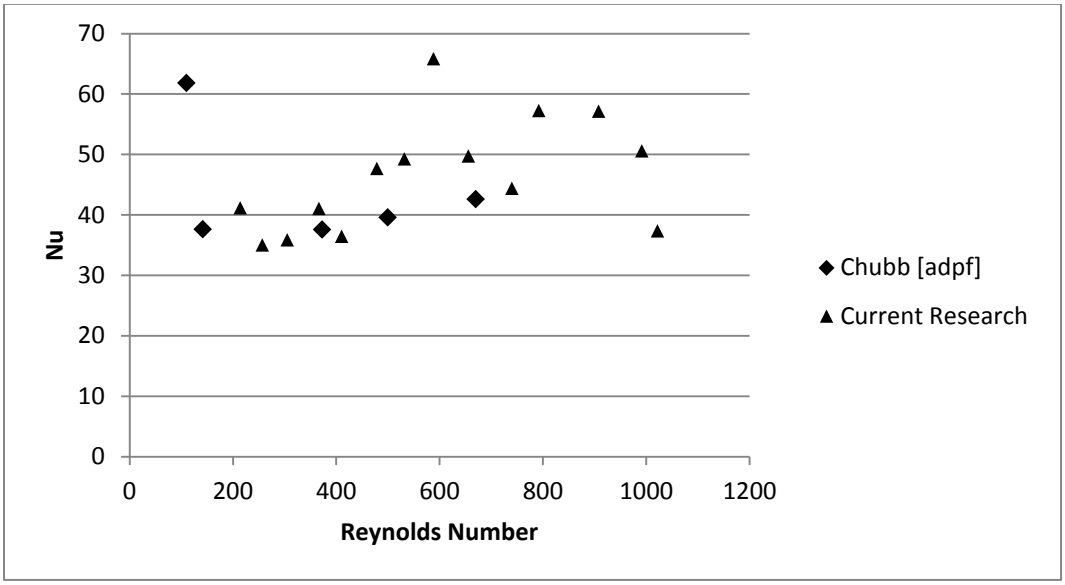


Figure 145: Nusselt Number against the Reynolds Number Heating Comparison

## Appendix O: Biot and Peclet Number Graphs

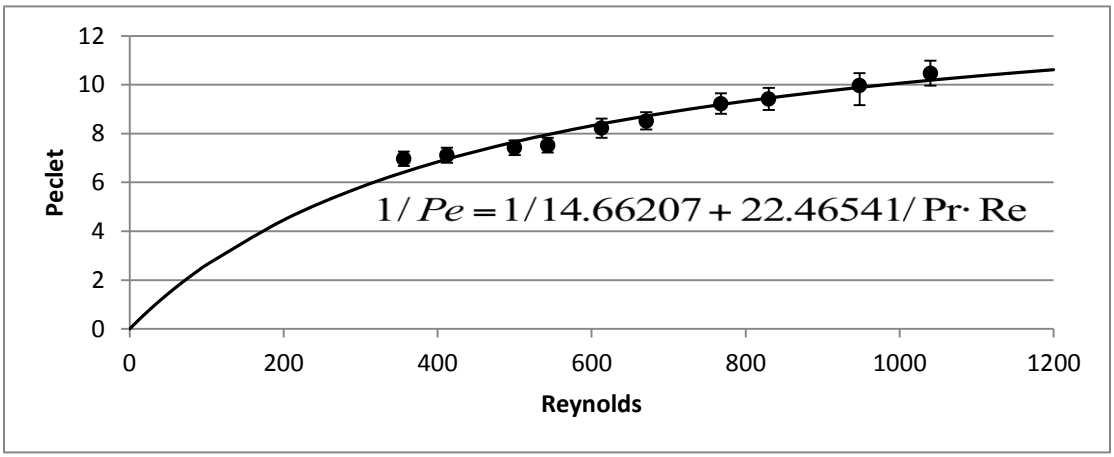


Figure 146: Peclet Number versus Reynolds Number for Countercurrent Cooling for Procedure B

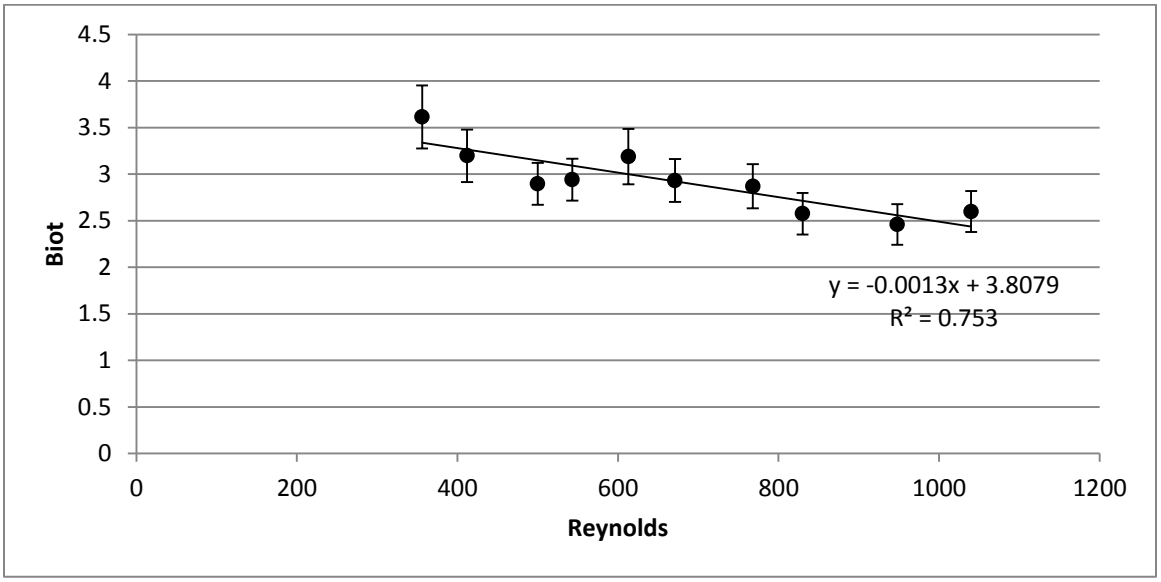


Figure 147: Biot Number versus Reynolds Number for Countercurrent Cooling for Procedure B

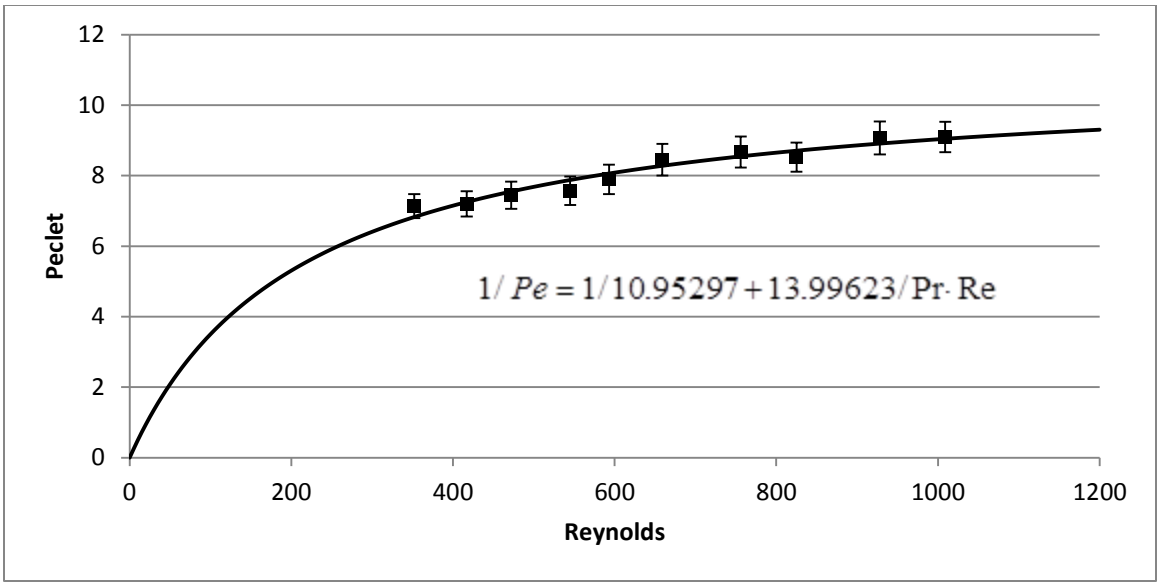


Figure 148: Peclet Number versus Reynolds Number Heating for Procedure B

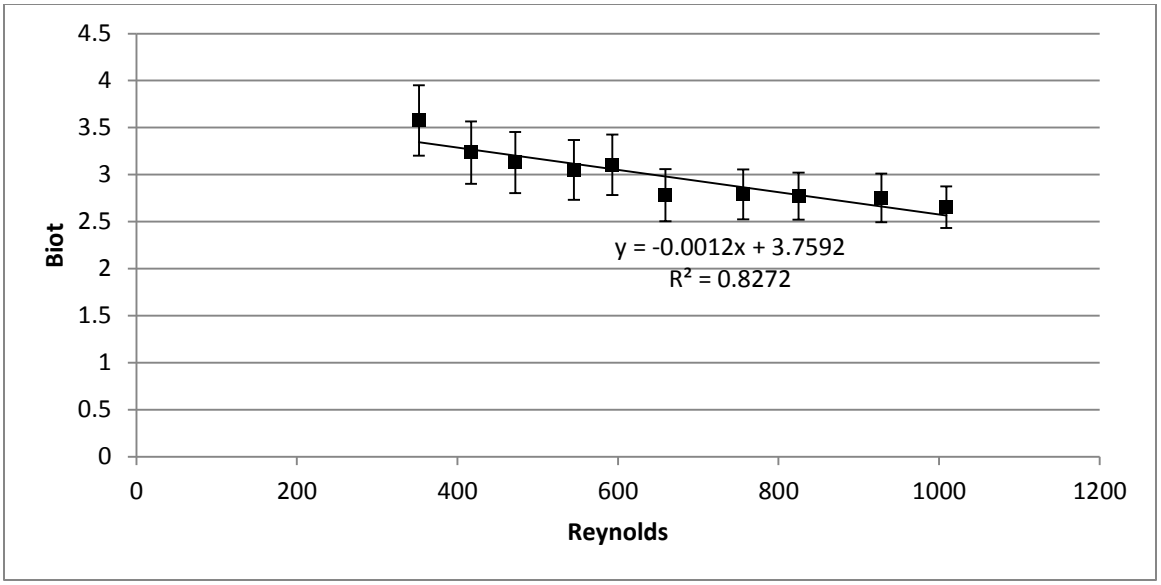


Figure 149: Biot Number versus Reynolds Number Heating for Procedure B

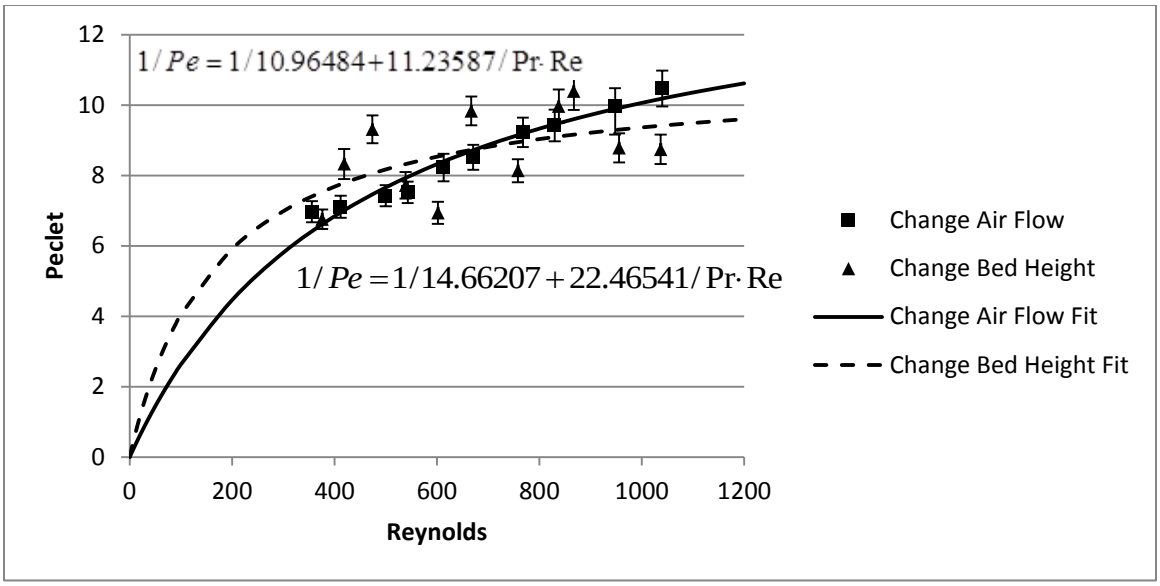


Figure 150: Peclet Number versus Reynolds Number Cooling Comparison for Both Procedures

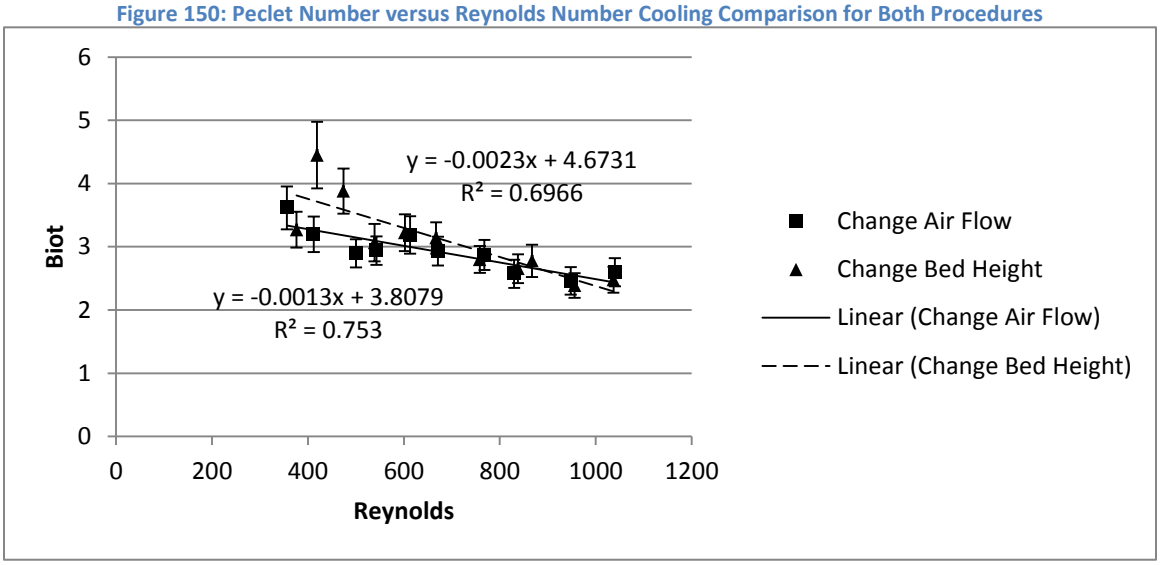


Figure 151: Biot Number versus Reynolds Number Cooling Comparison for Both Procedures

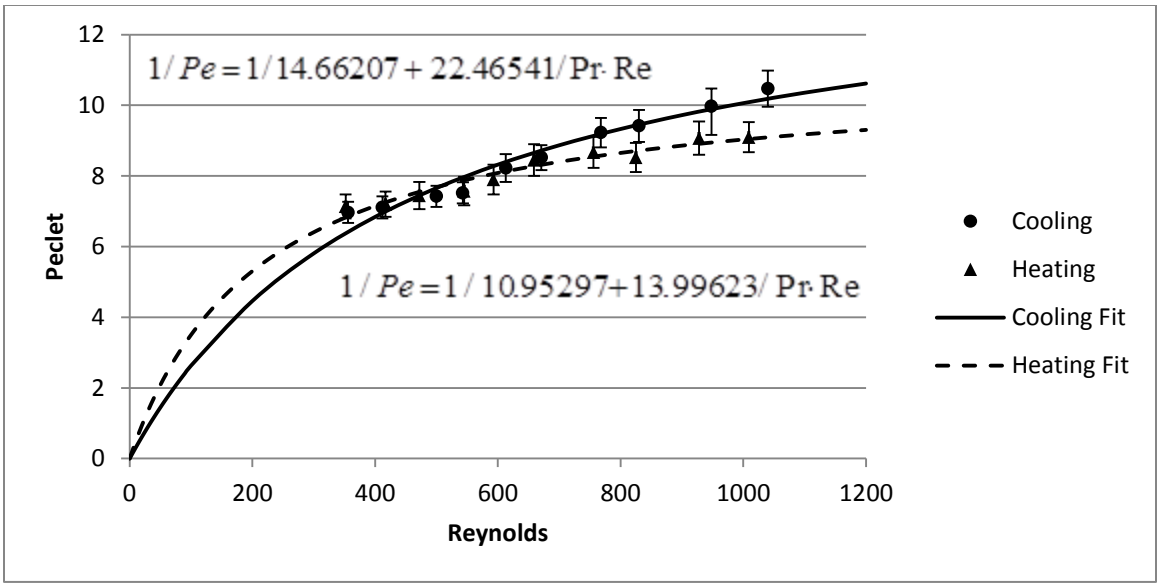


Figure 152: Peclet Number versus Reynolds Number Heating and Cooling Comparison for Procedure A

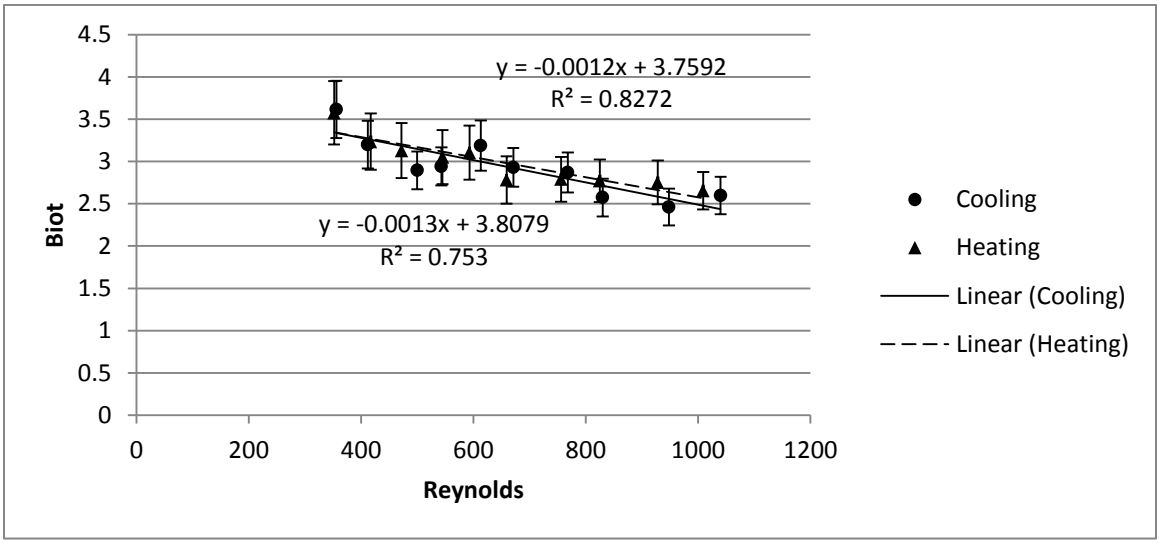


Figure 153: Biot Number versus Reynolds Number Heating and Cooling Comparison for Procedure A

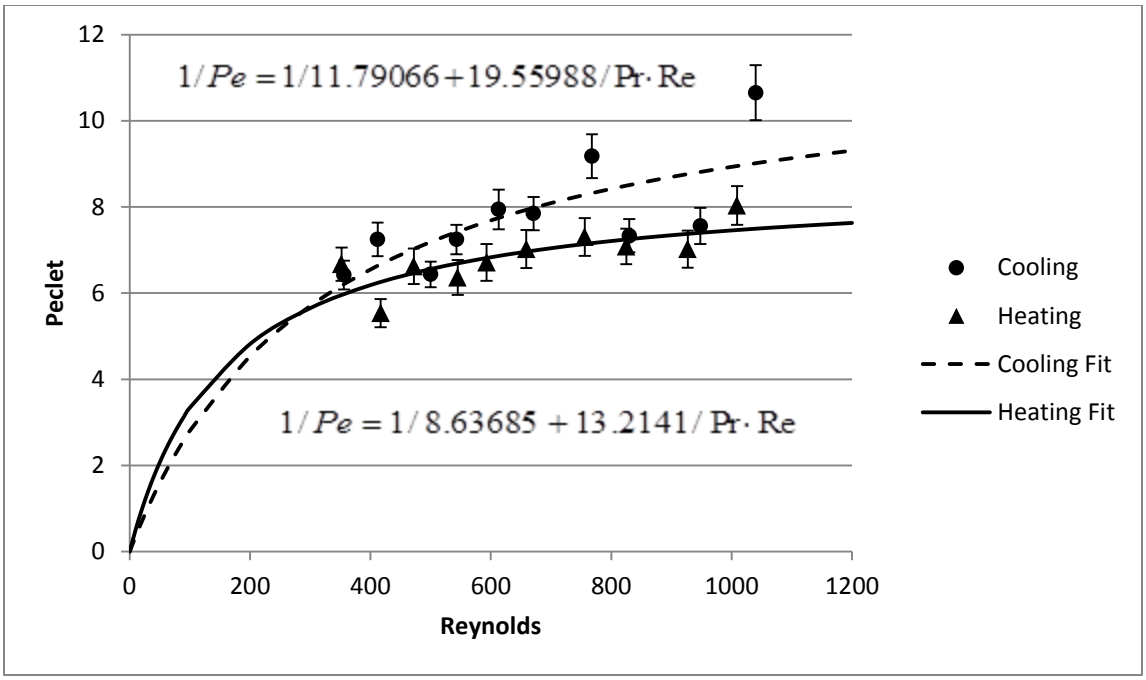


Figure 154: Peclet Number versus Reynolds Number Heating and Cooling Comparison for Procedure B without Center Thermocouple

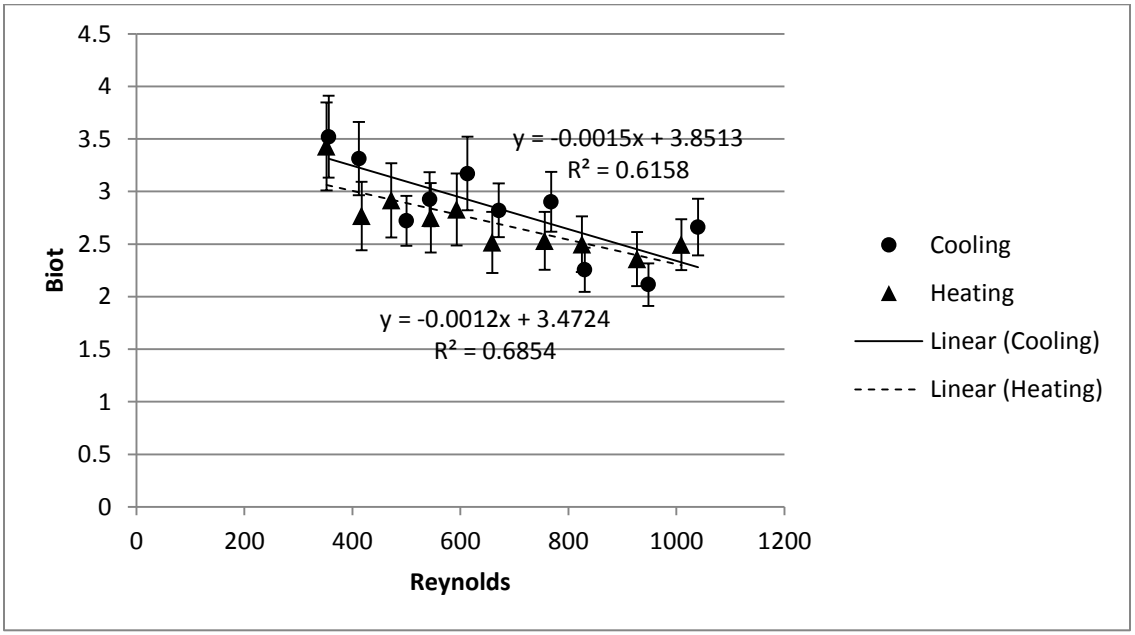


Figure 155: Biot Number versus Reynolds Number Heating and Cooling Comparison for Procedure B without Center Thermocouple

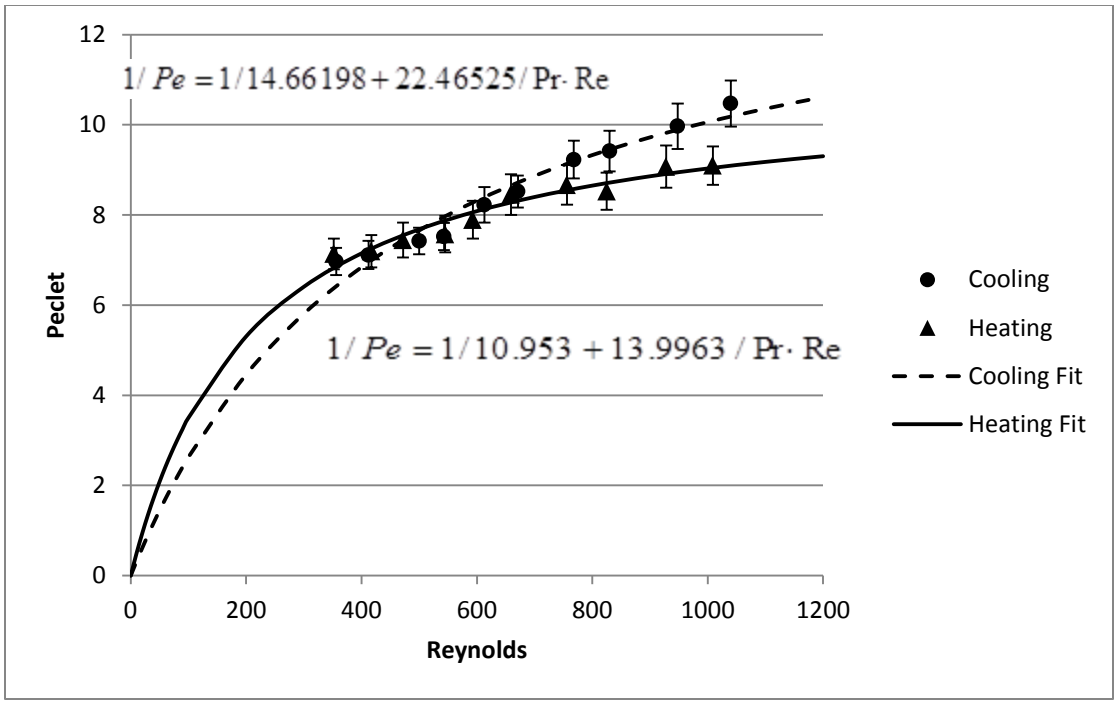


Figure 156: Peclet Number versus Reynolds Number Heating and Cooling Comparison for Procedure B with Center Thermocouple

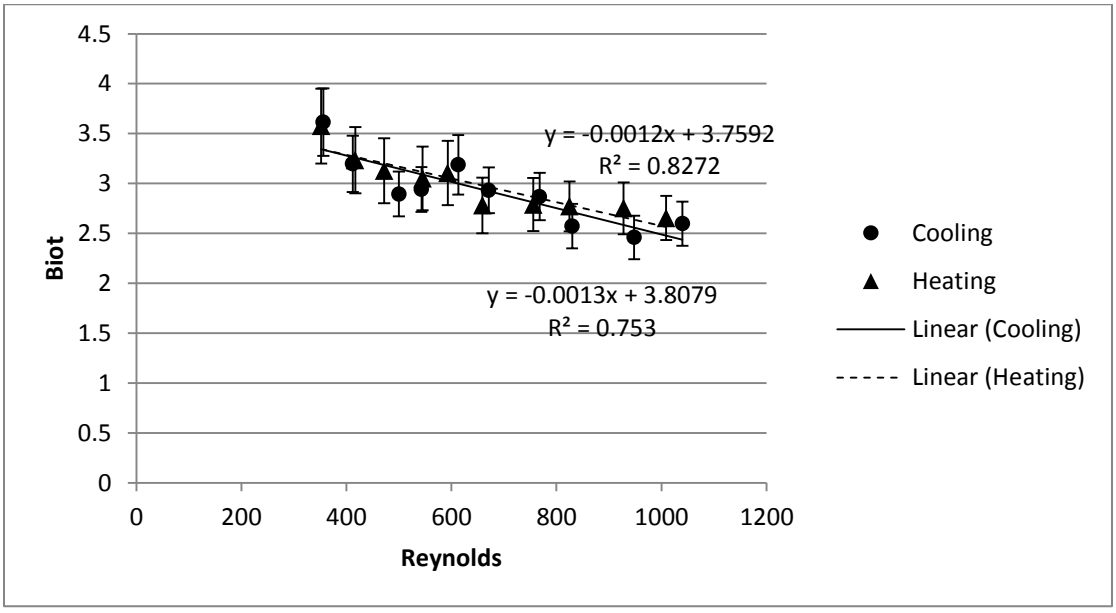


Figure 157: Biot Number versus Reynolds Number Heating and Cooling Comparison for Procedure B with Center Thermocouple